

IMPROVED ASSESSMENT METHODS OF LOWER EXTREMITY INJURIES IN VEHICLE-TO-PEDESTRIAN ACCIDENTS USING IMPACTOR TESTS AND FULL-SCALE DUMMY TESTS

Oliver Zander

Federal Highway Research Institute (BASt)
Germany

Dirk-Uwe Gehring

Peter Leßmann

BGS Böhme & Gehring GmbH
Germany
Paper Number 11-0079

ABSTRACT

A flexible pedestrian legform impactor (FlexPLI) has been evaluated by a Technical Evaluation Group (Flex-TEG) of the Working Party on Passive Safety (GRSP) of the United Nations Economic Commission for Europe (UN-ECE). It will be implemented within phase 2 of the global technical regulation (GTR 9) as well as within a new ECE regulation on pedestrian safety as a test tool for the assessment of lower extremity injuries in lateral vehicle-to-pedestrian accidents (UN-ECE 2010-1, 2010-2 and 2010-3).

Due to its biofidelic properties in the knee and tibia section, the FlexPLI is found to having an improved knee and tibia injury assessment ability when being compared to the current legislative test tool, the lower legform impactor developed by the Pedestrian Safety Working Group of the European Enhanced Vehicle-safety Committee (EEVC WG 17). However, due to a lack of biofidelity in terms of kinematics and loadings in the femur part of the FlexPLI, an appropriate assessment of femur injuries is still outstanding.

The study described in this paper is aimed to close this gap. Impactor tests with the FlexPLI at different impact heights on three vehicle frontends with Sedan, SUV and FFV shape are performed and compared to tests with a modified FlexPLI with upper body mass. Full scale validation tests using a modified crash test dummy with attached FlexPLI that are carried out for the first time prove the more humanlike responses of the femur section with applied upper body mass. Apart from that they also show that the impact conditions described in the current technical provisions for tests with the FlexPLI don't necessarily compensate the missing torso mass in terms of knee and tibia loadings either.

Therefore it can be concluded that an applied upper body mass will contribute to a more biofidelic overall behavior of the legform and subsequently an improved injury assessment ability of all lower extremity injuries addressed by the FlexPLI.

Nevertheless, the validity of the original as well as the modified legform for tests against vehicles with extraordinary high bumpers as well as flat front

vehicles still needs to be evaluated in detail. A first clue is given by the application of an additional accelerometer to the legform.

INTRODUCTION

The preamble of the Global Technical Regulation on Pedestrian Safety (GTR No. 9), published in January 2009, considers the flexible pedestrian legform impactor (FlexPLI) to replace the EEVC WG 17 pedestrian legform impactor which is currently used for type approval tests according to European Regulation (EC) 78/2009 in the near future. Therefore, a Technical Evaluation Group (Flex-TEG) of UNECE-GRSP has evaluated the FlexPLI within 12 meetings and has given final recommendations for the introduction within world-wide legislation. The introduction of the FlexPLI is also one of the main mid term activities on the agenda of the Pedestrian Subgroup of the European New Car Assessment Programme (Euro NCAP).

A study of the German In Depth Accident Database GIDAS in 2009 was aimed at examining the distribution of lower extremity injuries in lateral vehicle-to-pedestrian accidents focusing on the particular injury locations at 3 or 9 o'clock related to the pedestrian. All accidents with pedestrians crossing (from the left or the right only) and with the vehicle front, bonnet leading edge or bumper as injury causing part were taken into account. The described selection criteria resulted in a total of 6330 pedestrian injuries, thereof 1921 lower extremity injuries. Figure 1 shows the distribution in terms of injury location. 818 of the described injuries are located in the lower leg area, followed by 460 knee injuries and 226 femur injuries. 417 injuries are not clearly specified or occurred in other areas. Though the femur injuries represent the smallest group in this statistical analysis, they are of a high relevance in the actual accident scenario and thus cannot be neglected.

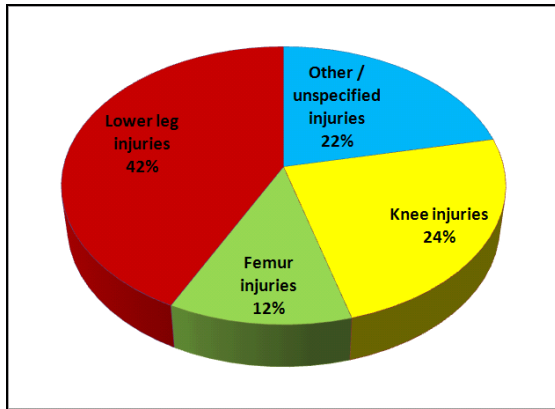


Figure 1. Distribution of lower extremity injuries (n=1921) in selected vehicle-to-pedestrian accidents within GIDAS (2009).

However, up to now the pedestrian protection potential of modern vehicle frontends is limited to the assessment using the FlexPLI, only taking into account the tibia bending moments acquired by four strain gauges as well as the elongation of medial collateral and cruciate ligaments measured by three string potentiometers. As the biofidelity of the FlexPLI is limited by the absence of a pedestrian torso or equivalent mass, femur injuries cannot be assessed appropriately.

The application of an additional upper body mass is meant to close this gap. Component tests with a modified FlexPLI against three different vehicles front shapes are validated by full scale dummy tests.

DERIVATION OF INJURY CRITERIA AND THRESHOLD VALUES

In one of its latest status reports to GRSP, the Technical Evaluation Group recommended threshold values for the FlexPLI tibia bending moments and ligament elongations that previously had been controversially discussed.

Threshold value for tibia bending moment

At the 8th GRSP Flex-TEG meeting in May 2009, two proposals for the tibia threshold value of the FlexPLI version GTR (also called Flex-GTR) were made by the Japan Automobile Manufacturers Association (JAMA) and the German Federal Highway Research Institute (BASt), coming to different conclusions.

JAMA derived the Flex-GTR tibia bending moment threshold using a linear transition equation between human and Flex-GTR finite element (FE) models derived from computer simulation results.

The average human tibia bending moment threshold value was taken from an injury risk curve of the 50th percentile male for tibia fracture, taking into account scaled male and female PMHS data

from Nyquist et al. (1985) and Kerrigan et al. (2004) under modification of the standard tibia length and standard tibia plateau height, making the assumption that the height scale factor and length scale factor should correlate to each other. The Weibull Survival Model was used to develop the injury probability function. The proposed final threshold value resulted in 380 Nm (JAMA, 2009-1 and 2009-2).

BASt derived the Flex-GTR tibia bending moment threshold also using the corresponding transition equation between human and Flex-GTR FE models. The average human tibia bending moment threshold value was taken from an injury risk curve of the 50th percentile male for tibia fracture, taking into account scaled male PMHS data from Nyquist et al. (1985) using the standard tibia plateau height provided by DIN 33402-2 German anthropometrical database. The cumulative Gaussian distribution was used to develop the injury probability function. The calculated threshold value under consideration of possible scatter of test results and of a reproducibility corridor derived from inverse certification test results was 302 Nm (Zander, 2009).

A comparison of both approaches revealed that the calculated threshold values mainly depend on

- the underlying set of PMHS data
- the consideration of female and / or male data
- the use of scaled or unscaled data
- the particular anthropometrical database based on which human data are scaled
- the injury risk to be covered
- the statistical procedure to develop an injury probability function

As consensus for both approaches BASt proposed a rounded average value of 340 Nm for the maximum tibia bending moment threshold.

In parallel to BASt proposing a rounded average value, JAMA conducted a correlation study on the EEVC WG 17 PLI tibia acceleration and FlexPLI tibia bending moment. As a result, they found that the 170 g EEVC WG 17 PLI tibia acceleration in GTR 9 was correlated to 343 Nm Flex-GTR tibia bending moment

As this was almost the value proposed by BASt as average value between the BASt and former JAMA proposals, the group agreed at the 9th TEG meeting in September 2009 on a consensus of the rounded value of 340 Nm.

Threshold value for MCL elongation

JAMA developed an MCL injury risk function as average function between the risk functions from Ivarsson et al. (2004) and Konosu et al. (2001), latter one revised using the Weibull Survival Model. In this function, a 50% risk of knee injury in terms of MCL rupture corresponded to a human knee bending angle of 19 degrees. This value was

converted to 19.2 mm MCL elongation, using a corresponding transition equation from computer simulation. After incorporating the effect of muscle tone the threshold value was calculated at 21.1 mm (JAMA, 2009-2). As this value was converted to 16.9 degrees of EEVC WG 17 PLI knee bending angle by using a corresponding transition equation which would be approx. 11 % more conservative than the GTR threshold value of 19 deg, a 5% more conservative approach, equal to 18 deg EEVC WG 17 PLI knee bending angle was proposed and transformed to 22 mm MCL elongation, using the same transition equation as before.

As BAST was not in the position to validate or double-check those results, they investigated a direct correlation between the EEVC WG 17 PLI knee bending angle and the FlexPLI MCL elongation as a verification of the JAMA results. A transition equation was developed, based on hardware test results of different vehicle categories and idealized tests. Thus, a knee bending angle of 19 degrees would correspond to 22.7 mm MCL elongation. In order to provide at least the same level of protection as the current GTR, a threshold value of 22 mm was proposed which was in line with the JAMA proposal (Zander, 2009-3).

At the 9th GRSP Flex-TEG meeting in September 2009, the group agreed on a Flex-GTR threshold value for MCL elongation of 22 mm.

Threshold value for ACL/PCL elongation

Currently, no injury risk curve for cruciate ligament injuries is available. BAST therefore carried out correlation studies between

- a) results for the shearing displacement of the EEVC WG 17 pedestrian legform impactor and FlexPLI ACL/PCL elongations,
- b) between FlexPLI MCL and ACL elongation results and
- c) between FlexPLI shearing displacement and ACL elongation,

and compared those with the results of PMHS tests described by Bhalla et al. (2003), stating that below a shear displacement of 12.7 mm sufficient protection is provided to the cruciate ligaments. Thus, having in mind that the FlexPLI should provide at least the same level of protection as the EEVC WG 17 PLI, BAST proposed a mandatory threshold value of 13 mm for ACL/PCL (Zander, 2010).

In contrast, JAMA stated that the percentage of isolated ACL/PCL injuries in real world data is low (less than 3%) and the biomechanical data limited, which did not allow the development of an injury probability function. Therefore, the tentative threshold value was suggested to be set for monitoring, subject to future modification to the tentative threshold based on additional biomechanical data.

The European Automobile Manufacturers Association (ACEA) was, for the time being, in favour of not considering an ACL/PCL injury assessment at all.

Current status within GRSP

During its 48th session in December 2010, GRSP discussed the phase of introduction of the FlexPLI within GTR No. 9 as well as the new ECE Regulation on Pedestrian Safety. The introduction will be based on the threshold values for the tibia bending moments and MCL elongation agreed by Flex-TEG, amended by a relaxation zone for bumper test widths of a maximum of 264 mm where the maximum tibia bending moment shall not exceed 380 Nm. Concerning the cruciate ligament elongations ACL/PCL, in case a vehicle does not comply with a threshold value of 13 mm, an additional test with the EEVC WG 17 PLI has to be carried out for the assessment of the shearing displacement which in that case shall not exceed 6 mm (UN-ECE, 2010-2). Table 1 shows an overview of the tentative Flex-GTR threshold values:

Table 1.
Tentative Flex-GTR threshold values

Leg region	Flex-GTR thresholds (tentative)	based on
Tibia	340 Nm	Nyquist et al. (1985) Kerrigan et al. (2004)
Relaxation zone	380 Nm	Feasibility
MCL	22 mm	Konosu (2001) Ivarsson et al. (2004)
ACL / PCL	13 mm	Bhalla et al. (2001) Zander (2009-3)

MOTIVATION AND MODIFICATION OF TEST SETUP

As the results of previously performed tests have proved, from built level GT on, the FlexPLI has shown biofidelic responses for the knee and tibia area in tests against Sedan and SUV shaped frontends. However, an injury assessment of the femur section was not possible due to the lack of an additional mass representing a pedestrian torso. Bovenkerk et al. (2009) therefore developed an additional pedestrian upper body mass that was applied to the FlexPLI built level GT and tested against an SUV shaped frontend. First test results seemed promising in terms of an improved injury assessment ability of the legform femur segments.

Zander et al. (2009-2) amended this study by tests against a Sedan frontend and found the additional mass having a positive effect on the femur as well as tibia and knee injury assessment ability, too.

In order to obtain more information on the applicability of the modified FlexPLI for the assessment of the pedestrian protection potential of a broader variety of vehicle frontends, the FlexPLI was attached to a Hybrid II crash test dummy and additional full scale tests against three different car front shapes representing a Sedan, SUV and FFV category have been carried out.

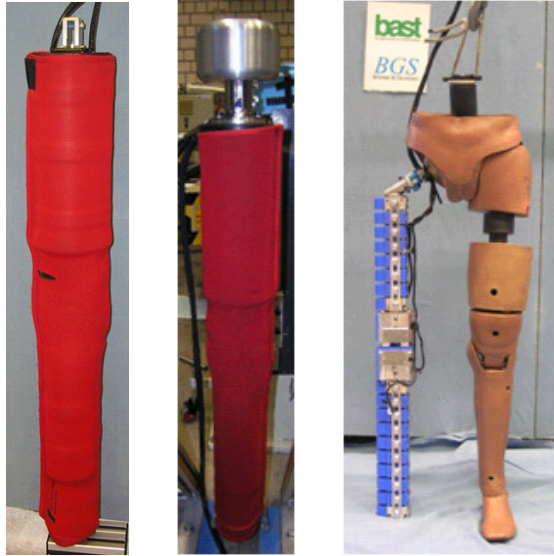


Figure 2. FlexPLI built level GT as standard version, with upper body mass and applied to Hybrid II pelvis.

To complete the data basis, further component tests with the Flex-GT with and without upper body mass against the FFV representative have been performed, so that in the end all three vehicle categories were tested using all three test setups. A complete test matrix is given in table 2.

**Table 2.
Test matrix**

Test #	Vehicle	Impactor	Test Location y [mm]	Impact Height [mm]
1	Sedan	Flex-GT	51	25
2	Sedan	Flex-GT	51	25
3	Sedan	Flex-GT	51	25
4	Sedan	Flex-GT	51	75
5	Sedan	Flex-GT	51	75
6	Sedan	Flex-GT	51	75
7	Sedan	Flex-GT-UBM	51	25
8	Sedan	Flex-GT-UBM	51	25
9	Sedan	Flex-GT-UBM	51	25
10	Sedan	Flex-GT-HII	51	25
11	Sedan	Flex-GT-HII	51	25
12	Sedan	Flex-GT-HII	51	25
13	SUV	Flex-GT	128	75
14	SUV	Flex-GT	128	75
15	SUV	Flex-GT	128	75
16	SUV	Flex-GT-UBM	128	25
17	SUV	Flex-GT-UBM	128	25
18	SUV	Flex-GT-UBM	128	25
19	SUV	Flex-GT-HII	128	25
20	SUV	Flex-GT-HII	128	25
21	SUV	Flex-GT-HII	128	25
22	FFV	Flex-GT	0	75
23	FFV	Flex-GT-UBM	0	25
24	FFV	Flex-GT-HII	0	25

DESCRIPTION OF IMPACT CONDITIONS AND TARGET POINTS

In order to obtain a better understanding of the validity of test results obtained in component tests with upper body mass as well as full scale dummy tests, three different vehicle categories have been chosen for a comparative study. The lateral impact locations have been selected in a way that the control of impact conditions within the dummy tests was acceptable. The impact height of the Flex-GT during the UBM and full scale tests was chosen at 25 mm above ground level. The baseline component tests were performed at 75 mm (and in case of the sedan additionally at 25 mm) as prescribed by legislation in order to compensate for the missing upper body mass in the tibia injury assessment.

The load paths in relation to the FlexPLI measurement items of all tests setups with an impact height of 75 mm are shown in figures 2-4.

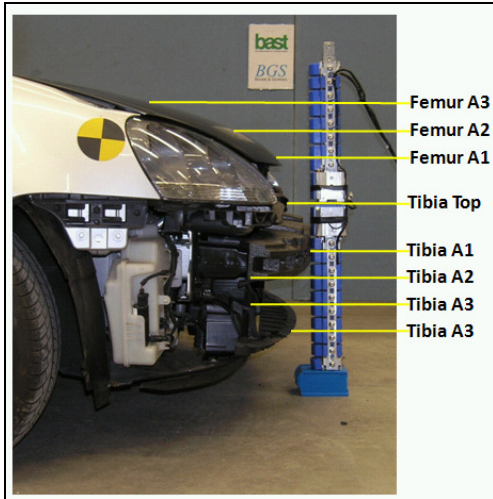


Figure 3. Load paths of sedan frontend in relation to Flex-GT measuring items at 75 mm impact height (baseline test setup).

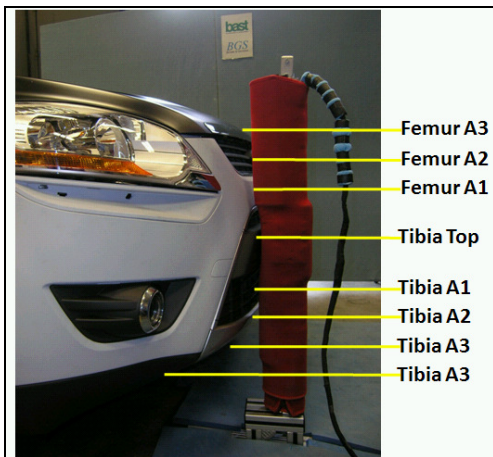


Figure 4. Load paths of SUV frontend in relation to Flex-GT measuring items at 75 mm impact height (baseline test setup).

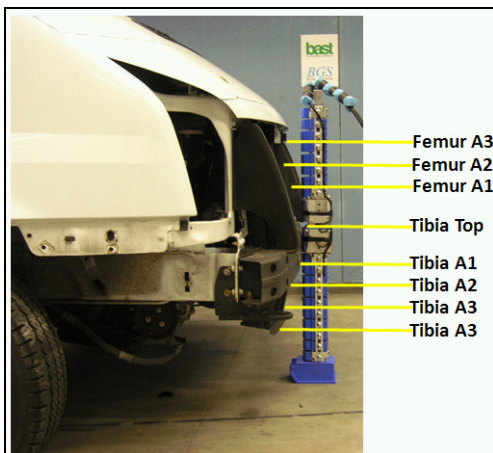


Figure 5. Load paths of FFV frontend in relation to Flex-GT measuring items at 75 mm impact height (baseline test setup).

SEDAN TESTS

Testing

A test series with the Flex-GT with and without upper body mass (UBM) had previously been carried out against a sedan shaped vehicle by Zander et al (2009-2). It was found that testing the standard impactor at an increased impact height that is foreseen for GTR phase 2 requirements cannot entirely compensate for the effects of an UBM. The quality of test results with UBM was recommended to be investigated further. Therefore, a series of full scale tests with the Flex-GT applied to a Hybrid II dummy with pedestrian pelvis at the identical impact location were meant as means of validation of the UBM tests.



Figure 6. Sedan against Flex-GT-HII test.

Test results and analysis

Three full scale tests with the sedan shaped vehicle against a Hybrid II dummy with Flex-GT have been performed at a lateral position of 51 mm from the vertical longitudinal midplane. Those tests have been compared to the previously conducted baseline tests with the Flex-GT at 25 and 75 mm impact height and the tests with the Flex-GT UBM. The peak femur bending moment results of all twelve tests are shown in figure 7.

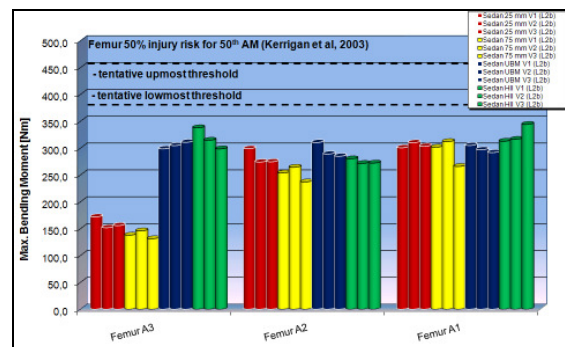


Figure 7. Femur bending moment results of Sedan tests.

In terms of peak results of the femur segments A3 and A2 the full scale tests confirmed the results acquired by the tests with the Flex-GT-UBM. Especially in segment A3 the results with applied UBM or dummy torso are significantly higher than without any additional mass. On the other hand, the increase of the impact height from 25 mm to 75 mm did not show any clear effect on the results. For femur A1, which is the section closest to the knee and the mid load path of the sedan, all results were in a comparable range.

The quite repeatable time history curves for femur segment A3 show that besides the significantly higher peak values for the FlexPLI with UBM or attached to the dummy torso the characteristics of the corresponding traces are completely different to the ones without additional mass (figure 8). In the tests with additional mass the duration of the main impact is much higher. On the other hand, an effect of the increased impact height within the tests with the unloaded legform is not mirrored by the corresponding curves.

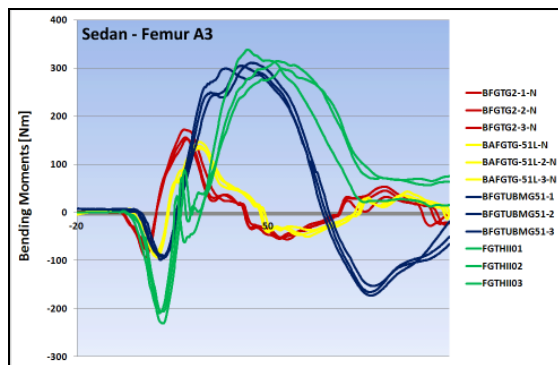


Figure 8. Time history curves for femur A3 bending moments in Sedan tests.

The time history curves for femur A2 and A1 as well as all other diagrams not presented in the main text can be found in the appendix.

Figure 9 shows the peak tibia bending moment results.

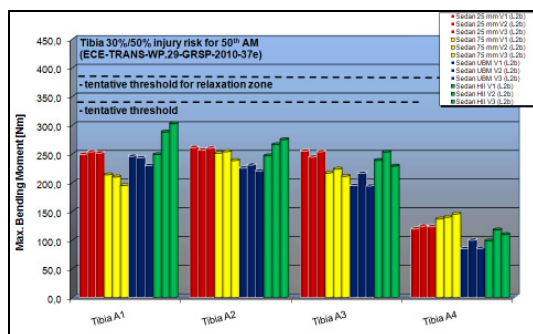


Figure 9. Tibia bending moment results of Sedan tests.

In all tests the sedan vehicle passes the tentative threshold values foreseen within the GTR and ECE regulations on pedestrian safety, while the tibia section shows the highest results on segment A1 when additionally attached to the Hybrid II torso. Under application of a torso mass the loadings on the tibia segments are consistently higher than with UBM. For the segments closest to the knee section, the application of an upper body mass or pedestrian torso does not show a consistent effect. With increased distance from the knee and vehicle mid load path the mass effect becomes more obvious in terms of lower maximum values (tibia A4). The corresponding time history curves put these observations into perspective. All traces show a relatively comparable behavior, even though the impact in tests with additional mass is higher.

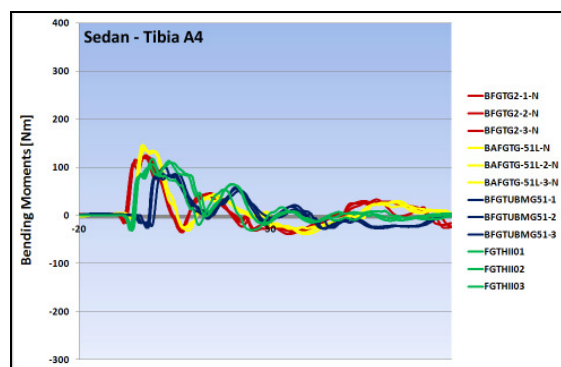


Figure 10. Time history curves for tibia A4 bending moments in sedan tests.

Altogether, the additional mass effect on most of the segments was proved to be not that high.

Regarding the knee elongations the influence of an additional mass are most obvious for the medial collateral ligament (MCL). Here, the peak values with UBM and dummy torso, both exceeding the tentative threshold values for legislation, are very similar. The mass effect can also be seen for PCL while for ACL the results with applied dummy were higher than the remaining ones, latter ones all in a comparable range.

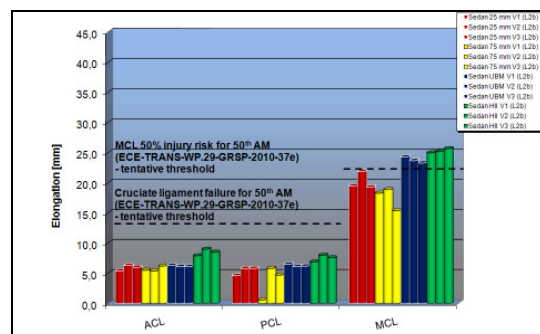


Figure 11. Knee elongation results of Sedan tests.

As for most of the femur and tibia segments, also the time history curves of MCL for legform with both UBM and dummy torso show different characteristics than the traces for the unmodified Flex-GT. Again, as shown in figure 12, the impact duration is significantly longer.

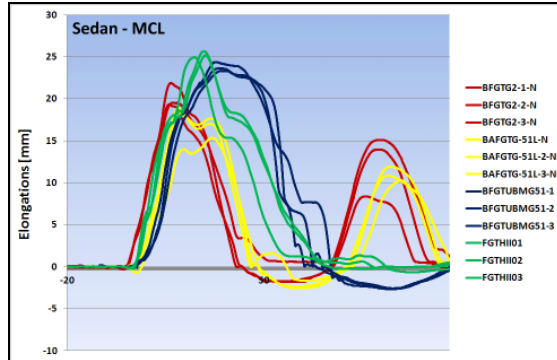


Figure 12. Time history curves for MCL elongations in Sedan tests.

SUV TESTS

Testing

As with the sedan, the Flex-GT attached to the pelvis of a Hybrid II dummy was tested three times within full scale tests against an SUV shaped vehicle. The aimed impact location in all tests was at a lateral position of 128 mm from the vertical longitudinal midplane.



Figure 13. SUV against Flex-GT-HII test.

Test results and analysis

The results of the full scale tests were compared to impactor tests with the Flex-GT at legislative impact height and tests with Flex-GT and applied UBM carried out by Bovenkerk et al (2009). Figure 14 shows an overview of the peak femur bending moment results in all tests.

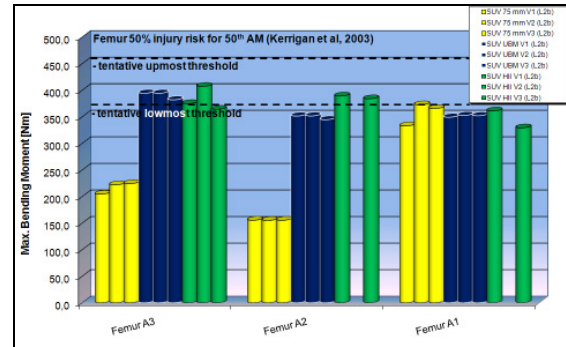


Figure 14. Femur bending moment results of SUV tests.

The tendency that had been observed during the sedan tests becomes much more obvious within the tests with the SUV representative. For tibia segments A3 and A2 the peak results with applied UBM or dummy torso are significantly higher than with the unmodified FlexPLI. At femur A1, the additional mass effects on the maximum loadings cannot be observed.

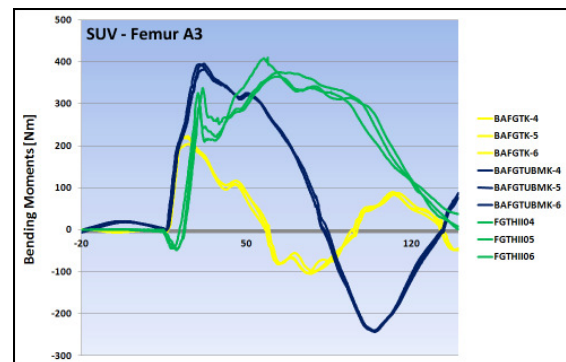


Figure 15. Time history curves for femur A3 bending moments in SUV tests.

Besides of a high repeatability, the time history curves show the different characteristics of the traces caused by the particular test setups. Figure 15 illustrates the characteristics for femur segment A3. Here, the dummy tests show a behavior different from the component tests with and without UBM. The impact duration for the full scale tests is the longest one, followed by the UBM tests.

The peak tibia bending moment results are given in figure 16. In tibia segments A1 and A2 the application of the additional UBM or dummy torso leads to significantly higher results. The influence decreases with an increasing distance between the segments and the impactor knee. At tibia A4, all maximum results are within the same range.

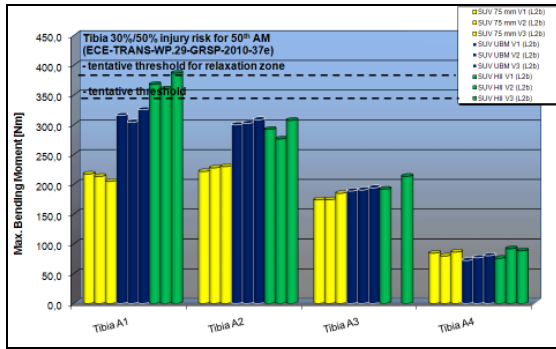


Figure 16. Tibia bending moment results of SUV tests.

The time history curves for tibia A1 (figure 17) underline different characteristics of tests with the unmodified impactor and tests with additional mass. Latter ones show a comparable behavior. Furthermore, the duration of impact in the full scale tests is the longest one, followed by the component tests with UBM.

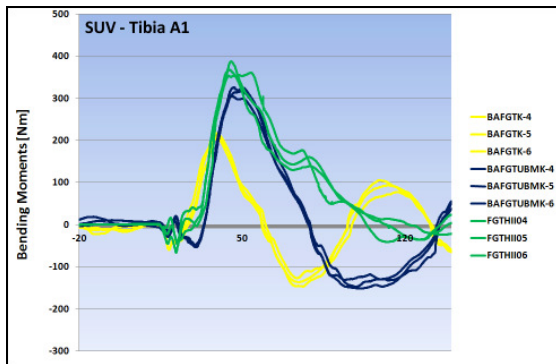


Figure 17. Time history curves for tibia A1 bending moments in SUV tests.

The significant effects of an additional mass within component and full scale tests on the knee elongation peak values are illustrated in figure 18.

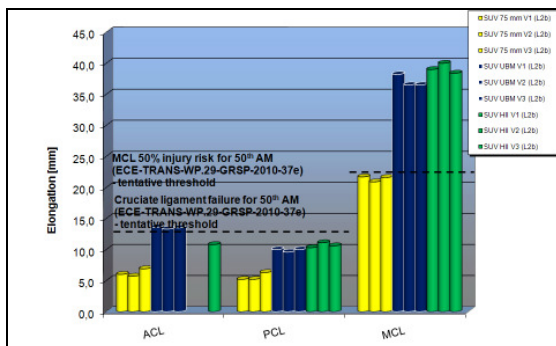


Figure 18. Knee elongation results of SUV tests.

In terms of the medial collateral ligament, the application of an additional mass leads to almost a duplication of the peak results when being

compared to the component tests conducted with the unmodified legform. For the cruciate ligaments (ACL and PCL), the effect is still obvious. The time history curves stress the observations made for the sedan tests. The traces show a good repeatability.

The impact duration of the tests with additional mass is significantly longer than within the component tests without unmodified legform, as shown in figure 19 for the elongations of MCL.

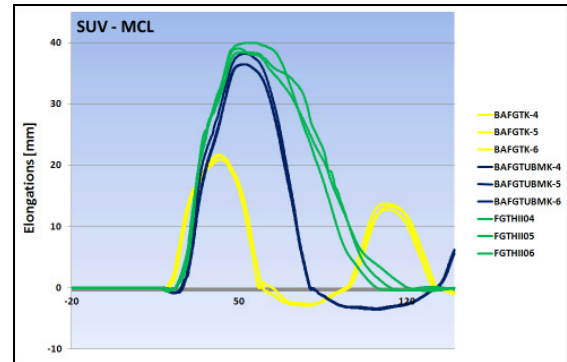


Figure 19. Time history curves for MCL elongations in SUV tests.

However, until achieving their maximum, the characteristics of the time history curves are quite alike. Most differences occur during the rebound phase. Figure 19 demonstrates this phenomenon for tests against the SUV representative.

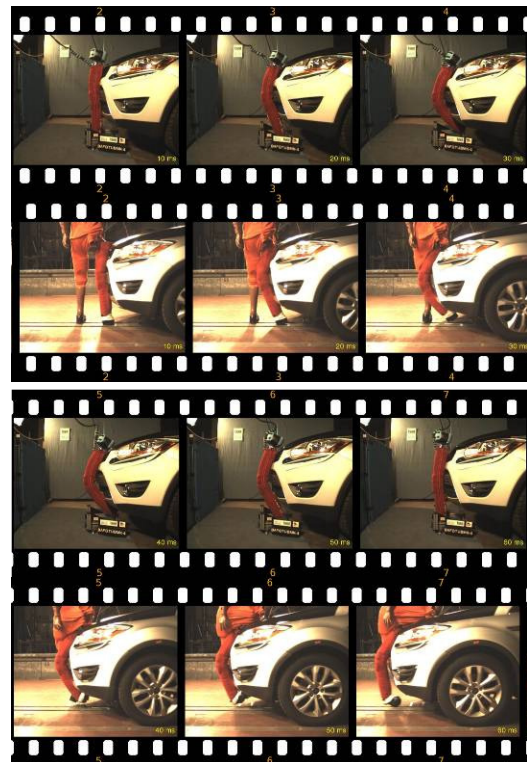


Figure 20. Flex-GT kinematics in tests with UBM and full scale tests against SUV.

FFV TESTS

Testing

To cover a broader range of vehicle frontends, the test series comprising of component tests with unmodified and UBM loaded legform and full scale tests has been amended by tests against a flat front vehicle representative. The impact location in all three tests was located on the vertical longitudinal midplane of the vehicle.



Figure 21. FFV against Flex-GT-HII test.

In addition to the acquisition of femur and tibia bending moments and knee elongations, two uniaxial accelerometers were applied to the lowest femur segment of the legform and to the knee bottom section at the accelerometers' position of the Flex-GTR, both at the non-struck side of the legform, to obtain additional information about potential injury causing parts (figure 22).

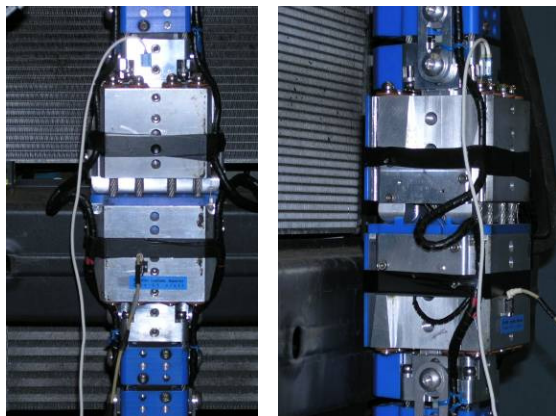


Figure 22. Location of knee bottom and femur bottom (knee top) accelerometers.

Figure 23 shows the peak femur bending moment results acquired in the three tests. As already observed within the tests with sedan and SUV, the peak results for the upper femur segments are significantly higher with applied UBM or dummy torso. In case of the FFV this statement is also valid for the remaining femur segments. Here, the higher

the distance to the knee of the legform and the bumper crossbeam of the vehicle, the higher the difference of the peak values.

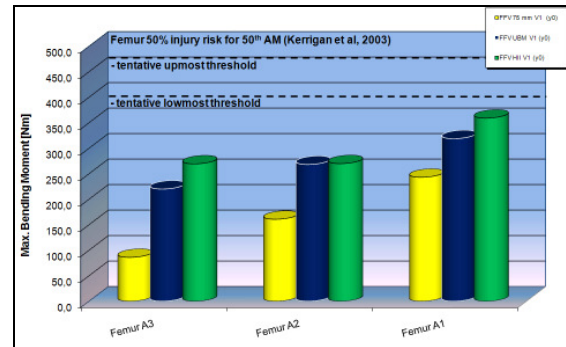


Figure 23. Femur bending moment results of FFV tests.

On the other hand, the characteristics of the particular time history curves are not comparable to each other. Even though the impact duration once again is longer in both tests with applied additional mass (UBM or dummy torso), the shape of all traces is different in all tests especially for femur segments A3 and A2. When getting closer to the mid load path of the vehicle, the curves become more alike, as it can be seen in figure 24.

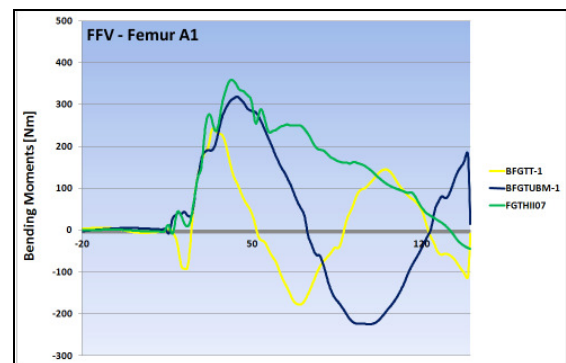


Figure 24. Time history curves for femur A1 bending moments in FFV tests.

Referring to the peak values, the tibia results show a reverse trend (figure 25). Both tests with additional mass give a slightly lower output than the baseline component test with unmodified impactor. Apparently, the mass leads to a shifted energy application of the tibia segments in comparison to the baseline test setup.

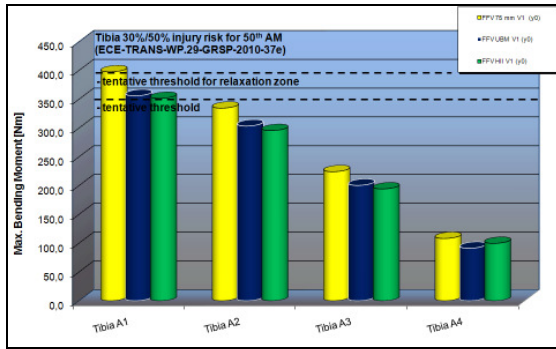


Figure 25. Tibia bending moment results of FFV tests.

Even though the impact duration in the tests with additionally loaded impactor is longer than in the test with baseline setup, the characteristics of the traces are more alike between the two component tests, as shown in figure 26 for tibia A1.

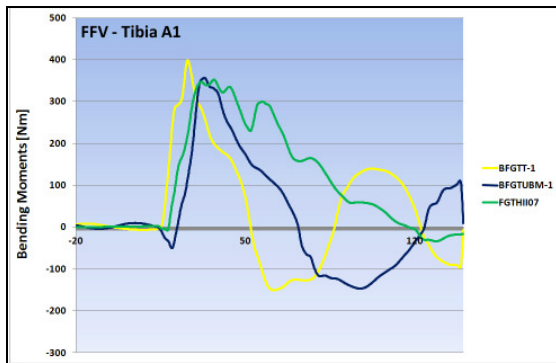


Figure 26. Time history curves for tibia A1 bending moments in FFV tests.

Finally, the peak knee elongations given in figure 27 show that the application of the upper body mass in component tests or the attachment of the legform to the dummy torso lead to higher loadings of MCL than in the baseline test. For ACL, no effect can be stated. For PCL, the conclusion remains unclear due to a potentiometer failure during the UBM test. However, no effect on the peak values can be seen in the comparison of the baseline to the full scale test.

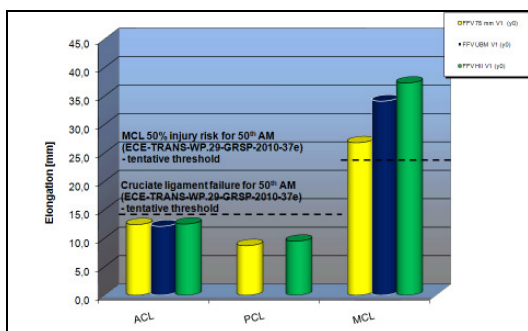


Figure 27. Knee elongation results of FFV tests.

The time history curves of the knee elongations underline the observations made within the analysis of the sedan and SUV tests. The full scale test results in the longest impact duration, followed by the component test with applied UBM. Figure 28 shows the traces for MCL.

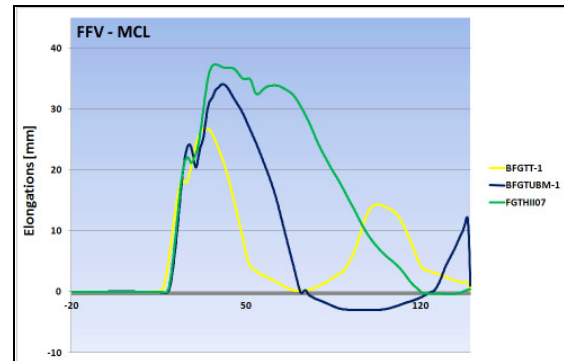


Figure 28. Time history curves for MCL elongations in FFV tests.

In terms of the acceleration signals partly high oscillations could be observed. On the other hand, for vehicles with flat frontends the acceleration of particular segments can give valuable additional information with respect to the loading of the leg during the impact, as illustrated in figure 29 for the test with upper body mass.

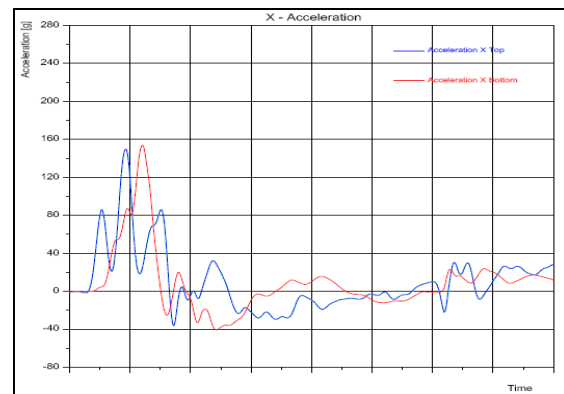


Figure 29. Time history curves for acceleration in FFV UBM test.

The peak accelerations of knee bottom and femur bottom are quite comparable. An effect of the different accelerometer locations on the test results is demonstrated in the baseline test with unmodified Flex-GT (figure 30).

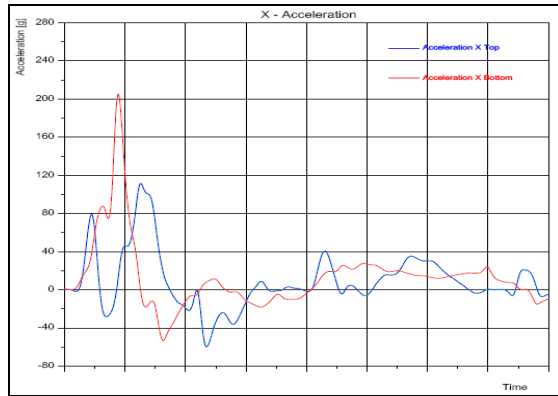


Figure 30. Time history curves for acceleration in FFV baseline test.

Here, the maximum acceleration at the bottom of the knee is significantly higher than at the bottom of the femur. A reason can be found in the alignment of the legform relative to the mid load path of the vehicle which directly impacts the knee bottom section with the bumper beam (see also figure 5). The application of additional accelerometers at the height of the main vehicle load paths therefore seems reasonable.

DISCUSSION

Simulations carried out by Konosu et al. (2007-2) showed that the injury assessment ability of the FlexPLI especially for its tibia section could be improved by modified impact conditions. Those were realized by an increased impact height at 75 mm above ground level. The application of an upper body mass developed by Bovenkerk et al. (2009), based on computer simulations with the THUMS pedestrian model against a large SUV front carried out by Compigne et al. (2009), indicated that the increased impact height of the baseline impactor could not compensate for the lacking torso mass, especially for SUV shaped vehicle frontends as well as the femur and MCL results of the sedan representative. Full scale tests carried out against a modified Hybrid II dummy with attached Flex-GT confirmed the disproportionately higher loading of the legform when tested with additional upper mass. Though the peak results acquired by the UBM tests could be reproduced within the full scale tests, the characteristics of the time history curves are not always in line.

For the tibia section in the sedan tests the results remain heterogeneous. Additional tests with a flat front vehicle representative confirm the tendencies observed within the SUV tests whereas the additional mass leads to slightly lower peak tibia bending moments. This can be explained by the alignment of the bumper beam which directly

impacts the tibia section of the legform in the baseline test.

Besides more realistic impact conditions related to the assessment of tibia and knee injuries, the modified Flex-GT offers for the first time the option of appropriately assessing injuries caused in the femur area. The application of accelerometers to the femur and tibia section can deliver additional information about segments loaded by rigid structures of the vehicle which are not entirely detected by the strain gauges.

CONCLUSIONS

Full scale tests with a sedan and SUV representative against a Hybrid II dummy with attached Flex-GT impactor were meant as validation of impactor tests with Flex-GT and upper body mass. The modified impactor introduces the possibility of femur injury assessment in lateral vehicle-to-pedestrian accidents which are of a high significance in real world vehicle-to-pedestrian accidents. For the SUV category, the impactor peak test results could be confirmed by the full scale tests for all impactor regions. For the sedan, the loadings of femur as well as the knee sections are represented well by the component tests with UBM. For the tibia region, the UBM reveals potential for being further optimized. In terms of the flat front vehicle representative, the UBM seems to be entirely applicable.

Though the maximum loadings of most of the segments are comparable in component tests with UBM and full scale tests, the characteristics of the corresponding traces are not always fully alike and further research is needed in this area. An optimization of the vertical and longitudinal alignment of the upper body mass could be done by additional simulations and component tests. Furthermore, the data basis should be amended by including further real car front shapes. Additionally, the development of transition equations between human model simulations and legform component tests with applied upper body mass for a variety of vehicle frontends representing different vehicle categories could contribute to the optimization of test results towards a realistic injury assessment.

Finally, the application of femur and tibia accelerometers can provide additional information on injury risks not captured by the strain gauges.

ACKNOWLEDGEMENT

The Federal Highway Research Institute (BAST) wants to thank Ford-Werke GmbH for the provision of a vehicle and spare parts, and JARI/JAMA for the loan of the Flex-GT impactor.

REFERENCES

- Bhalla K., Bose D., Madeley N., Kerrigan J., Crandall J. 2003. „Evaluation of the response of mechanical pedestrian knee joint impactors in bending and shear loading.“ Paper no. 429 of ESV conference proceedings.
- Bovenkerk J., Zander O. 2009. “Evaluation of the extended scope for FlexPLI obtained by adding an upper body mass.” Deliverable D333H of the European FP6 research project on Advanced Protection Systems (APROSYS).
- Compigne S., Martinez L. 2009. “New or improved test methods to address lower and upper leg impacts.” Deliverable D333B of the European FP6 research project on Advanced Protection Systems (APROSYS).
- Deutsche Industrie Norm DIN 33402-2. 2005. “Ergonomics – Human Body Dimensions – Part 2: Values.”
- Ivarsson J., Lessley D., Kerrigan J., Bhalla K., Bose D., Crandall J., Kent R. 2004. „Dynamic response corridors and injury thresholds of the pedestrian lower extremities.“ IRCOBI conference proceedings.
- Japan Automobile Manufacturers Association (JAMA) Pedestrian Safety WG. 2009. “Injury Criteria for Tibia - JAMA Proposal“ Doc TEG-084 of 8th Meeting of the GRSP Flex PLI Technical Evaluation Group. Cologne, May 19th.
- Japan Automobile Manufacturers Association (JAMA) Pedestrian Safety WG. 2009-2. “Injury criteria for Flex-GTR MCL and Tibia - JAMA Proposal.“ Doc TEG-097 of 8th Meeting of the GRSP Flex PLI Technical Evaluation Group. Cologne, May 19th.
- Kerrigan J., Bhalla K., Madeley N., Funk J., Bose D., Crandall J. 2003. „Experiments for establishing pedestrian-impact lower limb injury criteria.“ SAE World Congress, SAE paper no. 2003-01-0895
- Konosu A., Ishikawa H., Tanahashi M. 2001. „Reconsideration of injury criteria for pedestrian subsystem legform test - problems of rigid legform impactor -.“ Paper no. 01-S8-O-263 of ESV conference proceedings.
- Konosu A. 2004. “Discussion on injury threshold for pedestrian legform test.” Doc. INF/GR/PS/82 of 6th Meeting of the GRSP Informal Group on Pedestrian Safety. Paris, February 24th-26th.
- Konosu A., Issiki T., Suzuki H. 2007. “Information on Flexible Pedestrian Legform Impactor Type GT (Flex-GT).” Doc TEG-033 of 4th Meeting of the GRSP Flex PLI Technical Evaluation Group. Bergisch Gladbach, April 2nd.
- Konosu A., Issiki T., Tanahashi M., Suzuki H. 2007-2. “Development of a biofidelic flexible pedestrian legform impactor Type GT (Flex-GT).” Paper no. 07-0178 of 20th ESV conference proceedings.
- Nyquist G., Cheng R., El-Bohy A., King A. 1985. “Tibia bending: strength and response.” Proceedings of the 29th Stapp Car Crash Conference, SAE paper no. 851728.
- United Nations Economic Commission for Europe. 2010-1. “Proposal for Amendment 2 to global technical regulation No. 9 (Pedestrian safety).” ECE/TRANS/WP.29/GRSP/2010/37
- United Nations Economic Commission for Europe. 2010-2. “Amendments agreed to ECE/TRANS/WP.29/GRSP/2010/37 during the 48th session of GRSP.” GRSP-48-41
- United Nations Economic Commission for Europe. 2010-3. “Proposal for the 01 series of amendments to draft Regulation on pedestrian safety.” GRSP-48-09-Rev.1
- Zander O. 2009. “Flex-GTR: Proposal for Tibia Bending Moment Injury Threshold.” Doc TEG-098 of 8th Meeting of the GRSP Flex PLI Technical Evaluation Group. Cologne, May 19th.
- Zander O., Gehring D., Leßmann P., Bovenkerk J. 2009-2. “Evaluation of a flexible pedestrian legform impactor (FlexPLI) for the implementation within legislation on pedestrian protection.” Paper no. 09-0277 of 21st ESV conference proceedings.
- Zander O. 2009-3. “Flex-GTR: Proposal ACL/PCL and MCL injury thresholds.” 9th Meeting of the GRSP Flex PLI Technical Evaluation Group. Bergisch Gladbach, September 3rd-4th.
- Zander O. 2010. “Flex-GTR: Proposal for ACL/PCL Injury Threshold.” Doc TEG-130 of 11th Meeting of the GRSP Flex PLI Technical Evaluation Group. Bergisch Gladbach, April 21st.
- Zander O. 2010-2. “Status of the introduction of the FlexPLI within regulations on pedestrian protection.” Proceedings of 5th Praxiskonferenz Fußgängerschutz.

APPENDIX

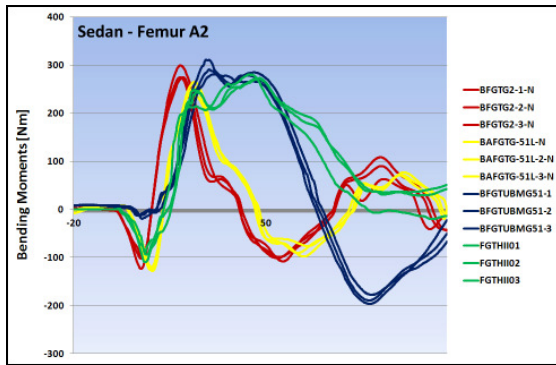


Figure 31. Time history curves for femur A2 bending moments in Sedan tests.

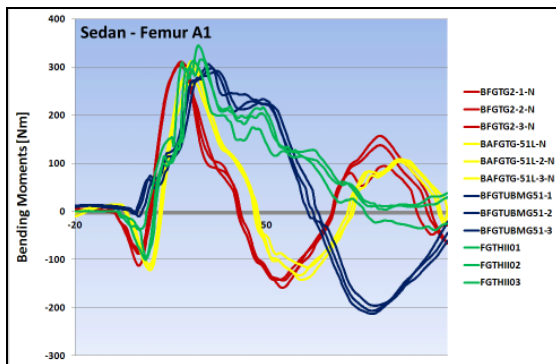


Figure 32. Time history curves for femur A1 bending moments in Sedan tests.

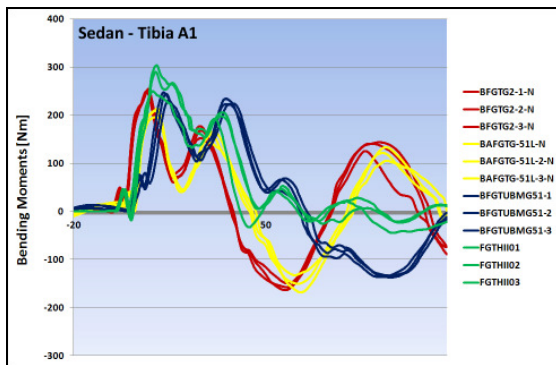


Figure 33. Time history curves for tibia A1 bending moments in Sedan tests.

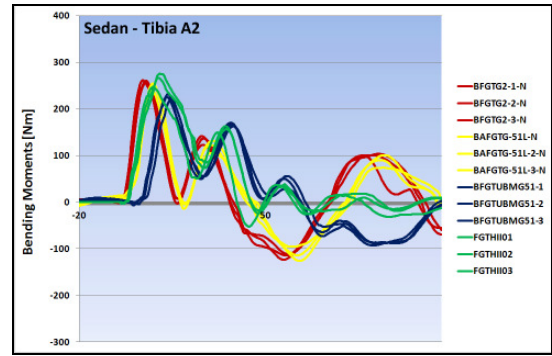


Figure 34. Time history curves for tibia A2 bending moments in Sedan tests.

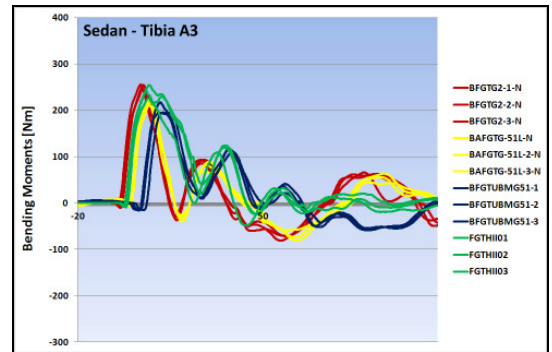


Figure 35. Time history curves for tibia A3 bending moments in Sedan tests.

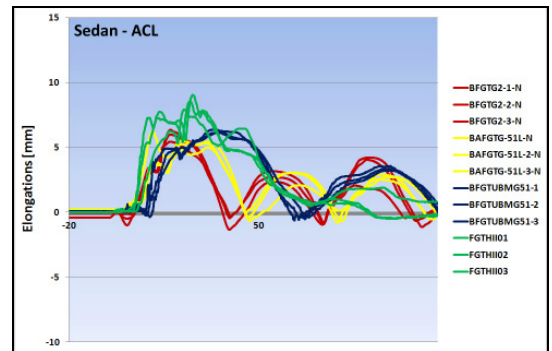


Figure 36. Time history curves for ACL elongations in Sedan tests.

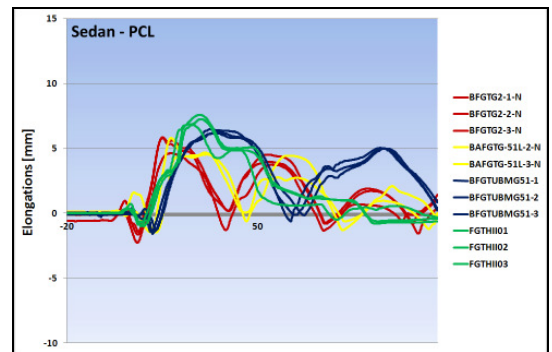


Figure 37. Time history curves for PCL elongations in Sedan tests.

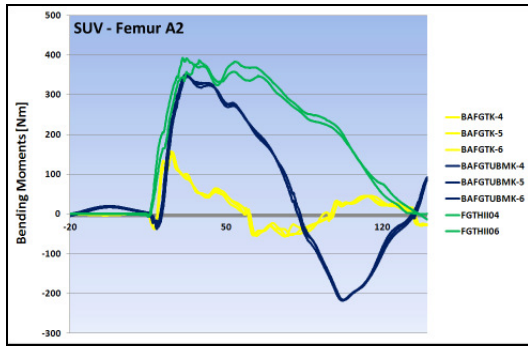


Figure 38. Time history curves for femur A2 bending moments in SUV tests.

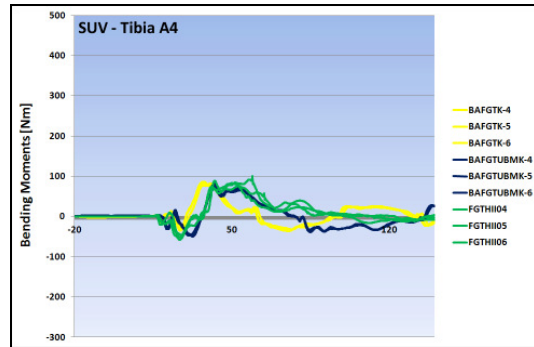


Figure 42. Time history curves for tibia A4 bending moments in SUV tests.

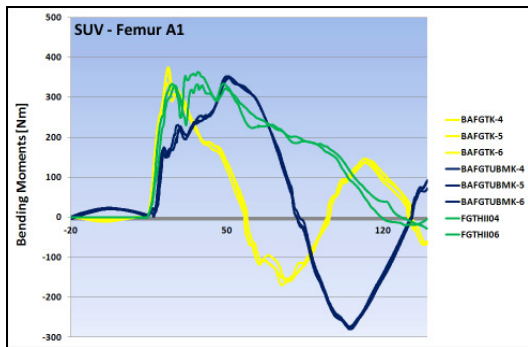


Figure 39. Time history curves for femur A1 bending moments in SUV tests.

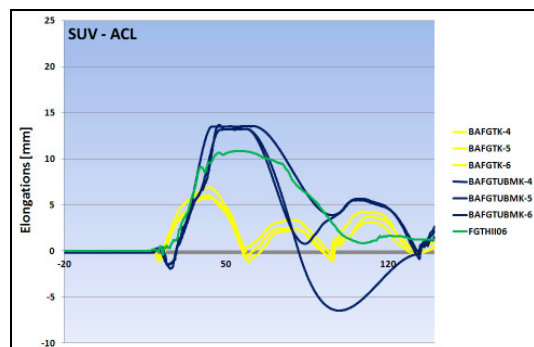


Figure 43. Time history curves for ACL elongations in SUV tests.

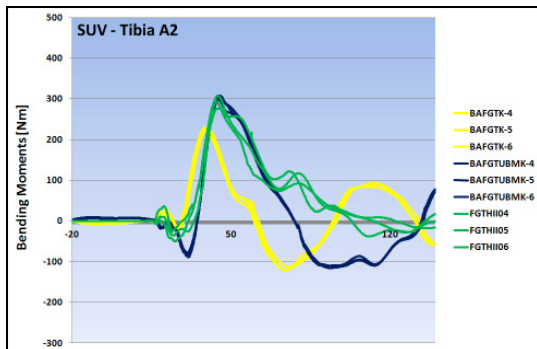


Figure 40. Time history curves for tibia A2 bending moments in SUV tests.

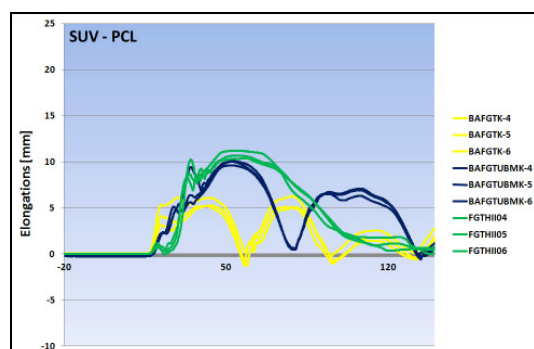


Figure 44. Time history curves for PCL elongations in SUV tests.

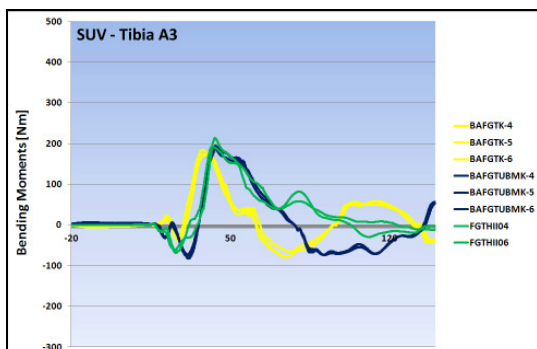


Figure 41. Time history curves for tibia A3 bending moments in SUV tests.

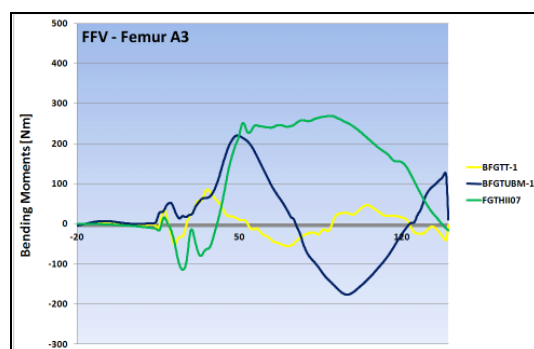


Figure 45. Time history curves for femur A3 bending moments in FFV tests.

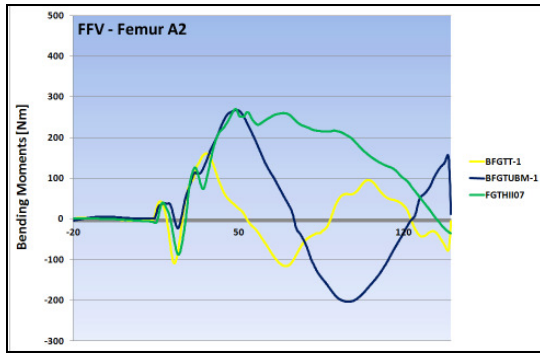


Figure 46. Time history curves for femur A2 bending moments in FFV tests.

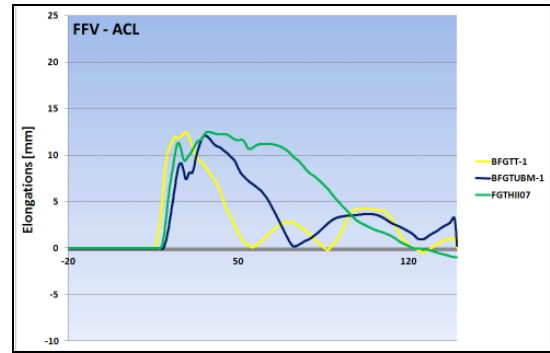


Figure 50. Time history curves for ACL elongations in FFV tests.

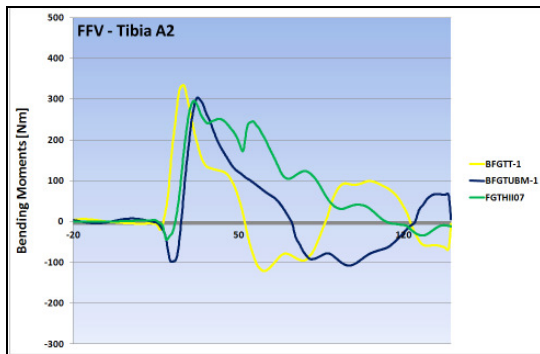


Figure 47. Time history curves for tibia A2 m bending moments in FFV tests.

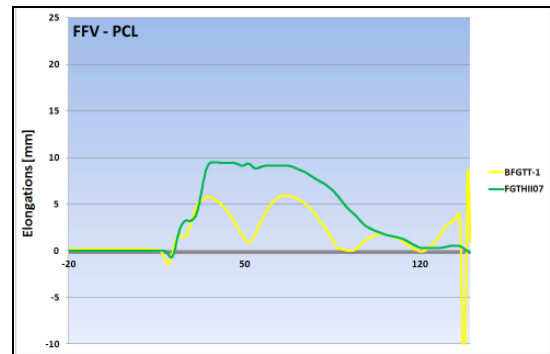


Figure 51. Time history curves for PCL elongations in FFV tests.

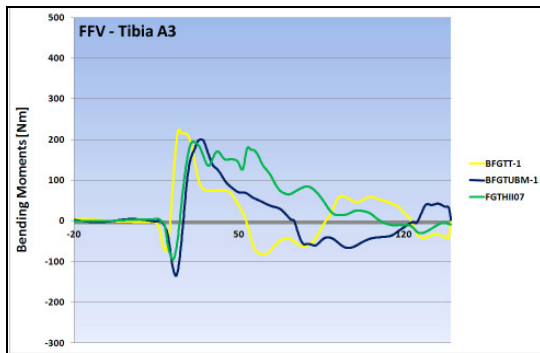


Figure 48. Time history curves for tibia A3 bending moments in FFV tests.

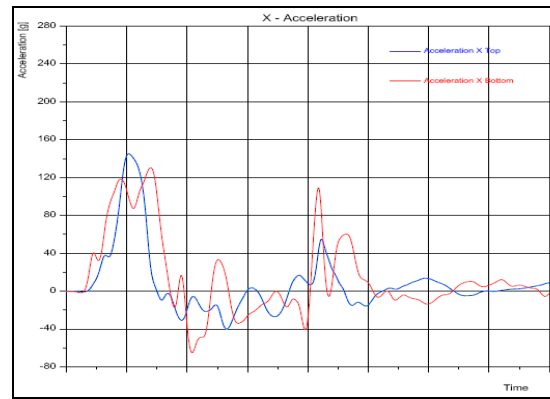


Figure 52. Time history curves for acceleration in FFV full scale test.



Figure 49. Time history curves for tibia A4 bending moments in FFV tests.

THE FLEXIBLE PEDESTRIAN LEGFORM IMPACTOR AND ITS IMPACT ON VEHICLE DESIGN



Thomas Kinsky
Dr. Flavio Friesen
Benjamin Buenger

Adam Opel AG / General Motors Europe Engineering
Germany

Paper Nr. 11-0328

ABSTRACT

In Japan, a new legform impactor for pedestrian protection testing has been developed during the past 10 years. This legform is called “Flexible Pedestrian Legform Impactor” (FlexPLI). Compared to the existing legform currently used in Europe, the FlexPLI is intended by its developers to better reflect the behavior of a human leg during an impact with a vehicle. In addition to a more humanlike knee section, the new impactor provides for the possibility to also assess injuries of the pedestrian's tibia.

In the first development phase, the legform was considered to be very biofidelic but testing robustness was limited. In its further development, the impactor was modified to better address the needs of a certification tool: The latest version of the legform is more robust than pre-versions, the handling is acceptable, the repeatability of test results seems to be acceptable and the legform fits into the current sub-system test scenario of the global technical regulation (gtr) No 9 on pedestrian safety.

Common vehicle designs use a forward-moved lower structure of the bumper as a load path to reduce the knee bending. However, these structures may cause higher strains in the tibia area of the FlexPLI (and consequently may indicate a risk for tibia injuries in real-world accidents). Therefore, for many vehicles the bumper systems designed to meet the requirements for the lower legform currently used in Europe will need to be redesigned to fulfill the FlexPLI targets.

Nevertheless, the FlexPLI has already been proposed to be used as certification tool in gtr No 9. The study presented below provides first results of tests in a manufacturer's lab with different vehicles of different categories and identifies general concepts for optimization towards FlexPLI requirements' fulfillment. The intention of this paper is to summarize the experiences gained for use as information for future vehicle developments.

DEVELOPMENT OF THE FLEXIBLE PEDESTRIAN LEGFORM IMPACTOR

About 10 years ago, experts of the Japan Automobile Research Institute (JARI) and of the Japan Automobile Manufacturers' Association (JAMA) presented a new legform impactor for pedestrian safety testing. The new legform is called “Flexible Pedestrian Legform Impactor” (FlexPLI).

The European legform impactor was never widely accepted in Japan. During the development of the first impactor and the respective test procedures, the experts of the European Experimental Vehicle Committee (EEVC; later renamed to European Enhanced Vehicle-Safety Committee) decided to prioritize knee ligament injuries while possible bone fractures were to be evaluated via the acceleration of the legform. However, a detailed assessment of fractures of the long bones was not intended [1].

Several pedestrian safety experts, especially the experts of Japan, pointed out that the design of the EEVC legform impactor with its rigid upper and lower part cannot simulate the human lower extremities' motion properly. Also, according to the Japanese experts the EEVC impactor may mislead the protection for the pedestrians' lower extremities since an injury assessment of the lower part of the leg is not possible [2]. Approximately 3 to 4 years ago, Japanese experts presented additional analyses of the Japanese accident statistics showing that around 87 % of all leg injuries were tibia fractures [3]. The missing ability of the EEVC Lower Legform Impactor (EEVC LFI) to assess fractures of the pedestrians' lower extremities in detail was the main reason for Japan to develop their new legform impactor.

During the past 10 years, the FlexPLI had been presented in different build levels: version 2000, version 2002/2003, version 2004, version G, version GT and version GTR. For the later versions, which were thought to be close to a final design, additional prototypes were presented. They were referred to as version xx alpha (or xx α). To improve robustness and reliability of the tool itself, repeatability of test results,

handling of the impactor etc., the impactor was modified significantly during the development process. The latest build level, FlexPLI version GTR (or Flex-GTR), has been available in its production version since early 2010. However, the manufacturer of the legforms still applies additional modifications during the current production to achieve further improvements and especially to be able to meet the agreed corridors for the impactors' certification [4].

COMPARISON OF THE EEVC LOWER LEGFORM IMPACTOR AND THE FLEXIBLE PEDESTRIAN LEGFORM IMPACTOR

The EEVC LFI is often referred to as “WG17 impactor” according to the EEVC working group responsible for the development of the impactor or as “TRL impactor” according to the company that had finalized the design and is merchandising the impactor now. It mainly consists of two stiff metal tubes, two deformable knee elements made of steel and a shear-spring system with a hydraulic damper (see figure 1). The two stiff metal tubes represent the femur and the tibia of a human leg. The deformable knee elements represent the human knee, specifically the ligaments, with the ability to withstand a certain bending. The metal “ligaments” are used to assess possible knee injuries. The shear-spring system simulates lateral shear displacement between femur and tibia at the knee level; the damper is necessary to limit vibrations caused by the mass of the shear-spring system. An accelerometer is used to indirectly measure the contact force applied to the tibia, representing a provisional assessment of the risk of bone fractures. For testing, the legform is covered with a 25 mm thick foam layer and a 6 mm neoprene skin, together representing the human's flesh and skin (see figure 2) [5].

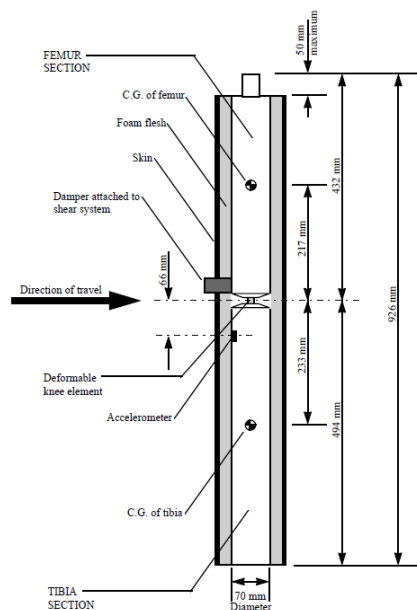


Figure 1. Design of the EEVC Lower Legform Impactor [6]



Figure 2. Photograph of the EEVC LFI without and with flesh and skin simulation [7]

The FlexPLI consists of a femur and a tibia, which are composed of bone cores made of fiber glass, and several nylon segments attached to them. The overall design of femur and tibia represents the human bones and their ability to be bent. Strain gauges, glued to the fiber glass core, are used to measure the bending moments at the different segments and thereby assess the risk of bone fractures. The knee element consists of two complex blocks, where string potentiometers assess the risk of ligament injuries (see figure 3).

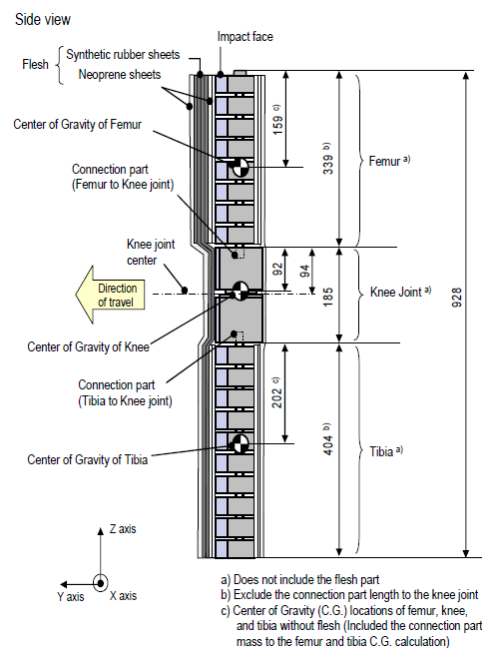


Figure 3. Design of the FlexPLI version GTR [8]

Human skin and flesh are formed by several layers of rubber and neoprene sheets. To closer follow the geometry of a human leg, the number of layers is different for femur, knee and tibia [8].

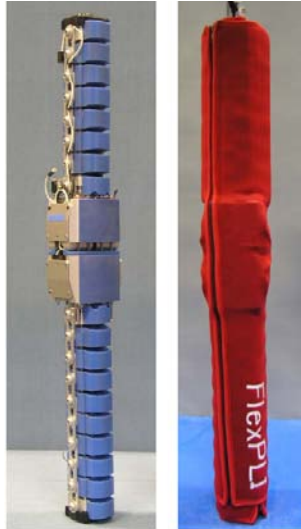


Figure 4. Photograph of the FlexPLI version GTR without and with flesh and skin simulation [9]

The EEVC LFI is a simplified design, approximately representing the human leg with the intention to measure specific loads at limited locations. In contrast, the FlexPLI especially in its earlier versions had been designed simulate the biomechanical behavior of a human leg when being impacted by a vehicle (see figure 5).



Figure 5. Principle behavior of the EEVC LFI compared to the FlexPLI

However, one compromise regarding biofidelity at the knee of the FlexPLI was necessary: The element is designed almost symmetrically, whereas the human legs have a mirrored position of the ligaments. This

was necessary to allow one single impactor to be used for vehicle testing and to avoid the necessity of using a right hand and a left hand legform impactor separately.

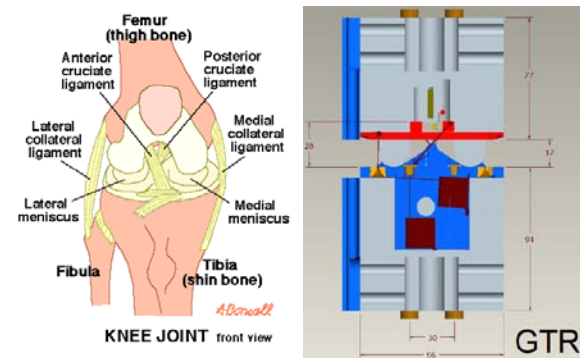


Figure 6. Comparison of a schematic view of the (right leg's) human knee joint [10] and a CAD drawing of the FlexPLI knee element [11]

In addition to the knee section with its improved biofidelity compared to the EEVC LFI (see figure 7), the FlexPLI provides for the possibility to assess injuries to the pedestrian's tibia in detail. For research purposes the FlexPLI may be equipped with up to 32 measurement channels recording e.g. the loads to the femur and the detailed motion of tibia and femur [11].

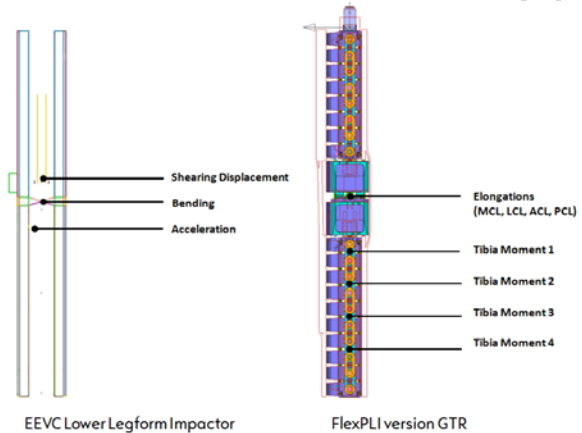


Figure 7. Comparison of the measurement abilities of the EEVC LFI and the FlexPLI as proposed for regulatory purposes

During first development phases, the FlexPLI had restrictions regarding its use as a test tool, e.g. a limited robustness. As mentioned, this improved significantly during the several development steps of the impactor. From the beginning, the legform had been designed to fit into the sub-system test scenario as it is currently standard for pedestrian protection in regulatory and consumer testing. Japan therefore proposed to use the FlexPLI for the pedestrian safety testing according to the grt No 9 [12].

TESTING OF DIFFERENT BUMPER CONCEPTS WITH BOTH LEGFORM IMPACTORS

During the development of the different FlexPLI build levels, the automobile industry had frequently impacted vehicles to assess the legform as a test tool. Tests were conducted by manufacturers in joint projects of the European Automobile Manufacturers' Association (ACEA) with partners or on their own. Usually, existing serial production vehicles were used for these trials. Those vehicles often have protruding lower structures of the bumpers as support to initiate rotation of the legform, which is necessary to meet existing regulatory and consumer testing requirements. Such devices are often referred to as "lower bumper stiffeners" (LBS). An LBS helps reducing the knee bending and therefore limits the knee loads.

However, test results indicated that bumper concepts with protruding LBS's may create high peaks in the tibia bending moment of the FlexPLI at the contact position with the LBS and consequently may lead to the risk for tibia injuries in real-world accidents. Therefore the bumper systems designed to meet the EEVC LFI requirements need to be optimized to fulfill the FlexPLI targets.

One question that could not be answered satisfactorily during earlier tests was whether such peaks in the bending moment can be controlled and how existing bumper systems can be modified to meet the injury criteria of the new legform. Trying to find an answer to this question, tests were conducted on-site at Adam Opel AG / General Motors Europe Engineering in late 2010. Three different bumper concepts, which are currently in production, were assessed. The concepts differ in their principle characteristics (see also figure 8):

- Concept A has an LBS with a medium (average) elastic displacement ability. This elastic displacement ability refers to the component characteristics and not to the material properties only. In vehicle x-direction, the offset between the LBS contact surface and the bumper main beam in this concept is relatively small. The force reaction surface of the vehicle front is quite homogenous.
- For concept B, the elastic displacement ability of the LBS is lower, the x-offset between the LBS contact surface and the bumper main beam is medium and the force reaction surface is not homogenous.
- The LBS of concept C shows a medium elasticity, the x-offset between LBS contact surface and the bumper main beam is quite large and the force reaction surface is also quite homogenous.

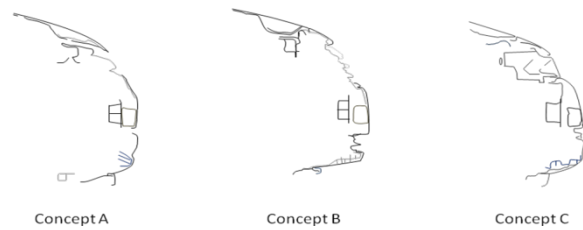


Figure 8. Sketches of different bumper concepts assessed with the FlexPLI in this study

All three concepts were assessed with the FlexPLI version GTR, even though none of the concepts needs to meet any requirements with this new impactor. The impact positions matched earlier tests with the EEVC LFI. Test results from regulatory as well as from consumer metrics tests were available for this impactor, to be evaluated against the new results.

In general, to compare the performances of the different bumper systems, the regulatory limit was considered to be 100 %. According to gtr No 9 [12] these limits for the EEVC LFI are:

- 19 degrees for the maximum dynamic knee bending angle;
- 6 mm for the maximum dynamic knee shearing displacement;
- 170 g for the acceleration measured at the upper end of the tibia.

For the FlexPLI, the limits were used as proposed for the amendments to gtr No 9 [8]. These limits are:

- 22 mm for the maximum dynamic elongation of the medial collateral ligament (MCL);
- 13 mm for the maximum dynamic elongation of the anterior cruciate ligament (ACL) and the posterior cruciate ligament (PCL);
- 340 Nm for the dynamic bending moments at the tibia; a possible relaxation zone as proposed for the gtr No 9 amendment was not considered in the initial assessment.

Values above 100 % consequently would represent an excess of the respective current or proposed regulatory limits. However, it also needs to be noted that, from a manufacturer's point of view, a margin to the pass/fail criterion is applied.

DISCUSSION OF TEST RESULTS

For bumper concept A with its medium (average) elastic displacement ability, the relatively small offset between the LBS contact surface and the bumper main beam plus the homogenous force reaction surface, the shearing and the bending reached around 50 % of the regulatory limits when being tested with the EEVC LFI (see figure 9). The tibia acceleration was slightly above 75 %.

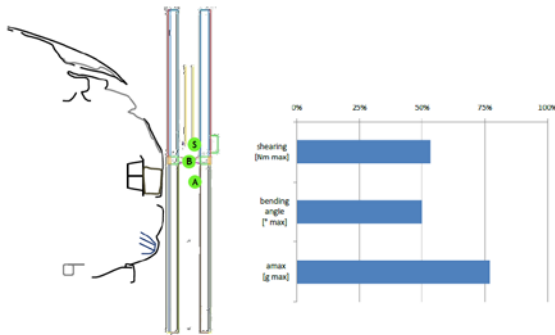


Figure 9. Test results of bumper concept A with the EEVC LFI

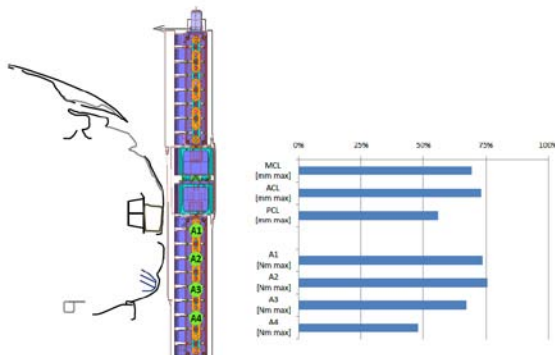


Figure 10. Test results of bumper concept A with the FlexPLI

Testing bumper concept A with the FlexPLI, the knee ligament elongations were close to 75 % for MCL and ACL and around 60 % for the PCL (see figure 10). The tibia bending reached its peak at around 75 % of the proposed regulatory limit at the measurement position 2 where the FlexPLI has the first contact with the bumper surface. The other measurement positions performed with round about 55 % and 75 % respectively of the proposed regulatory limit. In terms of vehicle engineering, concept A would be promising to meet the regulatory limits with both impactors as the characteristics of the respective bumper design seem to be sufficient. However, it needs to be noted that respective loads on the impactor's knee of this bumper concept were significantly lower with the EEVC LFI than with the FlexPLI.

Bumper concept B is characterized by the less elastic displacement ability, the medium offset between the LBS contact surface and the bumper main beam and the in-homogenous force reaction surface. When being tested with the EEVC LFI, this concept produced shearing and bending results well below 50 % but an acceleration of around 80 % of the regulatory limits (see figure 11).

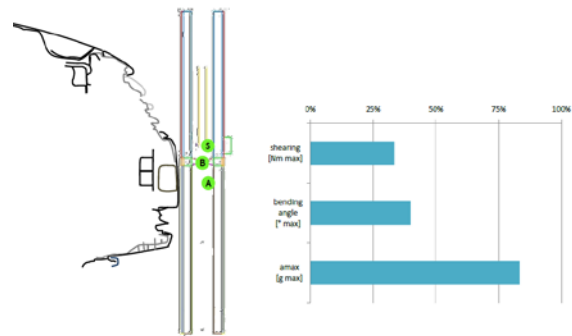


Figure 11. Test results of bumper concept B with the EEVC LFI

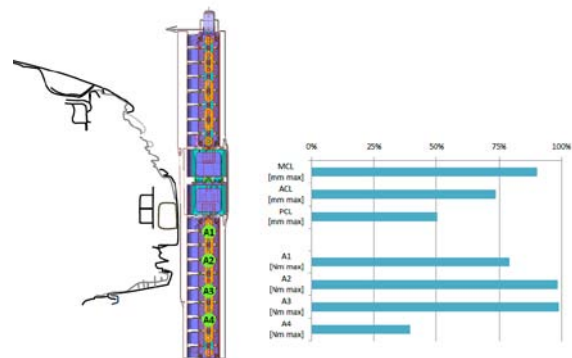


Figure 12. Test results of bumper concept B with the FlexPLI

With bumper concept B, the tibia bending of the FlexPLI was very close to the proposed regulatory limit for two of the four measurement positions. Only the test result at the position without contact to the vehicle surface during impact was well below 50 % of the limit. The elongations of the ligaments were between 50 % and 90 % of the future regulatory limits. From a vehicle engineering perspective, the bumper concept needs an extended review in terms of FlexPLI performance.

Bumper concept C, showing a medium elasticity, a quite large offset between LBS contact surface and the bumper main beam and a quite homogenous force reaction surface, also performed well with the EEVC LFI. The tibia acceleration was around 75 % of the regulatory limit. Shearing and bending were well below 50 % (see figure 13).

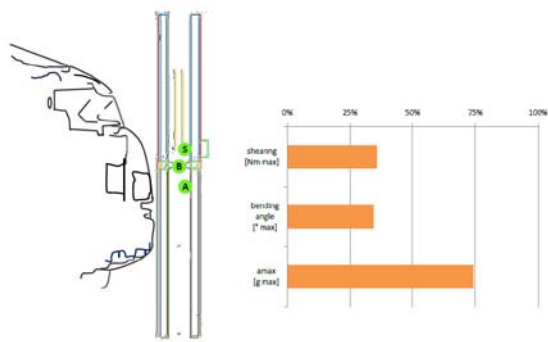


Figure 13. Test results of bumper concept C with the EEVC LFI

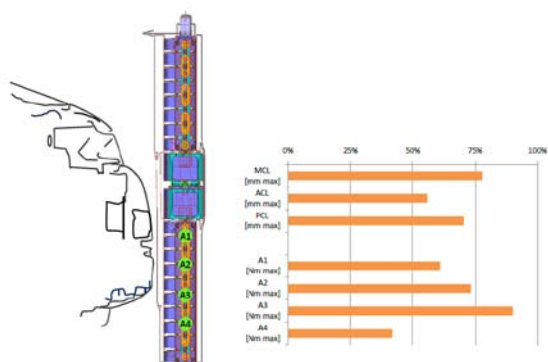


Figure 14. Test results of bumper concept C with the FlexPLI

However, with the FlexPLI this concept was closer to the limits. At the position near the first contact between impactor and bumper fascia, a peak bending moment occurred, reaching almost 90% of the proposed regulatory limit (see figure 14). The lower part of the impactor, without contact with the vehicle surface during the testing, was well below 50 % of the proposed limits. The elongations of the three ligaments were in the range of 55 % and 80 % of the future limits. Generally, the performance of this bumper concept is acceptable for meeting the proposed regulatory limits.

A comparison of the test results above implies that all three bumper concepts already comply with the future regulatory limits as proposed as the gtr No 9 amendments. However additional tuning or even re-design will be necessary to also meet top ratings in expected consumer metrics requirements which usually are more stringent than regulation.

Nevertheless, the bumper systems with a more homogenous reaction surface seem to have conceptual advantages. Also, a certain elasticity of the structure, allowing the FlexPLI to deform the bumper surface, seems to be favorable for meeting the future requirements. The main issues when testing

with the new legform are caused by high levels of stiffness of the LBS's or by large offsets between the LBS contact surface and the bumper main beam in longitudinal vehicle direction. However this was the main intention of the designers of the FlexPLI: to measure the load distribution in the tibia part of the legform in more detail.

Manufacturers may need to find other ways to address this, for example bumper surfaces with multiple force reaction supports. Additionally, design solutions need to control the rotation of the legform in order to avoid increased loads in the knee area and, consequently, to limit the risk of ligament injuries.

The vehicles tested in this study all comply with the current regulatory requirements on pedestrian safety in Europe and in addition have a good performance when being assessed in consumer metrics programs. The results of this study apply to the design characteristics of the three bumper concepts described above but cannot be generalized unconditionally to the variety of concepts existing in the market today.

CONCLUSIONS

Bumper systems that perform well when being tested with the EEVC lower legform impactor do not necessarily have the same performance level with the new Flexible Pedestrian Legform Impactor. However, first test results indicate that today's concepts, engineered to comply with current requirements for the legform tests, may not need to be completely redesigned from sketch or "reinvented" respectively. Generally, measures like a smooth geometry of the vehicle front end with a homogenous reaction surface and a certain elasticity of the bumper structure allowing an elastic displacement of the lower bumper stiffener help to comply with the requirements of the new legform. One focus needs to be on the design of the load paths. Structure and surface elements creating high peaks for the tibia bending moment should be avoided. Structures with multiple load supports are more promising.

However, it needs to be emphasized that the test results discussed above were produced at vehicles that already meet regulatory requirements and furthermore have a good performance in consumer metrics testing. Therefore, those vehicles are well positioned to meet the new requirements.

ACKNOWLEDGEMENTS

The authors would like to thank all team members at Adam Opel AG / General Motors Europe Engineering

that contributed to this study, especially Matthias Erzgraeber for his knowledge and support with all FlexPLI simulation activities.

FREQUENTLY USED ABBREVIATIONS

ACEA	European Automobile Manufacturers' Association
ACL	anterior cruciate ligament
EEVC	European Experimental Vehicle Committee, later renamed to European Enhanced Vehicle-Safety Committee
FlexPLI	Flexible Pedestrian Legform Impactor
gtr	global technical regulation
LBS	lower bumper stiffener
LFI	(Lower) Legform Impactor
MCL	medial collateral ligament
PCL	posterior cruciate ligament

REFERENCES

- [1] Proposal for methods to evaluate pedestrian protection for passenger cars; report of European Experimental Vehicles Committee (EEVC) Working Group 10, November 1994; available at the EEVC website www.eevc.org (13 February 2011)
- [2] Information on the Flexible Pedestrian Legform Impactor (Flex-PLI) from J-MLIT Research; presentation of representative of the Ministry of Land, Infrastructure and Transport, Government of Japan (J-MLIT) at the 7th meeting of the GRSP informal group on pedestrian safety (INF GR PS); Paris, 28 – 30 September 2004; available as document PS/106 at the UNECE GRSP website www.unece.org/trans/main/wp29/meeting_docs_grsp.html (18 February 2011)
- [3] JAMA's Explanation on the Pedestrian Safety GTR Phase 2; presentation at the 148th meeting of the „Technical Committee“ International Automobile Manufacturers Organization OICA; Paris, 14 – 15 October 2008 (internal working document)
- [4] Burleigh, M. (Humanetics): Changes to FlexPLI GTR Since Prototype Built, including BAST estimations of effects; document to the 12th meeting of the FlexPLI Technical Evaluation Group (FlexPLI TEG); Bergisch Gladbach, 2 December 2010; not yet available at the UNECE GRSP website
- [5] Lawrence, G.J.L. (TRL), Hardy, B.J. (TRL): Pedestrian Testing Using the EEVC Pedestrian Impactors; proceedings of the 16th ESV Conference, paper number 98-S10-O-03; Windsor/Canada, 31 May – 4 June 1998
- [6] Improved test methods to evaluate pedestrian protection afforded by passenger cars; report of the European Enhanced Vehicle-Safety Committee (EEVC) Working Group 17, December 1998 with September 2002 updates; available at the EEVC website www.eevc.org (13 February 2011)
- [7] Leßmann, P. (BGS Boehme & Gehring): Die Impaktoren [The impactors]; BGS training material; Bergisch Gladbach, 9 July 2008
- [8] Proposal for amendments to global technical regulation No. 9, submitted by the expert from Japan; document number ECE/TRANS/WP.29/GRSP/2010/2) for the 47th session of the UNECE Working Party on Passive Safety (GRSP); Geneva, 17 – 21 May 2010; available at the UNECE GRSP website www.unece.org/trans/main/wp29/meeting_docs_grsp.html (18 February 2011)
- [9] Gehring, D.-U. (BGS Boehme und Gehring), Leßmann, P. (BGS Boehme und Gehring), Zander, O. (BAST): Enhanced Requirements For Front Ends Due To The New Test Regulations For Pedestrian Protection; proceedings of the crash.tech 2010 Conference “Vehicle Safety 2020”; Leipzig, 13 – 14 April 2010
- [10] Knee joint front view; image in article “knee joint definition” at the website www.emedicinehealth.com (18 February 2011)
- [11] B. Been (FTSS Europe): Design Freeze Status, FlexPLI-GTR Development, Mechanical Design; presentation at the 6th meeting of the FlexPLI Technical Evaluation Group (FlexPLI TEG); Bergisch Gladbach, 31 March 2008; available as document TEG-054-Rev.1 at the UNECE GRSP website www.unece.org/trans/main/wp29/meeting_docs_grsp.html (18 February 2011)
- [12] Global technical regulation No 9: Pedestrian Safety, Established in the Global Registry on 12 November 2008; available at the UNECE WP.29 website www.unece.org/trans/main/wp29/wp29wgs/wp29gen/wp29age.html (15 March 2010)

REVIEW OF THE EURO NCAP UPPER LEG TEST

Nils Lubbe

Toyota Motor Europe, Belgium

Hiromi Hikichi

Hiroyuki Takahashi

Toyota Motor Corporation, Japan

Johan Davidsson

Chalmers University of Technology, Sweden

Paper Number 11-0137

ABSTRACT

The EEVC WG17 upper leg test as used in Euro NCAP was reviewed. Previous work revealed shortcomings of the EEVC WG17 test set-up. Recent published accident data show that injuries to the lower extremities by the bonnet leading edge, not including ground impacts, only accounted for 5% of all AIS2+ injuries and 4% of all AIS3+ injuries. Previous work and this data indicate a discrepancy in importance of the upper leg test between Euro NCAP and real-life injury frequencies.

Suggested legform impactor threshold values have so far not been based on human injury risk transferred to impactor values. The implications of the proposed improvements to the test set-up from Snedeker et al. (2005) for Euro NCAP test results have not been assessed. Both the above issues are aimed at in this study. They are important as only with the right targets and evaluation methods, traffic related injuries can be minimized.

Human injury threshold values for femur and pelvis impact were derived from applicable and original PMHS data. Data was scaled to a mid-sized male, survival analysis with Weibull fit was performed with exact femur 3-point bending data, logistic regression with doubly censored pelvis impact data. Legform thresholds were derived using a linear regression between impactor and THUMS values derived from tests conducted by Snedeker et al. (2005). It is assumed that THUMS and upper leg surrogates have a similar response. The implications of the new set-up and thresholds for Euro NCAP test results were assessed for results published 2009 and 2010 using empirical relationships between impact energy, measured force and moment.

Using this approach, the resulting thresholds to be used with the legform were determined to be 7.9-9.0 kN for the pelvis test and 300-365 Nm for the femur test. These values correspond to 5 and 20% fracture risk, respectively.

With the currently used set-up and limits, the average score for the upper leg test is 22% of the maximum score. With the proposed method and

limits, the average score calculated is 70%. With only 30% missing, the score matches better with the accident frequency of bonnet leading edge induced injuries to lower extremities.

INTRODUCTION

Aim

Euro NCAP uses a test developed by EEVC WG17 to rate a vehicle's ability to protect pedestrians from femur and pelvis fractures when impacted. Previous work and recently published accident data indicated a discrepancy between test results in Euro NCAP and real-life injury risk. Based on these findings Snedeker et al. (2005) suggested test set-up changes. However, suggested legform impactor threshold values have so far not been based on human injury risk that have been transferred to impactor values which might be required due to the limited biofidelity of the legform.

This work aimed at deriving legform impactor threshold values from applicable and original PMHS data to be used with the proposed test set-up from Snedeker et al. (2005). Finally, the implications for Euro NCAP test results and the match with real-life injury risk were assessed.

The Euro NCAP Upper Leg Test

The Euro NCAP upper legform test was developed by the European Experimental Vehicles Committee (EEVC) in the working groups (WG) 7, 10 and 17 since the 80s (Lawrence 2005). The final version was published in 2002 (EEVC 2002).

In Euro NCAP, the upper legform test is one part of the pedestrian protection assessment, and aims at measuring the level of protection for the femur and pelvis area. Car manufacturers can be awarded full score for the upper leg test when not exceeding impactor threshold force and moment values which are 5 kN and 300 Nm, respectively (upper performance limit) for any of the tested impact points. These values were adopted from EEVC WG17. When exceeding the lower performance limit, set by Euro NCAP, which is 6kN and 380 Nm, no score is awarded. Between the upper and lower performance limits proportional score is

awarded. The upper leg tests can provide up to 17% (6 points) of the total maximum achievable score in Euro NCAP (36 points, Euro NCAP 2009) and is therefore important.

The test uses a guided legform which is made to impact the bonnet leading edge (BLE) while force and bending moment are measured. Impact velocity, angle and energy are depending function of the vehicle geometry, namely BLE height and bumper lead, defined as the horizontal distance between upper bumper reference line (UBRL) and BLE, as depicted in figure 1. (EEVC 2002).

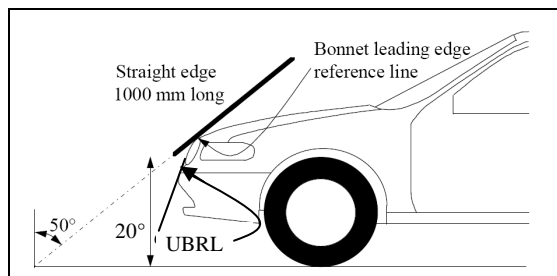


Figure 1. Geometric definition of BLE. Adopted from Euro NCAP (2009).

The used relations between impact velocity and angle and car geometries were established by full scale dummy tests (EEVC 2002, Lawrence 1998). The impact energy dependency on the vehicle geometry was developed by use of computer simulations by TRL. In their simulations a 50th percentile dummy model was used and deformation energy was estimated for several car shapes (EEVC 2002).

Acceptance levels or impactor thresholds were identified by accident reconstruction. For 39 accidents the dent depth on the forward bonnet area, close to the BLE was reproduced with the upper leg impactor (Rodmell and Lawrence 1998, Matsui 1998). Recording impactor bending moment and force as well as occurrence of femur or pelvis fracture allowed the construction of injury risk curves. Impactor thresholds are 5 kN and 300 Nm, defined from the 20% risk of fracture determined as the average values from logistic regression and cumulative normal distribution (EEVC 2002, Rodmell and Lawrence 1998).

Accident Data

Liers (2010) and Liers and Hannawald (2009) analyzed GIDAS pedestrian accidents occurring between 1999 and 2008 with the vehicle front of passenger cars at impact velocities up to 40 km/h. There was no restriction to model years, the average was 1991. Table 1 shows the classification of 517 AIS2+ injuries according to injury-causing vehicle part and injured body region.

Fredriksson et al. (2010) used GIDAS data from 1999 to 2008 to analyze pedestrians being hit by a vehicle front of passenger cars, resulting in a sample of 1030 cases. There was no restriction to model years. 161 pedestrians sustained at least one AIS 3+ injury, pedestrians sustaining at least one injury in the given body region are listed together with the injury causing vehicle part in table 2. Differently from Liers and Hannawald (2009), SUVs were not included but all impact velocities were considered.

Table 1. Injury causing vehicle part and injured body region for car to pedestrian accidents. Adopted from Liers (2010)

	Head /Face	Neck	Thorax	Abdomen	Spine	Upper Extr.	Lower Extr.	Total
Windscreen frame	31	0	6	0	3	5	0	45
Windscreen	74	0	1	0	3	5	0	83
Bonnet	15	1	7	4	5	8	5	45
BLE	1	0	0	6	0	1	17	25
Bumper	0	0	0	1	1	0	134	136
Other	3	0	5	2	3	3	12	28
Ground	92	0	18	0	7	27	11	155
Total	216	1	37	13	22	49	179	517

Table 2. Injury causing vehicle part and injured body region for car to pedestrian accidents. Adopted from Fredriksson et al. (2010)

	Head /Face	Neck	Chest ⁽¹⁾	Upper extremities	Lower extremities	Total
Windscreen incl. frame	40	0	20	1	3	64
Bonnet	8	1	23	5	10	47
BLE	1	0	1	0	8	10
Bumper	2	0	5	2	68	77
Other	5	1	5	0	3	14
Ground	19	0	15	7	6	47
Total	75	2	69	15	98	259

⁽¹⁾ Chest includes: Thorax, abdomen and spine

Comparison with Euro NCAP Test Results

It is important to note that the exact test zones in Euro NCAP might differ from injury-causing vehicle part in real life accidents. For example, depending on the vehicle geometry, only a part of the hood might be tested for head injuries in Euro NCAP while injury frequencies are given for the complete hood. Despite this limitation, accident

frequencies for the corresponding Euro NCAP pedestrian protection subtests can be taken from the accident data in table 1 and table 2.

For the type of accident targeted by the upper leg test, the relative injury frequency is calculated as the proportion of BLE induced injuries to lower extremities compared to all injuries without ground impact and others. This frequency was 5% for AIS2+ (table 1) and was 4% for AIS3+ injuries (table 2).

In contrast, the relative injury frequencies of adult and child head injuries from impacts to the windscreen and bonnet were 36% (AIS2+, table 1) and 24% (AIS3+, table 2).

Also injuries to the lower extremities (knee and tibia) when subjected to impacts by vehicle bumpers are much higher than the BLE related injuries. Lower leg injuries account for 40% (table 1) and 34% (table 2), of all injuries without ground impacts and others, respectively, and are thereby the most common type of injuries.

In Euro-NCAP, injuries from ground impacts are not considered even though they account for 30% of all AIS2+ injuries (table 1) and 18% of all AIS3+ injuries (table 2).

These relative injury frequencies can be compared to the score awarded to recent vehicles in Euro NCAP pedestrian protection testing. The comparison shown in figure 2 includes two different measures for indicated hazard. The real-life hazard is expressed by the relative injury frequencies at AIS3+ level presented above. The Euro NCAP indicated hazard is the fraction of the total pedestrian score not achieved in Euro NCAP. These statistics are given for a few combinations of vehicle parts and body regions.

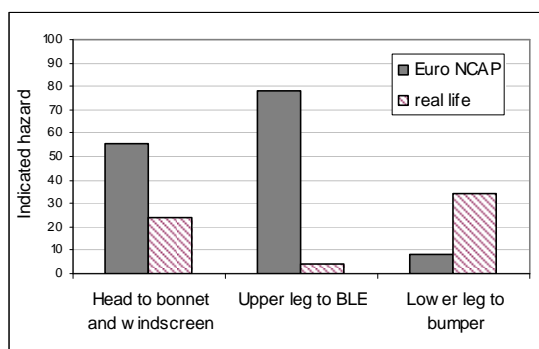


Figure 2. Euro NCAP and real-life indicated hazard for several body region – vehicle part combinations.

The fraction not achieved in Euro NCAP score can be expected to be particularly low for the tests corresponding to low injury frequency, as the level

of protection could be judged high from the accident data and thus the level of protection indicated by the Euro NCAP score should be high.

A low relative injury frequency can be demonstrated for BLE induced injuries, which means that the BLE is not a hazardous vehicle area in real-life. Despite this fact, the score awarded in upper leg test is low: the average score for this test is 1.44 points out of 6 points, which means that Euro NCAP is highlighting the BLE area as particularly hazardous. This is an apparent mismatch. Discrepancies between real-life relevance and test severity have been reported before. The majority of vehicles tested give legform test values that exceed the used thresholds while BLE to upper leg or pelvis injuries are scarce (EEVC 2002, Hardy et al. 2006, JARI 2004, Snedeker et al. 2003).

Review of the Test Set-Up

It has been argued that the bumper lead is not a significant parameter determining upper leg injuries, thus should be excluded from determining the impact energy (Matsui et al. 1998). The suggested impact energies are generally too high (Konosu et al. 1998, Honda 2001). The impactor test speed was shown to be inaccurate as bonnet roundness is not sufficiently reflected (Snedeker et al. 2003). Furthermore, a separation in femur and pelvis tests was suggested as the injury mechanisms differ (Honda 2001, Snedeker et al. 2005).

Snedeker et al. (2005) proposed a modified test set-up, addressing several of the highlighted issues. A wrap around contact definition is used, which was based on PMHS testing and computer simulation with THUMS, and which is summarized in figure 3. A small change in the geometric definition of the BLE is proposed. The impactor mass is fixed to represent human properties, the impactor velocity is defined from car geometry and the impact energy results accordingly. In the current set-up, impact energy and velocity are defined by the car geometry and the impactor mass results accordingly.

Legform Impactor Thresholds

Several legform impactor threshold values have been proposed and are summarized in table 3. In this table “the peak bending moment relates to the risk of femur fracture while the risk of pelvis fracture is more related to the peak force.” (Matsui et al. 1998).

Rodmell and Lawrence (1998) included 12 cases reported of Matsui et al. (1998) for the construction of their injury risk curve. However, it seems that

information from 2 cases (#5 and #7) was wrongly reported by Rodmell and Lawrence (1998) and should be corrected.

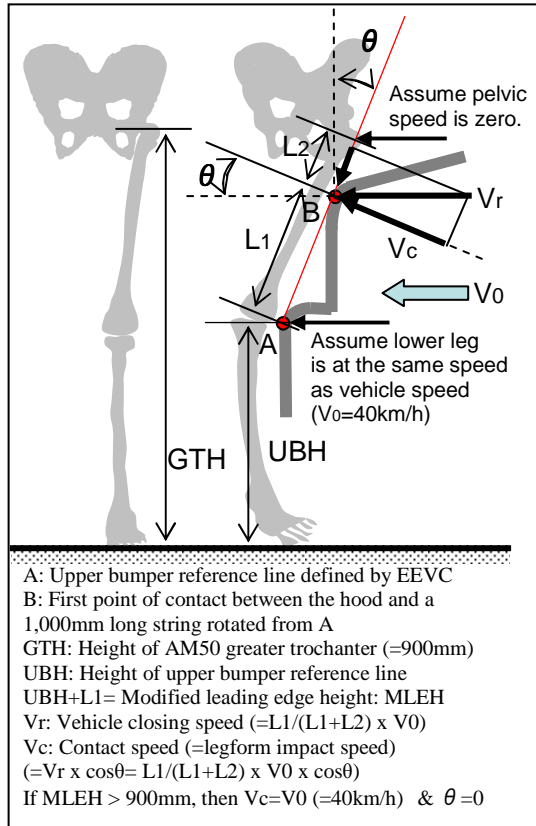


Figure 3. Proposed test set-up from Snedeker et al. (2005).

Table 3. Proposed legform impactor thresholds

Source	Pelvis	Femur	Basis
EEVC	4 kN	220	50% risk from accident reconstruction
WG10		Nm	
EEVC	5 kN	300	20% risk from accident reconstruction
WG17		Nm	
Matsui et al. 1998	7.5 kN	510	50% risk from accident reconstruction
TRL 2006	6.25 kN	375	Feasibility
EC/78/2009 (5 kN)		(300 Nm)	Monitoring only
Matsui et al. 2006	6.3 kN	417	20% risk from accident reconstruction
Snedeker et al. 2005	10 kN ⁽²⁾	320 Nm ⁽¹⁾	Human tolerance data: ⁽¹⁾⁽²⁾

⁽¹⁾base: Yamada (1971); Powell et al. (1975); Kress et al. (2001) ⁽²⁾base: Cesari (1982)

More fundamentally, one might question the quality of the proposed thresholds by EEVC WG17 when these were developed from matching dent depths caused by impacts with a human leg and the upper legform. As outlined above, biofidelity and kinematic representation have been questioned.

More commonly, impactor thresholds are developed by transferring human injury risk to impactor risk, using either proven biofidelity or some kind of transfer function. For the upper legform, Bovenkerk et al. (2008) recommend the use of a transfer function. None of the proposed thresholds listed in table 3 were developed from human injury risk subsequently modified by a transfer function.

METHODS AND MATERIALS

Legform Impactor Thresholds

Literature concerning human pelvis and femur fracture risk was selected when the following criteria were met:

- Measurement of bending moments for femur fracture or impact force for pelvis fracture;
- Identification of this measurement to be a suitable predictor for fractures;
- Dynamic testing;
- Listing of relevant specimen geometries to allow normalization;
- Only 3-point bending considered for femur fracture risk;
- Addressing pedestrian impact conditions for pelvis fracture risk.

Having identified applicable data as shown in table 4 and 5, pelvis and femur injury risk curves were constructed.

Femur Fracture risk was assessed using data published by Kerrigan et al. (2004) and Kennedy et al. (2004). All 70 data points were normalized to the size of an average male as proposed in these publications. The reference in Kerrigan et al. (2004) is a femur length of 448.5 mm taken from an implant measure and a cross sectional area of 467.26 mm² taken from the male average value in the sample in Kennedy et al. (2004). The bending moment was scaled to the third power of the length scale factor, i.e. fraction of femur length and fraction of the square root of the sectional area, as proposed in Kleinberger et al. (1998). As fracture was a force limiting event, thus data was exact, survival analysis was performed in line with the latest proposed recommendations from ISO WG6.

From the survival analysis, the hazard function was obtained. Confidence intervals were obtained adopting p-bootstrap methods proposed by Efron and Tibshirani (1993). The basic idea is that having a sample but no information on the underlying distribution, the sample itself is the best approximation. Thus, randomly taking equally sized samples of the original dataset (drawing with replacement), one obtains the possible variation of samples taken from the underlying distribution.

This resampling was executed 1000 times and 2.5 and 97.5 percentile values for each step in the hazard function were taken to give the 95% confidence intervals for each probability value.

The hazard function is a step function as given in equation (1) and as such not very convenient to use. To smoothen the curves, a Weibull function as given in equation (2) was fitted by least square optimization as given in Cullen and Frey (1999) for lower and upper confidence data as well as for the hazard function itself.

$$F(x_i) = P(X < x_i) = \frac{i - 0.5}{n}$$

where: $F(x_i)$: Fracture risk (CDF);
 x_i : bending moment of data point i ;
 n : sample size; $i = 1, 2, \dots, n$;
and $x_1 < x_2 < \dots < x_n$ (1).

$$F(x) = 1 - e^{-\left(\frac{x}{\alpha}\right)^\beta}$$

where: $F(x)$: Fracture risk (CDF);
 x : bending moment; α, β : shape parameter (2).

The resulting data and functions were checked for several potentially influential variables, i.e. whether these variables have an influence on the obtained risk curves and therefore would require the use of an appropriate sub-set. These variables were:

- origin of the dataset;
- bending direction ;
- specimen age;
- specimen gender.

These were identified as the most influential factors in this study as well as in Carrol and Hynd (2007). The check was done by two means.

Firstly, a Kolmogorov-Smirnov (K-S) test, as recommended for goodness-of-fit testing by Diamond (2001), was conducted from the survival data without Weibull fit to see if the cumulative distribution function (CDF) of subset A might originate from the data of subset B and vice versa at a significance level of 0.05.

Secondly, graphical evaluation was conducted. This means the injury risk curve and its confidence intervals of the subsamples were compared. Overlap of the confidence intervals indicated that there is no difference in injury risk due to the variable defining the sub samples.

Pelvis fracture risk was reviewed as listed in table 5. Only Matsui et al. (2003) aimed at reproducing pedestrian impact conditions and thus is used. Peak impact forces were scaled as proposed in Kleinberger et al. (1998), given in

equation (3), thus the scaling methodology of the original publication was not followed. The average normalized peak force remained at 9.1 kN, individual loads were up to 0.33 kN lower and 0.69 kN higher than originally proposed.

$$F_{scaled} = \left(\frac{75kg}{PMHSmass} \right)^{\frac{2}{3}} F_{peak}$$

where: F_{scaled} : normalized maximum force;
 F_{peak} : recorded maximum force for a mass of PMHSmass (3).

Impact energy was pre-set and equipment to indicate initial damage was not used, thus fracture was not necessarily a force limiting event. The data should be treated as doubly censored, i.e. it is only known that non-fracture cases withstand at least the maximum recorded force and fracture cases fail before maximum recorded force. For this type of data, logistic regression is suitable and was used.

Parameters for the logistic function in equation (4) were determined by maximizing log-likelihood based on all 4 fracture and 8 non-fracture cases, thus including one case of femur shaft and 3 of anterior pelvic ring fracture.

$$F(x) = \frac{e^{\beta_0 + \beta_1 x}}{1 + e^{\beta_0 + \beta_1 x}}$$

where: $F(x)$: Fracture risk (CDF); x : impact force;
 β_0, β_1 : shape parameter (4).

One might note that Matsui et al. (2003) performed statistical analysis with the Certainty Method. Implications for different statistical analysis and a comparison of the injury risk curves developed from Cesari et al. (1982) can be found in the discussion section.

Human injury thresholds for fracture risk were calculated at 20% level as done by EECV WG17. For femur fracture risk, the Weibull-survival function was used. For pelvis fracture risk, the average of normal CDF and logistic regression was taken, as done in EECV (2002). As Euro NCAP does not use a pass/fail threshold but an upper and lower performance limit, these limits also needed to be defined. Even though the current EECV recommendation is taken as the lower performance limit, it is thought to be more in line with the general philosophy to take this value as an upper performance limit. Thereby the test requires higher protection levels by the BLE in order to provide points to the overall assessment. The lower performance limit was set to 20% risk, the upper one to 5% risk. The current Euro NCAP lower limit corresponds 34% for moment and 37% for force while the upper limit is set to 20% for both.

Table 4.
Literature considered for human femur fracture risk. Applicable data is given on white background, omitted data on grey background

Author	Year	Impact condition	Data Scaling	N	Tabulated moment data	Proposed threshold
Yamada	1971	Static				182 Nm
Kress and Porta	2001	Dynamic, simply suspended leg	No	604	No	100-500 Nm
Matsui et al.	2004	Dynamic, simulated standing posture	Yes	13	No	8.8 kN
Kerrigan et al.	2003	Dynamic 3 point bending, L-M with surrounding flesh		7	Yes	412 Nm
Funk et al.	2004	Dynamic 3 point bending, L-M and A-P, isolated femur	No	15	Yes	458 Nm
Kerrigan et al.	2004	Dynamic 3 point bending, L-M, with surrounding flesh	Yes, femur length	12	Yes	372–447 Nm
Kennedy et al.	2004	Dynamic 3 point bending, L-M and A-P, isolated femur	Yes, cross sectional area	45	Yes	395 Nm

Note: Kerrigan et al. (2004) includes raw data from Kerrigan et al. (2003) and Funk et al. (2004)

Table 5.
Literature considered for human pelvis fracture risk. Applicable data is given on white background, omitted data on grey background

Author	Year	Threshold for	Impact condition	Data Scaling	N	Tabulated force data	Proposed threshold
Mertz et al.	2003	Vehicle occupant	Not specified	Yes, not specified	-	No	6 kN peak force
Matsui et al.	2003	Pedestrian	Full PMHS, restrained pelvis, dynamic ram	Yes, PMHS mass	12	Yes	8.9 kN peak force
Guillemot et al.	1997	Vehicle occupant	Isolated restrained pelvis, static	No	10	No	-
Zhu et al.	1993	Vehicle occupant	Load plate	Yes, PMHS mass	17	Yes	5 kN average force
Cavanaugh et al.	1990	Vehicle occupant	Load plate	Yes, PMHS mass	12	Yes	8 kN
Viano	1989	Vehicle occupant	Pendulum impact, suspended full PMHS	Yes	14	Yes	27% compression ⁽²⁾
Marcus et al.	1983	Vehicle occupant	Load plate	Yes, PMHS mass	11	No	-
Maltese et al.	2002	Vehicle occupant	Load plate	Yes, PMHS mass	36	No	-
Cesari et al.	1980	Vehicle occupant	Dynamic ram	No	36	Yes	5 kN
Cesari et al.	1982	Vehicle occupant	Dynamic ram	Yes (PMHS height & mass)	60 ⁽¹⁾	Yes	10 kN

Note: Cesari et al. (1982) includes raw data from Cesari et al. (1980)

⁽¹⁾out of those, 52 complete, unpadded cases were used ⁽²⁾Force was identified to not predict injuries

Transfer functions from human thresholds to legform thresholds were calculated using unpublished data from 20 tests with the physical impactor and THUMS simulations of the same impact conducted in the Snedeker et al. (2005) study as given in table 6.

The data can be used to establish a correlation between the physically measured values (tests with the leg form) and the corresponding human values. These are represented by the values measured with THUMS.

Table 6.
Test data for physical impact and THUMS simulation from Snedeker et al. (2005).

No	Bonnet edge radius	Femur moment [Nm]		Pelvis force [kN]		MLEH
		Test	THUMS	Test	THUMS	
1	0	397	177			778
2	50	385	189			763
3	100	397	180			746
4	250	206	174			670
5	500	165	171			627
6	0	725	275			904
7	50	520	300			885
8	100	325	305			868
9	250	295	255			799
10	500	210	235			735
11	0			30	13.8	1040
12	50			12.7	14.3	1014
13	100			14	20	984
14	250			11	17.5	895
15	500			8	14	852
16	0			9.1	8.9	904
17	50			9.2	11.8	885
18	100			10.3	14.4	868
19	250			7.1	11.1	799
20	500			5.5	7.5	735

The impactor limits were then used together with the test set-up from Snedeker et al. (2005) to assess the implications for Euro NCAP test results and the match with real-life injury risk.

Implications for Euro NCAP Test Results

It was estimated how the results in Euro NCAP scoring would change when applying the proposed method and thresholds from all vehicle ratings published in 2009 and 2010 as used in the initial comparison between Euro NCAP score and real-life injury risk. Vans and SUV were assessed with the pelvis test, other vehicles with the femur test from Snedeker et al. (2005).

First, the changes of impact energy, resulting from the proposed new set-up, were calculated for six modern cars, ranging from compact to van, and 3

impact points each from CAE geometry data as measured forces and moments are dependent on the impact energy.

For 32 vehicles, tested in Euro NCAP between 2004 and 2010, both the impact energy and the recorded force and moment were known for the impact point in the vehicle center. All these vehicles obtained some score in the upper leg area; therefore it can be presumed they were designed to comply with the test. Vehicles not designed to achieve score were excluded as this would give high response values no matter which impact energy was used and therefore misleading results. From these data a relationship between impact energy and recorded force and moment was calculated. Using the average of the previous calculated change in impact energy, the estimated average change in impactor measurements was determined.

The legform impactor measurements were reduced by this expected change as described above and Euro NCAP score was calculated with the proposed upper and lower performance limit. For comparison, the expected Euro NCAP score when using the performance limits from Snedeker et al. (2005) was calculated as well.

RESULTS

Human Femur Fracture Risk

Human femur fracture injury-risk curves were constructed by Weibull fit to survival analysis together with p-bootstrap confidence intervals. The evaluation of the origin of the dataset Kerrigan et al. (2004) or Kennedy et al. (2004), bending direction (anterior-posterior or lateral-medial), age and gender influence are depicted in figure 4 to 7. The best estimate is given as a solid line, the upper and lower confidence limit are given as dotted lines in the same color.

Figure 4 reveals overlap of pooled data with both individual data sets for all femur fracture risk levels. The K-S test indicated no significant difference between the curves. Therefore, origin of the dataset is not considered a major influence. Figure 5 shows that loading direction has almost no influence on the injury risk curve. The individual curves lie well within the confidence bounds of each other. The K-S test also shows no significant influence. Figure 6 depicts a lower fracture risk for females compared to males. The gender has a significant influence on the bending moment according to the K-S test. Figure 7 illustrates the fact that age had only negligible influence on the bending strength in this data set. It is important to note that the age span was limited to subjects of 40 years and older while Yamada (1971) found age to be influential based

on a wider span of subject ages. Further discussion can be found in Carrol and Hynd (2007).

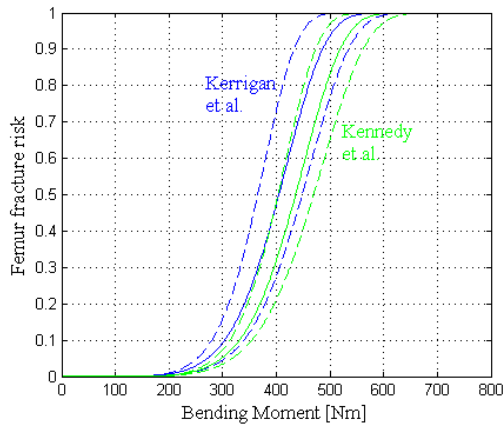


Figure 4. Influence of data source on the injury risk curve.

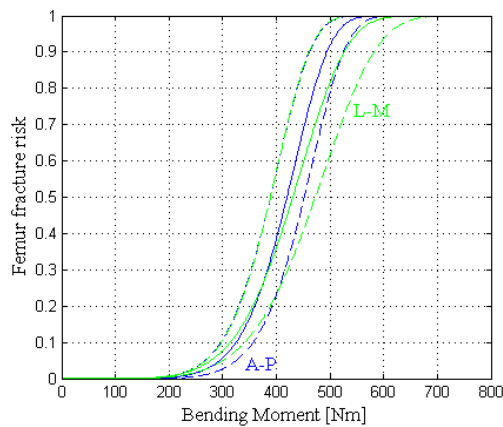


Figure 5. Influence of loading direction (A-P: Anterior-Posterior, L-M: Lateral-Medial) on the injury risk curve.

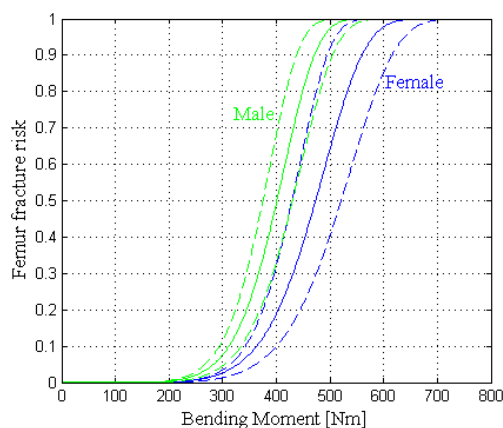


Figure 6. Influence of gender on the injury risk curve.

The evaluation led to the conclusion that only gender has a major influence and the data should therefore be restricted to male data. In conclusion, the injury risk curve was based on male PHMS data from Kerrigan et al. (2004) and Kennedy et al.

(2004), omitting not applicable female data as depicted in figure 8. The injury-risk curve is based on a Weibull fit. The parameters for the risk function as given in equation (2) are given in table 7. A fracture risk of 20% corresponds to 344 Nm and 5% to 283 Nm.

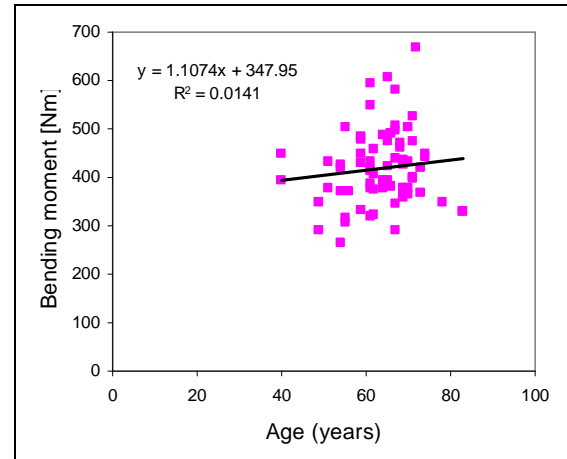


Figure 7. Influence of age on peak bending moment.

Table 7. Parameter for the femur fracture risk function

	Best estimate	Lower limit	Upper limit
α	420.9	393.5	450.4
β	7.48	7.67	7.50

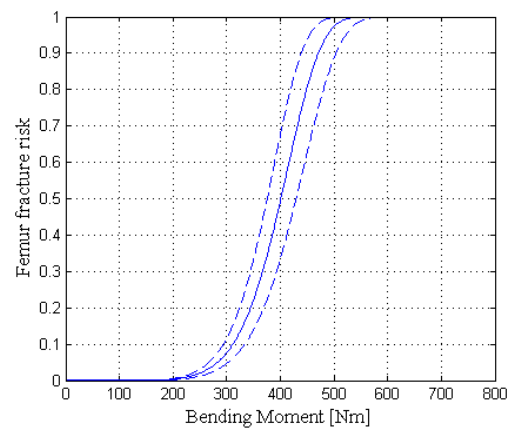


Figure 8. Injury risk curve for human femur fracture with 95% confidence limits.

Human Pelvis Fracture Risk

The pelvis fracture risk curve is shown in figure 9. The parameters for the logistic regression in the form of equation (4) are calculated to be $\beta_0 = -5.3378$ and $\beta_1 = 0.5065$. A fracture risk of 20% corresponds to 7.8 kN, 5% fracture risk corresponds to 4.7 kN.

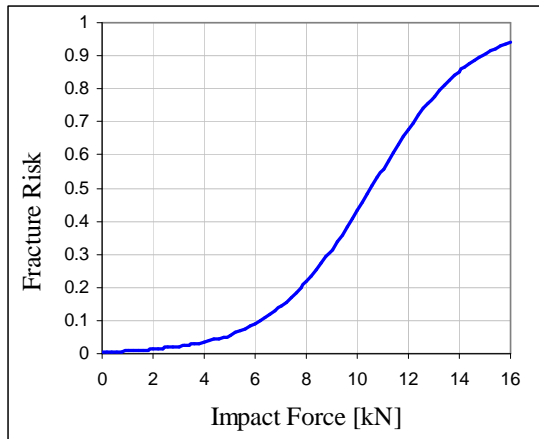


Figure 9. Injury risk curve for human pelvis impact.

Transfer Function

Not all values from the Snedeker et al. (2005) study as given in table 6 can be used for a regression. The proposed test method measures the force when the Modified Leading Edge Height (MLEH) is below 900 mm and the bending moment when above 900 mm. Thus the values from test 6, 15, and 17-20 are not applicable. Although test 14 lies slightly outside the corridor, it is used to increase the number of cases. Test 11 is identified as outlier. There seem to be two different linear trends for the tests 1-10. Figure 10 shows a linear relation for each group of small BLE radii (test 1, 2, 3, and 7) and large radii (test 4, 5, 8, 9, and 10).

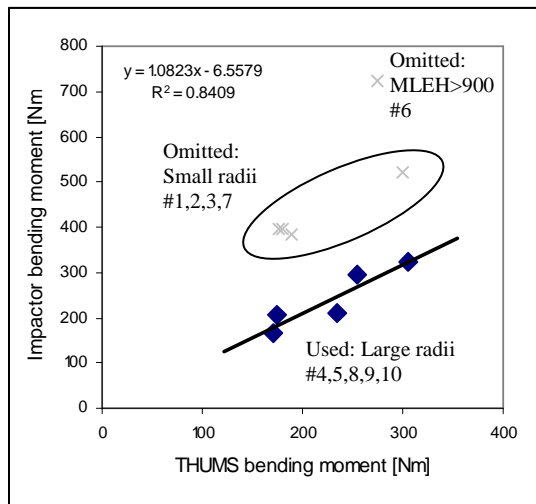


Figure 10. Transfer function human to impactor for femur bending moment.

This is not surprising as Snedeker et al. (2003) already found small radii leading to higher legform impactor measurements compared to full body simulations for sedan and van type vehicles. As most modern cars have large bonnet edge radii (Snedeker et al. 2003), this group was taken to establish a transformation function. For the pelvis

force no such split exists and all applicable values were used to calculate a transfer function as given in figure 11.

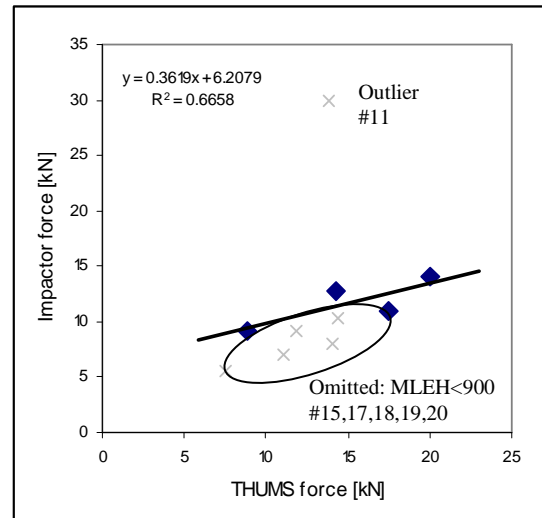


Figure 11. Transfer function human to impactor for pelvis force.

Legform impactor thresholds are listed in table 8. They are derived from human values using the transfer functions as given in figure 10 and 11.

Table 8.

Human and legform impactor values for 20% and 5% fracture risk

Fracture risk	Human values	Impactor values
20%	344 Nm 7.8 kN	365 Nm 9.0 kN
5%	283 Nm 4.7 kN	300 Nm 7.9 kN

Implications for Euro NCAP Test Results

For several vehicles currently on sale, the change of impact energy was calculated as given in table 9. On average, the impact energy was reduced by 431 J for the proposed femur test and by 60 J for the proposed pelvis test. The relationship between impact energy and vehicle response was derived from empirical relations for 32 vehicles, tested in Euro NCAP between 2004 and 2010, as shown in figure 12 and 13. From the calculated average reduction in impact energy and the linear regression equations for energy and legform impactor response, the average reduction for the pelvis test was calculated to be 0.26 N and the average reduction for the femur test is 60 Nm.

The expected influence on the Euro NCAP score was calculated by reducing the published legform impactor measurements for the 2009-2010 vehicles with the above values (0.26 kN and 60 Nm) and applying the proposed lower and upper performance limit (7.9-9.0 kN, 300-365 Nm). For comparison, the expected results when using the

limits 10 kN and 320 Nm from Snedeker et al. (2005) were calculated as well.

Table 9.
Impact energies using the EEVC WG17 method and the proposed changes for modern vehicles

Car	Point	EEVC		New energy	
		energy [J]	MLEH [mm]	Femur [J]	Pelvis [J]
Car 1 Sedan	PPU-1	700	895	327	
	PPU-2	700	863	321	
	PPU-3	700	915		686
Car 2 SUV	PPU-1	700	1005		686
	PPU-2	700	868	261	
	PPU-3	671	983		686
Car 3 Van	PPU-1	700	881	294	
	PPU-2	700	895	345	
	PPU-3	700	900	292	431
Car 4 Sedan	PPU-1	668	808	160	
	PPU-2	700	824	233	
	PPU-3	672	838	187	
Car 5 Sedan	PPU-1	564	783	104	
	PPU-2	508	813	185	
	PPU-3	700	980		686
Car 6 Sedan	PPU-1	700	839	195	
	PPU-2	700	807	194	
	PPU-3	651	868	230	
Average reduction [J]				431	60
Average reduction [%]				64	9

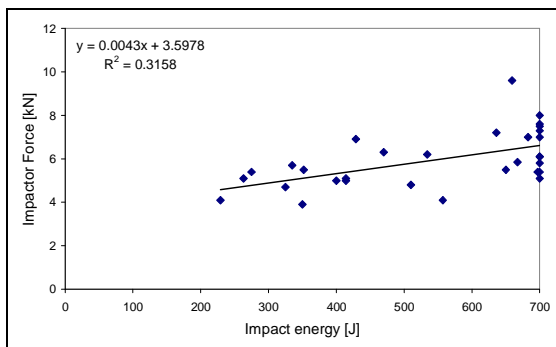


Figure 12. Impactor force dependency on impact energy.

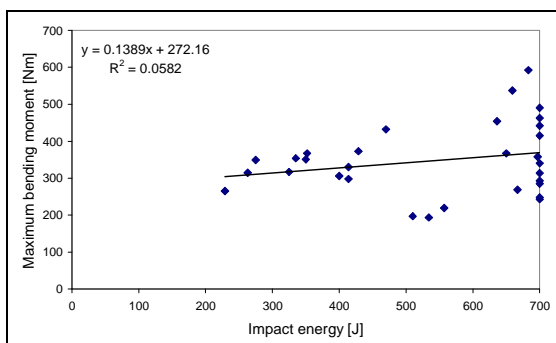


Figure 13. Impactor bending moment dependency on impact energy.

With the proposed method and limits, the average score calculated is 4.19 points, corresponding to 70% of the maximum score. By applying the limits from Snedeker et al. (2005), the average score is 4.47 points, corresponding to 75% of the maximum score. This is a significant increase compared to the score with the current method (1.31 points or 22% of the maximum score). Thus, the indicated hazard of this injury type, expressed as % gap to maximum score, is reduced to 30% for the proposed method and limits and to 25% when using the limits from Snedeker et al. (2005) as depicted in figure 14. It can be seen that the proposed changes for the upper leg test better reflect the real-life indicated hazard of this injury type. Still, the test might highlight the bonnet leading edge as more dangerous than it is.

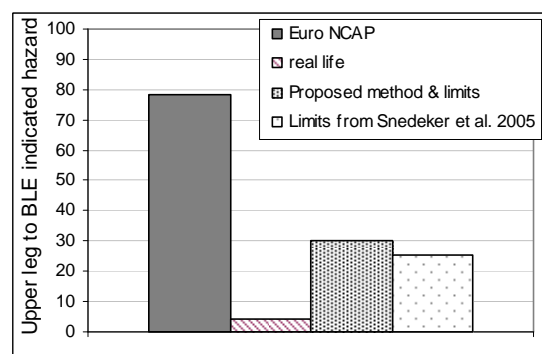


Figure 14. The proposed changes lead to a better match between Euro NCAP and real-life indicated hazard.

DISCUSSION

Construction of Injury-Risk Curves

For the construction of the injury-risk curves, survival analysis was applied for the exact data of femur fracture. For pelvis fracture logistic regression was used to construct injury-risk curves from the doubly censored data. Which methods are most appropriate for this purpose are still being discussed, e.g. in the ISO working group (TC 22/SC12/WG 6). Thus it can be argued that other methods should be applied.

In general, survival analysis, logistic regression and normal CDF are most commonly used, a variety of other methods exist (e.g. Certainty Method, Consistent Threshold Estimate, Median Rank method, Mertz/Weber method). Survival analysis has beneficial attributes such as zero risk at zero stimulus and monotonic increase of risk with increased stimulus, which logistic regression does not have (Kent and Funk, 2004). Figure 16 illustrated these properties. Furthermore, survival analysis is originally non-parametric, thus no assumption has to be made on the underlying distribution. The hazard function of a survival

analysis reduces to an empirical cumulative distribution function at Hazen plotting position when all data is exact as given in equation (1) in the notation of Cullen and Frey (1999), thus can be seen as unbiased. Fitting a Weibull function in a second step to smooth the curve and allow easy calculation still gives more freedom for the shape of the curve as the fit of a normal distribution does.

Survival analysis was used on the data for femur fracture risk curve in this study, due to its beneficial attributes as outlined above. Confidence intervals given for the resulting curve depict the inherent uncertainty. For the pelvis fracture risk curve, the data was assumed to be doubly censored. However, one might assume that pelvis fracture is a force limiting event, thus survival analysis or normal CDF could be applied. Figure 15 depicts injury-risk curves obtained from these statistical methods. 20% and 5% risk values from logistic regression are the most conservative estimate. Thus, the fracture risk is more likely to be overestimated than underestimated. Logistic regression appears to be the safe choice for the data at hand.

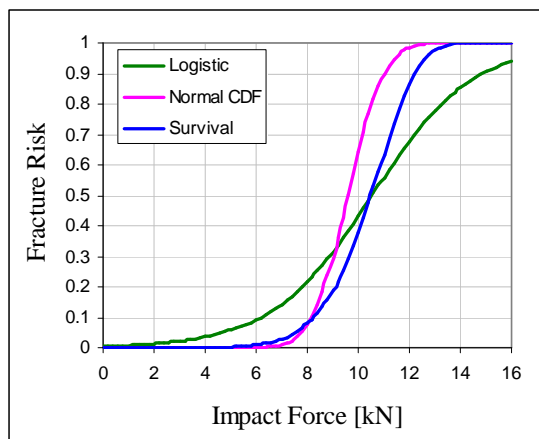


Figure 15. Injury-risk curves for pelvis impact obtained with different statistical methods.

Cesari et al. (1982) repeatedly tested the same pelvis until failure to be close to the exact failure load, thus recorded peak force levels, normalized according to equation (3), are not independent. This is a violation against pre-requisites for logistic regression which is shown in figure 16 to indicate substantial risk at zero stimulus. Normal CDF and survival analysis can be performed assuming failure load to be exact. The resulting failure loads for 5% and 20% fracture risk using the Cesari et al data of 5-6.2 kN and 7.2-9.2 kN are of the same order as the ones derived from Matsui et al. (2003) of 4.7 kN and 7.8 kN, thus not contradicting the findings.

Confidence intervals were not given as they only express the uncertainty related to fitting the data points to the selected distribution. It might be

misleading to give these confidence intervals as there is additional uncertainty on which distribution to select.

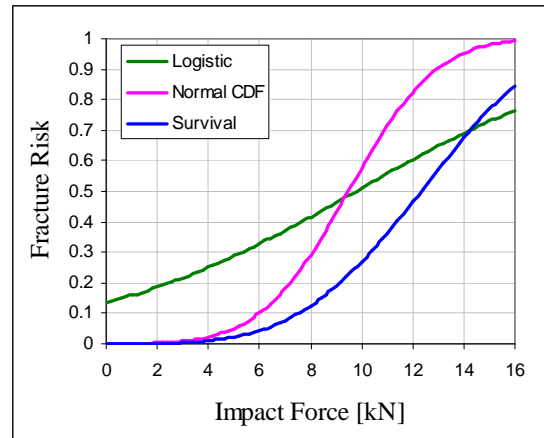


Figure 16. Injury-risk curves for pelvis impact developed from raw data of Cesari et al. (1982).

Data Scaling

Throughout this study, data was scaled to a mid-sized male as proposed in Kleinberger et al. (1998). Kerrigan et al. (2004) used this methodology, other sources had to be re-calculated. Kennedy et al. (2004) originally used multivariate regression, Cesari et al. (1982) adjusted for overweight and underweight, and Matsui et al. (2004) raised the mass fraction to the power of 1/2 instead of 2/3. While consistency has been achieved, consideration could be given whether this factor is too heavy. The rather surprising, but not necessarily invalid finding, that females have lower fracture risk could be explained: The unscaled data reveals the expected higher fracture risk for females, thus the scaling might have shifted the data too much. However, structural differences could explain the lower fracture risk as well.

Transfer Functions

The transfer from human thresholds to impactor thresholds was based on limited data and on the assumption that THUMS and human surrogate measurements are equal. Additional data could strengthen the relationships.

Snedeker et al. (2005) Test Set-Up

The proposed test set-up by Snedeker et al. (2005) addressed several of the highlighted issues with the current EEVC WG17 method as summarized earlier. In a more recent simulation study with THUMS, Compigne et al. (2008) have again highlighted differences in human and impactor kinematics as well as higher contact forces and vehicle damage using the EEVC WG17 upper leg test.

It has been shown that the set-up is expected to contribute to a better match between real-life injury data and Euro NCAP results. The authors advocate the use of this set-up as an improvement over the current one. It requires only small modifications to the test tool as a weight reduction of the legform for the femur test from 9.5 kg to 7.5 kg, thus below the current minimum weight, was suggested to be better aligned with the mass of a human thigh, and could be implemented with short lead time. New test tools might bring even further improvements but are not expected to be available in the near future.

Real-Life Relevance and Other NCAPs

Aside from Euro NCAP, the EEVC WG17 upper leg test is currently used in ANCAP and EU regulation.

In the EU directives 78/2009 and 631/2009, the upper leg test is prescribed for monitoring purposes with thresholds of 5 kN and 300 Nm. Monitoring means, that compliance with the thresholds is not required. The upper leg test is not included in JNCAP, US-NCAP and the global technical regulation on pedestrian safety (gtr No 9, ECE/TRANS/180/Add.9). The relevant section mentions that “some delegates had concerns about the biofidelity of the upper legform impactor and the limitations of the test tool in assessing injury”. Euro NCAP appears to give upper leg protection a higher weight and the EEVC WG17 test a higher relevance than other before mentioned parties do.

CONCLUSIONS

Previous studies have indicated a discrepancy between the EEVC WG17 upper leg test results in Euro NCAP and real-life injury risk as well as shortcomings in the test set-up. The test set-up proposed by Snedeker et al. (2005) was identified to address several of the highlighted issues and has the potential to be an improvement over the current test method. Legform impactor thresholds developed by EEVC WG17 and Snedeker et al. (2005) could be further improved constructing injury risk curves from applicable raw data. For the first time, these thresholds were based on human risk as defined in PMHS testing. These thresholds were then transferred to be used with the upper legform, thus potentially more favorable than the ones originally developed using accident reconstructions. Using the test method proposed by Snedeker et al. (2005) together with new performance criteria as proposed in this paper (7.9-9.0 kN for the pelvis test and 300-365 Nm for the femur test), the Euro NCAP test results could be better aligned with real-life injury risks. Setting the right targets and evaluation methods is crucial to

minimize the traffic related injuries as manufacturers might develop cars based on these tests.

REFERENCES

- Bovenkerk, J., Hardy, R.N., Neal-Sturgess, C.E., Hardy, B.J., van Schijndel - de Nooij, M., Willinger, R., Guerra, L.J., and Martinez, L. (2008), Biomechanics of real world injuries and their associated injury criteria, APROSYS, report number AP-SP33-001R.
- Carroll, J.A. and Hynd, D. (2007), Material Property Scaling for Human Body Modelling, APROSYS, report number AP-SP51-0048.
- Cavanaugh, J., Walilko, T., Malhotra, A., Zhu, Y., and King, A. (1990), “Biomechanical response and injury tolerance of the pelvis in twelve sled side impacts”, STAPP Conference Proceedings, SAE 902305, p. 1–12.
- Cesari, D., Ramet, M., and Clair, P.-Y. (1980), “Evaluation of pelvic fracture tolerance in side impact”, STAPP Conference Proceedings, SAE 801306, p. 231–253.
- Cesari, D. and Ramet, M. (1982), “Pelvic tolerance and protection criteria in side impact”, STAPP Conference Proceedings, SAE 821159, p. 145–154.
- Compigne, S., Guerra, L.J., Martínez, L., and Bovenkerk, J. (2008), Review of the current pedestrian lower and upper leg test procedures. APROSYS, report number AP-SP33-0016R.
- Diamond, W.J. (2001), Practical Experiment Designs: for Engineers and Scientists, Wiley.
- EEVC WG10 (1994), Proposals for methods to evaluate pedestrian protection for passenger cars. EEVC Working Group 10 Report
- EEVC WG17 (2002), Improved test methods to evaluate pedestrian protection afforded by passenger cars. EEVC Working Group 17 Report
- Efron, B. and Tibshirani, R.J (1993) An Introduction to the Bootstrap, Chapman & Hall.
- Euro NCAP (2009), Assessment Protocol- Pedestrian Protection. Version 5.0.
- Fredriksson, R., Rosén, E., and Kullgren, A. (2010), “Priorities of pedestrian protection - A real-life study of severe injuries and car sources” Accident Analysis and Prevention, 42(6), p.1672-81.
- Funk, J.R., Kerrigan, J.R., and Crandall, J.R. (2004), “Dynamic bending tolerance and elastic plastic material properties of the human femur”, 48th annual proceedings AAAM.

- Guillemot, H., Besnault, B., Robin, S., Got, C., LeCoz, J.Y., Lavaste, F., and Lassau, J.P. (1997) "Pelvic injuries in side impact collisions: A field accident analysis and dynamic tests on isolated pelvic bones", Stapp Conference Proceedings, SAE 973322, p. 91–100.
- Hardy, B.J., Lawrence, G.J.L., Knight, I.M., and Carroll, J.A. (2006), A study on the feasibility of measures relating to the protection of pedestrians and other vulnerable road users, report for the European Commission, Contract FIF.200330937.
- JARI, (2004), Technical Feasibility Study on EEVC/WG17 Pedestrian Subsystem Test, report number INF GR/PS/101.
- Kennedy, E.A., Hurst, W.J., Stitzel, J.D., Cormier, J.M., Hansen, G.A., Smith, E.P., and Duma, S.M. (2004), "Lateral and posterior dynamic bending of the mid-shaft femur: fracture risk curves for the adult population", Stapp Car Crash J, p. 27-51.
- Kent, R.W. and Funk, J.R. (2004) "Data Censoring and Parametric Distribution Assignment in the Development of Injury Risk Functions from Biomechanical Data", SAE paper 2004-01-0317.
- Kerrigan, J.R., Bhalla, K., Madeley, N.J., Funk, J.R., Bose, J., and Crandall, J.R. (2003), "Experiments for establishing pedestrian-impact lower limb injury criteria" SAE paper 2003-01-0895.
- Kerrigan, J.R., Drinkwater, D.C., Kam, C.Y., Murphy, D.B., Ivarsson, B.J., Crandall, J.R., and Patrie, J. (2004), "Tolerance of the human leg and thigh in dynamic latero-medial bending". *IJCrash*, 9(6) p.607-623.
- Kleinbaum, D. G. and Klein, M. (2005), *Survival Analysis. A Self-Learning Text*, Springer.
- Kleinberger, M., Sun, E., Eppinger, R., Kuppa, S., and Saul, R. Development of Improved Injury Criteria for the Assessment of Advanced Automotive Restraint Systems, NHTSA report.
- Konosu, A., Ishikawa, H., and Sasaki, A. (1998), "A Study on Pedestrian Impact Test Procedures by Computer Simulation - The Upper Legform to Bonnet Leading Edge Test", ESV conference, report number ESV 98-S 1 O-W- 19.
- Lawrence, G.J.L., (2005), "The next steps for pedestrian protection test methods", ESV conference, report number ESV 05-0379.
- Liers, H. (2010), Extension of the Euro NCAP effectiveness study with focus on MAIS3+ injured pedestrians, Report under contract of ACEA.
- Liers, H. and Hannawald, L., (2009) Benefit estimation of the EuroNCAP pedestrian rating concerning real-world pedestrian safety, Report under contract of ACEA.
- Maltese, M., Eppinger, R., McFadden, J., Saul, R., Pintar, F., Yognandan, N., and Hines, M. (2002) "Response corridors of human surrogates in lateral impacts", Stapp Car Crash J, p. 321–351.
- Marcus, J.H., Morgan, R.M., Eppinger, R.H., Kallieris, D., Mattern, R., and Schmidt, G. (1983), "Human response to injury from lateral impact", Stapp Conference Proceedings, SAE 831634.
- Matsui, Y., Ishikawa, H., and Sasaki, A. (1998), "Validation of Pedestrian Upper Legform Impact test – Reconstruction of pedestrian Accidents", ESV conference, report number ESV 98-S10-O-05.
- Matsui, Y., Kajzer, J., Wittek, A., Ishikawa, H., Schroeder, G., and Bosch, U. (2003), "Injury pattern and tolerance of human pelvis under lateral loading simulating car-pedestrian impact", 2003 SAE World Congress, SAE paper 2003-01-0165.
- Matsui, Y., Schroeder, G., and Bosch, U. "Injury pattern and response of human thigh under lateral loading simulating car-pedestrian impact", 2004 SAE World Congress, SAE paper 2004-01-1603.
- Mertz, H.J. and Irwin, A.L. (2003) "Biomechanical and Scaling Bases for Frontal and Side Impact Injury Assessment Reference Values", STAPP Car Crash Journal, p.155-188.
- Rodmell, C. and Lawrence, G.J.L. (1998), Further pedestrian accident reconstructions with the upper legform impactor, EEVC WG17 document 113.
- Snedeker, J.G., Muser, M.H., and Walz, F.H. (2003), "Assessment of Pelvis and Upper Leg Injury Risk in Car-Pedestrian Collisions: Comparison of Accident Statistics, Impactor Tests and a Human Body Finite Element Model", Stapp Car Crash J, p. 437-457.
- Snedeker, J.G., Walz, F.H., Muser, M.H., Lanz, C., and Schroeder, G. (2005), "Assessing Femur and Pelvis Injury Risk in Car – Pedestrian Collisions: Comparison of Full Body PMTO Impacts, and a Human Body Finite Element Model", ESV conference, report number ESV 2005-103.
- Viano, D.C. (1989) "Biomechanical response and injuries in blunt lateral impact", STAPP Conference Proceedings, pp.113–142, SAE 892432.
- Zhu, J.Y., Cavanaugh, J.M., and King, A.I. (1993), "Pelvic biomechanical response and padding benefits in side impact based on a cadaveric test series", Stapp Conference Proceedings, p. 223–233, SAE 933128

INJURY RISK ASSESSMENT AT THE TIMING OF A PEDESTRIAN IMPACT WITH A ROAD SURFACE IN A CAR-PEDESTRIAN ACCIDENT

Kenji Anata

Atsuhiko Konosu

Takahiro Issiki

Japan Automobile Research Institute

Japan

Paper Number 11-0119

ABSTRACT

In a car-pedestrian accident, there are two major phases that exist when a pedestrian injury occurs. One is the timing of a pedestrian colliding with a car body (denoted initial collision hereafter). The other is the timing of a pedestrian colliding with a road surface (denoted secondary collision hereafter) which occurs after the initial collision.

Up until now, pedestrian protection has been considered mainly for the initial collision, and several countermeasures have been developed by automobile manufacturers. On the other hand, pedestrian protection issues in a secondary collision have not been considered in depth, therefore, collision phenomenon and pedestrian protection methods in a secondary collision have not been investigated deeply. The purpose of this study is to clarify the risk to a pedestrian in a secondary collision using traffic accident data as well as a computer simulation analysis method.

First, the reality of accidents relevant to a secondary collision was investigated by using car-pedestrian accident data. As a result, it was found that the rate of road surface causing pedestrian injury is twice the rate of injuries caused by a bonnet and fender of a car, both of which are targeted by regulations of pedestrian head protection worldwide.

Next, the phenomenon of car to pedestrian collisions was analyzed by using JARI pedestrian models which are calculated by MADYMO (Tass) and these base models' biofidelity was validated by using Post Mortem Human Subject test data. Computer

simulation analyses were carried out in a total of 45 conditions which consisted of combinations of three kinds of vehicle models (sedan type, sports utility type, van type), five kinds of pedestrian models (six-year old child, fifty-year old male and female, seventy-year old male and female, because such ages are frequently involved in car-pedestrian accidents) and three collision velocities of car to pedestrian (20, 30, 40km/h). The results showed that the HIC_{15} value in a secondary collision was higher than that of the initial collision in 38 of the 45 conditions. In addition, the HIC_{15} value in 30 of those 38 conditions was over 2000.

Based on this analysis, it became clear that it is necessary to not only focus on the initial collision but also focus on a secondary collision in car-pedestrian traffic accidents.

For our future plans, we are going to conduct additional analysis by using additional sizes of human models and additional analysis conditions, and also have a plan to develop more effective countermeasures for pedestrian protection in secondary collisions to reduce pedestrian injuries which are generated by secondary collisions in the real-world.

INTRODUCTION

Approximately, 700,000 traffic accidents occur and about 4,500 lives are lost per year in Japan. However, the number of fatalities from traffic accidents has been declining in the last decade, as shown in Figure 1 [1]. In addition, the same set of statistics show that while the number of people riding in a vehicle is

declining, the number of pedestrians is increasing. Furthermore, the number of pedestrians is higher than that of those riding in a vehicle in recent years. For this reason, it is important to reduce traffic accident fatalities even further and in particular, to reduce fatalities in pedestrian accidents.

In a car-pedestrian accident, there are two major phases when pedestrian injuries occur. One is the timing of a pedestrian colliding with a car body (denoted initial collision hereafter). The other is the timing of a pedestrian colliding with a road surface or other object (denoted secondary collision hereafter) which successively occurs after the initial collision.

Until now, pedestrian protection has been considered mainly for the initial collision, and several countermeasures have been developed by automobile manufacturers such as head or leg protection countermeasures. On the other hand, pedestrian protection issues in a secondary collision have not been considered in depth, therefore, protection countermeasures for pedestrians in a secondary collision have not been sufficient. Moreover, the collision phenomenon and injury risk in a secondary collision have not been clarified. It is clear that there is a delay of protection countermeasures for pedestrians in a secondary collision, while those in the initial collision have been advancing.

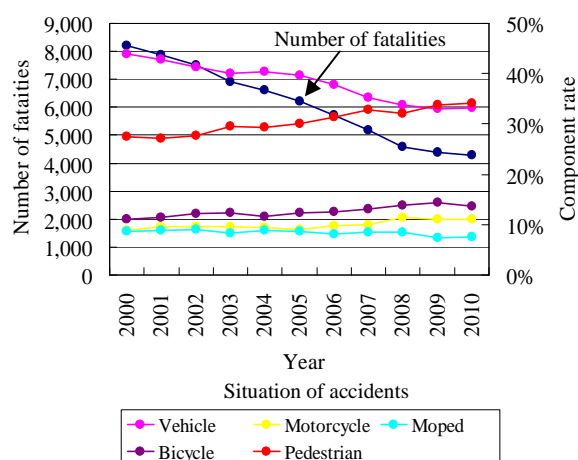


Figure 1. Transition of fatalities from traffic accidents and situation, from 2000 to 2010

The purpose of this study is to clarify the injury risk to a pedestrian in secondary collisions using traffic accident data as well as computer simulation analysis methods. In addition, countermeasures to protect pedestrians in a secondary collision are considered. This study focuses on head injuries because in an analysis of the area of injury responsible for death, head injuries caused 56% of the fatalities, as shown in Figure 2 [2].

RESEARCH RELEVANT TO A SECONDARY COLLISION IN PPEDESTRIAN ACCIDENTS

The reality of accidents relevant to a secondary collision were investigated by using car-pedestrian accident data [3] which was issued by the Institute for Traffic Accident Research and Data Analysis (ITARDA). The report was analyzed by using case examples of accident data for nine years from 1993 to 2001. Pedestrian subjects in this study totaled 104 people.

Figure 3 shows the percentage of parts of the vehicle and such as a road surface causing pedestrian head injuries (AIS2-6). Figure 4 shows the percent of a road surface causing pedestrian head injuries for each vehicle type (AIS2-6). Figure 3 shows that the percentage of a road surface causing pedestrian head injuries is approximately 20% of the total. The

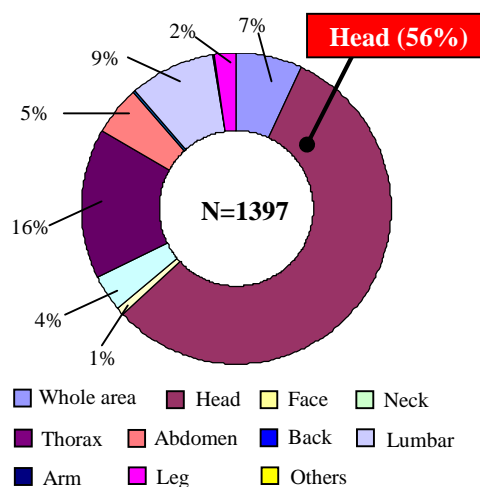
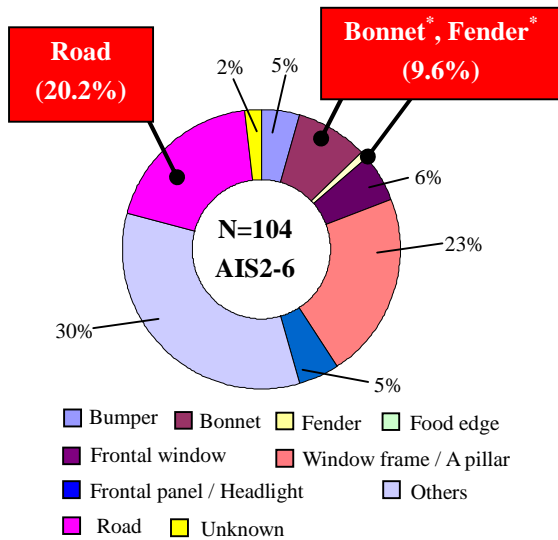


Figure 2. The percent of area of injury responsible for death in traffic accidents in Japan, 2008



*These parts are targeted by regulations of pedestrian head protection worldwide.

Figure 3. The rate of parts of the vehicle, road surface, etc. causing pedestrian head injuries (AIS2-6)

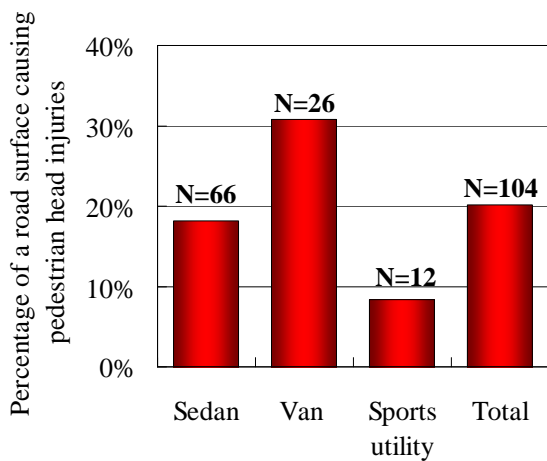


Figure 4. The percentage of a road surface causing pedestrian head injuries for each vehicle type

percentage is approximately twice that of the rate of the bonnet and fender of a car, which are parts targeted by regulations of pedestrian head injury protection worldwide. Figure 4 shows that the percentage of a road surface causing pedestrian head injuries when a pedestrian collides with a van type vehicle is highest of the vehicle models.

For these reasons, an effective countermeasure for pedestrian protection is to prevent or absorb impact of a pedestrian's head on a road surface in a secondary collision.

CLARIFICATION OF PHENOMENON OF A SECONDARY COLLISION IN PEDESTRIAN ACCIDENTS USING COMPUTER SIMULATION ANALYSIS METHODS

In the previous section, it became clear that injury risk in a secondary collision is high in pedestrian accidents. However, it is difficult to observe the phenomenon in a secondary collision using car-pedestrian accident data. An additional problem is that the number of cases investigated in the data was low. Therefore, in this section, car to pedestrian collisions are analyzed by MADYMO (Tass), to clarify the phenomenon in a secondary collision in car-pedestrian accidents. The pedestrian models and vehicle models in this study are made on software (AJAK) in which it is possible to automatically adjust parameters such as the pedestrians' weight and height, bonnet leading edge height, bumper skirt height and ground clearance, and so on [4].

Pedestrian models

First, the age of fatalities in pedestrian accidents was investigated to determine subject pedestrians in the model. Figure 5 shows the age distribution of fatalities in car-pedestrian accidents [2]. The figure shows that adults aged fifty and over have the highest fatality rate in car-pedestrian accidents.

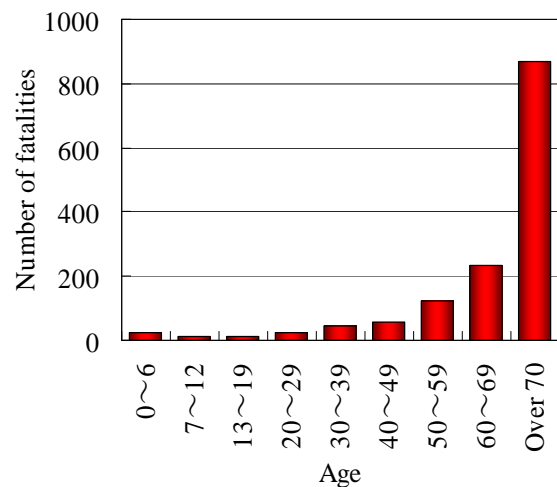


Figure 5. The age distribution of fatalities in car-pedestrian accidents (In Japan, 2008)

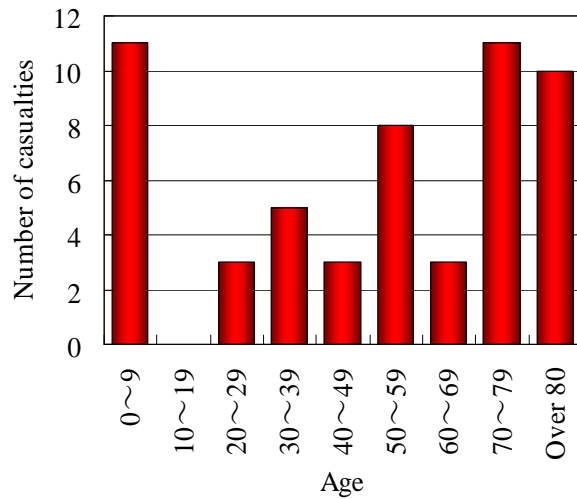


Figure 6. The age distribution of pedestrians who suffered head injuries in car-pedestrian accidents

Moreover, Figure 6 shows the age distribution of pedestrians who suffered head injuries in car-pedestrian accidents [5]. It was analyzed by using case examples of accident data for twelve years from 1994 to 2005. Pedestrian subjects in this study totaled 54 people. The figure shows that head injuries occurred chiefly in children aged nine or younger, and in adults aged fifty or over in pedestrian accidents. From the results, pedestrian models of a child and adults aged fifty or over were chosen for this study.

Next, height and weight of the chosen ages were investigated using literature (shown in Table 1) [6]. From the results, gender-segregated data of height and weight from one-year old to nine-year old children was inserted. From that data, it was found that the height and weight differences of gender are not so large in children of the same age, but differences between ages are significant. Therefore, data for the average height and weight of a six-year old male and female was used for the child model because it is a median in the intended age and gender difference is not large. For adults aged fifty and over, gender-segregated data of height and weight of adults in their fifties, sixties and aged seventy or over was inserted. From the data, it was found that age difference was not so large but gender difference is significant. Therefore, a total of four adult models were made which were based on height and weight data for males and females in their fifties

and males and females aged seventy or over.

Hence, a total of five pedestrian models were made in this study: one child model (based on six-year olds' data, denoted CH06 hereafter) and four adult models (based on data of males and females in their fifties, denoted AM50 and AF50 hereafter, and based on data of males and females in their seventies, denoted AM70 and AF70 hereafter). Table 2 shows the data of height and weight of each pedestrian model and Figure 7 shows each model.

These models were created using a scaling method with the JARI pedestrian model in which these base models' biofidelity was validated using Post Mortem Human Subject test data. The scaling method used in this study followed the method stated in the user manual of MADYMO version 5.4 as a reference.

Table 1. Height and weight data by age (abridgment)

Age	Male		Female	
	Height [m]	Weight [kg]	Height [m]	Weight [kg]
1	0.807	10.9	0.782	10.1
2	0.894	12.5	0.879	12.0
3	0.961	14.6	0.971	14.3
4	1.051	16.9	1.035	16.8
5	1.098	18.7	1.097	18.7
6	1.172	21.2	1.156	20.7
7	1.214	24.5	1.226	23.9
8	1.267	27.6	1.280	26.0
9	1.329	29.3	1.341	31.8
⋮	⋮	⋮	⋮	⋮
50-59	1.673	66.6	1.545	55.0
60-69	1.640	64.2	1.514	53.6
Over 70	1.605	59.3	1.468	49.8

Table 2. Height and weight data of each pedestrian model

Model	Height	Weight
	[m]	[kg]
Child (CH06)	1.164	21.0
Fifties Female (AF50)	1.545	55.0
Seventies Female (AF70)	1.468	49.8
Fifties Male (AM50)	1.673	66.6
Seventies Male (AM70)	1.605	59.3

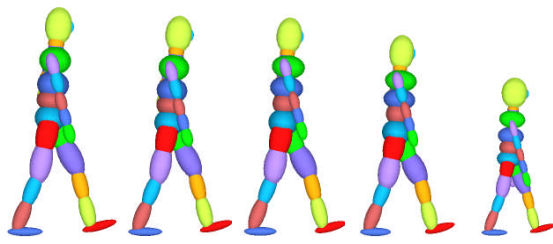


Figure 7. Pedestrian models

Vehicle models

A total of three vehicle models were made in this study which were sedan type, sports utility type and van type, to clarify collision phenomenon for all kinds of vehicle type. Figure 8 shows the construction of a vehicle model's front parts as used in this study. The model consists of some plane elements and some cylindrical elements. Each element is given stiffness which is shown in Figure 9. Figure 10 shows vehicle models used in this study. These models were made based on the data of the average shape of each vehicle from IHRA WG researched results [7].

Collision conditions

The vehicle models collided with the pedestrian

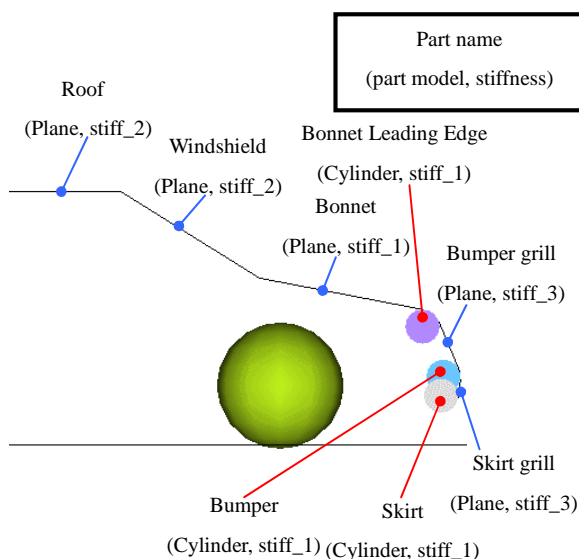


Figure 8. Construction of a vehicle model's front section

models at three collision velocities which were 20km/h, 30km/h and 40km/h. Thereafter, the vehicle models slowed down with deceleration of 0.5G. The stance of pedestrian models was set up as shown in Figure 11 and Table 3. The pedestrian's standing position was made the center of the vehicle models. The pedestrian model was set up for each contact condition to be able to impact the vehicle models and the road surface model.

The road surface model was given stiffness of a real road which was determined by analysis using MADYMO. The data used for analysis was obtained

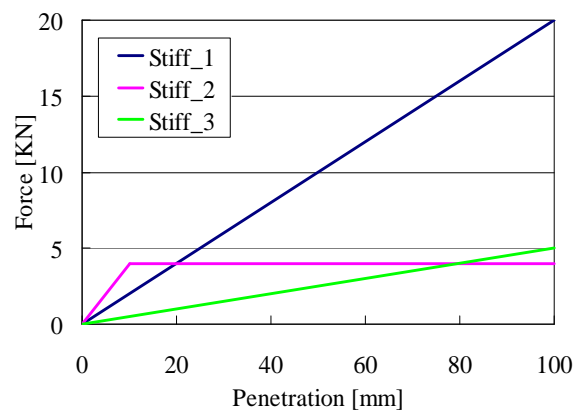


Figure 9. Stiffness of vehicle model

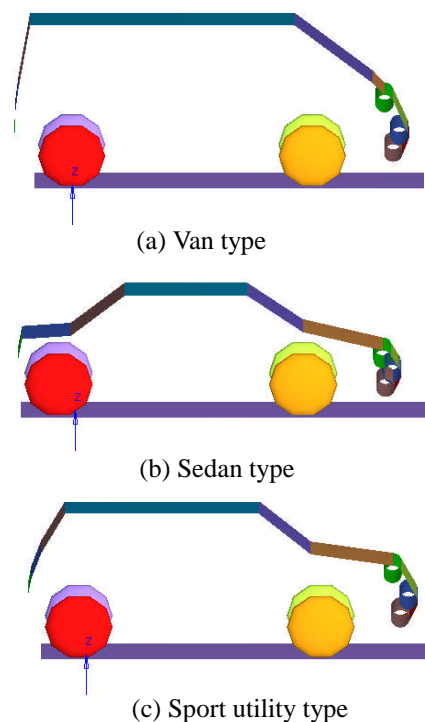


Figure 10. Vehicle models

from an experiment in which a head impactor fell to a real road surface. From those results, the stiffness of the road surface model was shown by the following, Equation 1.

$$F = 1 \times 10^5 x \quad (1)$$

Here F is the force [kN], x is the penetration [m].

All conditions were calculated by using MADYMO version 7.1 in this study.

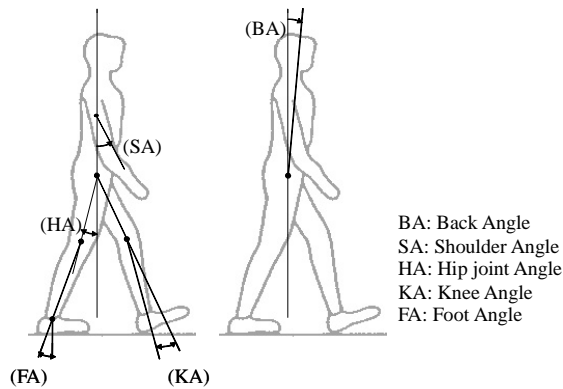


Figure 11. The stance of pedestrian model definition angle

Table 3. The value of the stance of pedestrian model definition angle

	Left	Right
BA (deg.)	+5	
SA (deg.)	-15	+15
HA (deg.)	+29	-12
KA (deg.)	-14	-10
FA (deg.)	0	+22

Results and Discussion

Behavior in collision Figure 12 shows an example of collision behaviors when each vehicle model collides with the child model (CH06) at 40 km/h. The figure shows that the timing of the pedestrian's head impact with the road surface is different according to vehicle model. Specifically, the pedestrian impacts with the road surface at 200ms in the sports utility type, at 400ms in the van type and at 800ms in the sedan type. In addition, behaviors until the pedestrian's head impacts with the road surface vary greatly. Moreover, behaviors of the pedestrian model after colliding with the vehicle models vary greatly as an overall trend when one condition is changed among the pedestrian models, vehicle models and collision velocities.

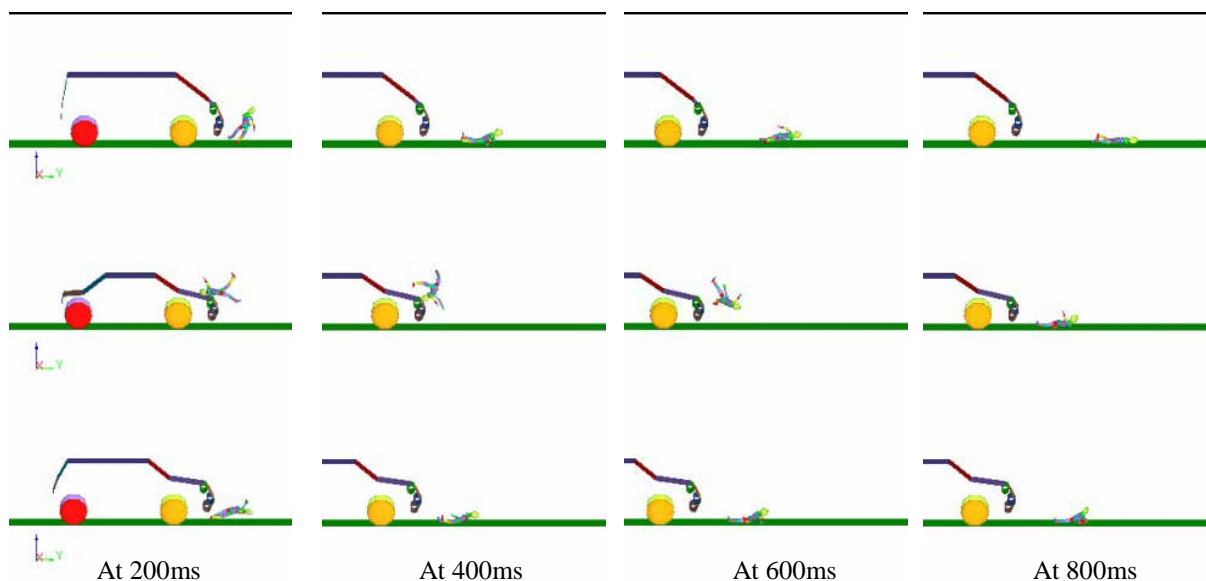


Figure 12. The collision behavior when each vehicle model collided with the child model (CH06) at 40 km/h. Upper: van type, Middle: sedan type, Lower: sport utility type

Comparison of HIC of the initial collision with the secondary collision

Table 4 shows the HIC₁₅ value in each analysis condition to compare injury risk between the initial collision and the secondary collision. In the table, the cases are highlighted in yellow when the HIC₁₅ value is higher in the secondary collision. (That is, the HIC₁₅ values which are highlighted are for the secondary collision). The cases which are not highlighted are when the HIC₁₅ value is higher in the initial collision (That is, HIC₁₅ un-highlighted values are for the initial collision). For the values that are higher in the initial collision, the HIC₁₅ value of the secondary collision is given in parenthesis.

The table shows that the HIC₁₅ value in the secondary collision is higher than that of the initial collision in 38 of the 45 conditions. Additionally, the HIC₁₅ value in the secondary collision exceeds 1000 in three cases when the HIC₁₅ value in the initial collision is higher than that of the secondary collision. (When the HIC₁₅ value exceeds 1000, head injuries generally occur). The HIC₁₅ value in those 38 cases was over 2000 in 30 of the conditions.

Comparison of injury risk in vehicle models

Table 5 shows the average of the HIC₁₅ value for each vehicle model. The results shown in the table are calculated by maximum HIC₁₅ value for each case. The table shows that risk increases in order of sedan type, van type, and sports utility type when comparing the average of the HIC₁₅ value for each vehicle model.

Behavior in collision with the road surface

It was found that a pedestrian's head impacted with the road surface in all conditions in this study. When focusing on behavior of a pedestrian's head impact with a road surface, two major patterns exist. One is the case of a pedestrian's head impacting with a road surface first (shown in Figure 13 a), and the other is the case of any part of a pedestrian, except the head, impacting with the road surface first. Moreover, this second pattern may be further categorized into cases where one pedestrian part (except the head) impacts first, followed by head impact as seen in Figure 13b, and in cases where two or more parts of the body impact first, followed by head impact, Figure 13c. Thus behavior of pedestrian head impact with a road

surface can be categorized by order of impact.

Table 4. HIC₁₅ value in each analysis condition to compare injury risk between initial collision and secondary collision

(a) CH06			
	Vehicle speed [km/h]		
	20	30	40
Van	3048	4401	4434
Sedan	2708	3446	7758
Sports utility	4924	7655	4463
(b) AM50			
	Vehicle speed [km/h]		
	20	30	40
Van	3766	3669	5868
Sedan	1023	1469	19729
Sports utility	4399	4554	3374
(c) AM70			
	Vehicle speed [km/h]		
	20	30	40
Van	7687	4626	961 (125)
Sedan	497 (115)	1361 (1255)	3663
Sports utility	736	3549	2019
(d) AF50			
	Vehicle speed [km/h]		
	20	30	40
Van	2655	6665	2717 (669)
Sedan	400	8751	3630 (2894)
Sports utility	786	35580	13870
(e) AF70			
	Vehicle speed [km/h]		
	20	30	40
Van	1199	910 (317)	10524
Sedan	809	1992	3424 (1852)
Sports utility	5295	2556	10468

Table 5. Average of HIC value in each vehicle model

	Van	Sedan	Sport utility
CH06	3961	4637	5681
AM50	4434	7407	4109
AM70	6157	3663	2101
AF50	4660	4576	16745
AF70	5862	1401	6106
Average	5015	4337	6949

Table 6 shows the relationship between behaviors of impact as categorized above and HIC₁₅ values at that time. The table shows that the HIC₁₅ value becomes low when there is more impact frequency of pedestrian parts except the head with the road surface before the pedestrian's head impacts. This is because the velocities and energy in the pedestrian's head impact with the road surface is decreased when pedestrian parts impact before the head.

Table 6. The relationship between behaviors of impact categorized as above and HIC values at that time

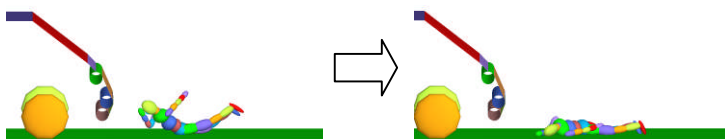
	Pattern (shows the fig. 13)		
	a	b	c
HIC ₁₅ Ave.	9449	3817	2407

STUDY ON COUNTERMEASURES FOR PEDESTRIAN PROTECTION IN SECONDARY COLLISIONS

From the results of accident data research and computer simulation analysis, it was clarified that a secondary collision has a high risk in pedestrian accidents. However, pedestrian protection countermeasures in a secondary collision have not been developed. Therefore, in this section, road characteristics influencing the secondary collision were investigated using computer simulation methods for pedestrian protection.



(a) The case of a pedestrian's head impacting with the road surface first



(b) The case of one pedestrian part, except the head, impacting with the road surface then followed by head impact



(c) The case of more than two pedestrian parts, except the head, impacting first followed by the head

Figure 13. Patterns of pedestrian impact with a road surface

Influence of road characteristics on a pedestrian in a secondary collision

Road stiffness The material was rubber sheet (thickness: 6mm, rubber hardness: A45) which was applied to the road surface in this study. Computer simulation analysis was carried out for two conditions of road surface characteristics which were one layer of rubber, and three layers of rubber. Each characteristic was given the stiffness of a real road which was determined by analysis using MADYMO. The data used for analysis was obtained from an experiment in which a head impactor fell to the road surface for each condition. From those results, the stiffness of one layer of rubber is shown by the following, Equation 2, and three layers of rubber is shown in Equation 3.

$$F = 4 \times 10^3 x \quad (2)$$

$$F = 1 \times 10^3 x \quad (3)$$

Here F is the force [kN], x is the penetration [m].

Analysis conditions Computer simulation analyses were carried out in a total of 90 conditions which consisted of combinations of three kinds of vehicle models (sedan type, sports utility type, van type), five kinds of pedestrian models (CH06, AM50, AM70, AF50, AF70), three collision velocities of car to pedestrian (20, 30, 40km/h) and two kinds of road surface characteristic (one layer of rubber, three layers of rubber). The pedestrian models and vehicle models were those used in the previous sections.

Result and Discussion Figure 14 shows the HIC₁₅ value for each road model. Table 7 shows the number of HIC₁₅ values that exceed 1000 in the secondary collision for each road model.

Figure 14 shows that the HIC₁₅ value is low in all pedestrian models when the road model is changed from characteristics of a real road to characteristics using a buffer such as rubber. In addition, the HIC₁₅ value becomes lower if three layers of rubber are used, compared to one layer of rubber. Table 6 shows that the number of HIC₁₅ values exceeding 1000 in the secondary collision is lower when a buffer is applied.

Therefore, it was found that the rate of a pedestrian's head injury occurring in the secondary collision was favorably influenced by the application a buffer such as rubber and expanded polystyrene to the characteristic of the road surface. Therefore, a buffer is an effective countermeasure to protect a pedestrian's head in a secondary collision. However, decreasing road stiffness greatly decreases the durability of a road surface and travelling performance. Therefore, it is necessary to consider other effective countermeasures including those developed by automobile manufactures for protecting pedestrians from head injuries. In particular, controlling pedestrian behavior after colliding with a vehicle, aimed at reducing injuries when they are knocked to the road in a secondary collision.

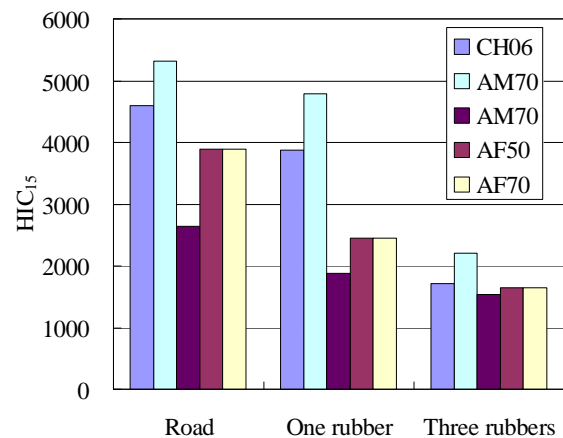


Figure 14. HIC value in each road model

Table 7. The number of HIC values exceeding 1000 in a secondary collision for each road model

	Road	One rubber	Three rubbers
CH06 (9)	9/9	9/9	6/9
AM50 (9)	9/9	8/9	5/9
AM70 (9)	6/9	5/9	4/9
AF50 (9)	7/9	5/9	4/9
AF70 (9)	7/9	7/9	7/9
Total (45)	38/45	34/45	26/45
Probability	84%	76%	58%

CONCLUSION

In this study, the risk to a pedestrian in a secondary collision was investigated using traffic accident data as well as computer simulation analysis methods. From the results of researched traffic accident data, the rate of a road surface or construction causing pedestrian injury is twice the rate of the bonnet and fender of a car, both of which are targeted by regulations of pedestrian head protection worldwide. From the results of computer analysis methods, the HIC₁₅ value in a secondary collision was almost always higher than that of the initial collision. In addition, the HIC₁₅ of the higher value cases was over 2000 in 30 of the 38 conditions. From these results, it became clear that the secondary collision has a high risk of causing injury. It is necessary to not only focus on the initial collision but also focus on a secondary collision in car-pedestrian traffic accidents.

From the modeled results, countermeasures for pedestrian protection in a secondary collision were considered. It was found that one effective countermeasure to protect a pedestrian from head injury is to apply a characteristic of a buffer such as rubber and expanded polystyrene to the road surface. However, such a countermeasure would affect road durability and performance. Therefore, in the future it is necessary to consider other effective countermeasures for protecting pedestrians from head injuries. In particular, controlling pedestrian behavior after colliding with a vehicle, aimed at reducing injuries when they are knocked to the road in a secondary collision.

REFERENCES

- [1] National Police Agency Traffic Planning Division, Traffic accident statistics (2010), 2010
- [2] Ministry of Land, Infrastructure, Transport and Tourism, Road Transport Bureau, 11th Automobile safety symposium, 2010
- [3] Institute for Traffic Accident Research and Data

Analysis (ITARDA), Report of research and analysis of case examples of traffic accidents in 2002, 2002

[4] Kounosu, A., JARI pedestrian model generation and editing software (AJAK), 2004

[5] Institute for Traffic Accident Research and Data Analysis (ITARDA), Report of research and analysis of case examples of traffic accidents in 2008, 2008

[6] Ministry of Health, Labour and Welfare, Report of research of health and nutrition in 2006, 2009

[7] Mizuno, Y., SUMMARY OF IHRA PEDESTRIAN SAFETY WG ACTIVITIES (2005) - PROPOSED TEST METHODS TO EVALUATE PEDESTRIAN PROTECTION AFFORDED BY PASSENGER CARS, ESV Proceedings, Paper Number 05-0138, 2005

VALIDATION OF A PEDESTRIAN SEDAN BUCK USING A HUMAN FINITE ELEMENT MODEL

Shunji Suzuki

Yukou Takahashi,

Masayoshi Okamoto

Honda R&D Co., Ltd.,

Japan

Rikard Fredriksson

Autoliv Research

Sweden

Shinsuke Oda

Autoliv Japan Ltd.,

Japan

Paper Number 11-0277

ABSTRACT

For the purpose of reproducing complex vehicle-pedestrian interactions using a simplified and standardized vehicle model, a previous study has developed a computational model for a generic buck to reproduce car-small sedan interaction using a standardized vehicle front model. Although the previous study validated the buck model using a finite element (FE) model for a pedestrian dummy in terms of pedestrian kinematics and vehicle-pedestrian contact forces, the buck structure has not been further validated with regard to responses of injury measures against a more biofidelic tool such as a human FE model.

The objective of this study was to evaluate the buck model representing a small sedan developed in the previous study (Untaroiu et al., ESV 2009) against a human FE model in terms of pedestrian kinematics and injury measures from comparisons between the buck and full vehicle models.

A human FE model developed by Takahashi et al. (IRCOBI 2010) was used in the current study. For the purpose of validating the buck model, an FE vehicle model representing the same small sedan was also used for comparisons. The pedestrian model was hit by the center of both vehicle models laterally at a baseline impact velocity of 40 km/h used by the previous study. In order to evaluate robustness of the buck model against impact velocity, impact simulations were performed at 20 and 60 km/h as well.

The results of the comparisons showed that the pedestrian kinematics and values of injury parameters were generally well reproduced by the buck model compared to the vehicle model. It was also found that for enhanced representation of the responses of injury measures to the pelvis and lower limb, some modifications to the buck

components are suggested in terms of geometry, material property and structure.

INTRUCTION

The percentage of pedestrian fatalities in traffic accidents is considerably high worldwide from OECD data sets (International Traffic Safety Data and Analysis Group, 2010). Pedestrian fatalities account for over one thousand annually in USA (4378 people, 12% of all road user fatalities), Korea (2137, 36%), Japan (2012, 35%) and Poland (1467, 32%). Especially in Japan, the percentage of pedestrian fatalities exceeds that of vehicle occupants (21%). Therefore, a demand for pedestrian safety technology is increasing to provide safer environments for vulnerable road users.

A study done by IHRA (International Harmonized Research Activity) (Mizuno 2005) showed that in severe injuries to pedestrians, the percentage of lower extremity is one of the highest of all body regions, with severe injury defined as Abbreviated Injury Scale (AIS) 2-6. In the following three countries, the lower extremity accounted for the highest percentage of all body regions (39% in USA from Pedestrian Crash Data Study (PCDS) between 1994 and 1999, 40% in Germany from German In-Depth Accident Study (GIDAS) between 1985 and 1998, 42% in Japan from collected data by Japan Automobile Research Institute (JARI) between 1987 and 1988 and by Institute for Traffic Accident Research and Data Analysis (ITARDA) 1994 and 1998). In Australia, the lower extremity accounted for the second highest percentage (31%) from at-the-scene investigations of pedestrian collisions in the Adelaide metropolitan area in 1999 and 2000. The data from these countries show high priority of

lower extremity protection.

Among lower extremity injuries, pelvic fracture is most important from a viewpoint of threat to life, because pelvic fracture links to a substantial factor in pedestrian morbidity and mortality (Eastridge et al. 1997). Pelvic fracture may cause high blood loss because of the arteries located inside of pelvic ring.

Research for the relationship between pedestrian pelvic fracture and vehicle shape was made by Snedeker et al. (2003, 2005). Takahashi et al. (2010) analyzed pelvic injury patterns due to car-pedestrian collisions and identified three different impact locations relative to the pelvis that lead to different loading mechanisms. These studies analyzed details of pelvis injury mechanism using human FE models and vehicle models to investigate the effect of vehicle front geometry on injury parameters. However, the effect of vehicle stiffness characteristics has not been investigated.

Untaroiu et al. (2009) developed FE pedestrian sedan buck models representing a mid-sized sedan and a large sedan to investigate the influence of vehicle front end structures on pedestrian kinematics and loading. Although the buck models were validated using POLAR II (Akiyama et al. 2001) FE model by comparing pedestrian dummy kinematics and reaction forces with the results of impact simulations using vehicle FE models, the buck models have not been validated in terms of injury parameters.

In this study, injury levels exerted on the pelvis and lower limb along with whole-body kinematics were evaluated using the human FE model developed by Takahashi et al. (2010) by performing car-pedestrian impact simulations using the mid-sized sedan buck model proposed by Untaroiu et al. and a vehicle FE model. Pelvis deformation, femur bending moment, MCL (Medial Collateral Ligament) tensile strain and tibia bending moment were chosen as injury parameters. Pedestrian kinematics was also compared. In addition, the influence of impact velocity was also evaluated by changing the impact velocity.

METHODOLOGY

Human FE Model

In the current study, all the FE simulations were run using PAM-CRASH. The human FE model used in this study was developed by Takahashi et al. (2010). The model represents a mid-sized male anthropometry. The FE lower limb model was extensively validated against numerous published human data as presented by Kikuchi et al. (2006). The pelvis model was validated against the results of the dynamic lateral loading tests using isolated human pelvis performed by Salzar et al. (2008). The upper part of the body was represented using

articulated rigid bodies with the neck and lumbar models divided into seven and five segments, respectively, to represent flexibility of these regions in a biofidelic manner. The kinematics of the full body model was validated in sedan and SUV impacts as performed by Kikuchi et al. (2008), confirming that all the trajectories were within the trajectory corridors developed using the data from published full-scale car-pedestrian impact tests using human surrogates.

Car-Pedestrian Impact Simulations

The pedestrian model was hit laterally from the left by the center of an FE vehicle model and an FE buck model. Figure 1 shows the simulation models for a vehicle model representing a mid-sized sedan and a buck model simulating the vehicle developed by Untaroiu et al. (2009) at the time of initial contact. A gravitational field was applied to the pedestrian model. The lower limbs were rotated about the latero-medial axis by ten degrees with the right limb forward to represent a gait stance. A baseline impact velocity was chosen at 40 km/h as this velocity is used as the standard velocity in regulations and new car assessment programs worldwide. Real world pedestrian accident data show that cumulative frequency of pedestrian accidents is over 90% at 60 km/h in USA, Japan, Germany and Australia (Mizuno 2005). For this reason, in addition to 40 km/h impact, 20 km/h and 60 km/h were also chosen for evaluating robustness of the buck performance against impact velocity.

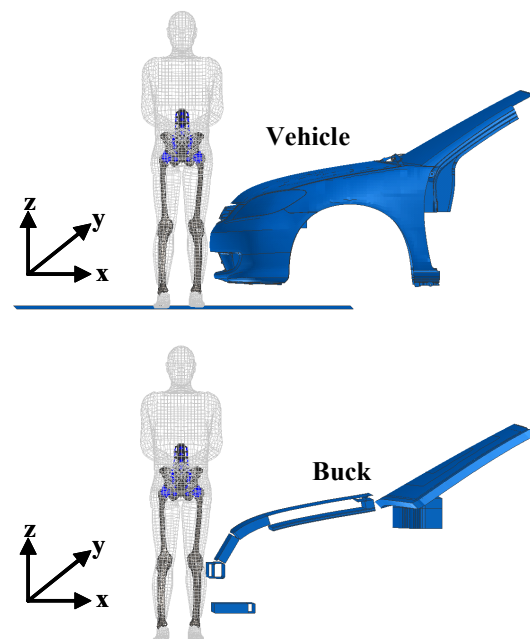


Figure 1. Full scale impact simulation models for mid-size sedan vehicle and buck models.

Injury Parameters

Some injury parameters that correlate with pelvis and lower limb injuries were compared between the full-vehicle and buck models. Ikeda et al. (2010) investigated injury indices for pelvic fracture using a human FE model, and found that lateral compression of the pelvis is the best predictor of pubic rami fracture. Based on this finding, the current study used deformation between the left and right acetabulum for pubic rami fracture as shown in Figure 2. Femur and tibia bending moment were used as injury measures for fracture of these bones. The locations of the cross-sections at which bending moment was recorded are presented in Figure 2. Five and three sections were chosen on the femur and tibia of the struck-side, respectively. Since maximum bending moment was always seen at the distal and proximal cross-sections of the femur and tibia, respectively, only the moment time histories at these cross-sections were used for the analysis. Tensile strain was used as an injury measure for failure of the knee ligaments. Although tensile strain generated at every ligament was recorded, only MCL strain was used in the analysis since maximum strain was always generated in the MCL. Figure 3 shows the locations of the datum points from which MCL tensile strain was calculated.

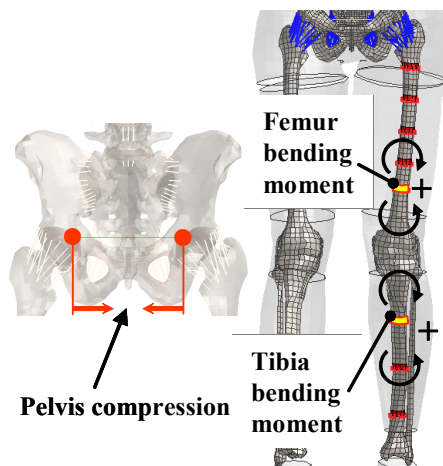


Figure 2. Measurement locations for pelvis deformation, femur and tibia bending moment.

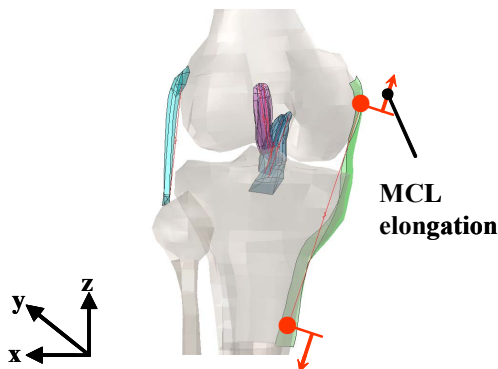


Figure 3. Datum point for MCL tensile strain.

Kinematics

Untaroiu et al. (2009) compared trajectories of the head CG (Center of Gravity), T1 (1st thoracic vertebra), T8 (8th thoracic vertebra) and pelvis of the POLAR II FE model between the vehicle and buck FE models. These locations were used to develop trajectory corridors from full-scale car-pedestrian impact tests using human surrogates for determining performance specifications of pedestrian dummies (J2868 SAE information report). In this study, the same procedure was applied to compare kinematics of the human model between the vehicle and buck FE models.

RESULTS

Injury parameters and kinematics at 40km/h

Figure 4 shows the time history responses of injury parameters generated on the human FE model. Positive pelvis deformation corresponds to decrease in the distance between the datum points defined in Figure 2 (compression). Close magnitude is shown for both the vehicle model and the buck model until 11 ms. After 11 ms up to 32 ms, the result from the vehicle model shows larger pelvis deformation than that from the buck model. At 32 ms, pelvis deformation from both models becomes close again. After 32 ms, the result from the buck model shows larger deformation than that from the vehicle model.

Positive femur bending moment corresponds to femur bending convex to the medial side of the pedestrian. General trend is similar to that of pelvis deformation. Femur bending moment is close between the vehicle and buck models until 9 ms. After 9 ms up to 17 ms, the result from the vehicle model shows smaller femur bending moment than that from the buck model. From 17 ms to 29 ms, close femur moment is shown between both models. After 29 ms, femur moment is larger with the buck model.

As for MCL tensile strain, the vehicle model shows negative strain up to 5 ms but the buck model shows almost no strain up to 3 ms. After 3 ms, both models show increase in MCL strain. Always the buck model shows larger strain than the vehicle model.

Positive tibia bending moment is defined in the same manner as femur moment. Tibia bending moment from both models shows no increase until 6 ms. The result from the buck model shows increase in tibia moment after 6 ms. The result from the vehicle model shows negative peak value at 8 ms and then starts to increase. Between 6 ms and 18 ms, the result from the buck model shows higher moment than that from the vehicle model.

Figure 5 compares trajectories from the human FE model between initial contact to 130 ms. This

termination time was chosen because at this timing the head contacted the windshield with the vehicle model, which was slightly earlier than that for the buck model. Thin lines represent vehicle model results and thick lines show buck model results. Overall, the trajectories match well between the results from the vehicle and buck models, with maximum difference at 130 ms 69 mm for head z-displacement and 41 mm for pelvis x-displacement.

Effect of impact velocity change on injury parameters and kinematics

Figures 6 and 8 compare injury parameter time histories at 20 km/h, 40 km/h and 60 km/h for the vehicle and buck models, respectively. Table 1 summarizes the comparison of the difference in peak injury measures between 20 km/h and 40 km/h and between 40 km/h and 60 km/h. No evident positive peaks of pelvis deformation are identified for the vehicle model. In contrast, both negative and positive peaks of pelvis deformation are seen with the buck model. For this reason, negative peaks of pelvis deformation (pelvis tension) identified for both the vehicle and buck models were compared in Table 1. As for femur bending moment, both negative and positive peaks are identified for both the vehicle and buck models. Overall peaks of femur bending moment are reached on a positive side for all cases except the vehicle model result at 60 km/h. In addition, positive peaks are due to direct contact of the vehicle front structure with the thigh, while initial negative peaks are primarily due to loading to the leg and knee. For this reason, positive peaks of femur bending moment are compared in Table 1. The differences between vehicle and buck models are not significant with the MCL tensile strain and tibia bending moment. As for the pelvis deformation, a larger difference between vehicle and buck models are seen when impact velocity is changed from 20 km/h to 40 km/h. In contrast, for femur bending moment, the difference between the vehicle and buck models is more evident when impact velocity is changed from 40 to 60 km/h. Figures 7 and 9 compare full-body kinematics between 20 km/h, 40 km/h and 60 km/h for the vehicle and buck models, respectively. Similar general trends are seen for both vehicle and buck models. For all trajectories, the horizontal coordinates at 130 ms increased as the impact velocity increased.

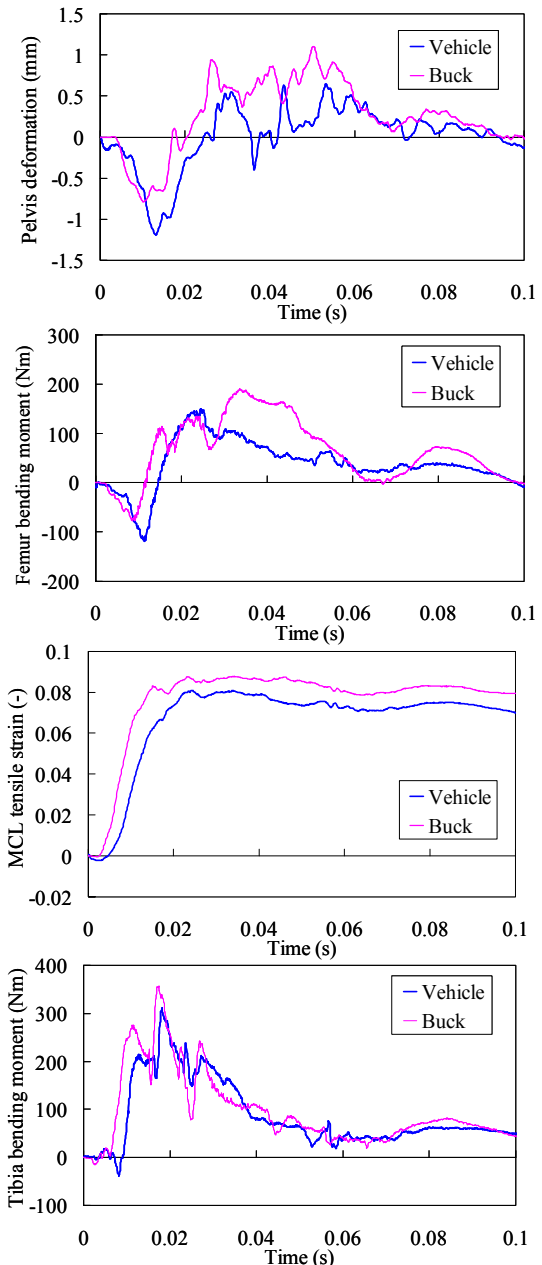


Figure 4. Comparison of time histories of injury parameters between vehicle and buck models.

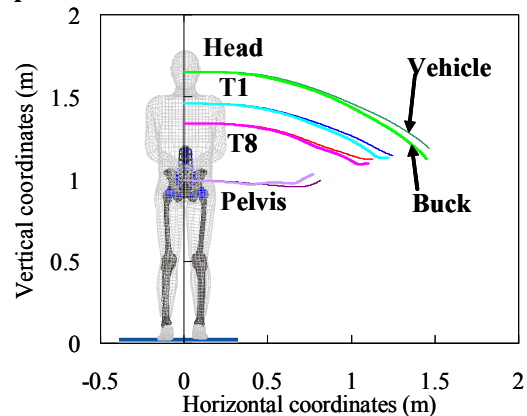


Figure 5. Comparison of full-body kinematics between vehicle and buck models.

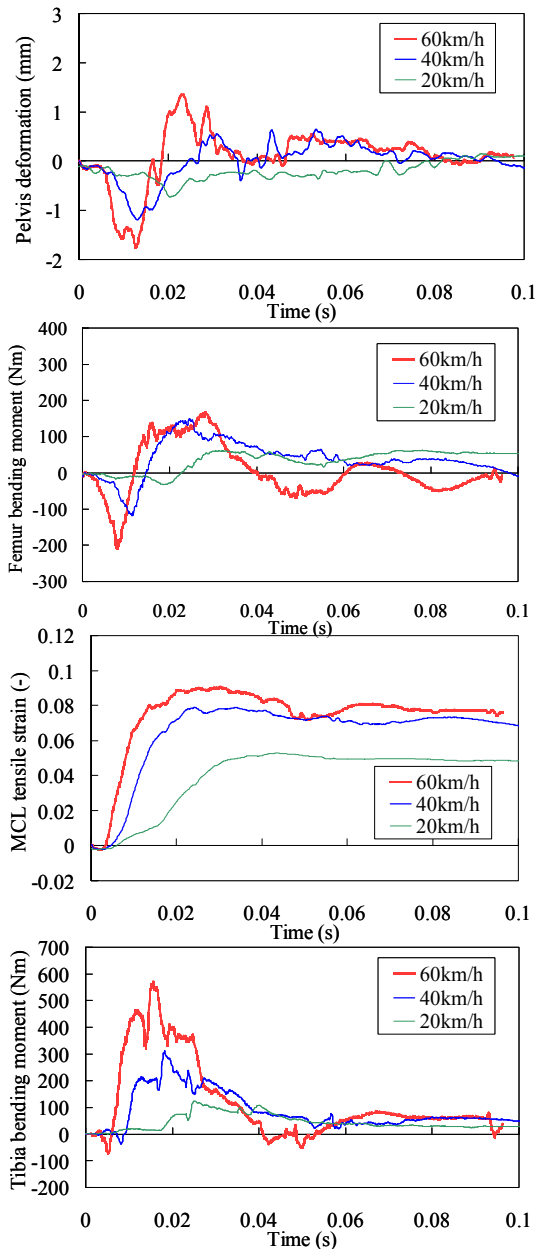


Figure 6 . Comparison of injury parameter time histories between 20 km/h, 40 km/h and 60km/h for vehicle model.

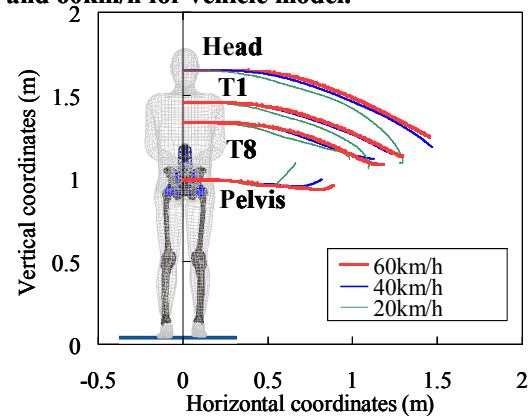


Figure 7 . Comparison of full-body kinematics between 20 km/h, 40 km/h and 60km/h for vehicle model.

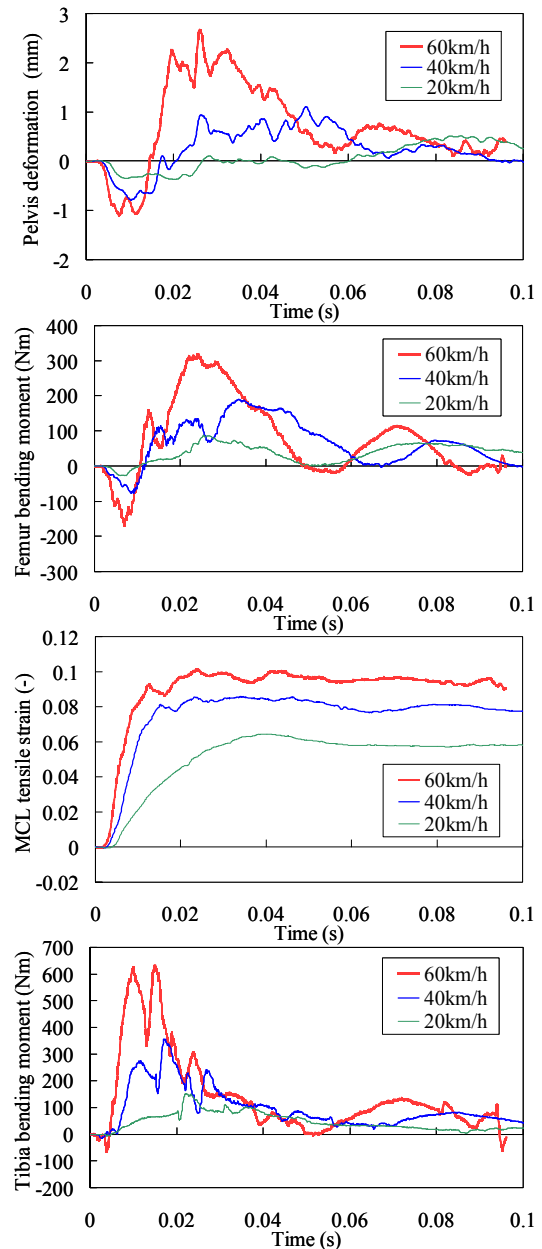


Figure 8 . Comparison of injury parameter time histories between 20 km/h, 40 km/h and 60 km/h for buck model.

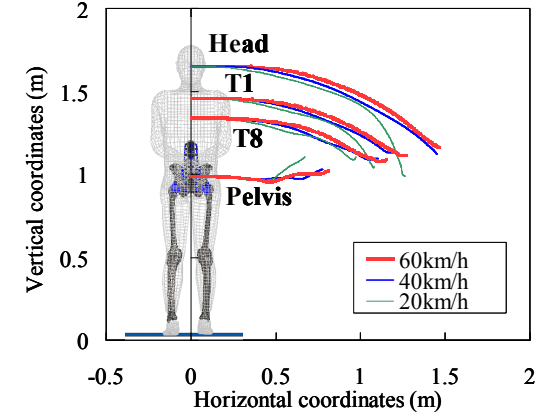


Figure 9 . Comparison of full-body kinematics between 20 km/h, 40 km/h and 60 km/h for buck model.

Table 1 . Comparison of maximum injury parameters ratio from 20 km/h to 40km/h and from 40 km/h to 60km/h

	Pelvis tension		Femur bending moment		MCL tensile strain		Tibia bending moment	
	Vehicle	Buck	Vehicle	Buck	Vehicle	Buck	Vehicle	Buck
20 → 40km/h	165	214	246	219	149	133	115	118
40 → 60km/h	147	139	111	168	249	233	184	177

Unit:%

DISCUSSION

For designing bucks for reproducing car-pedestrian impact, characteristics of loading from the buck to a pedestrian (magnitude, location and timing) are key factors that determine pedestrian injury value and kinematics. Based on this understanding, the effect of the difference in loadings applied to a pedestrian on pedestrian impact responses is discussed.

Since difference in pedestrian kinematics was not significant between the vehicle and the buck in 40 km/h impact, the effect of difference in pedestrian loadings on injury parameters is investigated at this impact velocity. In impact velocity changes from 20 km/h to 40 km/h and from 40 km/h to 60 km/h, similar change in pedestrian kinematics was identified between the vehicle and buck models. In addition, no significant difference in the change of peak MCL tensile strain and tibia bending moment was seen. Therefore, the effect of impact velocity change on negative peak of pelvis deformation and positive peak of femur bending moment is discussed in this section.

Difference in impact force time histories

Difference in injury parameters at 40km/h.

Figure 10 shows the center cross-sections of the vehicle and buck models. In order to investigate onset timing of impact force, all dimensions in x-direction were measured relative to the front end of the bumper face. In order to investigate location of point of application of the force relative to the pedestrian, all dimensions in z-direction were measured relative to the ground level. Since injury is normally assessed by the maximum value of injury parameters, difference of injury parameters was analyzed up to the timing when maximum value was reached.

Figure 11 shows impact force time histories of the hood, grille, bumper face and bumper lower of the vehicle and buck models. The ratios of z-component to x-component of the impact force from the hood, grille, bumper face and bumper lower were 63%, 33%, 18% and 31%, respectively, from a preliminary analysis. Since the ratio of z-component of the impact force was exceptionally large for the hood, both x-component and z-component were compared for the hood, while only x-component was compared for the grille,

bumper face and bumper lower.

Impact force time histories from the hood, grille, bumper face and bumper lower obtained from impact simulations using the vehicle and buck models were classified into four time phases, depending on the difference in loading configuration and magnitude between the vehicle and buck models.

Phase-I: From initial contact up to 5 ms, both the bumper face and bumper lower contacted the lower limb for the vehicle model. In contrast, only the bumper face contacted the lower limb for the buck model. This difference resulted in larger MCL tensile strain for the buck model due to larger rotation of the leg underneath the bumper caused by the lack of loading from the bumper lower. This can be attributed to difference in horizontal location of the bumper lower of the buck model from that of the vehicle model (9 mm difference as shown in Figure 10).

Phase-II: Between 5 ms and 13 ms, two major differences in pedestrian loading situation were identified. The first one is that the grille along with the bumper face and bumper lower applied load to the pedestrian for the vehicle model, while only the bumper face and bumper lower contacted the pedestrian for the buck model. This difference in loading configuration resulted in difference in further difference in MCL tensile strain due to the lack of contact of the thigh with the grille for the buck model, which would yield larger rotation of the thigh. The difference in loading configuration also yielded less impact force applied from the buck model to the distal thigh, resulting in 1) less tensile force at the hip joint and thus earlier shift of pelvis deformation from tension (negative) to compression (positive) and 2) earlier shift of femur moment from negative to positive. The difference in loading configuration can be attributed to difference in horizontal location of the front end of the grille between the vehicle and buck models (9 mm difference as shown in Figure 10).

The second major difference in pedestrian loading situation is that the magnitude of impact force from the bumper face was larger for the buck model, while that from the bumper lower was larger for the vehicle model. Due to higher force from the bumper face of the buck model, tibia bending moment was also higher with the buck model. The lower impact force from the bumper lower of the buck model, along with the previously mentioned

difference, resulted in higher MCL tensile strain due to larger rotation of the leg underneath the bumper. These differences can be attributed to difference in structure and material property of the bumper face and bumper lower, and horizontal location of the front end of the bumper beam between the vehicle and buck models (20 mm difference as shown in Figure 10).

Phase-III: Between approximately 25 ms and 42 ms, both the grille (in x-direction) and the hood (in x- and z-direction) generated higher impact force for the buck model compared to that for the vehicle model. Due to this difference in impact force, pelvis positive deformation (compression) and femur bending moment were both higher for the buck model relative to that for the vehicle model. This can be caused by difference in material property of the grille and hood between the vehicle and buck models.

Phase-IV: Between approximately 42 ms and 55 ms, the magnitude of impact force from the grille was similar between the vehicle and buck models. In this phase, the hood (in x- and z-direction) generated higher impact force for the buck model compared to that for the vehicle model. Due to this difference in impact force, pelvis positive deformation (compression) and femur bending moment were both higher for the buck model relative to that for the vehicle model. This can be attributed to difference in material property of the hood between the vehicle and buck models.

Difference in effect of velocity change As presented in the RESULTS section, a larger difference in pelvis deformation between the vehicle and buck models was seen when impact velocity was changed from 20 km/h to 40 km/h. As for the femur bending moment, the difference between the vehicle and buck models was more evident when impact velocity was changed from 40 km/h to 60 km/h.

Regarding the difference in peak negative pelvis deformation (tension) due to the change in impact velocity from 20 km/h to 40 km/h, peak deformation was reached in Phase-II as described in the previous sub-sub-section. Difference of change in impact force from the bumper face is crucial because 1) this force was predominant compared to the forces from the bumper lower and grille, and 2) the bumper force applied to the knee and distal femur yields tensile force at the hip joint. The ratio of peak impact force from the bumper face between 20 km/h and 40 km/h was 376 % and 256 % for the buck model and vehicle model, respectively. The larger increase in the peak impact force from the bumper face for the buck model can explain the larger increase in negative pelvis deformation (tension). This can be attributed to the difference in rate sensitivity of material property of the bumper face and/or the difference in the

effective mass of the deformed portion of the bumper face.

As for the difference in peak positive femur bending moment due to the change in impact velocity from 40 km/h to 60 km/h, peak bending moment was reached in Phase-III as described in the previous sub-sub-section. In this phase, the ratio of peak impact force between 40 km/h and 60 km/h for the hood in x- and z-direction and the grille in x-direction were all larger with the vehicle model than with the buck model. Since this does not explain the difference in the change of peak positive femur bending moment (larger change with the buck model), other factors must be involved. A possible explanation would be the difference in deformed shape of the hood and grille. At 60 km/h, the foam material representing the stiffness characteristics of the hood and grille of the buck model bottomed out, resulting in concentrated impact forces applied to the thigh from the hood leading edge and upper part of the grille. In contrast, the hood and grille of the vehicle model provided much more distributed loads to the thigh. Since a distributed load yields less maximum bending moment relative to a concentrated load, the difference in load distribution level can explain the more significant increase in femur bending moment with the buck model than that with the vehicle model. This can be attributed to the difference in crash stroke of the hood and grille up to bottoming between the vehicle and buck models.

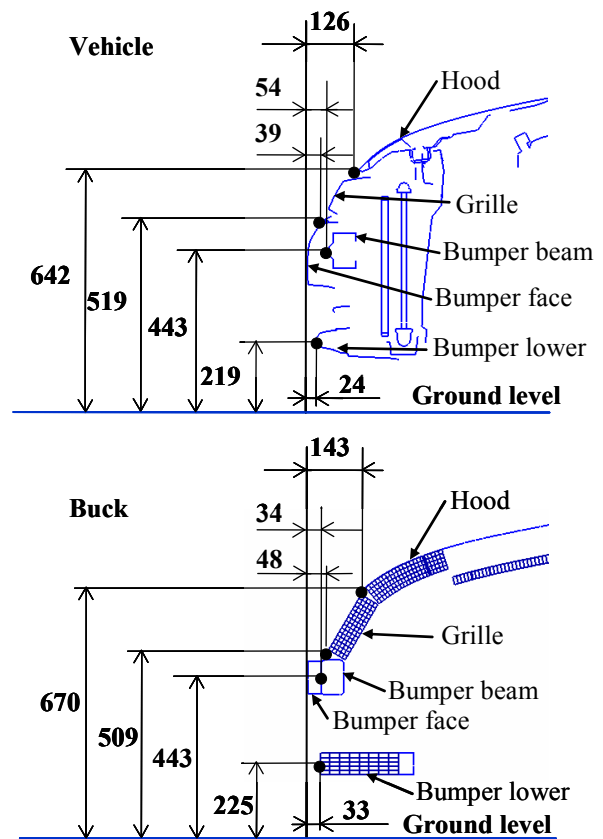


Figure 10. Geometry of vehicle and buck models.

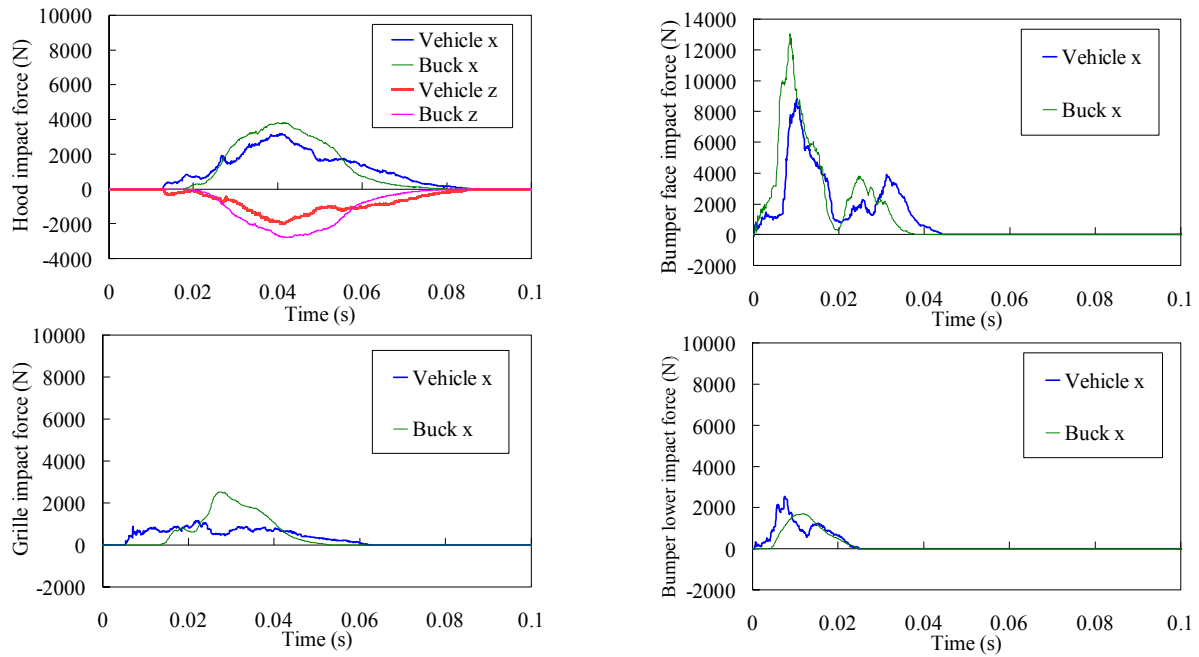


Figure 11. Comparison of impact forces between vehicle and buck models.

Table 2 . Suggested modifications to buck components

Components	Design parameters			Effect on injury parameters
	Geometry	Material	Structure	
Hood		Decreased stiffness		Pelvis positive deformation Femur positive bending moment in phase III and IV
			Increased crash stroke	Femur positive bending moment at velocity change from 40 km/h to 60 km/h
Grille	Front end of grille to be located 9 mm forward			Pelvis deformation from negative to positive Femur bending moment from negative to positive MCL tensile strain in phase II
		Decreased stiffness		Pelvis positive deformation Femur positive bending moment in phase III
			Increased crash stroke	Femur positive bending moment at velocity change from 40 km/h to 60 km/h
Bumper face	Front end of bumper beam to be located 20 mm backward	Decreased stiffness	Decreased stiffness	MCL tensile strain Tibia positive bending moment at phase II
		Less rate-sensitive material	Decreased effective mass	Pelvis negative deformation at velocity change from 20 km/h to 40 km/h
Bumper lower	Front end of bumper lower to be located 9 mm forward			MCL tensile strain at phase I
		Increased stiffness	Increased stiffness	MCL tensile strain at phase II

Suggested modification items for buck components

To enhance reproducibility of interaction with a pedestrian relative to the actual vehicle, suggested modifications to the buck components obtained from the analysis described in the previous sub-sub-section are summarized in Table 2. The reasons for the suggestions are also summarized in Table 2 from a viewpoint of difference in responses of injury parameters. Although the results from the impact simulations using the buck model were in general agreement with those from the vehicle model in terms of injury parameters and kinematics, these suggested modifications to the buck model would provide an enhanced representation of pelvis and lower limb injury parameter responses when impacted by an actual vehicle.

FUTURE WORK

In this study, the buck designed to represent a mid-sized sedan was validated. Due to low profile of the front end geometry of the vehicle, all the impact simulations using the vehicle and buck models resulted in only small pelvis deformation. In order to develop a standardized vehicle model for investigating biofidelity of anthropomorphic tools for evaluating pelvis injuries, bucks representing vehicles with higher bonnet leading edge such as SUVs or minivans that would yield larger pelvis deformation need to be developed.

CONCLUSIONS

In this study, a buck model developed in a previous study was validated against a vehicle model represented by the buck by performing impact simulations using a human FE model. Injury parameters on the pelvis and lower limb along with trajectories of each body region were compared between the vehicle and buck models at various impact velocities.

As a result of comparisons of injury parameters and kinematics, it was found that the buck results generally represent injury and kinematic responses of a pedestrian when impacted by the mid-sized sedan. In order to enhance representation of responses of pelvis and lower limb injury measures, it was also found that the following items are suggested to be modified;

- 1) Geometry of the grille, bumper face and bumper lower
- 2) Stiffness of the hood, grille, bumper face and bumper lower
- 3) Rate sensitivity and effective mass of the bumper face
- 4) Crash stroke of the hood and grille

REFERENCES

- [1] International Traffic Safety Data and Analysis Group Data Sets, <http://internationaltransportforum.org/irtad/pdf/roaduse.pdf>
- [2] Y. Mizuno. 2005, "Summary of IHRA Pedestrian Safety WG Activities – Proposed Test Method to Evaluate Pedestrian Protection Afforded by Passenger Cars", *Paper 05-0138, Proceedings of the 19th Conference on the Enhanced Safety Vehicle (ESV)*
- [3] Brian J. Eastridge, and Andrew R. Burgess, 1997, "Pedestrian Pelvis Fractures : 5-year Experience of a Major Urban Trauma Center", *The Journal of TRAUMA, Volume 42(4), April 1997, pp. 695-700*
- [4] J. G. Snedeker, M. H. Muser and F. H. Walz. 2003, "Assessment of Pelvis and Upper Leg Injury Risk in Car-Pedestrian Collisions: Comparison of Accident Statics, Impactore Tests and a Human Body Finite Element Model", *Stapp Car Crash Journal, Vol 47 (October 2003), pp.437-457*
- [5] J. G. Snedeker, F. H. Walz, M. H. Muser and C. Lanz. 2005 "Assessing Femur and Pelvis Injury Risk in Car-Pedestrian Collision: Comparison of Full Body PMTO Impacts, and a Human Body Finite Element Model", *Paper 05-0103, Proceedings of the 19th Conference on the Enhanced Safety Vehicle (ESV)*
- [6] Y. Takahashi, S. Suzuki, M. Ikeda and Y. Gunji. 2010, "Investigation on Pedestrian Loading Mechanisms using Finite Element Simulations", *International Research Council on the Biomechanics of Impact (IRCOBI)*
- [7] C. Untaroiu, J. Shin, J. Crandall, R. Fredriksson, O. Bostrom, Y. Takahashi, A. Akiyama, M. Okamoto and Y. Kikuchi. 2009, "Development and Validation of Pedestrian Sedan Buck using Finite Element Simulations: Application in Study in the Influence of Vehicle Automatic Breaking on the Kinematics of the Pedestrian Involved in Vehicle Collisions", *Paper 09-0485. Proceedings of the 21th Conference on the Enhanced Safety Vehicle (ESV)*
- [8] A. Akiyama, M. Okamoto and N. Rangarajan. 2001, "Development and Application of New Pedestrian Dummy", *Paper 463, Proceedings of the 17th Conference on the Enhanced Safety Vehicle (ESV)*
- [9] Y. Kikuchi, Y. Takahashi and F. Mori. 2006, "Development of a Finite Element Model for a Pedestrian Pelvis and Lower Limb", *SAE World Congress, paper Number 2006-01-0683*

[10] R. S. Salzar, D. Genovese, C. R. Bass, J. R. Bolton, H. Guillemot, A. M. Damon and J. R. Crandall. 2008, "Load Path Distribution within the Pelvic Structure under Lateral Loading", *International Crashworthiness Conference*

[11] M. Ikeda and Y. Takahashi. 2010, "Investigation on Pelvis Injury Indices Using a Human Finite Element Model", *SAE World Congress, Paper Number 2010-01-1169*

[12] J2868, "Pedestrian Dummy Full Scale Test Results and Resource Materials" *Surface Vehicle Information Report, Society of Automobile Engineers (SAE)*

PEDESTRIAN PROTECTION – PHYSICAL AND NUMERICAL ANALYSIS OF THE PROTECTION OFFERED BY THE WINDSCREEN

**Christian Pinecki,
Laurent Fontaine,
Céline Adalian,
Clément Jeanneau,
Richard Zeitouni.**

PSA Peugeot Citroën
France

Paper number 11-0432

ABSTRACT

Pedestrian head protection is mainly focused on energy absorption when impacting the bonnet. But the technical solutions for mitigating the impact are completely different for the head protection when impacting the windscreen.

Even if regulations do not require an assessment of the protection offered by the windscreen in case of pedestrian impacts, consumerism increased requirements incite us to study in-depth the windscreen, its shape, its boundary conditions and its bonding to optimise adult pedestrian head protection.

Large amount of physical tests were performed with varying all the parameters in order to assess the relative influence of each one.

In parallel, correlation modelling and prediction modelling were performed. Different meshing formulations were also investigated.

The results will be presented showing the effects on the different parameters and the difficulty of modelling them.

This study results in the release of new technical specifications for the windscreen that has to be compatible with the other mechanical and acoustical requirements that need to be fulfilled as well.

INTRODUCTION - AIM OF THE STUDY

Every year, approximately 8,000 pedestrians and cyclists are killed and 300,000 others injured in road accidents in Europe. The accidents are particularly frequent in urban zones. Even when cars are driving at relatively reduced speeds, very severe injuries can occur.

Below a speed of approximately 40 km/h, it is nevertheless possible to considerably reduce the gravity of injury with modifications of the frontal parts of vehicles

So, since 2005, a new European Directive [1] (called “phase 1”) requires the car manufacturers to treat their new vehicles for pedestrian protection.

Moreover, the consumerist organization Euro NCAP assesses the pedestrian protection offered by a new car through component tests [2], [3]. The level of pedestrian protection is then ranked by attributing the vehicle a given number of stars.

The assessment of pedestrian protection offered by a vehicle is made through three different and independent component test procedures corresponding to different body segments:

- the first one is related to the assessment of the protection of the leg. The test is called “legform to bumper test”

- the second one is related to the upper leg. The test is called “upper legform to bonnet leading edge”

- the last one is related to the head, adult head impact and child head impact. The tests are called “Adult and Child headforms to bonnet and windscreen test”

Four specific body form impactors are used in these tests. They are propelled against the front part of the vehicle (from the bumper up to the windscreen depending on the type of test) and they are equipped with several sensors in order to measure biomechanical criteria that are used to assess the risk of injuries (see Figure 1).

Because of the increasing requirements on the pedestrian protection performance in the Euro NCAP new rating (overall rating), the performance of head in the windscreen tests becomes more and more sensible.

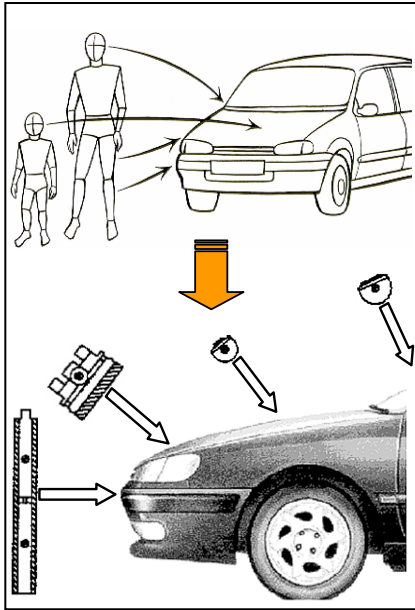


Figure 1. Euro NCAP Pedestrian tests made of body form impactors propelled against the car front-end.

This paper aims to assess the scattering in test and to propose an enhanced numerical model to represent the test of an adult head impactor on the windscreen.

THE ADULT HEAD EURO NCAP TEST PROTOCOL [2]

An adult head impactor is made of a rigid sphere made in Aluminium surrounded by a rubber flesh. The overall radius of the adult head impactor is 82.5 mm, and the mass is 4.5kg.

The test is made by a free flight of the impactor at 40 km/h against the windscreen with an angle of 65° with respect to horizontal (tests can also be performed on the bonnet). The impact zone is defined from wrap around distance measured from the ground.

Pedestrian protection is assessed via a total score of 36 points from which 12 points are dedicated to the adult head tests. The adult zone is divided in sixth. Each sixth will have an impact point. Therefore, each sixth will received a maximum score of 2 points.

For these adult head tests, only one biomechanical criterion is computed: the well known Head Injury Criterion (HIC) calculated from the head acceleration.

$$HIC = \max \left[\frac{1}{t_2 - t_1} \int_{t_1}^{t_2} a dt \right]^{2.5} (t_2 - t_1) \text{ with } (t_2 - t_1) \leq 15ms \quad (1)$$

In this paper, unless specified, the tests presented are carried out following Euro NCAP test protocol:

- head impactor mass 4.5 kg (*),
- impact speed: 40km/h,

- impact angle: 65°,
- damped accelerometer.

(*) Some tests were performed with the head impactor of 4.8 kg because it was the Adult head impactor used by Euro NCAP up to 2009.

DESCRIPTION OF THE PROBLEM

As already explained, head impactor test can be carried out on the upper part of the bonnet, or the windscreen. Experience shows that windscreen tests present a very high scattering level which prevents us to be predictive.

In addition to the usual scatterings experienced in the other type of tests (such as the scattering on the impact velocity), other parameters are supposed to influence the results when testing a point on the windscreen:

- the adhesive that glue the windscreen to the car,
- the curved shape of the windscreen,
- the windscreen thickness,
- the supplier,
- the distance to the windscreen pillar,
- the distance to the dashboard.

These different parameters have to be represented in the modelling which makes this modelling more complex.

This paper presents the study of the following parameters in test:

- the windscreen supplier,
- the distance to the windscreen pillar,
- the windscreen thickness,

In addition, the study presents some possible improvements for the modelling of the phenomenon.

DESCRIPTION OF THE ACCELERATION CURVE OF A HEAD IMPACTOR TEST INTO THE WINDSCREEN

Deceleration curves of head impactor test into the windscreen follow the same trend.

As shown in the following example (see Figures 2 and 3), the head impactor first undergoes an increased deceleration representative of the contact between the windscreen and the impactor and of the start of the cracking (from 0 to 5 ms). Then, a second phase of deceleration occurs, which is smaller in magnitude but longer in duration. This second phase is characteristic of the windscreen stiffness (from 7 to 30 ms).

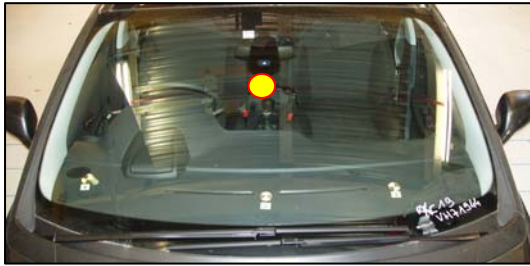


Figure 2. Impact point localisation on the upper part on the windscreen – Car A.

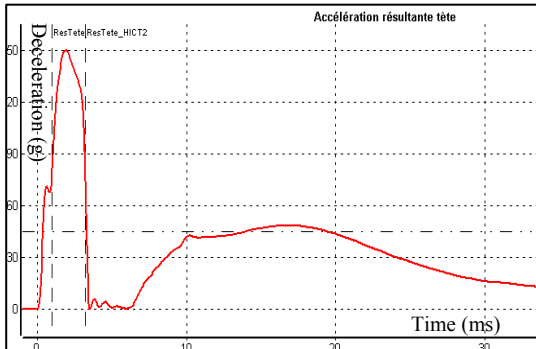


Figure 3. Deceleration curve measured on the impact point as shown in Figure 2.

Sometimes, the first peak is made of several small consecutive peaks.

If the test is made in the lower part of the windscreen, a secondary impact may occur (head impactor to the dashboard) that may overlay the second phase and give a deceleration peak that can be greater than the initial peak ; depending on the dashboard stiffness (see Figures 4 and 5).



Figure 4. Impact point localisation on the lower part on the windscreen – Car A.

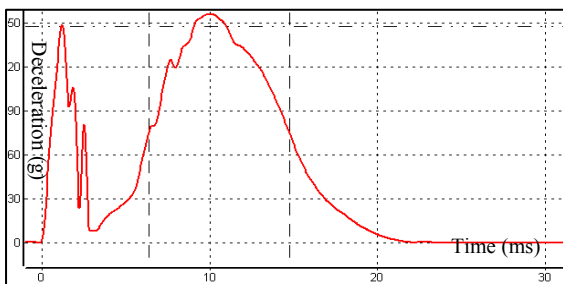


Figure 5. Deceleration curve measured on the impact point as shown in Figure 4.

PHYSICAL STUDY

Influence Of The Windscreen Type

Two types of windscreen have been tested, from two different manufacturers (M-#A and M-#B) with the same test conditions:

- same impact points,
- same windscreen thickness (4.47mm)
- same impactor and test velocity (head impactor of 4.8 kg as used by Euro NCAP up to 2009).

A car model different from the one presented in figure 2 to 5, was used in this test series. It is called “Car B”.

Each test point is tested twice: one with a dashboard, the other without (in order to characterise the windscreen behaviour by itself).

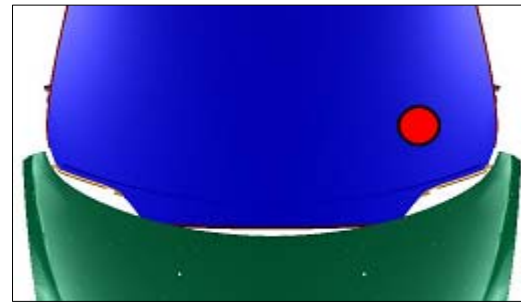


Figure 6. Impact point localisation on the lower part on the windscreen – Car B.

Deceleration curves measured with the windscreen M-#A and M-#B are presented in Figure 7 and 8.

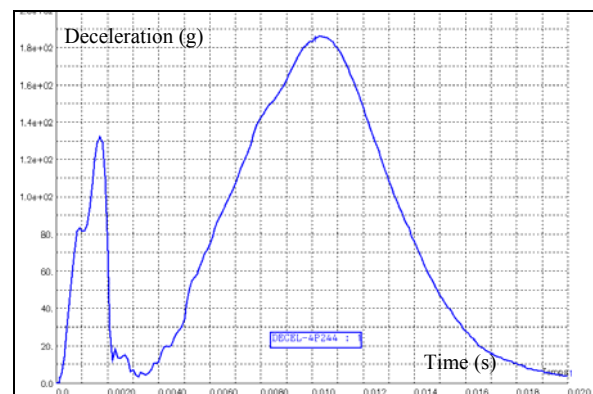


Figure 7. Deceleration curve measured on the impact point as shown in Figure 6 with the M-#A windscreen.

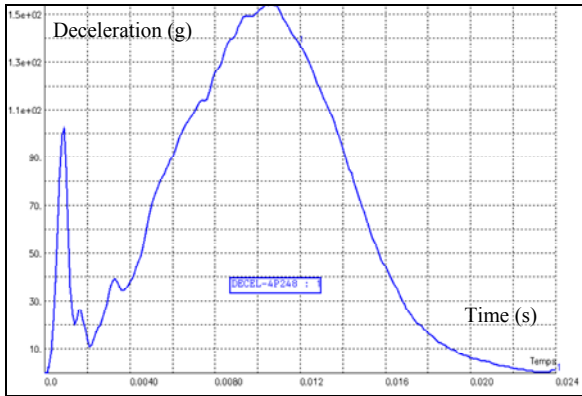


Figure 8. Deceleration curve measured on the impact point as shown in Figure 6 with the M-#B windscreen.

Pictures presented in Figure 9 and 10 clearly show that the post test deformation and cracks are different between the two windscreens. M-#B breaks into tiny pieces whereas M-#A breaks into bigger pieces.



Figure 9. Post impact picture of test with M-#A windscreen



Figure 10. Post impact picture of test with M-#B windscreen

In order to remove the dashboard stiffness influence from the windscreen behaviour, additional tests were performed without the dashboard. The deceleration curves of these tests are presented in Figure 11.

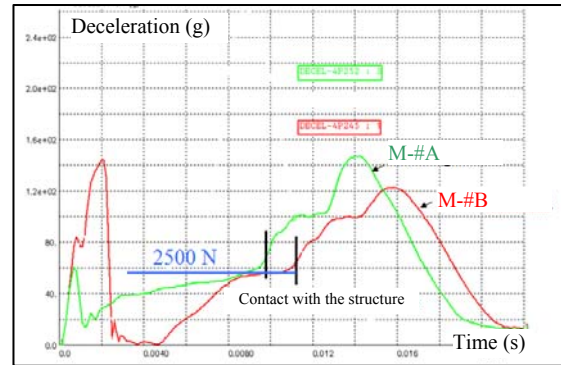


Figure 11. Comparison of the deceleration curves measured on car B without dashboard with the two windscreens.

Although the dashboard was not fitted on the latter tests, a secondary impact is still present (at 10 to 12 ms), because of the impact with structural elements present below the dashboard.

The following curves (Figure 12) show the energy absorbed in function of head displacement into the windscreen with the two windscreens and with and without dashboard.

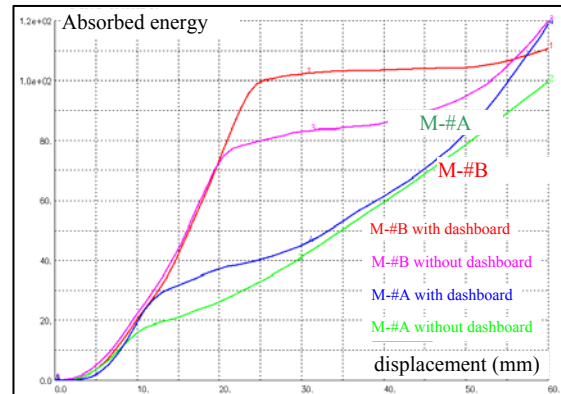


Figure 12. Comparison between the energy absorbed in function of head impactor displacement into the windscreen with the two windscreens and with and without dashboard

The curves shown in Figure 12 highlight the different behaviour between the two types of windscreens, especially during the phase when there is no interaction with the dashboard or its structure below.

The M-#B windscreen dissipate quickly the energy (high initial load peak) then a plateau occurs (from 20 mm to 50 mm of head impactor displacement).

Whereas the M-#A windscreen dissipates the energy in a progressive and linear way.

After 50 mm of head impactor displacement the tests with the dashboard evolves in a different way that the test without the dashboard

The windscreen behaviour differs between the manufacturers. The energy dissipated in windscreen M-#B is slightly greater than the M-#A one (up to 50mm displacement).

Moreover, after the first peak, the load crush level are similar (around 2500 N, see figure 11).

In conclusion, if the dashboard is farther than 50 mm from the windscreen, in order to dissipate more energy, M-#B windscreen is to be privileged to minimise the energy to dissipate into the dashboard.

Influence Of The Impact Point Localisation With Respect To The Windscreen Pillar

In order to characterize the windscreen behaviour when impacted close to its pillar, the following tests were performed.

- Car A with M-#B / 4.47mm thickness windscreen
- same impact points at WAD 2100 (in order to avoid a secondary impact to the dashboard),
- same impactor and test velocity
- different distances from the windscreen pillar are tested (80-95-110 mm)

Figure 13 and 14 present the test carried out at 80 mm from the windscreen pillar and its deceleration curve.



Figure 13. Impact point at 80 mm from the windscreen pillar – Car A.

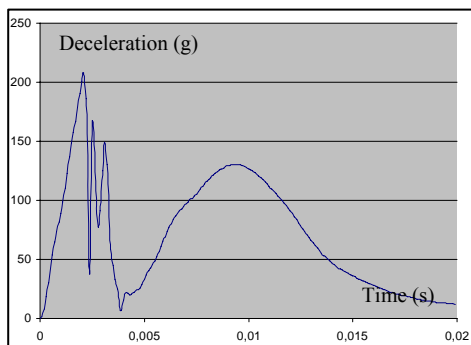


Figure 14. Deceleration curve measured on the 80 mm impact point as shown in Figure 13.

The first peak is 207g, then there is a second phase with a maximum deceleration of 131 g. This gives an HIC of 1111 which corresponds to a score of 1,37 points (out of 2 points). It is important to notice that there is no contact between the head impactor and the windscreen pillar during the test.

Figure 15 and 16 present the test carried out at 110 mm from the windscreen pillar and its deceleration curve.



Figure 15. Impact point at 110 mm from the windscreen pillar – Car A.

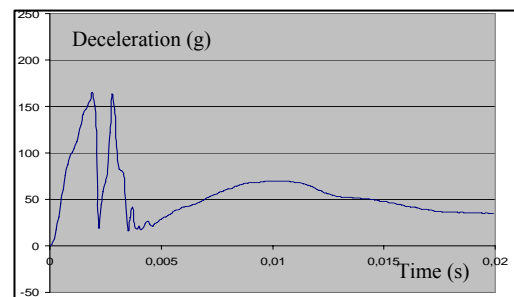


Figure 16. Deceleration curve measured on the 110 mm impact point as shown in Figure 15.

In this last test, the first peak is 165g, then, the maximum deceleration of the second phase is 80 g. This gives an HIC of 430 which corresponds to a full score (2 points). For sure, in this test again, there is no contact between the head impactor and the windscreen pillar during the test.

This latter test (110 mm) was reproduced a second time. The second curve is shown in Figure 17.

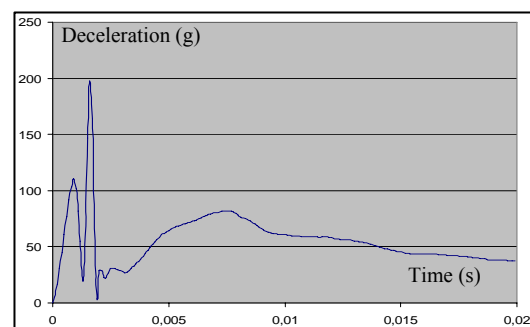


Figure 17. Deceleration curve measured on the 2nd test made at 110 mm.

In this 2nd test, the first peak is 197, then the maximum deceleration of the second phase is 80 g. This gives an HIC of 452 (compared to 430 in the 1st test) which corresponds to a full score (2 points). HIC values are therefore similar even if the first 5 ms of the deceleration curves are different.

By analogy with the adult head impactor size (diameter is 165 mm), we can then conclude that a distance equivalent of the radius of the impactor (82,5 mm) is not sufficient to get 2 points. It is needed to be at 110 mm at least to get the full score at Euro NCAP.

Influence Of The Windscreen Thickness

Another part of the test series was to study the influence of the windscreen thickness. For this purpose, two thicknesses were tested in the same test configurations: 3.96 mm and 4.47mm, with dashboard and M-#B windscreen. Every test configuration is repeated twice.

The impact point is presented in Figure 18.

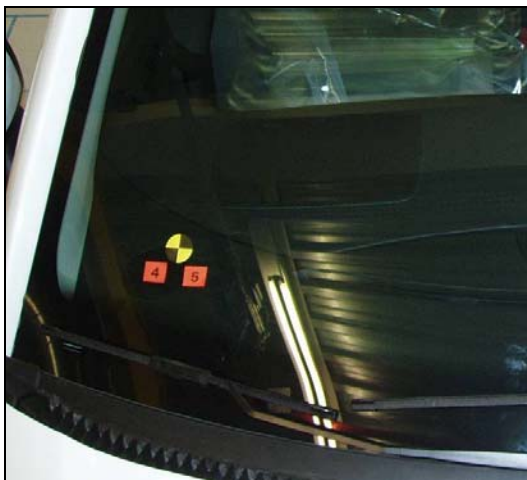


Figure 18. Impact point for the test of the windscreen thickness influence – Car C.

Deceleration curves of the two tests with the 4.47 mm thickness are presented in Figure 19.

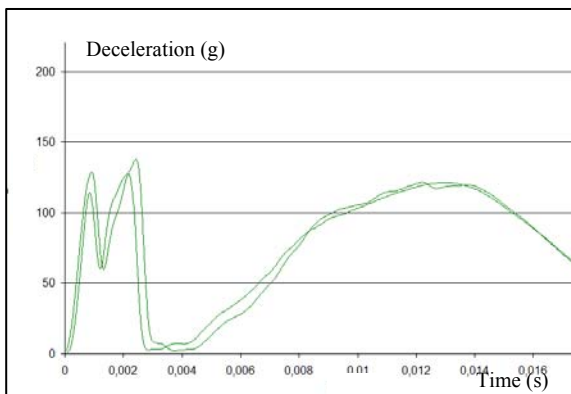


Figure 19. Deceleration curves of the two tests with the 4.47 mm thickness.

Between 0 to 4 ms, two peaks appear on both curves. First peak is 110 to 130 g and 2nd peak is 120 to 140g. Then, there is a drop and a second phase where the deceleration reaches 120 g.

Deceleration curves of the two tests with the 3.96 mm thickness are presented in Figure 20.

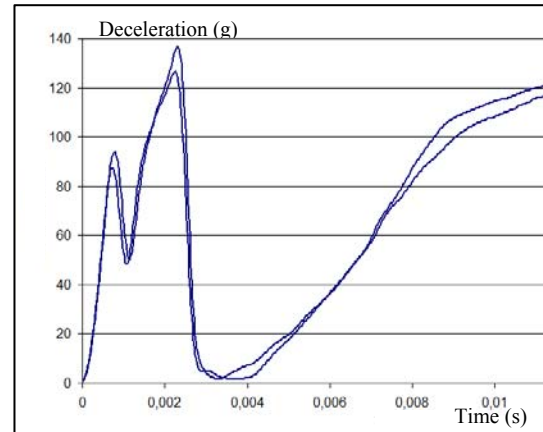


Figure 20. Deceleration curves of the two tests with the 3.96 mm thickness.

Here again, between 0 to 4 ms, the two peaks appear. First peak is 80 to 100 g and the 2nd peak is 120 to 140g. Then, there is a drop and a second phase where the deceleration reaches 120 g.

A comparison between the average curve of the 3.96 mm windscreen and the 4.47 mm one is presented in Figure 21.

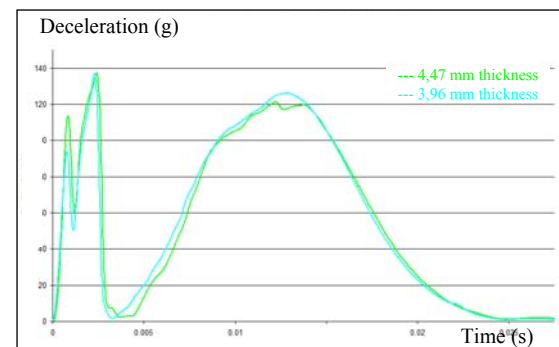


Figure 21. Comparison of the deceleration curves for the two thickness (3.96 mm and 4.47 mm thickness).

Except the magnitude of the first peak, the deceleration curves are very similar between the two thicknesses. The magnitude of the first peak is lower with the 3.96 mm windscreen because its inertia (its mass) is lower.

In conclusion, these tests show that the windscreen thickness is not a key parameter for reducing the head to windscreen HIC (for a 12% variation of the thickness). HIC are approximately the same for these four tests: between 1040 and 1140.

But other parameters are important to clearly understand the headform impactor test on the windscreen and they have to be clearly understood. For this reason, an additional study was carried out based on numerical analysis to create an enhanced modelling of the windscreen. This is presented in the following chapter.

NUMERICAL STUDY

Five-Points Flexion Test

The purpose of this test is to validate the modelling of the windscreen without taking into account any other influence, such as the dashboard or the windscreen proximity.

The test configuration chosen, in order to represent a head impactor test into the windscreen, is a five-points flexion test. The load is applied on the centre of the windscreen and the contact with the test trig is made via non-friction balls fixed between two plates attached to the windscreen extremities.

The load is applied by a displacement controlled hydraulic jack. The displacement velocity is 50 mm/mn.

Several windscreens were tested up to rupture.

The following measurements were made with a 200 Hz sampling frequency:

- load applied by the jack
- jack displacement
- a total of 36 strain gages glued on the inner part and the outer part of the windscreen (45° set of strain gages)

Figure 22 presents an overall view of the test rig.

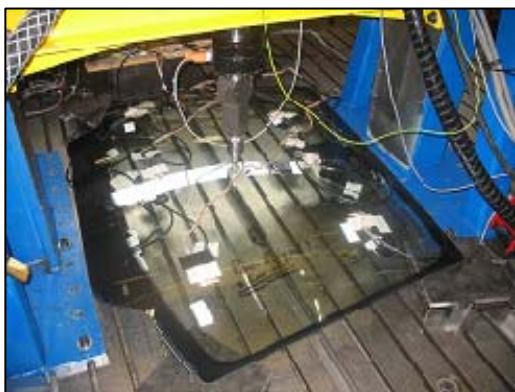


Figure 22. Overview of the test rig used for the windscreen flexion characterisation

Results get from the different tests are presented in Figure 23.

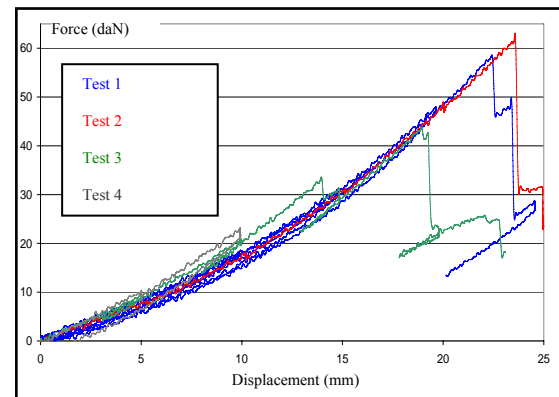


Figure 23. Load vs displacement of the windscreen tested in five-points flexion.

The results in terms of stiffness are very similar and we can state that this test shows good repeatability.

But the level of rupture is significantly scattered, but this can be expected for a fragile material such as glass.

Windscreen Modelling

In the first part of the section, we will present the model formulation used for the windscreen. And the next section, we will present the correlation between physical tests and modelling.

Some glass models with rupture have already been developed and presented to the scientific community [4], but the calculation time is really important which make them difficult to use in the automotive industry, for the development of a project of vehicle.

Indeed, these models request size meshes of 0.1 mm, whereas we are currently using meshes of 5 to 10 mm.

A standard windscreen is made of 3 layers:

- The first layer (external layer) is made of glass. Thickness can be from 1.8 mm to 3.15 mm,
- The second layer is made of "PVB" (Polyvinyl Butyral) of 0.76 mm,
- The third layer (internal layer) is made of glass. Thickness can be from 1.8 mm to 2.1 mm.

The windscreen under study had the following characteristics:

- The external layer had a thickness of 2.1 mm,

- The second layer is 0.76 mm,
- The internal layer had a 1.6 mm of thickness.

Figure 24 describes the 3 layers as modelled via the crash software (Radioss®).

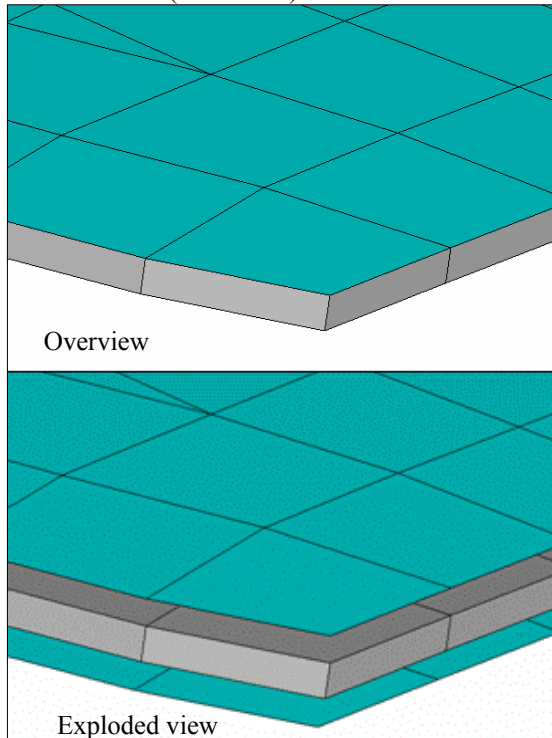


Figure 24. Overview and exploded view of the mesh and model.

The two layers of glass are modelled via a shell formulation with the actual thickness taken into account. The mesh corresponds to the neutral fibre position.

On the other hand, the middle layer (PVB) is modelled by 8 nodes brick elements.

In order to get a consistent mesh, the thickness of PVB has to be modified.

Its mesh thickness is then its own thickness + half the thickness of the internal and external layers. For this reason, the constitutive law of PVB had to be modified (stiffness and density).

Correlation Between Physical Tests And Modelling

Figure 25 compares physical test and modelling as defined in the previous section.

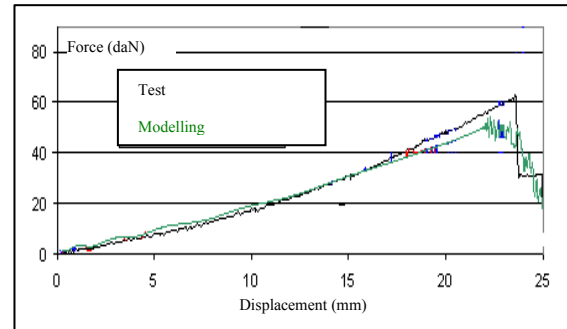


Figure 25. Correlation between test and modelling of the 5-points flexion tests.

In the first model, the constitutive law for the two glass layers was a “fragile elasto-plastic” law with an elastic limit (von Mises stress) of 75 MPa.

Two other calculations were made with an elastic limit of 50 and 100 MPa. The consequences can be found on the load at rupture as shown by Figure 26.

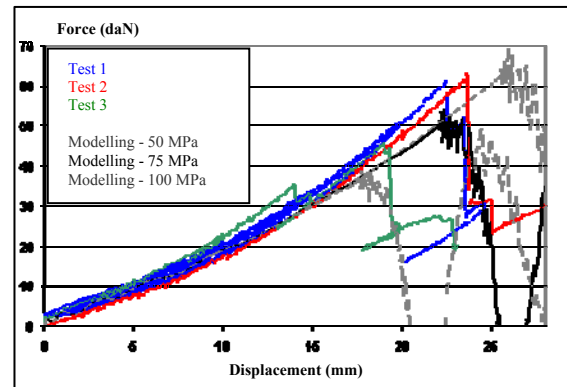


Figure 26. Comparison between test and modelling and influence of the load at rupture.

Following this comparison, it seems that the threshold at 75 MPa is closer to reality than the two other ones.

Modelling Of The Headform Test On The Windscreen

The model correlated thanks to the 5-points flexion tests was used to represent the behaviour of the windscreen when impacted by a 4,8 kg headform impactor at 35 km/h and with an impact angle of 35°.

Test results were X, Y, Z deceleration vs time curves from which we can calculate HIC.

Figures 27 and 28 present the test results.

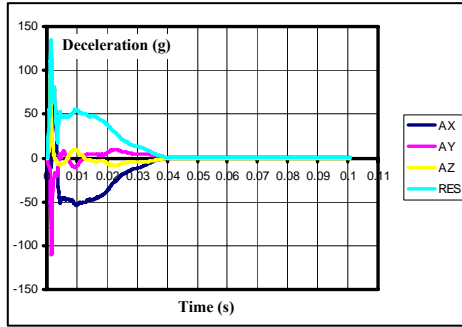


Figure 27. Test results of a head impactor on the windscreen.

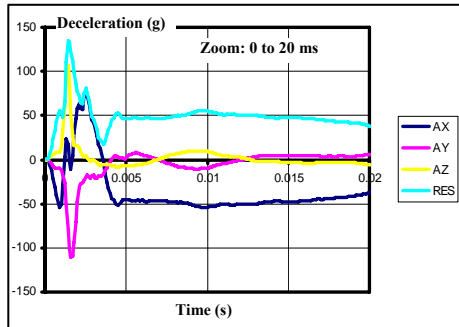


Figure 28. Test results of a head impactor on the windscreen (zoom 0 to 20ms).

As already mentioned, at the very beginning of the test, there is a first peak (135 g at 2 ms in X) which can be described as a dynamic initiation of the glass rupture. Then, the second phase occurs, (longer, at a level of 50 g in X) which can be described as the propagation of the crack in the glass.

In this test, HIC was 360.

Figure 29 presents an overview of a head impactor modelling for a vehicle project.

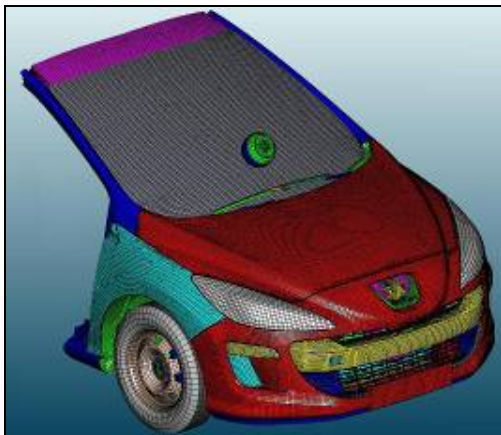


Figure 29. Overview of a head impactor modelling for a vehicle project

As already explained, we used the “shell-brick-shell” modelling for the windscreen. When comparing this model to the physical test, resultant

acceleration does not give a good correlation, as shown in Figure 30.

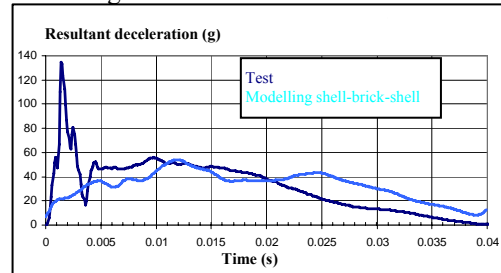


Figure 30. Comparison between test and shell-brick-shell modelling.

The initial peak deceleration is not present in the modelling and the HIC value in the model is 283 (for 352 in the test).

In order to optimise the modelling and enhance the correlation, some numerical and some physical parameters have been studied. Each parameter was studied independently from the others, as presented in the following sections.

Stiffness Of The Adhesive Bead Of The Windscreen

The first parameter under study was the stiffness of the adhesive bead. In order to magnify the influence of this stiffness, we carried out modelling where we artificially increased it by a 100 times with respect to the reference model (see Figure 31).

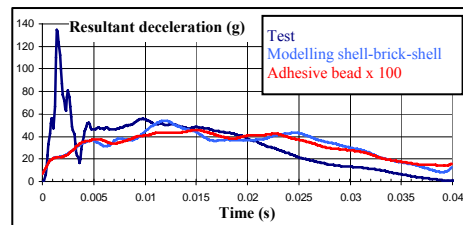


Figure 31. Influence of the windscreen adhesive bead on the head impactor deceleration.

Clearly, the influence of the adhesive bead is not a key parameter to improve the modelling of the headform impactor deceleration.

Stiffness Of The Contact Interface Between Headform Impactor and Windscreen

Another parameter under study was the type of contact defined in the modelling. This is a purely numerical parameter following the “penalty method”.

Several values were tried :1000, 500, 200, 100, 50 (see Figure 32):

- 100 and 50 were used with the headform as the master element of the contact surface.

- For 1000, 500 and 200 values, too much additional and artificial mass was added by the software to keep the calculation stable.

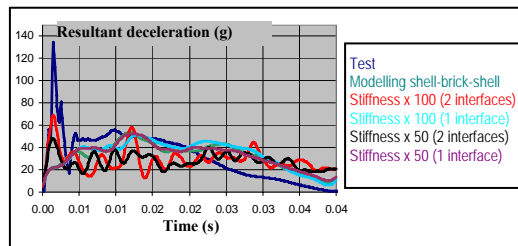


Figure 32. Influence of the stiffness of the head impactor to windscreen interface on the deceleration.

We can see in Figure 32 that the initial peak can be improved (2 interfaces – stiffness 100) but this worsens the rest of the curve.

Rigid Body Model For Headform Impactor and Embedment For Windscreen

In order to see if the initial peak is due to a difference in stiffness between the windscreen and the headform impactor, one idea was to define the headform impactor as a rigid body and the adhesive bead as a complete embedment. The result of this numerical model is shown in Figure 33.

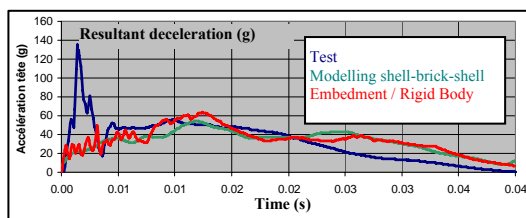


Figure 33. Influence of the type of modelling (rigid body model for headform impactor and embedment for windscreen) on the deceleration.

No significant influence is shown with this type of modelling.

Influence Of The Strain Rate

Radioss software proposes two formulations (ICC 1 and ICC 2) to take into account the influence of the strain rate as shown in Figure 34.

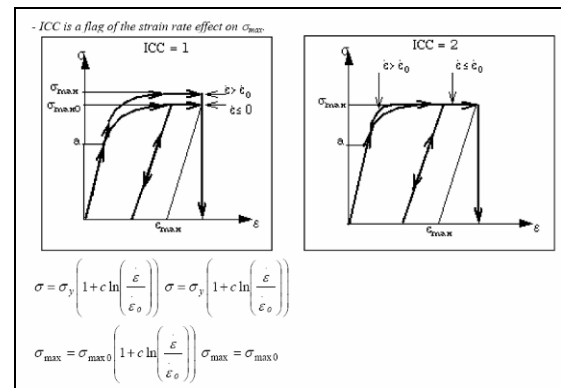


Figure 34. Influence of the strain rate as proposed in the software.

Two strain rate coefficients were tested, with the two Radioss formulation (ICC 1, ICC2) but with little influence, again, as shown in Figure 35.

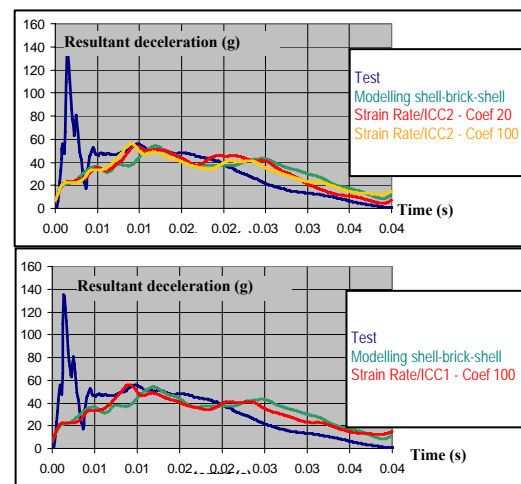


Figure 35. Influence of the strain rate on the headform impactor deceleration using different modelling parameters.

Influence Of The Time Step

Recommendation of modelling experts at PSA Peugeot Citroën is to use a $1 \cdot 10^{-6}$ s time step. But we also tried another time step ($2 \cdot 10^{-7}$ s) as shown in Figure 36 ; unfortunately without any influence.

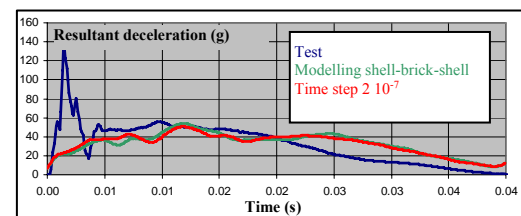


Figure 36. Influence of the time step on the headform impactor deceleration.

Influence Of The Damage Parameters

The glass is modelled via type 27 law in Radioss. The different input parameters of type 27 are shown in Figure 37.

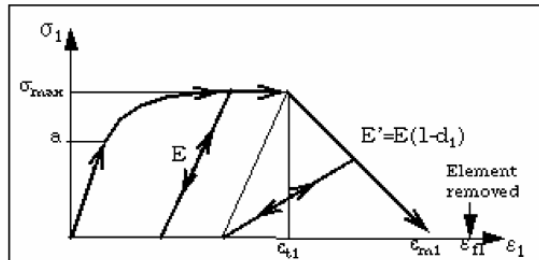


Figure 37. Input parameters of the Type 27 law.

Standard parameters such as σ_{Max} , a , E , ϵ_{t1} and d_1 are defined in literature. But ϵ_{m1} et ϵ_{f1} , characterising the damage undergone by the element, are not well known and not described in literature. Therefore, we studied the influence of these parameters on the headform impactor deceleration.

Influence of ϵ_{m1} and ϵ_{f1} .

In the reference model (named shell-brick-shell modelling), ϵ_{m1} was set at $2.7 \cdot 10^{-3}$ and ϵ_{f1} was set at $2.71 \cdot 10^{-3}$.

Other calculations were made with ϵ_{m1} set at $5 \cdot 10^{-3}$, $1 \cdot 10^{-2}$ and $2 \cdot 10^{-2}$. The results are shown in Figure 38.

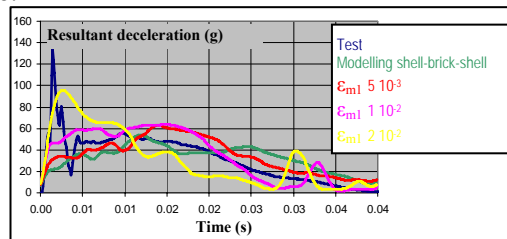


Figure 38. Influence of ϵ_{m1} on the headform impactor deceleration.

Same philosophy was applied to ϵ_{f1} set at $5 \cdot 10^{-2}$, $2.7 \cdot 10^{-2}$ and $2.7 \cdot 10^{-1}$ (see Figure 39).

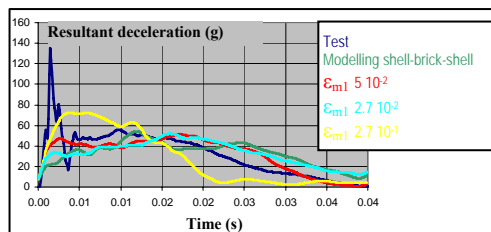


Figure 39. Influence of ϵ_{f1} on the headform impactor deceleration

A final modelling was made by changing the two parameters at the same time (see Figure 40).

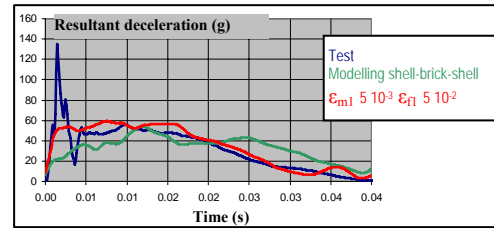


Figure 40. Combined influence of ϵ_{m1} and ϵ_{f1} on the headform impactor deceleration.

The corresponding HIC are 352 for test, 283 for the reference modelling and 410 for the combined influence.

Here again, no significant improvement is shown by this parameter study.

Influence of the mesh size

The size of the mesh in the reference modelling is $14 \times 14 \text{ mm}^2$ for the windscreen.

In order to highlight any influence of the mesh size, we decided to divide the mesh size by two in the windscreen; except for the number of element in the middle layer (PVB).

The consequence on the headform impactor deceleration is presented in Figure 41.

Unfortunately, here again, no significant improvement is found whereas the time step decreased from $1 \cdot 10^{-6}$ to $0.2 \cdot 10^{-6}$ s.

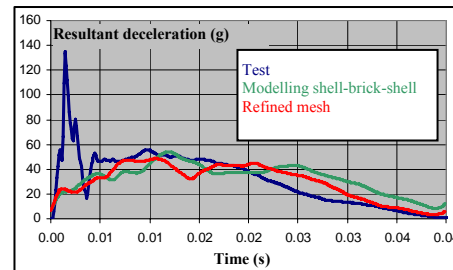


Figure 41. Influence of the mesh size on the headform impactor deceleration.

Another combination was carried out with a refined mesh and the damage parameters. The consequence on the headform impactor deceleration is presented in Figure 42.

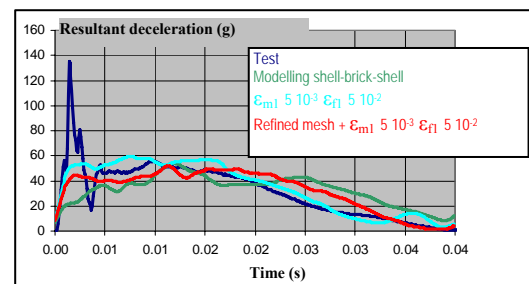


Figure 42. Combined influence of $\epsilon_{m1} + \epsilon_{f1}$ and mesh size on the headform impactor deceleration

A final mesh refinement was made by dividing the initial mesh by 4 in order to have a mesh size of $3.5 \times 3.5 \text{ mm}^2$. This could be done with the same time step as previously presented ($0.2 \cdot 10^{-6} \text{ s}$). And this last change helped to approximate accurately the test results (see Figure 43).

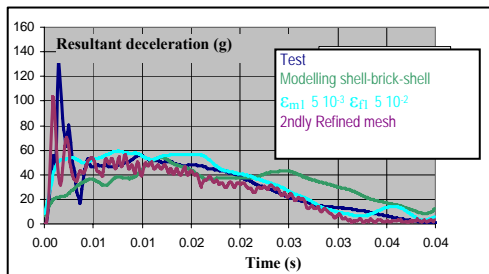


Figure 43. Combined influence of $\epsilon_{m1} + \epsilon_{r1}$ and mesh size on the headform impactor deceleration.

The corresponding HIC are 352 for test, 283 for the reference modelling, 410 for the combined influence of damage parameter and first mesh refinement (mesh size divided by 2 with respect to the reference modelling), and finally HIC is 271 for the secondly refinement (mesh size divided by 4 with respect to the reference modelling).

Conclusion of the numerical modelling

The modelling correlated with static test is therefore not able to represent the dynamic impact of the headform to the windscreen. We have highlighted that the size of the mesh needs to be strongly refined to represent the dynamic impact that last only a few milliseconds. Otherwise the load peaks with short duration are not “caught” by the mesh. Moreover, because of the fragile behaviour of the glass, predicting the windscreen rupture is a very difficult task without doing a large number of tests. Finally, the parameters of the constitutive law used to represent the glass behaviour can have a strong influence on the correlation between test and modelling.

CONCLUSION

As shown in the first part of the study, the biomechanical results of a headform impactor into the windscreen are influenced by several parameters and present a high scattering.

Energy absorption depends on the type (manufacturer) of the windscreen and this implies a different risk of head impact to the dashboard. Moreover, impact point proximity with the windscreen pillar strongly increases the

biomechanical values and a distance of 110 mm is needed to get HIC below 1000.

Finally, biomechanical results are not strongly influenced by the thickness of the glass layers. Head deceleration over time and HIC values are very similar even with an increase of 12% in the thickness. The only change is seen in the first peak of deceleration.

In the second part of the study, we highlighted the high difficulty to model the windscreen and reproduce its dynamic behaviour.

The mesh size needs to be very small (smaller than the usual mesh size recommendation for an overall car model calculation) to be able to reproduce the first peak of deceleration. But this has a strong influence in the time step and therefore the running time of calculation.

Finally, some other parameters, not analysed in this study, may have a strong influence on the modelling, such as windscreen curvature and adhesive properties of the bonding. These parameters will be part of a future study.

REFERENCES

- [1] European Directive 2003/102/EC of the European Parliament and of the Council relating to the protection of pedestrians and other vulnerable road users before and in the event of a collision with a motor vehicle
- [2] Euro NCAP Pedestrian Testing Protocol - Version 4.3 and 5.2
- [3] Euro NCAP Assessment Protocol And Biomechanical Limits - Version 4.3 and 5.0
- [4] M. Timmel, S. Kolling, P. Osterrieder, P.A. Du Bois - ‘A finite element model for impact simulation with laminated glass’- International Journal of Impact Engineering 34-2007 -1465–1478

ACKNOWLEDGMENTS

The authors wish to thank all the members of the laboratories involved in this study as well as the PSA research team. A special thank to Mr David Bosse, Mr Marc Louvigne and Mr Arnaud Delaye from PSA Peugeot Citroën.

ACCIDENTS BETWEEN PEDESTRIANS AND INDUSTRIAL VEHICLES: FROM INJURY PATTERNS TO DUMMY AND TRUCK PROTOTYPES

Philippe Beillas, Mario Mero, Steve Belon, Alain Maupas

Université de Lyon, F-69000, Lyon, France
Ifsttar, LBMC, UMR_T9406, F-69675, Bron
Université Lyon 1, F-69622, Villeurbanne
France

Hervé Desfontaines, Philippe Deloffre

Renault Trucks SAS – Volvo 3P, 99 route de Lyon. F-69806 Saint-Priest
France

Pierre-Yves Lapauw, Laurent Huet

Segula Technologies Sud, BU-CALCUL, R&I, F-69800 Saint-Priest
France

Sébastien Charnaux

Plastic Omnium Auto Extérieur, Research and Innovation Dept, F-01150, Sainte Julienne
France

Paper Number 11-0355

ABSTRACT

This paper provides new results on the safety of pedestrians involved in accidents with industrial vehicles such as trucks and buses. The analysis of two accident databases highlighted the importance of the frontal impacts, run over scenario and the thorax loading for this accident type (when using car pedestrian accidents as a reference). The accidents were then studied using full scale tests conducted with three standard industrial vehicles, one prototype and two pedestrian dummies (including a new modified dummy). The test results include an analysis of the kinematics and of dummy signals. Beyond specific test results, the study describes the development of a possible methodology to improve the safety of vulnerable road users involved in accidents with industrial vehicles and discusses a possible strategy.

INTRODUCTION

Recent research on pedestrian safety has been mostly focused on accidents involving cars and sometimes light trucks and vans. In comparison, only few studies deal specifically with the safety of vulnerable road users (VRU) such as pedestrians and two-wheelers involved in accidents with industrial vehicles such as trucks and buses. The main objectives of the study were:

- (1) Better understand accidents between VRU and industrial vehicles using epidemiological, testing and modeling approaches,
- (2) Formulate strategies to reduce the injury due to primary impact and the run over risks,
- (3) Implement and evaluate some of these strategies on a prototype truck.

The scope of the study was limited to accidents and vehicles relevant for an urban environment.

The work was performed within a 42 months French national project called PRUDENT-VI. The project involved industrial vehicle manufacturers, suppliers and academic partners from the Lyon Urban Trucks and Buses 2015 competitive cluster. The current paper provides a partial overview of the results obtained during the project.

METHODS

Epidemiological approach

Existing epidemiological results from the literature were supplemented by the detailed analysis of two French databases.

Renault Trucks fatal accidents database This database contains details about 192 fatal cases involving one truck and at least one pedestrian or two-wheeler. It is composed of 170 police reports and 22 detailed accident reports collected by CEESAR (Nanterre, France) for Renault Trucks. All accidents occurred in France after 2001. For the current study, the analysis was restricted to the 112 cases (114 VRU) that occurred in urban areas.

Rhône Road Trauma Registry This database is an epidemiological registry managed by ARVAC and Ifsttar (Bron, France). It aims to collect information about all road accidents occurring in the Rhône district for which an injured victim is seen by a doctor. Each report includes a detailed description of the injuries (AIS codes) and a brief description of the circumstances (sometimes accompanied by the police report). After selecting

the pedestrian and cyclist cases (10031 for the period 1996-2005), the vehicles were organized in trucks with flat front (n=281), buses (n=315) and cars (used as reference, n=9088).

Full scale testing with pedestrian dummies and industrial vehicles

Thirty-two full scale tests were performed using two dummies and the following industrial vehicles:

- A Medium Duty Truck (MDT), with a flat front cab. This is a midsize truck typically used for delivery. It will be referred to as MDT1.
- A Light Duty Truck, with an inclined front similar to a large van. This smaller size truck is also typically used for delivery. It will be referred to as LDT.
- A bus (whose data will not be presented in detail in the current paper)
- A version of the MDT1 modified for the current project. It will be referred to as MDT2.

The first three vehicles are standard models that were selected to represent typical industrial vehicles used in an urban environment.

Autoliv-Chalmers pedestrian dummy The first test series (14 tests) was performed using an experimental pedestrian dummy (Fredriksson et al., 2001) developed by Autoliv Research and Chalmers University (Sweden). This dummy will be referred to as Autoliv-Chalmers or AC dummy. It is designed for pedestrian lateral impact and composed of parts from various 50th percentile dummies: Eurosid 1 head and neck, US-SID thorax, Hybrid II abdomen, standing Hybrid III pelvis, Hybrid III lower and upper legs. Custom components (neck mount, lumbar spine and knees) are used to link these parts. The lumbar spine is very flexible compared to seated dummies. It uses a metal spring surrounded by steel cables to limit the range of motion. The modified knees include deformable steel cylinders whose properties were selected to approximate the EEVC WG17 (2002) knee bending corridors. The dummy was instrumented with linear accelerometers at the center of gravity of the head (X, Y, Z), thorax accelerometers at T1, T12, lower and upper ribcage (Y), a thorax potentiometer (deflection), pelvis linear accelerometers (X, Y, Z), upper tibia accelerometer (Y), femur load cell (forces and moments on X, Y, Z), upper and lower tibia load cells (forces X, Z, moments X, Y). Only the impacted leg (i.e. left) was instrumented.

Iffstar-Autoliv pedestrian dummy This dummy was used during the second test series (18 tests). It was developed based on the same principles as the Autoliv-Chalmers dummy in an attempt to improve the dummy based on

observations from the first test series. More specifically, the thorax (and neck) regions were replaced by Eurosid 2 parts while other standard dummy components remained the same. The custom components were also modified: the lumbar design was changed to facilitate the spring replacement and to prevent the rotation at its base during the impact. Similarly, the knee design was changed in order to be able to tighten the deformable elements sufficiently to prevent axial rotation during impact. An adjustable neck mount was added to link the Eurosid 2 parts in a standing posture. Lengths, masses and relevant characteristics of deformable components (lumbar spring and knee cylinder) were kept from the previous design. The new dummy has a height of approximately 1.80m and a weight of 77kg. Because the abdomen of the Hybrid II dummy was not completely filling the space between pelvis and thorax, a raiser made of the upper part of a Hybrid III pelvis dummy foam was added above the pelvis. The instrumentation was the same as the AC dummy except that the thorax deflections were measured in three locations. The dummy will be referred to as the Iffstar-Autoliv or IA dummy.

The bending responses of deformable elements were characterized to verify that they were close to the EEVC corridors (Figure 1). Illustrations of the two dummies and of the new components are provided in Figure 2.

Test setup In order to minimize the risk of dummy damage due to run over, the vehicle cab was mounted without its wheels on a deceleration sled available at Iffstar (Figure 3). In the dummy impact area, the ground level was raised by about 1.2m using a platform (scaffolding). During the impact, the sled was going under the platform while the test vehicle and the dummy were above. Two narrow slots in the platform let the vehicle fixture go through.

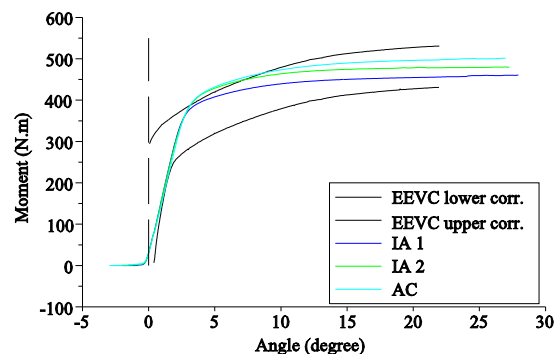
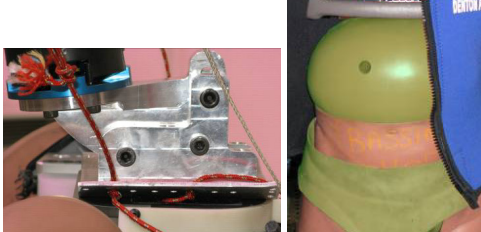


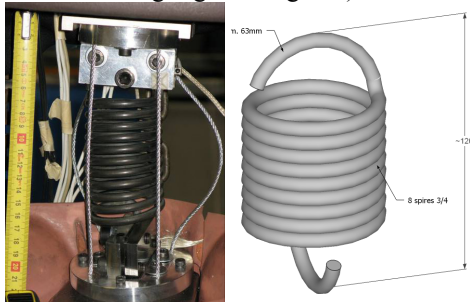
Figure 1: Bending response of knee deformable elements. Legend: AC=provided with the Autoliv-Chalmers dummy. IA= manufactured for the Iffstar-Autoliv dummy. Corridors from EEVC (2002).



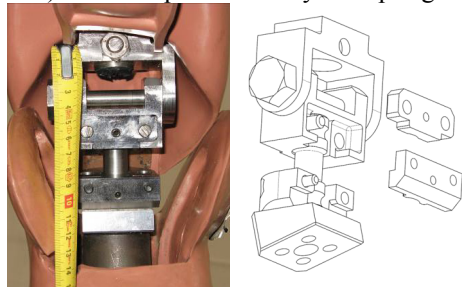
a) AC (left) and IA (right) dummies



b) Neck mount and abdomen raiser between abdomen and pelvis (abdomen and pelvis highlighted in green)



c) Lumbar spine assembly and spring



d) Knee assembly

Figure 2: Pedestrian dummies and new components of the Ifsttar-Autoliv dummy.

A typical test included the following steps: the dummy was positioned on the edge of the platform (Figure 3) and suspended to an electromagnet by two ropes. The sled (with the vehicle on top) was accelerated up to target speed and separated from the pulling cable when approaching the platform.

Then, 100ms before dummy contact, a wireless contact mounted on the sled was triggered, leading to the release of the electromagnet and the dummy. After the dummy contact, the sled continued freely for about 2.5m and before being stopped in less than 1m. The dummy ended its trajectory on mattresses positioned on the platform in order to reduce the severity of the ground impact (Figure 3). Four Visario (Weinberger) cameras with a three dimensional calibration were used to follow the impact. Fuji Prescale Ultra Low pressure sensitive paper positioned on the vehicle helped identify the contact areas.

After each test, the damage to the dummy and the vehicle were assessed and damaged components were replaced. The knee flexion angles were measured using photographs of the deformable components on a calibrated flat surface.

Injury criteria In the absence of standard procedures or injury criteria for this impact scenario and these impact dummies, a list of injury criteria and tolerances that could be used to evaluate the severity of the impacts was compiled (Table 1). The criteria and their injury assessment reference values were selected because they were (1) already used for the Autoliv-Chalmers dummy or (2) used for dummy regions in other configurations (e.g. Eurosid 2 in side impact) or (3) used for EEEVC subsystems.



Figure 3: Overview of the test setup. Top left: Test vehicle on sled (partially under the platform). Top right: dummy in impact position on the edge of the platform. Bottom left: dummy impact (above the platform). Bottom right: final position. All photos with the MDT2.

Table 1: List of candidate injury criteria

Region	Criteria, limit and comments
Head	HIC15<1000: used in many regulations including with EEVC headform
Thorax	TTI<85g: used with US-SID in regulations (but not ES2) Deflection <42mm: used with ES2 in regulations (but not US-SID)
Pelvis	Acc.<130g: used in FMVSS214 (not with standing HIII pelvis)
Femur	Force<5kN and Moment<300N.m: used with EEVC legform
Knee	Flexion<15deg: used with EEVC legform
Tibia	Acc.<150g: used with EEVC legform TI <1.3: only used for frontal impact

Full scale modeling with pedestrian dummy and industrial vehicles

Dummy simulations matching the physical tests were performed all along the project, from the test preparation phase to the design of the MDT2 and the analysis of the final results. Simulations were performed using the Radioss (Altair, Troy, MI) finite element code. The model of the AC dummy was already available in the Radioss dummy library. It was modified as the physical dummy to create a model of the IA dummy. As an alternative modeling approach, the EEVC legform was also compared with the full dummy.

Standard vehicle models Vehicle models were modified for use in pedestrian impacts. In order to characterize the standard vehicles and validate the corresponding models, the vehicle front were tested using rigid impactors matching the shape and mass of the EEVC head and upper leg. An illustration of the process is provided in Figure 4.

Design of the MDT2

The modified truck (MDT2) was designed starting from the full scale simulations, the first series of tests, epidemiological and literature results. The objectives of the new design were (1) to reduce the risk of run over by better managing the kinematics and (2) to reduce the severity of the impact on the front of the vehicle.

The stiffness and shapes of the struck areas at various heights were adjusted using simplified models of the truck impacted by leg subsystems and full dummies. They were then implemented using new parts for the front lid, bumper, grill, head lamps, front underrun protection system, etc. For the prototype, the parts were machined or molded. Due to budget constraints, molding was not performed using final materials. Foam blocks positioned behind the front lid, bumper and aisle were used to provide the needed stiffness. The

dimensions and densities of the foam blocks were determined by simulation. Illustrations of the process are provided in Figure 5.

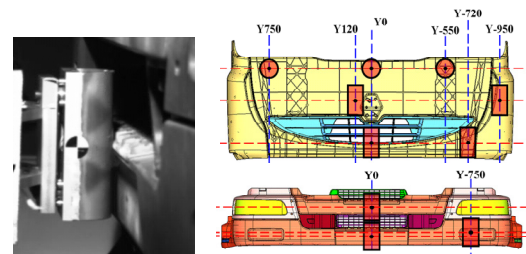
The reference speed of 35km/h was selected to dimension the stiffness of the various components.

RESULTS

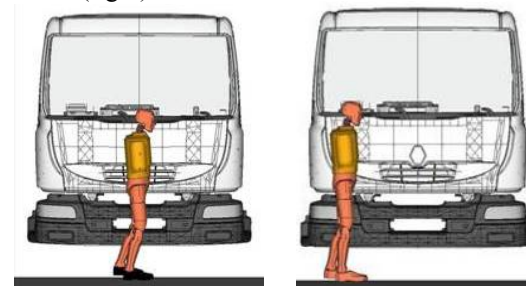
Epidemiological approach

Renault Trucks VRU Database Out of the 112 urban cases selected for the study, 51% (n=57) were pedestrians and 13% (n=14) were cyclist. The remainder (32%) was composed of various types motorized two-wheelers. 68% (n=39) of the pedestrians were 61 years or older, while only 5% (n=4) were less than 18 years old. The tendencies were different for the two wheeled victims since 11% were over 61 (n=6, including 4 cyclists) and 75% were between 13 and 40 years.

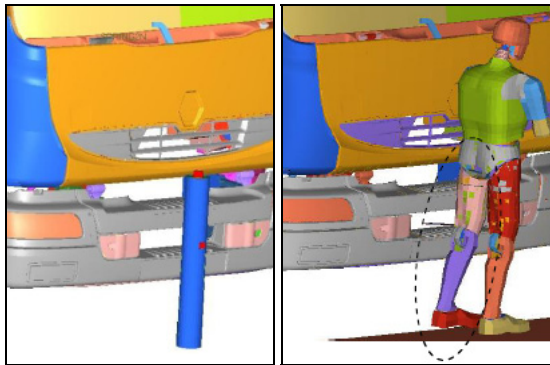
For the pedestrian victims, the impact was frontal (from the truck's viewpoint) in 79% of the cases. For the two wheeled victims, only 46% of the cases were frontal and 46% were lateral impacts (30% on the right and 16% on the left side). The truck was going forward in 72% of the cases (n=81) and not moving in 18% of the cases (n=20). The accident typically occurred at an intersection (62%, n=70). Regarding the vehicle type, 54% had of the trucks no trailer and 55% were used as delivery trucks.



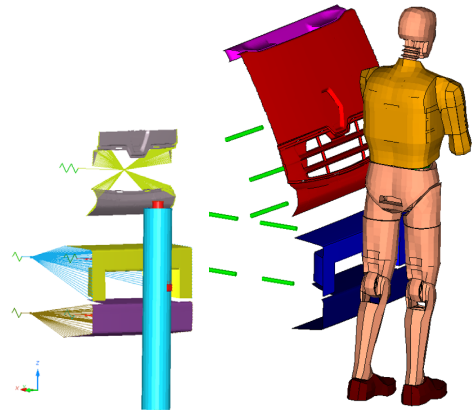
a) Example of stiffness characterization with rigid impactors (left) and location of impact points on MDT1 (right)



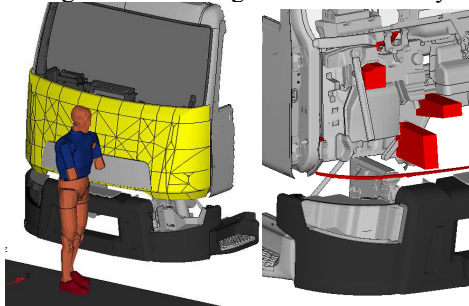
b) Full cab model with AC dummy in position
Figure 4: example of MDT1 model preparation for pedestrian impact.



a) EEVC legform or IA dummy against the MDT1



b) Simplified truck model with regional stiffness interacting with EEVC legform or IA dummy.



c) MDT2 with IA dummy. Foam blocks (red) used to simulate the stiffness in the prototype

Figure 5: Overview of the MDT2 design process

While no information was available on injury type or location in the database, run over – defined as at least one wheel of the truck rolling over at least one part of the body – occurred for two thirds of the victims (Table 2). 75% of the pedestrians (n=43) and 79% of the cyclists (n=11) were run over. The only category for which run over cases were not a majority was the motorcycles (6 out of 17).

The analysis was further detailed for the pedestrians. For pedestrians struck by the front of the truck, a speed could be estimated in 31 cases. The speed was estimated between 30 and 50km/h in 10 cases (pedestrian crossing away from crosswalk not aware of the danger), below 10 km/h in 15 cases (impact close to or at a crosswalk, with the truck just starting or restarting), and between 5 and 25 km/h in 6 cases (the truck started and turned

left or right). In the most typical scenario, the pedestrian was crossing the road (38 cases out of 52 known activities), walking (37 out of 49). Out of the 30 cases for which the pedestrian maneuver just prior to impact was known, there were no maneuver at all in 15 cases (no perception of danger or no time), a reaction in 14 cases (try to avoid, falls, speed up, stops, etc) and one case was a suicide. When the initial and final positions were documented, the pedestrian ended at 5m or less from the initial impact position in 68% of the cases (n=28).

Rhône Registry Analysis Most of the accidents occurred on regular streets (74% or more of the cases with known location). The lowest percentage was for trucks for which a few cases of accidents with pedestrians occurred on freeways (n=17 or 8.3%).

Out of the 281 cases selected for the trucks, 73% (n=205) were pedestrians, the remainder being cyclists. The proportions were 90% (n=283 out of 315) and 76% (n=6907 out of 9088) for the buses and cars, respectively. For pedestrians, fatalities represented 12.7% (n=26) of the cases for trucks, 4.2% (n=12) for buses and 2.4% (n=166) for cars. For cyclists, the number of fatal cases in the sample was very small for the trucks (n=4) and buses (n=1). It represented 1.4% of the cases (n=30) for the cyclist involved in accidents with cars.

VRU between 16 and 60 represented a majority of cases for all vehicle classes (Table 3). However, VRU over 61 years were more represented in the fatal cases: they were 50% (n=15) of the fatalities with trucks, 62% (n=8) with buses and 48% (n=94) with cars. Percentages of VRU not sustaining at least one serious injury (AIS3+) also decreased for populations over 61 (Figure 6).

For the analysis of the injury location, only pedestrians were considered. Spinal injuries were distributed onto the abdomen or the thorax based on their location. Thorax, abdomen and pelvis were also grouped in a large zone called trunk. This was done to facilitate possible determination of impact zones on the vehicle.

Table 2: Cases of run over by vulnerable road user type in the Renault Trucks database

VRU	Run over	Not run over
Pedestrian	43	14
Cyclist	11	3
Moped	8	6
Scooter	8	4
Motorcycle*	6	11
Total	76	38

*50cm³ or more

Table 3: Pedestrians and cyclists in the Rhône Registry (1996-2005): percentages by age class and total number. (Killed are in parenthesis).

	Buses	Trucks	Cars
0-15 (%)	18.8 (15.4)	13.2 (3.3)	29.3 (10.8)
16-60 (%)	60.5 (23.1)	61.9 (46.7)	54.8 (40.2)
61+ (%)	20.7 (61.5)	24.9 (50.0)	15.9 (49.0)
Total (%)	100 (100)	100 (100)	100 (100)
Number of VRU	314 (13)	281 (30)	9065 (194)

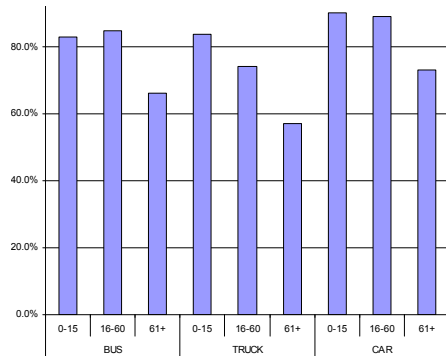


Figure 6: Percentages of pedestrians and cyclists not sustaining an AIS3+ (by age and vehicle)

Results are provided in Figure 7. Overall:

- multiple injuries per pedestrian or region are typical (sum of percentages superior to 100%);
- For AIS 1 or 2: the most commonly injured regions are the lower extremities and the head.
- For AIS 3, 4 and 5: trunk injuries are more prevalent for trucks and buses. For AIS3+ with trucks and buses, there are more pedestrians with an injury to the trunk than to the head.
- For all levels: trunk injuries are more common for trucks and buses than for cars. For example, for pedestrians with AIS2+, AIS2+ lesions to the trunk are almost twice more frequent for trucks and buses than cars (29.2%, 27.7% and 15.5%, respectively). The proportions remain similar for AIS3+ injuries (36.9%, 38.2% and 21.9%). This increase affected both thoracic and abdominal injuries.
- For AIS6: head and thorax are the only two contributing regions, with the head region leading. The samples are small as injuries are not specified for many fatal cases. Fatal injuries for trucks and buses were typically crushes of the head or thorax.

Run over is suggested in the optional free description field of the database for 6 of the 13 fatal cases for the buses, and 11 of the 30 fatal cases for the trucks.

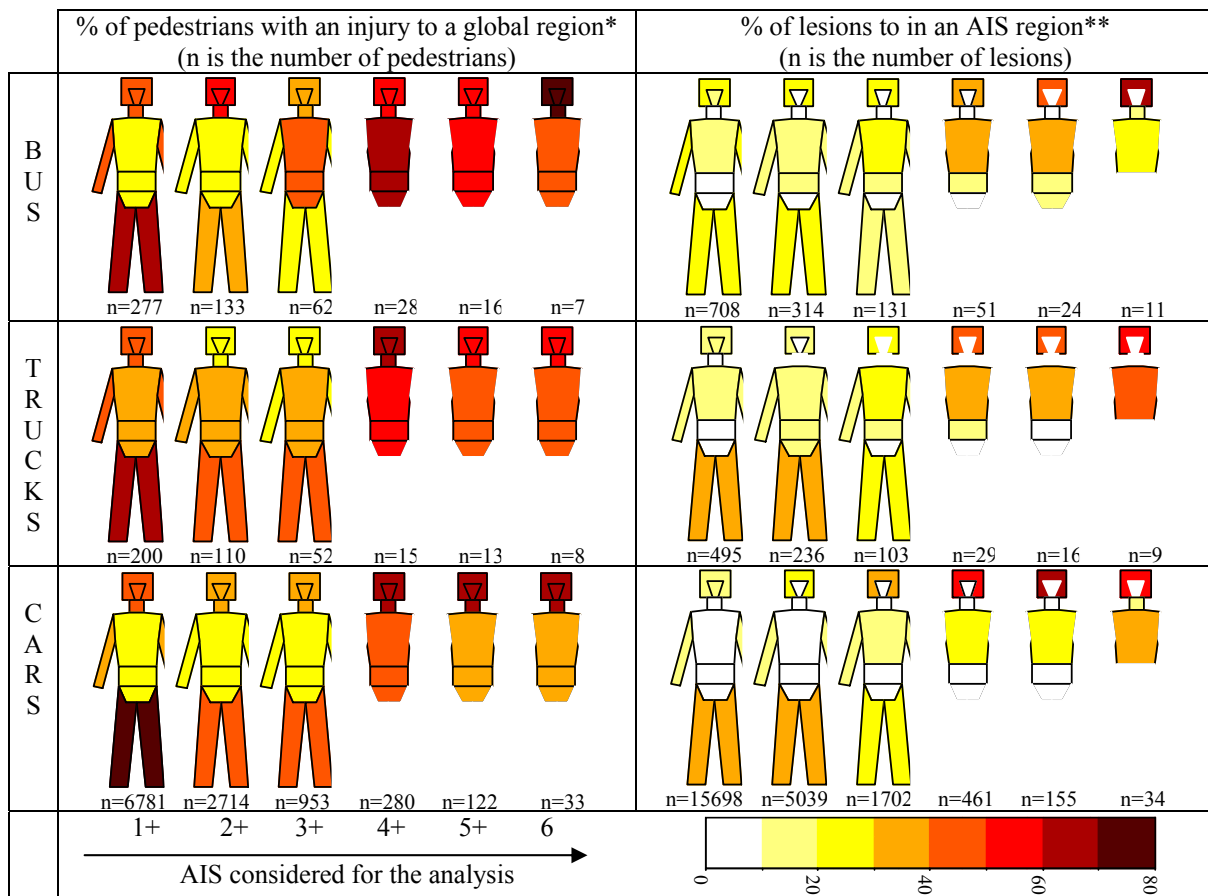


Figure 7: Overview the injured regions in pedestrian accidents with trucks, buses and cars based on the analysis of the Rhône Road Trauma Registry. Notes: *Global regions: head/face/neck, thorax/abdomen/pelvis, upper ext., lower ext. **Except spine distributed onto neighboring regions

Comparison of simulations with subsystems and dummy

When comparing EEVC legform and dummy for the MDT1, their kinematics were similar at the very beginning of the impact, and the lower leg angles (below the knee) were relatively close all along the simulation (Figure 8a). However, the top of the EEVC legform moved away from the vehicle (visible from 12 ms) while the weight of the upper body of the dummy continued to push the upper leg, leading to a higher knee flexion angle (36.5 vs. 12.3 degrees). This difference could be reduced by adding a mass to the top of the legform (e.g. a 10kg mass led to an angle of 25.3 degrees, Figure 8b). The differences between the dummy and the EEVC legform were smaller when used against a car that complied with European pedestrian regulations (Figure 8c).

Full scale testing with pedestrian dummies and industrial vehicles

Thirty two tests were performed in two test series. In summary (Table 4), the MDT1 and MDT2 were tested in centered position up to 35km/h with the IA dummy while the speed was limited to 27km/h for all other configurations. Most tests were performed at the center position and the LDT and the bus were only tested with the AC dummy (Beillas, 2009). Some impacts were repeated three times with the IA dummy. Small modifications of the prototype were performed along the test series.

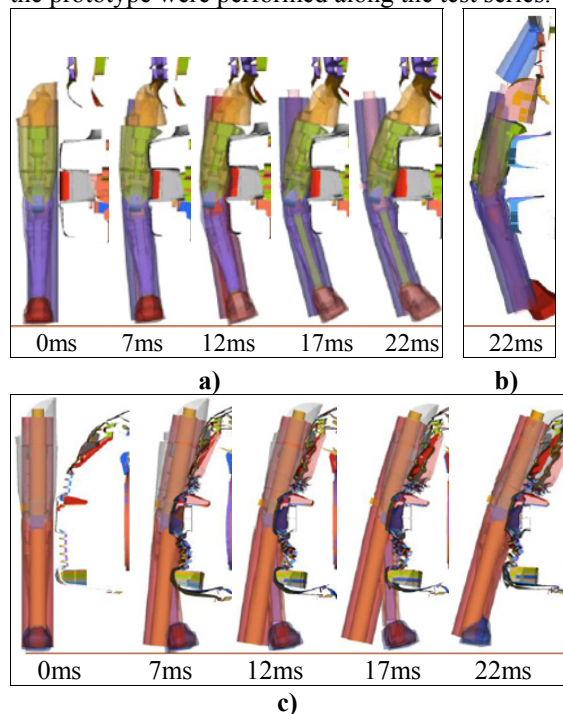


Figure 8: EEVC legform vs. full dummy simulations at 40km/h: a) Against MDT1. b) Legform with additional 10kg mass at the top against MDT1 c) Standard legform against car.

Vehicle damage varied from no damage in centered impacts at low speed on the MDTs to extensive damage at high speed against the MDT2 (which includes numerous breakable parts). The damage to the dummies included shoes, ankles (second test series), foam components, lumbar springs, lumbar cables, one load cell and a few accelerometers. None of the custom designed components were damaged in the second test series despite the higher test speeds (35km/h).

Kinematic response of standard vehicles The kinematic response of the dummy was affected by the vehicle type and the dummy. The kinematic response with LDT was relatively similar to the response of a large van (Figure 9) and will not be further detailed.

Typical kinematic responses of the two dummies with the MDT1 are shown on Figure 10 for tests at the center with intermediate speeds. The two dummies had similar kinematic responses. The contact was first established on the thorax, with the pelvis and lower extremities following. The thorax deformed the hood until the head impacted. The motion of the dummies was mostly horizontal during that phase. Then the dummies bounced and fell rapidly to the floor. At low speed, the dummy was impacted a second time on the floor despite the sled being stopped about 3m after the impact point.

One difference that could be observed between the two dummies was the rotation about the vertical axis: for the Autoliv-Chalmers dummy, the thorax remained mostly aligned with the direction of impact, with a slight tendency to rotate its front face towards the vehicle. The opposite trend (rotation of the dummy front away from the vehicle) was much more marked for the Ifstar-Autoliv dummy.

Repeatability of the kinematics For the tests that were repeated three times, some variations were observed on the initial posture of the dummy due to the softness of the lumbar spine making difficult the positioning. These differences did not seem to increase along the trajectory as illustrated in Figure 11 for MDT1 tests. A similar repeatability was observed with MDT2 tests at low speed as illustrated in the Figure 12.

Table 4: Partial Test matrix (without the bus)

Test	Vehicle Dummy Position Speed*	Observation (D=Damage)
01	MDT1 AC C 12	
02	MDT1 AC C Low	
03	MDT1 AC R Low	D=bumper and front lid
04	LDT AC C Low	D=bumper
05	LDT AC R Low	D=front lid
06	LDT AC C 19	D=bumper and front lid
07	LDT AC C Med	D=bumper and front lid
08	LDT AC R Med	D=bumper and front lid
13	MDT1 AC C Med	D=bumper and front lid
14	MDT1 AC R Med	D=bumper and front lid
21	MDT2 IA C Low	D=bumper
22	MDT2 IA C Low	No measures
23	MDT2 IA C Low	No video; dummy drop delay
24	MDT2 IA C Low	
25	MDT2 IA C Med	D=front lid
26	MDT2 IA C Med	D=front lid
27	MDT2 IA R Low	D=head lamp, aisle, front lid
28	MDT2 IA R Med	D=head lamp, aisle, front lid
29	MDT2 IA C Med	D=front lid
30	MDT2 IA C High	D=front lid
31	MDT2 IA C High	Upper bumper support removed; D= front lid, bumper, aisle, bumper support beam (attached to FUPS**) bent, head lamp
32	MDT2 IA C High	Upper bumper support removed; spoiler foam and supports reduced; D=same as PRU31 + front lid hinges
33	MDT1 IA C Low	
34	MDT1 IA C Low	
35	MDT1 IA C Low	
36	MDT1 IA C Med	D=front lid
37	MDT1 IA R Med	D=front lid
38	MDT1 IA C High	D= windshield cracked (head contact), bumper, front lid

*Speed: in km/h or level: low=14.4-17.5km/h, medium=24.5-27.1km/h, high=34.9-35.1km/h

**FUPS: Front underrun protection system.



Figure 9: Kinematics of the AC dummy against a LDT at medium speed (25km/h)

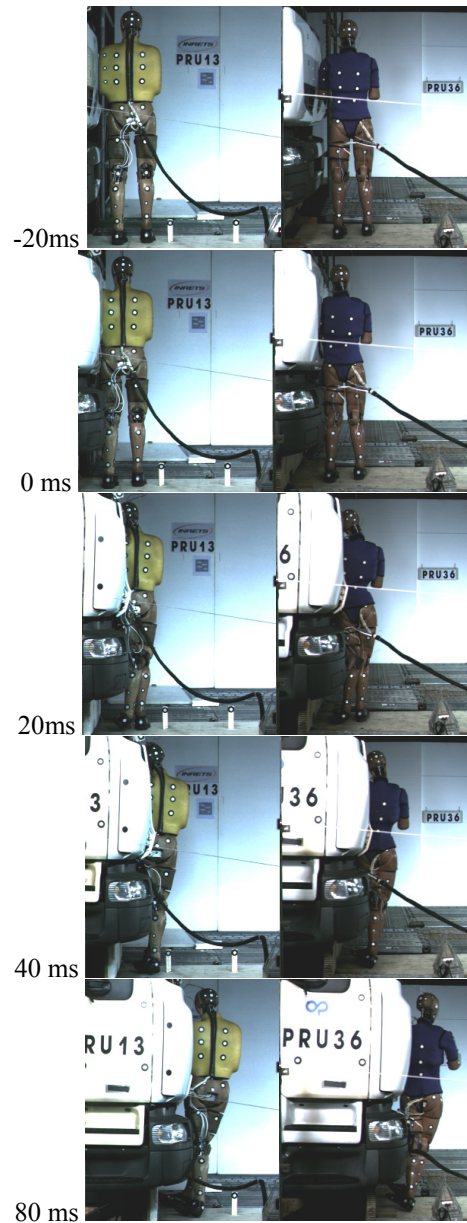


Figure 10: Comparison of the Autoliv-Chalmers (left) and Ifsttar-Autoliv (right) dummies with the MDT1 at medium speed.



Figure 11: Superimposed kinematics from three low speed tests (around 17km/h) with the Ifsttar-Autoliv dummy and the MDT1. Each test has a different color and the images are at 0 (contact), 150 and 400ms

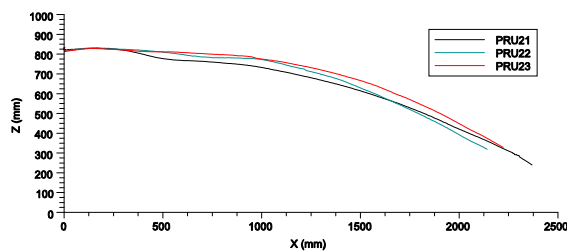


Figure 12: Repeatability of the trajectory of a pelvis target of the IA dummy in three low speed tests with the MDT2 (projected from 3D tracking; Z vertical up, X horizontal away from the vehicle with zero at the platform level).

Kinematics for the MDT2 The changes made in the MDT2 affected the dummy kinematics. For the MDT1, the contact was occurring first on the thorax and then on the lower extremities. For the MDT2, the contact occurred on the lower extremities and on the thorax almost at the same time. In consequence, while the thorax was ahead of the lower extremities and had a trajectory towards the ground in MDT1 test, the lower extremities were ahead for the MDT2 and the thorax and pelvis were pushed upwards.

The highest vertical impulse was observed for the test 31 for which the upper bumper supports were removed to leave the upper bumper move under the pelvis inertia. A comparison between this test and the corresponding MDT1 test is provided in Figure 13. This vertical impulse appeared to be highly dependant on the vehicle characteristics as it was not as prominent in the tests 30 and 32.

In order to quantify this effect on the kinematics, the trajectory of the pelvis target was tracked until the dummy legs interacted with the mattresses. The trajectories obtained for the MDT1 test 38 and the MDT2 test 31 are provided in Figure 14. The trajectories and their extrapolations suggest a difference in projection distance between 1.5 and 2m between the MDT1 and MDT2.

Dummy signals and injury criteria for the centered impact with the MDT trucks The order of the contacts depending on the vehicle type, it was decided to zero the time for all channels when the knee accelerometer reached 10 m/s². An overview of the dummy channels for nine tests is provided in Figure 15. Injury criteria values for all tests are available in the Table 5.

For low speed tests, there were no or little head impacts on the vehicle as the thorax was pushed away before head contact. At higher speeds, the head contact resulted in a large peak on the acceleration curves. The timing and amplitude of the peak were dependent on the dummy and vehicle. The peaks occurred later on the MDT2 due

to the earlier leg contact (Figure 15). At medium speed with the MDT1, the peak acceleration was lower with the IA than with the AC dummy as the initial thorax acceleration phase was higher due to shoulder loading. For the targeted design speed (35km/h), the MDT2 design led to much lower head accelerations than the MDT1. For the test 32, the head impact occurred earlier than in the other tests at the same speed (30 and 31) and it was associated with a rupture of the hinges holding the front lid. HIC15 were all below 1000 (Table 5), with the 35km/h MDT1 test being very close at 992 (head impact on the lower windshield leading to a crack in the glass). All HIC values were below 200 for the MDT2.

For the thorax, differences were also observed between dummies: for all test with the AC dummy and vertical vehicles, the maximum deflection varied very little (between 26 and 31mm) despite testing at two speeds. The variations were larger with the IA dummy and the speed sensitivity was more pronounced (Table 5). Also, for some tests with the IA dummy, an acceleration peak appeared on the lower rib during the unloading phase of the thorax (after 60ms). The reasons for this peak are unknown and the TTI were only computed based on the first 60ms. For comparable tests, the TTI values were similar for both dummies. TTI and maximum deflection were both below their respective limits of 42mm and 85 despite some values being close to these limits. Also, for the IA dummy, high TTI did not always correspond to high deflections (e.g. tests 30 and 32 in Table 5). While the rib deflections were relatively easy to interpret on the IA dummy, the rib accelerations were associated with large vibrations on both dummies, making difficult the interpretation of specific curves (Figure 15).

The pelvis accelerations were very similar with the two dummies on the MDT1 (Figure 15). The MDT2 had higher acceleration maxima than the MDT1 in corresponding tests (Figure 15 and Table 5) until the upper bumper support was removed (at test 31). Overall, the accelerations were much lower than the 130g limit (highest value of 87g).

The resultant femur forces were lower for the tests with the MDT2 than the MDT1, and with the IA than the AC dummy. All maximum forces were below 5kN, and the highest forces were reached for tests at high speed. On the contrary, femur moments were similar for the two dummies (tests 13 and 36) and, while being in average slightly smaller for the MDT2 than the MDT1, almost all maxima were largely above 300N.m (Table 5), with several values around 600N.m. Femur maximum moments did not seem to be affected by the impact speed either.

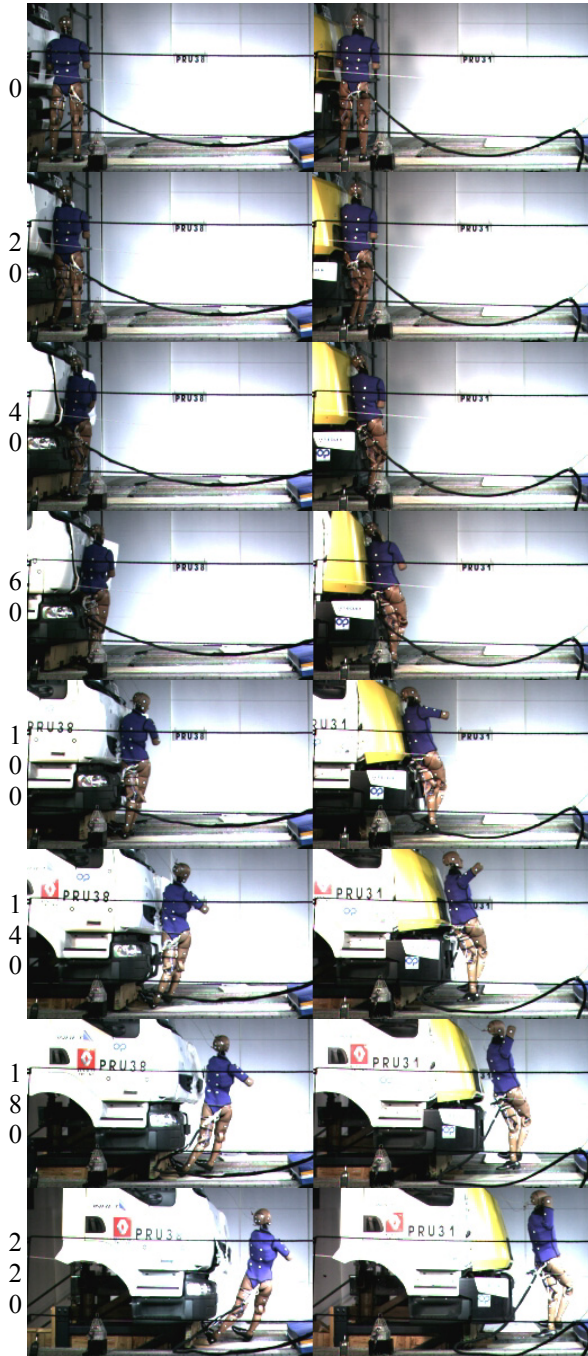


Figure 13: IA dummy kinematics at 35km/h with MDT1 (38) and MDT2 (31). Left: time (ms)

For the IA dummy, the upper tibia moments curves followed the overall trend of the femur moments but with lower values. Still, the level of 400N.m was reached for several tests despite the absence of the Z component in the calculation of the resultant. Most upper TI (Table 5) were above the 1.3 limit. The response curves were very different for the AC upper tibia moments: after a very short peak, there was a rebound and the main loading occurred much later. Moments were also associated with very large vibrations (up to 1000N.m) that were not present on the femur or on the lower tibia. As a consequence, upper TI and upper tibia moments were only computed based on the first 60ms of impact in Table 5.

Lower tibia moments were mostly unaffected by the vehicle change (MDT1 to MDT2) and dummy. They were lower than upper tibia moment and the TI values were also lower than 1.3. However, the damage of the ankle stops in axial rotation suggests that the Z component of the moment – that was not measured – may have been important.

The upper tibia accelerations were lower for the MDT2 and the IA dummy compared with the MDT1 and the AC dummy. For the MDT2, accelerations were just above the 150g limit proposed in EEVC, down from values above 300 for some of the tests with the MDT1.

Finally, the knee flexion angles measured on the deformable elements after the test were also generally reduced by the change of vehicle but seemed slightly higher for the IA dummy (tests 35 and 36 vs. tests 33 to 36).

Dummy channels for other configurations

Other configurations were not tested up to the high speed range. Due to space constraints, the results from these tests will not be detailed. In general, the impact to the right of the MDTs followed similar trends as the impacts at the center (Table 5). When compared with the MDT1, the criteria obtained with the LDT had a tendency to be higher for the lower body (e.g. knee flexion angle) and lower for the upper body (e.g. head).

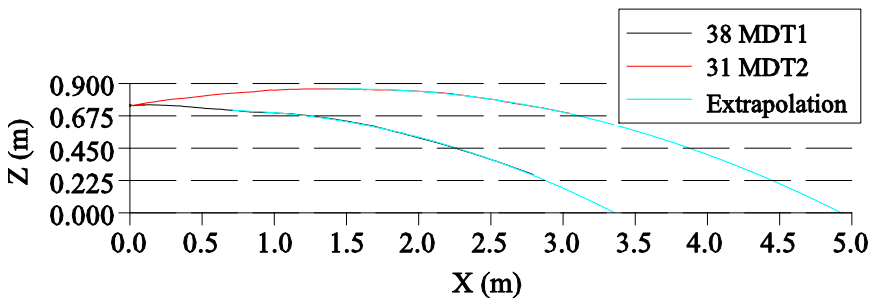


Figure 14: Pelvis target trajectories for MDT1 and MDT2 at 35km/h. Initial positions were aligned at their average. X is horizontal; Z is vertical pointing up with the origin at the ground. Parabolas were computed based on the last 200 positions (least square)

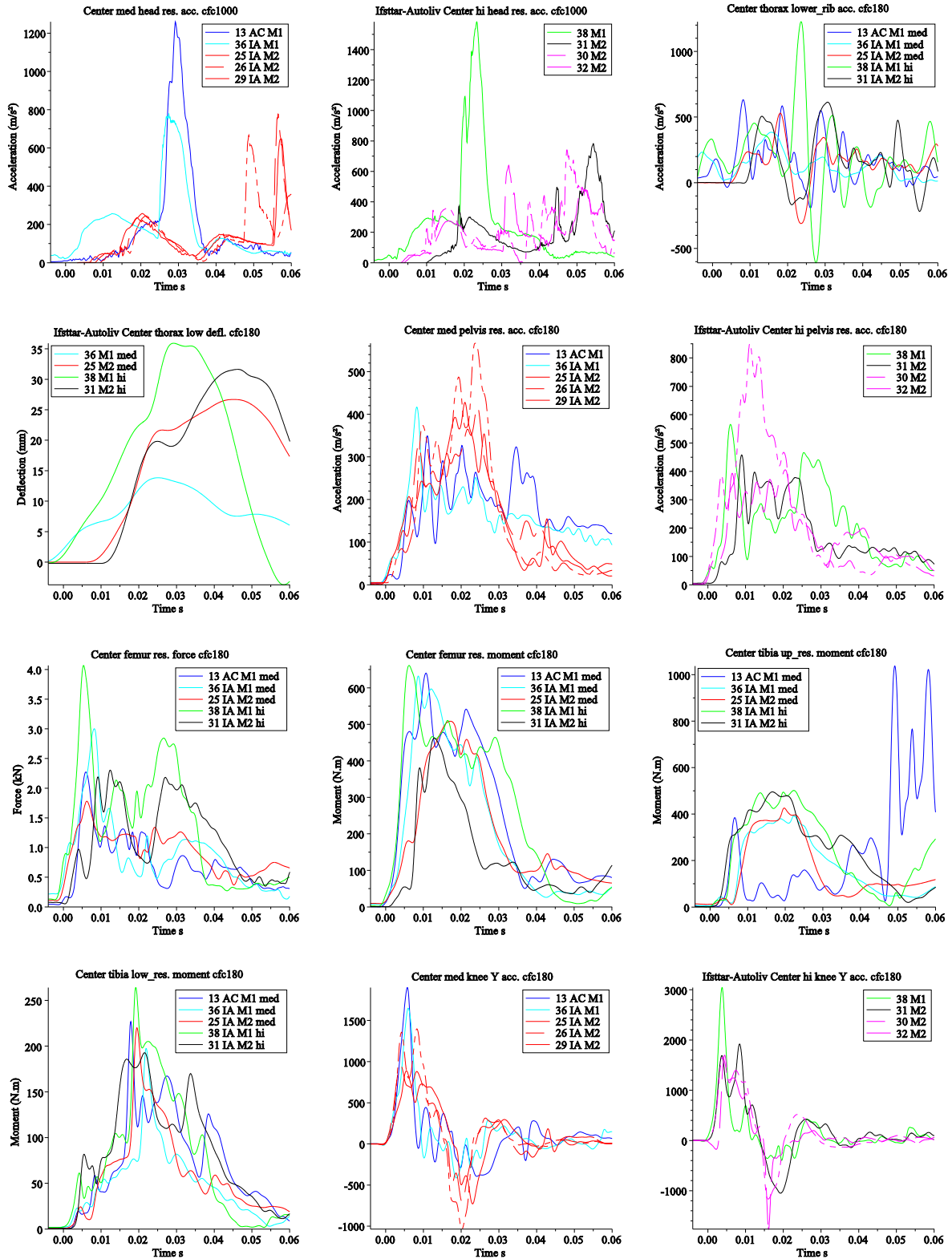


Figure 15: Summary of the dummy results obtained for nine tests with the MDT1 (M1), the MDT2 (M2), the Autoliv-Chalmers (AC) and the Ifsttar-Autoliv (IA) dummies for centered impacts at medium (med) or high (hi) speed. See Table 4 for full test description by number. The test 38 is the most severe test with the standard vehicle and the test 31 corresponds to the test with the best combination of dummy signals and kinematics. Colors were conserved between plots. The resultant of the tibia moments were only calculated based on the X and Y components (since Z was not measured). All results in the dummy reference frame.

Table 5: Summary of injury criteria values. All criteria were computed using the 200ms after the beginning of the impact (except upper tibia index and TTI: 60ms). Criteria were computed using SAE J211 or EEVC recommendations for filtering. Legend: MDT1=standard medium duty truck; MDT2=modified medium duty truck; LDT=low duty truck; AC=Autoliv-Chalmers dummy; IA=Ifsttar-Autoliv dummy; C=impact to the center of the vehicle; R=impact to the right of the vehicle; low=speeds between 14.9 and 17.5 km/h; med=speeds between 24.5 and 27.1 km/h; hi=speeds between 34.9 and 35.1 km/h. Channel data not available for test 22.

Test	Vehicle Dummy	Location	Speed	HIC15	TTI (g)	Rib defl. (mm)	Pelvis acc(g)	Femur mom. (N.m)	Femur force (kN)	Tibia acc (g)	TI upper	TI lower	Tib up mom (N.m)	Tib low mom (N.m)	Left Knee angle (°)	Right Knee angle (°)	
01	MDT1	AC	C	12	10	18.5	26.3	21.1	125	1.30	45	-	0.56	455	125	-	-
02	MDT1	AC	C	low	32	27.9	27.1	37.4	117	1.59	66	-	0.70	276	157	4.5	5.7
03	MDT1	AC	R	low	30	26.8	27.2	47.5	375	1.68	124	-	0.26	123	58	0.3	1.4
04	LDT	AC	C	low	8	18.2	23.4	30.9	549	1.71	72	-	0.62	234	138	4.7	0.3
05	LDT	AC	R	low	15	17.0	27.1	39.3	561	1.31	47	-	0.71	411	160	6.5	0.4
06	LDT	AC	C	19	21	31.4	26.4	37.9	701	2.78	79	-	0.76	545	169	9.3	0.3
07	LDT	AC	C	med	117	46.2	29.5	57.0	754	2.71	256	-	0.84	1047	188	18.5	0.8
08	LDT	AC	R	med	72	43.0	29.7	64.4	772	2.30	172	-	0.71	310	160	16.3	1.9
13	MDT1	AC	C	med	565	42.7	31.0	35.3	640	2.22	194	-	1.01	1064	227	9.6	0.6
14	MDT1	AC	R	med	483	71.9	28.9	86.2	487	4.22	320	-	0.81	977	181	5.7	-
21	MDT2	IA	C	low	4	23.1	21.3	27.4	399	1.34	53	1.14	0.61	255	133	0.3	0.3
23	MDT2	IA	C	low	5	21.3	15.0	25.7	431	1.10	75	1.73	1.01	387	225	5.2	0.0
24	MDT2	IA	C	low	16	31.2	24.8	25.6	489	1.04	65	1.72	0.88	384	196	5.5	0.0
25	MDT2	IA	C	med	59	37.8	26.7	43.2	508	1.77	90	1.90	0.98	427	220	9.6	3.1
26	MDT2	IA	C	med	97	47.3	26.4	57.5	503	2.28	143	1.91	1.02	426	229	8.7	1.2
27	MDT2	IA	R	low	5	20.8	15.5	18.6	299	0.76	66	1.22	0.73	272	163	0.0	0.0
28	MDT2	IA	R	med	46	38.2	25.6	27.4	375	1.56	118	1.98	1.39	442	311	0.4	1.2
29	MDT2	IA	C	med	83	37.8	22.5	42.6	441	1.46	98	1.14	1.02	255	228	12.5	4.4
30	MDT2	IA	C	hi	184	70.0	24.5	87.1	453	1.91	169	2.27	1.08	508	243	16.5	16.8
31	MDT2	IA	C	hi	192	52.4	31.6	46.5	462	2.31	196	2.22	0.86	496	193	19.7	2.4
32	MDT2	IA	C	hi	85	51.2	37.4	40.9	388	1.64	173	2.38	1.00	535	222	13.3	7.7
33	MDT1	IA	C	low	4	15.2	13.7	29.8	613	2.19	62	1.65	0.69	371	156	6.7	0.0
34	MDT1	IA	C	low	6	28.2	15.9	27.2	655	2.57	53	1.73	0.68	388	153	8.6	1.0
35	MDT1	IA	C	low	12	25.5	15.9	24.3	619	2.16	53	1.66	0.73	373	163	7.5	0.2
36	MDT1	IA	C	med	266	37.9	23.6	42.4	632	2.94	168	1.76	0.88	393	198	12.2	0.0
37	MDT1	IA	R	med	87	67.8	33.7	54.2	597	2.76	309	1.72	0.73	386	162	14.1	0.0
38	MDT1	IA	C	hi	992	70.2	40.1	57.0	661	3.88	310	2.28	1.18	503	264	23.8	5.5

DISCUSSION

Epidemiological approach

The analysis performed in the current study was based on two complementary databases: Renault Trucks (RT) and the Rhône Registry (RR). The first database includes only fatal cases with trucks and the second includes mostly non fatal cases with all vehicle types. For urban accidents, the analysis was mostly focused on pedestrian as they were the larger category of vulnerable road users. The results from the two databases are mostly in agreement with literature data from other countries and sources. More specifically:

- the most common scenario was by far the pedestrian crossing the road while the industrial vehicle was moving forward. The impact occurred mainly on the front of the vehicle (RR, RT and AP-SP83-D835, 2006).

- accidents involving trucks or buses were more often fatal than accidents with cars (RR). The numbers were within the range of European results as reviewed by Niewöhner and Hoogvelt B. (2006).

- a majority of the pedestrians involved in accidents with trucks and buses were adults between 16 and 60 (RR) but a majority of the killed were older (RR, RT)

- there was a run over in 75% of the pedestrian fatal cases with trucks (RT).

- for all vehicle types (RR), injuries to the lower extremities were predominant for lower AIS levels while head injuries were predominant for the highest levels. However, thorax injuries were much more common for trucks and buses than for cars (RR). This has also been suggested for flat front vehicles by Tanno et al. (2000) and for light trucks and vans by several authors including Longhitano et al. (2005).

While no impact speed was directly available from the databases, the accident scenarios obtained for 31 cases of the truck fatal cases (RT) suggest speeds lower than 25km/h for 21 cases, and between 30 and 50km/h in 10 cases. Tanno et al. (2000) suggested a median speed of about 30 km/h for the cases with an injury severity score superior to 16 for flat front vehicles. In general, while relatively low speeds are suggested, better speed

estimates and a better knowledge of the relationship between speed and injury outcome would be useful to improve the understanding of the injury mechanisms.

This data, combined with literature sources, were useful to help selecting impact conditions for the subsequent phases of the study (accidents involving the front of the vehicle with a pedestrian crossing). This is similar to the choice made in the Aprosys project (Feist and Mayrhofer, 2005). The results also emphasized the need to study both pedestrian kinematics issues (problem of run over) and primary impact issues (with a special attention to the thorax).

Pedestrian dummies and impactors

Because of the need to study the kinematics in relation with a possible run over, the exclusive use of EEVC like subsystems was not possible. Furthermore, when used against the MDT1, the EEVC legform model started rotating with its upper end going away from the vehicle. This kinematics would not be possible with a human (or a dummy) due to the mass of the upper body and the softness of the front lid. For the MDT1, simulations suggested that the legform kinematics was closer to the dummy response after adding a mass (e.g. 10 kg) on top of the legform. Similar sensitivity of the legform to the position of the impact point has been already pointed in the past (e.g. Yasuki, 2005).

The choice was made to use a physical dummy and its corresponding FE model for most of the study. The availability of the FE model was critical for the methodology that was put in place: the model was used to prepare the tests, simulate impact velocities that could not be tested, and most importantly, support the design of the modified truck.

The first dummy used was the Autoliv-Chalmers dummy and its Radioss model. The modification of this dummy to create another one (numerical at first and then physical) was motivated by the following observations from the first test series:

- (1) while the thorax is a region of interest based on epidemiological results, its deflection seemed largely insensitive to the impact speed and accelerometer signals were difficult to interpret. The thorax also seemed unable to detect localized loading and the absence of shoulder was suspected to possibly affect the kinematics (considering the sequence of contacts)
- (2) large vibrations occurred at the upper tibia load cell. They were attributed to the difficulty to tighten the knee deformable elements
- (3) the lumbar spine spring was also difficult to tighten to prevent the rotation of dummy thorax.

When comparing the responses of the two dummies (AC and IA), their kinematics were similar except the tendency of their thoraces to rotate vertically about Z in opposite directions. This was attributed to the presence of the arm and shoulder in the IA dummy. A similar tendency was observed in Lessley et al. (2010). The changes also affected some of the signals (e.g. head, thorax deflection, upper tibia). However, most signals remained comparable (shape and amplitude) and the modified dummy appears to be more an evolution than a radical change from the original.

Besides the need for better evaluation of the global dummy response and of the selected injury criteria, the following observations – that could lead to future improvements in the short term – were made during the testing:

- at 1.80m, the dummy may be too tall. A modification of the Hybrid III lumbar spine bracket could allow reducing the dummy height and removing the abdomen spacer currently needed.
- the repeatability of the dummy position prior to impact should be improved as it can affect the order of the contacts in the current scenario. This could be achieved by defining detailed positioning procedures and perhaps modifying the lumbar spine to reduce its initial compliance

Other pedestrian models were also evaluated for the current impact scenario. First, a pedestrian Madymo human model was used against the MDT1. However, numerical issues in the Madymo-Radioss coupling prevented the exploitation of the simulation results. Then, the pedestrian HUMOS2 model was used against the MDT1 and MDT2. However, the base model required many modifications to run and it was plagued with severe numerical issues that could not be solved (computing cost, hourglass deformation modes, etc). Overall, while these two approaches can provide additional information about the current impact scenario, their use was deemed impractical (for now at least) for the current design process.

Impacts with standard vehicles

For the LDT, while there was some wrap around kinematics of the pedestrian dummy, it was more limited than in Kerrigan et al. (2009) or Snedeker et al. (2005) as the profiles of vehicles used in these studies seemed lower. The LDT profile seemed closer to some configurations used in Fredriksson et al. (2007) but only seated dummies were used in their study. Despite the limited wrap around, the kinematics contrasted with the one observed for the vertical vehicles: for these, there was no wrap around at all and the short throw distance in front of the vehicle suggested a high risk of run over.

Most of the injury criteria were found sensitive to the impact speeds. It is therefore important to remember in the overall view that only the low and medium speeds were tested with the LDT and the bus. Overall, most injury criteria that were calculated were below their limit for the upper body (pelvis, thorax and head). Several values were very close to the limits (e.g. head at 35km/h for the MDT1 and some thorax deflections). This contrasted with the lower extremities for which numerous values were largely above the limits (e.g. upper TI, knee flexion angles, tibia accelerations, etc). While this overview is in overall agreement with the epidemiological results for the lowest injury levels (run over not being considered in testing), it cannot be assured that the dummy and criteria provide accurate risk estimates for the impact selected scenario. For example, the consistently high values of femur moments and their apparent insensitivity to speed would need to be further investigated. Also, the criteria used for the tibia only partially take into account the applied loads. However if the overall results are considered, it appeared reasonable to use the dummies and their criteria to compare vehicle designs or impact scenarios between each other.

Comparison of the MDT1 and MDT2

Using dummy and subsystem simulations, a modified medium duty truck (MDT2) was designed and dimensioned with following objectives (1) the reduction of injury criteria values associated with the primary impact and (2) the reduction of the risk of run over. In terms of design constraints, it was decided to evaluate what type of improvements could be obtained without changing the type of the truck (i.e. without transforming the truck into a large van or adding a large extension as in Feist and Fassbender, 2008). The resulting design, which has a limited footprint in terms of vehicle length, was implemented into a physical prototype.

During the final evaluation in the second test series, the new design led to a reduction of the values of most injury criteria. The reduction was sometimes very large (e.g. head, tibia acceleration at 35km/h). One exception was the lower tibia index which did not seem affected to be by the design changes (or even increased slightly). However, despite these reductions, some of the criteria were still largely above the limits for the lower extremities (e.g. femur moment).

The design changes also led to a vertical impulse for the dummy and a higher throw distance. However, the increase of distance was relatively small until the upper bumper support was removed (test 31). It was also less prominent in the test 32.

This can be attributed to the early collapse of the front lid under the thorax. These results highlight the importance of the relative stiffness of the truck regions to control the dummy kinematics.

With this kinematic change, the trajectories of dummy pelvic targets were shifted by more than 1.5m between the MDT2 (test 31) and the MDT1 (test 38). Based on the extrapolated trajectories (Figure 14), this corresponds to an increase of about 40% of the distance between impact and intersection between pelvis trajectory and ground (about 5m vs. 3.5m). For the run over of vital zones by the wheels (which is the criteria proposed by Feist and Mayrhofer, 2005), the possible sliding/rebound on the ground, the distance between the wheels and the pedestrian at the position at impact and the distance between head and pelvis (since the feet are closest to the truck when the dummy stops on the ground) could all affect favorably the risk of run over.

While the run over is inevitable if the vehicle does not stop, the optimal braking performance of a truck is around 6m/s^2 , or 7.9m from 35km/h. While it is far from certain that the kinematic change would provide sufficient time for the truck to stop, the combination of this change (possibly increased by further modifications of the truck's front) and emergency braking (triggered by the impact or just before the impact) could provide a viable protection strategy against pedestrian run over. Such a strategy could be compatible with existing vehicle architectures. It could also be a complementary solution to active pedestrian systems for which an early triggering (at least 7.9m to avoid impact at 35km/h) may be problematic in an urban setting with numerous pedestrians.

One limitation of these results is that it is difficult to know how realistic the increase of throw distance is for several reasons: (1) the feet were almost always in contact with the floor for the MDT1 tests and the lower limb stiffness under gravity may have affected the fall; (2) the ability of the dummy to dissipate energy is unclear (viscous dissipation as opposed to elastic storage leading to rebound). These aspects should be further investigated in the future.

Finally, while the impacts on the right of the MDT2 were also associated with reductions of the injury criteria, the impact was too centered to evaluate the effect of the increased curvature on the corner of the MDT2. The efficacy of this curvature to push the pedestrian on the side should be further evaluated.

CONCLUSIONS

A methodology was developed to study the safety of pedestrians involved in accidents with industrial vehicles such as trucks and buses. The methodology is based on the combined use of testing and simulation using pedestrian dummies. An experimental dummy was modified specifically for this purpose. The methodology was applied to (1) study accidents with three standard industrial vehicles and (2) evaluate the possible benefits from a new design aiming to reduce the risk of run over and consequences of the primary impact. The results from the evaluation appeared to be encouraging. They could lead to a possible protection strategy if combined with emergency braking.

ACKNOWLEDGMENTS

The research was performed within the PRUDENT-VI project by partners of the Lyon Urban Trucks and Buses 2015 competitive cluster. The project was made possible by the support of the French Ministry of Industry (DGCIS), the city of Lyon (Grand Lyon), the Rhône-Alpes Regional Council (Conseil Régional Rhône Alpes) and the Rhône district council (Conseil Général du Rhône).

The authors would like to thank Mr Rikard Fredriksson (Autoliv Research) for his precious help during the project. They would also like to thank all personnel that helped in the current study.

REFERENCES

AP-SP83-D835 (2006) *Characteristics of Heavy Trucks versus pedestrians and/or Cyclists*. APROSYS SP8.3 Deliverable D8.3.5. Available online at www.aprosys.com. Accessed March 7, 2011

Beillas P., (2009) *Protection des Usagers vulnérables lors d'un accident de la route contre un Véhicule Industriel*. Seminar on Vulnerable Road Users and Health. GO2/Predit 4. July 2-3 2009.

EEVC Working Group 17 (2002) *Improved test methods to evaluate pedestrian protection afforded by passenger cars*. Report. December 1998 with September 2002 updates.

Feist and Mayrhofer (2005) *APROSYS SP2 Preliminary Aggressivity Index Report*. AP-SP21-0047. Available online on www.aprosys.com. Accessed on March 07, 2011

Feist and Fassbender (2008) *Demonstration of truck front design improvements for vulnerable road*

users. APROSYS SP2 Project report. AP-SP21-0088. Available online on www.aprosys.com. Accessed on March 07, 2011

Fredriksson R., Håland, Y., and Yang J. (2001). *Evaluation of a new pedestrian head injury protection system with a sensor in the bumper and lifting of the bonnet's rear part*. 2001 ESV Conference. Paper number 131.

Fredriksson R., Flink E., Boström O., and K. Backman (2007). *Injury Mitigation In SUV-to-Pedestrian Impacts*. ESV Conference 2007. Paper number 07-0380

Kerrigan J., Arregui C. and Crandall J. (2009) *Pedestrian Head Impact Dynamics: Comparison of Dummy and PMHS in Small Sedan and Large SUV impacts*. 21st ESV Conference. Stuttgart, Germany, June 15–18, 2009. Paper Number 09-0127

Lessley D., Shaw G., Parent D., Arregui-Dalmases C., Kindig M., Riley P., Purtsezov S., Sochor M., Gochenour T., Bolton J., Subit D., Crandall J., Takayama S., Ono K., Kamiji K. and Yasuki T. (2010) *Whole-Body Response to Pure Lateral Impact*. Stapp Car Crash Journal, Vol. 54 (November 2010), pp. 289-336

Longhitano D., Ivarsson J., Henary B., and Jeff Crandall (2005) *Torso Injury Trends for Pedestrians Struck by Cars and LTVs*. The 19th International Technical Conference on the Enhanced Safety of Vehicles (ESV) - Washington D.C. June 6-9, 2005.

Niewöhner W. and Hoogvelt B. (2006) *Real-world crashes involving trucks and cars, cyclists or pedestrians – Results of the EU Research Subproject APROSYS SP8.3*. DEKRA/VDI Symposium Safety of commercial vehicles, Neumünster, October 12th-13th 2006

Snedeker J.G., Walz F.H., Muser M.H., Lanz C., G. Schroeder (2005) *Assessing Femur and Pelvis Injury Risk in Car Pedestrian Collisions: Comparison of Full Body PMTO Impacts, and a Human Body Finite Element Model*. ESV Conference 2005. Paper number 05-103

Tanno K., Kohno M., Ohashi N., Ono K., Aita K., Oikawa H., Myo-Thaik-Oo, Honda K., Misawa S. (2000) *Patterns and mechanisms of pedestrian injuries induced by vehicles with flat-front shape*, Legal Medicine, Vol 2, 2000, pp 68-74

Yasuki T. (2005) *A Survey on the Biofidelity of the Knee Bending Angle of the TRL Lower Leg Impactor*. 17th ESV Conference. 2005. Paper Number 05-0101

HOLLAND: VRU PARADISE GOES FOR THE NEXT SAFETY LEVEL

Margriet van Schijndel - de Nooij

Stefanie de Hair-Buijssen

Ton Versmissen

TNO

The Netherlands

Rikard Fredriksson

Erik Rosén

Jan Olsson

Autoliv Research

Sweden

Paper Number 11-0094

ABSTRACT

In Europe there has been a large focus on increasing pedestrian safety by requiring protection capability of cars, both using regulations and consumer tests, however none of this involved the safety of bicyclists in car crashes. The increasing use of bicycles in many major cities leads to the expectation that the number of cyclist fatalities will increase in the coming years, unless proper actions are taken.

In the Netherlands, a country with many cyclists, there were 720 road fatalities in 2009, of which 69 pedestrians and 185 cyclists. About half of the cyclist fatalities were directly related to an impact by a passenger car. In protection of cyclists and pedestrians, cornerstones are infrastructure, training, visibility/detectability of the vulnerable road user (VRU), and VRU friendliness of the vehicle. The first three cornerstones are dealt with in several (national) projects; the latter so far gained little activity within the Netherlands.

Initiated by the Dutch Cyclists' Union, the Dutch Ministry of Transport commissioned a project on the vehicle VRU friendliness. The overall target is to decrease the number of VRU fatalities and severe injuries. The preparation phase contained experiments and simulations studying cyclists' movements during the last seconds prior to impact. These activities were combined with accident reconstruction tests of a dummy riding a bike that was impacted by a passenger car. A study to the protection potential has been initiated, aiming to determine the number of fatally and severely injured (AIS3+) VRUs potentially saved by different types of countermeasures. This study focuses on the Dutch situation covered by the Dutch BRON database, enriched with GIDAS. While the effectiveness calculations remain to be done, the study shows that cyclists hit the windscreen area on a higher location than pedestrians. For all VRUs, the windscreen area is the main injury source. In the cases studied, ground

impact accounts for 20% of all AIS3+ injuries. AIS3+ survivors sustain in most cases a single AIS3+ injury (80% for cyclists, 70% for pedestrians), while the majority of fatalities suffered from AIS3+ and AIS4+ injuries to more than one body region. Cyclists suffer from leg injuries considerably less than pedestrians.

The current phase of the project is on the development and evaluation of a Proof of Concept of a VRU protection system. The major part of this phase consists of a Sensor Field Test, in which the vision system for classification of cyclists, pedestrians and "other objects", to trigger an airbag and/or automatic braking system, is further developed and tested. This Sensor Field Test runs for a year in order to encounter enough close-to-accident situations needed to develop a system with a high detection rate in combination with a sufficiently low number of false positives. The Proof of Concept will also be evaluated in laboratory tests, in crash and pre-crash situations, using the "Beyond NCAP" protocols of Euro NCAP. When proven successful, a larger Field Test covering several European countries would be an essential step towards further implementation of these types of systems.

INTRODUCTION

In most EU countries bicycles are mainly used for sporty activities. However, in the Netherlands the bike is a widely accepted means of daily transport for distances up to 10-12 km. With the increasing number of both cyclists and passenger cars in a shared environment, the issue of safety becomes increasingly important. For the physical safety of the car driver, accidents with cyclists are normally not catastrophic. On the other hand, the cyclist is much more vulnerable, just like pedestrians. Therefore, passenger car-to-cyclist/pedestrian accidents often cause severe or fatal injuries to the VRU [4]. While a lot of worldwide attention is being paid to the safety of car occupants as well as of motorcyclists

in almost any type of accident, pedestrian and pedal cyclist safety has been lagging behind. With an increasing number of cyclists that use the bike as an environment friendly means of transport [19], e.g. in major cities such as Paris, London, Barcelona and Berlin, cyclist safety starts to gain the attention it deserves. Figure 1 shows that safety of VRUs is at stake in many major European cities.

To improve cyclist safety there is a number of important instruments available, which include:

- Training
- Infrastructure/separation of traffic
- Cyclist visibility, especially at dawn and at night
- Pedestrian & cyclist friendliness of the vehicle.

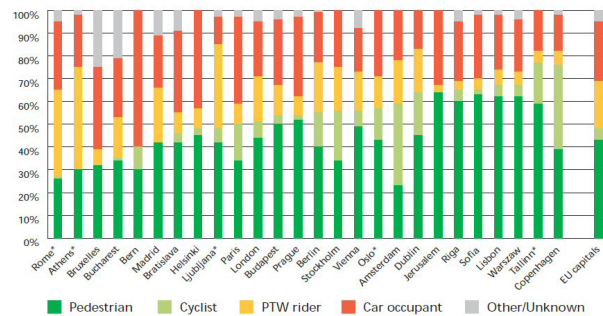


Figure 1. Distribution of road deaths by road user groups (2004 – 2006) [1]

In the Netherlands the number of fatalities in road traffic has been reduced from over 3000 per year in the 1970s to 720 in 2009. However the number of cyclist fatalities has been stable at around 185 per year for a long period [15]. Concerned by this situation the Dutch national government started some years ago to be more active in increasing cyclist safety. This is supported, stimulated and in some areas initiated by interest organisations such as the Dutch Cyclists’ Union.

A major Dutch project in the field of cyclist and pedestrian protection, called SaveCAP, was initiated by the Dutch Cyclist Union and the Dutch Ministry of Infrastructure and Environment. The main objective of SaveCAP is the development of an evaluated Proof of Concept for VRU safety systems. A consortium was formed, including also TNO, Autoliv and Dutch insurance company Centraal Beheer Achmea. Since 2008, they cooperate within SaveCAP. The Dutch Ministry of Infrastructure and Environment strives towards less than 500 road fatalities in 2020 and sees this project as an instrument to achieve this, while being its main funder. TNO acts as project leader and development partner, as well as the organizer of the Sensor Field Test and Proof of Concept Evaluation. Autoliv works on the system development, for the sensor and

protection system, including development of new test methods for cyclists based on accident data in Sweden and Germany. Funding has been provided for parts of this work by the Swedish Transport Administration and the Swedish government (FFI; Strategic Vehicle Research and Innovation). Centraal Beheer Achmea and the Dutch Cyclist Union support with project focus and supply real life data on car-to-VRU accidents, and cyclist needs.

The focus of this paper is on the protection potential of countermeasures on the vehicle towards fatally and severely injured cyclists and pedestrians. The paper starts with a short overview of the recent history of pedestrian protection. Many lessons learned here can be used for cyclist protection. This part is followed by case studies found in the Netherlands, enriched with data from the German In-Depth Accident Study (GIDAS). It is followed by an injury study based on GIDAS accident data. This section shows the distribution of severe injuries sustained by cyclists and pedestrians. Furthermore, it includes a description of the injury producing sources, such as ground, bonnet and windscreen. A study on the protection potential of several countermeasures is partially based on this, indicating the potential benefits for road safety in the Netherlands. Countermeasures taken into account are a VRU airbag, a pedestrian airbag, automatic braking and a deployable bonnet. For systems detecting the Vulnerable Road User (VRU) prior to impact, a reliable detection system is necessary. The last technical section will focus on the running Sensor Field Test for development and evaluation of such a detection system.

DEVELOPMENTS IN PEDESTRIAN AND CYCLIST SAFETY

Pedestrian safety research has been conducted since the 1970’s but it was with the introduction of consumer tests (Euro NCAP) in 1997 and legal tests in Japan and Europe 2005 [5] [16] that the development of pedestrian countermeasures gained momentum. Passive solutions for the bumper, headlights, bonnet, wing and scuttle areas have been presented and to some extent been introduced [2] [10]. While later Euro NCAP improved leg test results show that the bumper area has proven feasible to accommodate solutions, the bonnet area is more challenging. To give the energy absorption distance necessary and keep design freedom of the car, deployable bonnets have been developed and introduced in a number of car models (e.g. Jaguar, Citroën, Honda, BMW, Mercedes-Benz, Cadillac, Nissan and Porsche).

While current legal tests do not evaluate the windscreen area, this is included in Euro NCAP tests. This in combination with the recent introduction of combined rating of occupant and pedestrian protection [7] is expected to give increased focus on windscreen area solutions. Different airbags for the lower windscreen and a-pillars have been presented [3] [14] [12].

Another solution to increase the safety for pedestrians is aiding the driver in reducing the impact speed, and in some cases even avoiding the accident completely. Brake-assist, a system which aids the driver to optimize the braking in panic situations, was mandated in Europe 2008. The shortcoming of this system is that the driver needs to initiate the braking action. Since it is common in car to pedestrian accidents that no braking action is taken [11], probably due to that the driver does not notice the pedestrian before the impact; a natural next step is developing automatic braking systems. Automatic braking systems that gently or fully apply the brakes when a pedestrian is detected have been introduced recently [13] [20].

Both automatic braking systems and bonnet/windscreen countermeasures have been estimated to potentially save 27-44% of severely or fatally injured pedestrians when impacted by a car front, and over 60% if these systems are combined in an integrated system [8] [17]. While focus has been on pedestrian protection, less focus has been laid on cyclist safety so far. Within SaveCAP, first tests on accident reconstructions with cyclists have been performed. First, tests with volunteers were done, showing the last-moment moves that cyclist are capable of, in an attempt to avoid an accident. Furthermore, accident reconstruction full crash tests were performed, with a dummy (Hybrid III pedestrian) riding a bike, impacted by a car. Car speeds used were up to 50 kph, the bike speed was ¼ of the vehicle speed, see Figure 2.

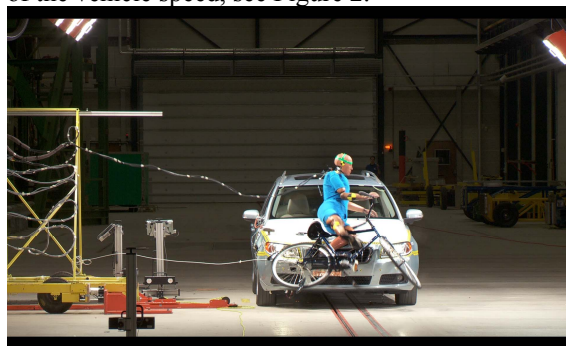


Figure 2. Biking dummy impacted by a car, under lab conditions

ANALYSIS OF VRU SAFETY SITUATION IN THE NETHERLANDS

Method

When starting the project SaveCAP, the first action was to look into the relevant accident information for the Netherlands, to gain deeper insight in the actual numbers of cyclist and pedestrian fatalities and severe injuries, as well as the accident scenarios. In this study, the following data sources were used:

1. Dutch National Accident databases (BRON),
2. German in-depth data bases (GIDAS) [23],
3. Insurance company data (Centraal Beheer Achmea),
4. Results of EU projects eIMPACT [22] and APROSYS [21].

BRON and GIDAS (see also Table 1) were used to obtain dedicated figures representative for the Netherlands. BRON was used as the base data source and was enriched with GIDAS data, since some of the important categories are not present in BRON. It was assumed that certain aspects of GIDAS data are representative for the Dutch situation.

Table 1. BRON and GIDAS databases

Topic	BRON (Netherlands)	GIDAS (Germany)
Data sources	Based on police reports	Specialist teams on accident location.
Registration criteria	Accident reported to the police	Accident reported to the police, rescue services and fire department headquarters and involving personal injury.
Coverage	Covers 80% of all cases in entire Netherlands	Covers most cases in regions of Hannover and Dresden, in which a person gets injured. The data is representative for the situation in Germany.
Database owner	SWOV (Dutch institute for road safety research)	GIDAS is a joint project between FAT (Automotive Industry Research Association) and BAST (German Federal Road Research Institute)

Injury level included	AIS1+, no distinction on severity level	All AIS levels included, distinction can be made
Years used in current study	2006-2008	1999-2007
Relevant data for current study	<ul style="list-style-type: none"> • Number of fatalities and severely injured • Age • Road type • Vehicle type • Frontal accident • Weather and lighting conditions 	<ul style="list-style-type: none"> • Ratio AIS1+ : AIS3+ • Head injury level • Impact location • Head impact location • Car braking level

In this study only the severe injuries (fatalities and AIS3+ (Abbreviated Injury Scale)) were taken into account. The AIS3+ and fatality cases are most relevant target groups to be saved by the countermeasures considered. The BRON database contains only figures of severity level AIS 1+ injuries, and beside fatalities no other injury levels are distinguished. The relation AIS1+, AIS3+ and fatal injuries from GIDAS were used to obtain AIS3+ figures representative for the Netherlands.

The ability of VRU safety countermeasures to reduce fatalities and mitigate injuries depends on several factors. The main factors taken into account are:

- type of vehicle,
- whether the VRU strikes the front of vehicle,
- speed of vehicle,
- whether the vehicle brakes or not,
- age of the VRU,
- impact location of head on vehicle,
- lighting conditions,
- weather conditions.

For the Netherlands representative numbers and their interrelation to the above mentioned categories were obtained (using BRON and GIDAS data). The data was handled in two steps.

The first step The data was filtered from the reference group (all accidents in which a VRU is severely or fatally injured) to the target group (those that can potentially be helped by the considered countermeasures). This target group consists of those cases in which a VRU is hit by the front of a moving passenger vehicle on a road with speed limit lower than or equal to 80 km/h (since very few VRU related

accidents occur on these Dutch roads). The resulting target group was used as input for the second step.

The second step A so called data tree was filled. The tree shows the number and cases and due to which combination of main factors the VRU became injured.

Table 2 gives an overview the categories used in the data trees and the origin of data used to fill the data trees. Furthermore it is explained how the data was divided over the different categories.

Table 2. Categories used in the data trees

Road type
The accident data was categorized according to the speed limit of the roads: <ul style="list-style-type: none"> • urban roads: speed limit ≤ 50 kph. All roads with a maximum speed limit of at most 50 kph, • rural roads: speed limit > 50 kph The roads with a maximum speed limit higher than 50 kph, but with a maximum of 80 kph. Roads with higher speed limits were not taken into account, as very few VRU related accidents occur on these Dutch roads.
VRU Age
The accident data was categorized according to the ages of the injured VRUs in BRON. Based on their age the cases were allocated to the appropriate category: <ul style="list-style-type: none"> • child: age ≤ 12, • adult: $12 < \text{age} \leq 65$, • senior: age > 65. The cases in which the age of the VRU was not specified were excluded.
Car braking*enriched
In GIDAS the car deceleration level is registered, a derived parameter, for example from the braking marks on the road and accident reconstruction simulations. This deceleration level was used to make a distinction between the following categories: <ul style="list-style-type: none"> • car is braking • car is not braking (deceleration is zero or the vehicle is accelerating). The GIDAS ratio between braking and not braking was used to enrich the BRON data. The cases with unknown braking levels were excluded.
Severe head injury*enriched
The GIDAS database contains a variable showing the VRU's head injury severity. The level is specified in AIS levels. Two categories are distinct: <ul style="list-style-type: none"> • severe head injury: head injury level is AIS3+ • no severe head injury: no head injury or a head injury of AIS1 or AIS2 The ratio between these two categories was used to enrich the BRON data. The cases with unknown head injury severity were excluded.

Head impact location*^{enriched}

The GIDAS database contains a variable which denotes on which zone of the car the VRU's head strikes the car. The zones are visualised in Figure 3. Zone 4 represents the windscreen. The 'no windscreen' cases were represented by impact to the car by the bonnet zones 1, 2 and 3 and the roof 5 or by cases in which the head does not hit the car (e.g. ground impact). The unknown cases were excluded from the data taken into account.

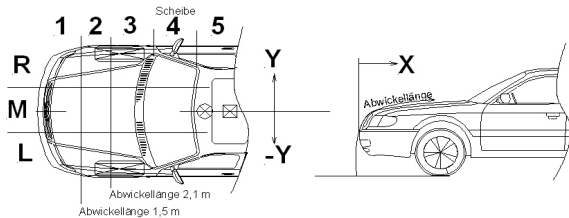


Figure 3. GIDAS definition of head impact location

Given that the victim's head strikes the windscreen, the method needed to distinguish between whether the head strikes the top or the bottom of the windscreen. The GIDAS variable does not make a distinction between the top and the bottom of the windscreen. To obtain this information the GIDAS photo material was used to investigate all cases in which the VRU's head struck the windscreen. On the basis of this information, visualized in Figure 4, a distinction was made between the cases that struck the top or bottom of the windscreen.

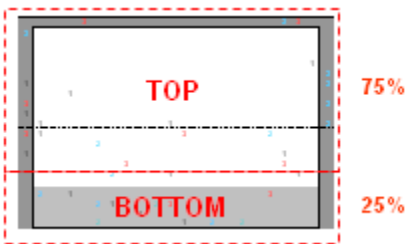


Figure 4. Schematic representation of windscreen containing the definition of windscreen TOP (upper 75%) and BOTTOM (lower 25%)

Lighting conditions

The lighting conditions were taken from the BRON database. The cases were divided over the following categories:

- darkness,
- daylight: meaning daylight and twilight.

The cases in which the lighting conditions were not specified are excluded.

Weather

The BRON data offers the weather conditions. The cases were divided over the following categories:

- normal weather: dry weather and hard wind,
- adverse weather: rain, fog, snow, hail.

The cases in which the lighting conditions were not specified were excluded.

Several data trees were setup taking the following categories into account: severely injured versus fatalities, cyclist versus pedestrians and countermeasure type. The data trees were first filled with available BRON data, complemented by using the relations retrieved from a comparable data tree setup with GIDAS data (see next section on the results). Since the number of relevant cases in GIDAS is very small, there are cells in the data tree without any cases. In these cases the proportion of a representative other subcategory was used. For example, in GIDAS no data was available about fatally injured children in urban areas, whereas in BRON there were. In order to obtain data for the Dutch situation for the braking and no braking cases for this category, overall mean values of the adult category were used to calculate the number of braking and not braking cases.

Results

The first step: determination target group

The resulting target group size was 398 (out of 905 from reference group) severely-injured cyclists and pedestrians for one year, based on detailed information available over the years 2006-2008. For fatalities, the target group was 93 (out of 228 from reference group) cyclists and pedestrians.

Table 3: Filtering from reference to target group

# cases 1 year (cyclists & pedestrians)	Reference group	Target group
Severely injured	905	398
Fatally injured	228	93

The second step: data trees

The data tree is structured around braking and severe head injury, based on the assumption that the head injury is the main injury. If head injury could be prevented, the VRU involved could be saved. Based on newest insights (see next section) the structure of the data trees should be extended. Beside head injuries chest injuries should also be taken into account, in order to draw conclusions on the protection potential of the considered countermeasures. The data trees are shown in Table 4 till Table 7.

In these tables, weather and lighting conditions are not included. Each table contains a section on urban cases and a section on rural cases. For both locations, a split is made into three age categories: children, adults and seniors. Thus, Table 4 shows e.g. for severely injured pedestrian children in the urban environment 21,3 cases, of which 6,6 sustained severe head injury. From this number, 3 cases of

severe head injury were caused by a head impact on the bottom of the windscreen. Furthermore, the table shows that out of the 21,3 cases, in 13,3 cases the car was braking before impact.

In the calculations run to fill the tables, the rounding of digits was done in the latest stage possible. This causes the small errors that can be found when adding the final numbers.

Most fatalities sustained a severe head injury, for cyclists in a majority of the cases caused by the top of the windscreen area. In the group fatalities, elderly are overrepresented.

Table 4. Pedestrians - severely injured. Number of cases for 1 year.

Note: No compensation included for under-reporting of AIS3+ injured compared to fatalities

VRU Age group	Severe Head Injury		Head impact location on Windscreen		Braking		
Urban 65,6							
Child	21,3	Y	6,6	Top	0	Y	13,3
				Bottom	3		
				No	3,3		
N		14,6					
Adult	30	Y	17,6	Top	2,6	Y	15,6
				Bottom	6		
				No	2,6		
N		19					
Senior	14,3	Y	2,6	Top	0,3	Y	9
				Bottom	1,6		
				No	0,6		
N		11,6					
Rural 7,6							
Child	1	Y	1	Top	0	Y	0,6
				Bottom	0,3		
				No	0,3		
N		0					
Adult	5,3	Y	0,6	Top	0,3	Y	3,6
				Bottom	0		
				No	0,6		
N		4,6					
Senior	1,3	Y	1,3	Top	0	Y	0,6
				Bottom	0,6		
				No	0,6		
N		0					
Total 73,3							

The results show that cyclists in general hit higher on the windscreen than pedestrians. Most accidents take place in urban area (speed limit ≤ 50 kph). On rural roads, a large majority of the VRUs (severely injured and fatalities) have (also) severe head injury.

For the severely injured VRUs, there is found a large share of non-severe head injuries. The share of children amongst the severely injured pedestrians is three times higher than their share amongst severely injured cyclists. This effect is not found for fatalities.

Table 5. Cyclists - severely injured. Number of cases for 1 year.

Note: No compensation included for under-reporting of AIS3+ injured compared to fatalities

VRU Age group	Severe Head Injury		Head impact location on Windscreen		Braking		
Urban 269							
Child	24,3	Y	9,6	Top	2,3	Y	9,6
				Bottom	0		
				No	7,3		
N		14,6					
Adult	192,6	Y	71	Top	43,6	Y	101
				Bottom	22		
				No	5,3		
N		121,6					
Senior	52	Y	2,6	Top	1,6	Y	9,6
				Bottom	6		
				No	6		
N		38,6					
Rural 55,3							
Child	5,3	Y	5,3	Top	1,3	Y	2,3
				Bottom	0		
				No	4		
N		0					
Adult	38,6	Y	38,6	Top	19,3	Y	19,3
				Bottom	0		
				No	19,3		
N		0					
Senior	11,3	Y	11,3	Top	11,3	Y	4,6
				Bottom	0		
				No	0		
N		0					
Total 324,3							

Table 6. Pedestrians - fatally injured. Number of cases for 1 year

VRU Age group		Severe Head Injury		Head impact location on Windscreen		Braking		
Urban								21
Child	1,3	Y	1,3	Top	0	Y	0,6	
				Bottom	0,6			
				No	0,6			
		N			0	N	0,6	
Adult	9,3	Y	6,3	Top	1,3	Y	4,6	
				Bottom	3,6			
				No	1,3			
		N			3	N	4,6	
Senior	10,3	Y	9	Top	2,6	Y	6,3	
				Bottom	6			
				No	0,6			
		N			1,3	N	4	
Rural								9
Child	1,3	Y	1,3	Top	0	Y	0,6	
				Bottom	0,6			
				No	0,6			
		N			0	N	0,6	
Adult	5,6	Y	4	Top	0,6	Y	1	
				Bottom	2,3			
				No	0			
		N			1,6	N	4,6	
Senior	2	Y	2	Top	0,6	Y	1	
				Bottom	1,3			
				No	0			
		N			0	N	1	
								30

Table 7: Cyclists - fatally injured. Number of cases for 1 year

VRU Age group		Severe Head Injury		Head impact location on Windscreen		Braking		
Urban								38,6
Child	2,3	Y	2	Top	0,3	Y	1,6	
				Bottom	0			
				No	1,3			
		N			0,3	N	0,6	
Adult	17	Y	14,6	Top	11,6	Y	14,3	
				Bottom	3			
				No	0			
		N			2,3	N	3	
Senior	19,3	Y	14,6	Top	7,3	Y	9,6	
				Bottom	7,3			
				No	0			
		N			5	N	9,6	
Rural								24
Child	2,3	Y	2,3	Top	0,6	Y	1,6	
				Bottom	0			
				No	2			
		N			0	N	0,6	
Adult	12,3	Y	12,3	Top	4	Y	8,3	
				Bottom	8,3			
				No	0			
		N			0	N	4	
Senior	9,3	Y	9,3	Top	9,3	Y	6,6	
				Bottom	0			
				No	0			
		N			0	N	2,6	
								62,6

INJURY PATTERN STUDY FOR CYCLIST AND PEDESTRIANS

Method

The GIDAS database from 1999 to 2008 was used to study the injury pattern of cyclists and pedestrians in real-world, road traffic accidents. GIDAS uses the AIS injury classification system (1998 version), dividing the body into eight different body regions: head, face, neck, thorax, abdomen, spine, and upper and lower extremities [2]. In this study, head and face were combined in a new category called “head”. Thorax, abdomen, and spine were combined in a category called “chest”. Further, lower and upper extremities were called “leg” and “arm” respectively.

The AIS scale comprises six levels of injury severity, where AIS1 denotes minor injury, 2 moderate, 3 serious, 4 severe, 5 critical, and 6 maximal injury. The fatality risk from a single injury increases with the AIS score. In this study, injuries with AIS scores equal to or higher than AIS3 (i.e. AIS3+) were considered severe.

The GIDAS database was queried for all severely and fatally injured cyclists and pedestrians struck by the front of a passenger car or van. This yielded a study group comprising 14 fatally and 88 severely injured cyclists together with 41 fatally and 120 severely injured pedestrians. This group of 263 vulnerable road users suffered from a total of 643 AIS3+ injuries. Injury mechanisms for the pedestrians in this study group were analysed by Fredriksson et al [9].

Results

For fatalities, the majority of cyclists and pedestrians in the study group suffered from AIS3+ and AIS4+ injuries to more than one body region. For both cyclists and pedestrians, approximately 80% had AIS3+ head injuries and 80% had AIS3+ chest injuries. Nearly 60% of the pedestrian fatalities had AIS3+ leg injuries, while only 20% of the cyclist fatalities had AIS3+ leg injuries. At the AIS4+ level, head and chest injuries were even more dominating for both groups.

For AIS3+ injured survivors, it was more common to sustain a single AIS3+ injury compared to the fatalities: 80% of the cyclist and 70% of the pedestrian survivors had only a single AIS3+ injury.

Combinations of AIS3+ injured body regions for fatalities and severely injured survivors are shown in Figure 5 and Figure 6. The fatalities were associated

with AIS3+ injuries to more than one body region, whereas the survivors most often had AIS3+ injuries to only one body region. As many as 70% (17 of 24) of the VRUs with AIS3+ injuries to both head and chest (but no other body regions) died (the average fatality rate for the five injury combinations in the top of Figure 6 (all including head and chest) was 80%). This can be compared to the fatality rate of 11% (7 of 61) for the VRUs with only AIS3+ head injuries and fatality rate of 3% (1 of 31) for those with only AIS3+ chest injuries.

The full meaning of this finding has yet to be investigated. However, it indicates that a countermeasure able to protect from either AIS3+ head injuries or AIS3+ chest injuries would offer a substantial reduction of the fatality risk. On the other hand, cases with AIS3+ injuries to both head and chest were associated with higher maximum AIS, car impact speed and VRU age compared to cases with AIS3+ injuries to only head or chest.

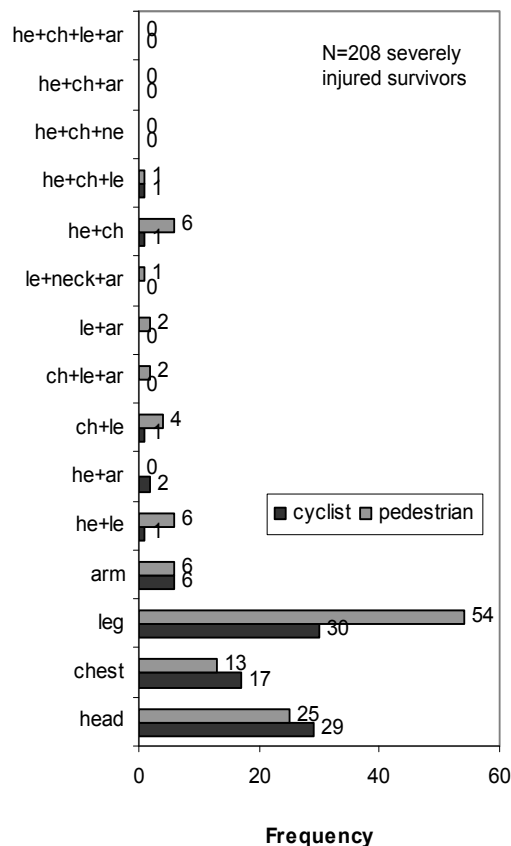


Figure 5. AIS3+ injury combinations for the 208 (88 cyclists, 120 pedestrians) severely injured VRU survivors. The horizontal axis shows the frequency of severely injured survivors with the particular injury combination

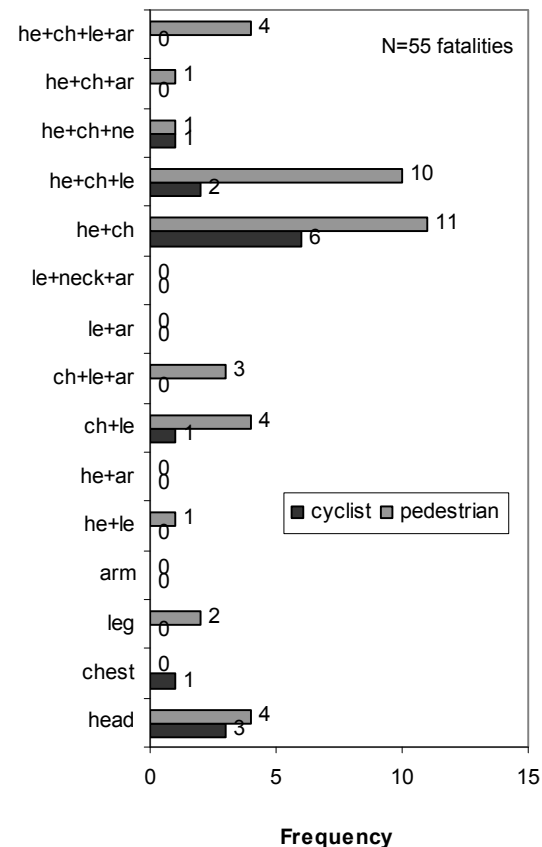


Figure 6. AIS3+ injury combinations for the 55 (14 cyclists, 41 pedestrians) VRU fatalities. The horizontal axis shows the frequency of fatalities with the particular injury combination

Figure 7 shows the distribution of AIS3+ injuries for the total study group (i.e., cyclists and pedestrians as well as survivors and fatalities treated together). Furthermore, Figure 7 shows injury causing parts for each body region. For all VRUs, the windscreen area is the main injury source. In fact, it can be seen that countermeasures for the bonnet and the full windscreen area would have addressed a little over 60% of all AIS3+ head and chest injuries. This in turn made up 45% of all AIS3+ injuries in the study group. Finally, we note that impacts to the ground constituted 20% of all AIS3+ injuries.

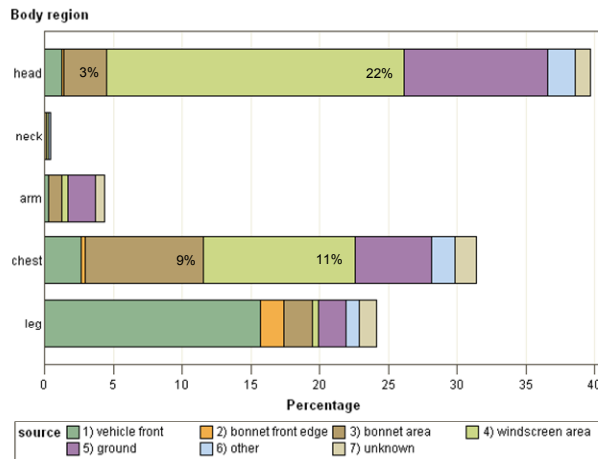
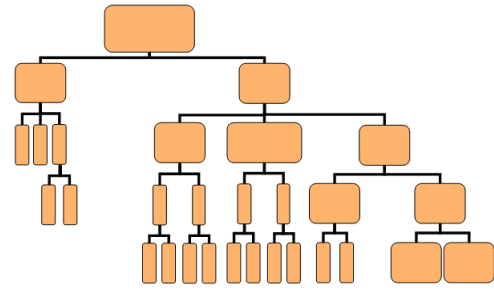


Figure 7. Distribution of AIS3+ injuries for fatally and severely injured cyclists and pedestrians struck by the front of a passenger car or van. Note that a combination of the injuries could be attributed to a single person

Protection potential of vehicle countermeasures

The data analysis described in the previous sections is the first step to get insight in the protection potential of VRU protection countermeasures. A next and future step will be an effectiveness calculation. In this calculation an objective, realistic estimation will be made on the effectiveness of the considered countermeasures (automatic braking, pedestrian airbag, VRU airbag, and deployable bonnet) based on available information (like risk curves, accuracy, airbag geometry, robustness, velocity distributions). This section describes the methodology which can be used to calculate the effectiveness of the considered countermeasures. The reference scenario used to determine the effectiveness potential is the current situation, based on the average of three years of Dutch accident data (2006-2008).



$$\begin{aligned} \text{Number (Data trees)} &= \# \times \# \\ \text{Effectiveness (Effectiveness trees)} &= \# \times \# \\ \text{Reduction of \# Fatalities or MAIS3+} &= \Sigma (\dots\dots\dots) \# \# \end{aligned}$$

Figure 8. Schematic representation of the procedure to determine the effectiveness

The basis of the effectiveness methodology is a tree structure capturing all relevant accident conditions. The structure of the tree is explained before.

The procedure to determine the effectiveness is:

1. The relevant conditions are placed in different levels of the tree. The levels of the tree correspond to the factors determining the effectiveness of the considered countermeasures. Based on the newest insight the tree structure will be extended.
2. Information from databases (BRON & GIDAS) is used to fill the tree with casualty data. This shows under which condition the most injuries/fatalities are inflicted.
3. The extent to which the countermeasure will be effective for VRU protection are estimated and put in the tree, where effectiveness is defined to be the percentage of the VRUs who did NOT die or VRUs who did NOT get injured as a result of the considered countermeasure. The percentages are based on injury risk curves such as illustrated in Figure 9.

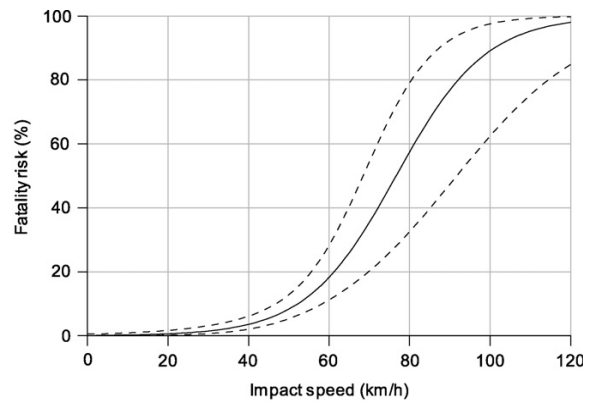


Figure 9. Pedestrian fatality risk curve [18]

- By multiplying the numbers of step 2 with the percentages of step 3 (at each level) the reduction of the number of fatalities or severely injured VRUs is estimated. This step assumes independence between the levels in the tree.

The outcome of the effectiveness study will show:

- the potential reduction of fatalities among pedestrians and cyclists by the various measures,
- the potential reduction of severely injured pedestrians and cyclists by the various measures;
- a comparison between the various measures.

SENSOR FIELD TEST

Intelligent VRU protection systems are in many cases still in a development phase. The road towards implementation of these systems includes field testing, starting with a small group of test vehicles, which can later on be extended. It has to be ensured that these systems undertake their actions only in case there truly is an imminent risk of impact. This means that the triggering of the system should include an absolute minimum of False Positives.

The SaveCAP consortium has recently started a Sensor Field Test (SFT), in which five identical vehicles are equipped with a system for cyclist and pedestrian detection and recognition. The objectives of this SFT are:

- Reduce number of false alarms by improving sensor algorithm
- Capture realistic near-accident situations for further sensor system development
- Speed up the development from testing in laboratory environment to test drives with VRU protection system on the road
- Make major step in VRU protection system development process towards a mature product.

In this Sensor Field Test (SFT), five vehicles are driving in two large Dutch cities. Two vehicles drive in The Hague, with many different types of traffic situations, while three vehicles are driving in Utrecht, where mixed traffic and narrow streets are common situations, and where there is a lot of student traffic. The Sensor Field Test will run for a full year, thus meeting many different traffic situations, as well as all possible weather conditions. The vehicles are used by service technicians of a Dutch telecomm company, KPN. They follow their normal routine and do not have to perform additional tasks. Accident situations are not needed to have a successful SFT.



Figure 10: Overview of SFT test vehicles

The SFT is about improving the activation capacity of the sensor systems for VRU protection countermeasures. Therefore the main component of the system is the sensor itself: a stereo vision camera. Since the focus of the SFT is on false positives, the contact sensor is not included, nor are the VRU protection countermeasures (deployable bonnet, airbag, active braking system). An overview of the SFT equipment incorporated in the vehicle is visualized in Figure 11.

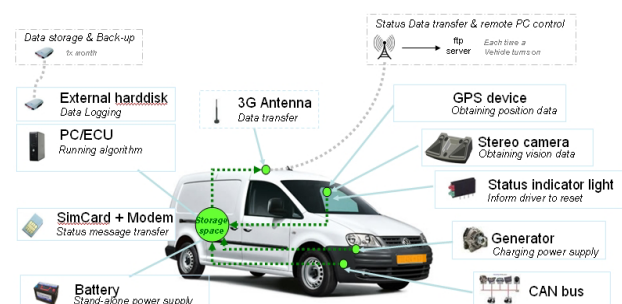


Figure 11: Equipment used in the Sensor Field Test

The stereo camera is positioned at the front windscreen close to the rear view mirror and the vehicle is equipped with data logging equipment, GPS and a 3G antenna for transferring status messages. Furthermore, information from the vehicle CAN bus and an additional ESP sensor is recorded: vehicle speed, yaw rate, braking actions and

windscreen wiper status. Hard discs are used for storing the data. In order to comply with the privacy legislation the data is anonymised.

The SFT system logs only data of potential impacts or critical situations. An interesting situation is defined as a situation in which an object is within a time-to-collision of 0.9s from the test vehicle. The recorded time frame is 16 seconds before estimated impact and 4 seconds after that moment. Per day about 30 events are estimated. A screen shot showing a situation of interest, recorded during the SFT, is given in Figure 12.



Figure 12: Image of real life situation, captured in the SFT

Every three months, the sensor software will be updated, based on the analysis of the measurements in the previous period. Thus, the number of False Positives (FP) will be decreasing during the project, based on real life information. This is essential to come to a properly working system. The sensor system cannot be optimized for a low FP rate only by laboratory tests, or by tests using professional test drivers. A minimized number of False Positives is essential for implementation of systems like this in the vehicle fleet.

DISCUSSION AND CONCLUSIONS

The SaveCAP project aims at improving safety for both cyclists and pedestrians in impacts with passenger cars. In doing so, it is important to understand which areas of the car impose most frequent and most severe injuries. This has been studied for the actual road situation in the Netherlands. In the study presented here, some assumptions needed to be made, such as appointing head injury as main injury in some of the data trees. In future studies, it would be good to verify these assumptions.

It was seen that as many as 80% of the VRUs with AIS3+ injuries to both head and chest died. This can be compared to the fatality rate of 11% for the VRUs with only AIS3+ head injuries and fatality rate of 3%

for those with only AIS3+ chest injuries. The full meaning of this finding has yet to be investigated. However, it indicates that a countermeasure able to protect from either AIS3+ head injuries or AIS3+ chest injuries would offer a substantial reduction of the fatality risk. This can be achieved by several of the vehicle-side countermeasures studied. On the other hand, cases with AIS3+ injuries to both head and chest were associated with higher maximum AIS, car impact speed and VRU age compared to cases with AIS3+ injuries to only head or chest.

Most probably due to the higher location with which cyclists impact the car, they suffer in far less cases from severe leg injury than pedestrians (AIS3+, 20% of the fatalities vs. 60% of the fatalities). This can also explain the finding that cyclists hit the windscreen area on a higher location than pedestrians. For all VRUs, the windscreen area is the main injury source. In the cases studied, ground impact accounts for a minor share of all AIS3+ injuries.

Continuing work like the Sensor Field Test and the Proof of Concept evaluation will lead to a large amount of (real life) close-to-accident information which is worldwide missing so far. This information will have a positive impact on future developments for VRU protection.

After the Sensor Field Test is finalized, the sensor system will be combined with a VRU airbag as test case, and evaluated according to the Beyond NCAP protocols. This will be done in several pre-crash and crash scenarios. Based on the outcomes of these tests as well as the outcomes of the Sensor Field Test, it will be decided how to proceed the drafted developments. Most probably, the scale of testing will be enlarged to a Field Operational Test in several countries, as a step towards implementation of this kind of live saving systems.

REFERENCES

- [1] AAAM, 2001. The Abbreviated Injury Scale: 1990 Revision, update 1998. Association for the Advancement of Automotive Medicine, Barrington, IL, USA.
- [2] Belingardi G, Scattina A, Gobetto E., Development of an hybrid bonnet to improve pedestrian safety in case of vehicle impact. Paper presented at: 21st International Technical Conference on the Enhanced Safety of Vehicles (ESV); 2009; Stuttgart, Germany. Paper No. 09-0026.

- [3] Crandall JR, Bhalla KS, Madeley NJ. Designing road vehicles for pedestrian protection. *BMJ*. May 11 2002; 324(7346):1145-1148.
- [4] EC. CARE database - reports and graphics. 2010; http://ec.europa.eu/transport/road_safety/specialist/statistics/care_reports_graphics/index_en.htm. Accessed 2010-12-27.
- [5] EC. Directive 2003/102/EC of the European Parliament and of the Council of 17 November 2003 relating to the protection of pedestrians and other vulnerable road users before and in the event of a collision with a motor vehicle and amending Council Directive 70/156/EEC. In: UNION, T. E. P. A. T. C. O. T. E., ed. 2003/102/EC. Brussels: Official Journal of the European Union; 2003.
- [6] ETSC, European Transport Safety Council, PIN annual report 2009
- [7] EuroNCAP. Assessment Protocol - Overall Rating Version 5.0: European New Car Assessment Programme (Euro NCAP); 2009.
- [8] Fredriksson R, Rosén E. Integrated pedestrian countermeasures - potential of head injury reduction combining passive and active countermeasures. Paper presented at: IRCOBI (International Research Council On the Biomechanics of Impact) Conference; 2010; Hannover, Germany.
- [9] Fredriksson, R., Rosén, E., Kullgren, A., 2010. Priorities of pedestrian protection – A real-life study of severe injuries and car sources. *Accid. Anal. Prev.* 42, 1672–1681.
- [10] Han YH, Lee YW. Development of a vehicle structure with enhanced pedestrian safety. Paper presented at: SAE (Society of Automotive Engineers) World Congress; 2003.
- [11] Hannawald L, Kauer F. Equal effectiveness study on pedestrian protection. Technische Universität Dresden, 2004.
- [12] Kalliske I, Bovenkerk J, Asadi M, Puppini R, Hashemi R and Hardy R, APROSYS deliverable D.3.4.2.C, Concepts of protection to address child and adult head impacts, 2009
- [13] Lexus. Advanced pre-collision system (APCS) with driver attention monitor. 2011; http://www.lexus.com/models/LS/features/safety/advanced_precollision_system_apcs_with_driver_attention_monitor.html. Accessed 2011-01-13.
- [14] Maki T, Asai T, Kajzer J. Development of future pedestrian protection technologies. Paper presented at: 18th International Technical Conference on the Enhanced Safety of Vehicles (ESV); 2003; Nagoya, Japan. Paper No. 03-0165.
- [15] Ministerie van Verkeer en Waterstaat, Kerncijfers verkeersveiligheid uitgave 2010, 2010
- [16] Nishimoto T. Introduction of the regulation of pedestrian head protection in Japan. Paper presented at: 18th International Technical Conference on the Enhanced Safety of Vehicles (ESV); 2003; Nagoya, Japan. Paper No. 503-O.
- [17] Rosén E, Källhammer J-E, Eriksson D, Nentwich M, Fredriksson R, Smith K. Pedestrian injury mitigation by autonomous braking. *Accident Analysis and Prevention* 2010; 42(6):1949-1957.
- [18] Rosén E, Sander U, Pedestrian fatality risk as function of car impact speed, *Accident Analysis and Prevention* 2009; 41; 536-542.
- [19] Thiemann-Linden J. Bicycle Use Trends in Germany. German Institute of Urban Affairs (Deutsches Institut für Urbanistik), 2010, Berlin.
- [20] Volvo. A revolution in pedestrian safety - Volvo's automatic braking system now reacts to people as well as vehicles. 2010; www.volvocars.com/za/top/about/news-events/pages/default.aspx?itemid=24. Accessed 2010-08-22.
- [21] www.aprosys.com. European FP 6 project on advanced protection systems. One of its subprojects focussed on protection of pedestrians and cyclists.
- [22] www.eIMPACT.info; European FP 6 project on "Socio-economic Impact Assessment of Stand-alone and Co-operative Intelligent Vehicle Safety Systems (IVSS) in Europe".
- [23] www.gidas.org; the German In-Depth Accident Study. Covers most cases in regions of Hannover and Dresden, in which a person gets injured. The data is representative for the situation in Germany. The detailed data is gathered by specialist teams at the accident site.

Development of Nissan Approaching Vehicle Sound for Pedestrians

Toshiyuki TABATA

Vehicle Performance Engineering Department, Nissan Motor Co.Ltd., 1-1 Morinosatoaoyama, Atsugi-city, Kanagawa,243-0123, Japan

Heather KONET

Technology Planning, Nissan Technical Center North America, Inc., 39001 Sunrise Dr. Farmington Hills, MI.48331, USA

Tsuyoshi KANUMA

PV Performance Development Department No1., Nissan Motor Co.Ltd., 560-2, Okatsukoku, Atsugi-city, Kanagawa,243-0192, Japan

Paper Number 11- 0097

Abstract—Electric Vehicles are very quiet at low speeds therefore people (especially the visually impaired) have difficulty recognizing that these vehicles are approaching. To address this concern, Approaching Vehicle Sound for Pedestrians system development has been discussed worldwide. In Japan, USA, Europe and China, government regulation is currently under study. As a solution to meet this concern, Nissan has developed the VSP (Approaching Vehicle Sound for Pedestrians) system for implementation on Nissan’s first mass production Electric Vehicle. Nissan VSP emits a futuristic sound to satisfy 3 key stakeholders’ concerns; for pedestrians to provide detectability, for drivers and neighborhoods to maintain a quiet environment. The sound emitted during forward motion has a “twin peaks and one dip” frequency signature, with modulation (or rhythmic structure) to accommodate human-beings ear frequency sensitivity, hearing loss due to aging and ambient noise conditions. Additionally, special emphasis is placed on the forward sound emitted when the vehicle is “taking-off”(starting forward motion) to notify pedestrians that the vehicle is about to move, in response to real world feedback gathered in surveys with visually impaired in Japan and USA. The system also includes a reverse motion or “backing up” sound that has an easy to recognize cadenced(or rhythmic structure) characteristic.

Keywords— “electric vehicle, hybrid electric vehicle, approaching vehicle sound, pedestrians, safety”

1. Background

Electric Vehicles are very quiet at low speeds (see Figure1), therefore pedestrians (especially the visually impaired) have difficulty recognizing that these vehicles are approaching. In Japan, USA, Europe, and China, regulation is currently under study. The Japanese government published VSP guide-lines in February 2010, and USA National Highway Traffic Safety Administration published a research report “Quieter Cars and the Safety of Blind Pedestrians: Phase I” in April 2010. [1] [2]

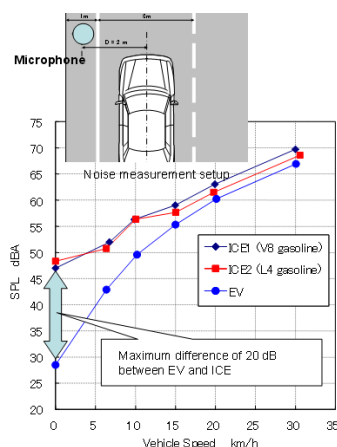


Figure 1: Vehicle noise level comparison EV vs. ICE (Internal Combustion Engine) vehicle[1]

2. Solution by Nissan

As a solution to meet this concern, Nissan has developed the VSP system for implementation on Nissan’s new mass production Electric Vehicle. This system addresses 3 key stakeholders’ concerns; for pedestrians to provide good detectability, for drivers and neighborhoods to maintain a quiet environment.

The design concept of Nissan VSP is as follows (from 1 to 3 are followed by Japanese guideline):

1. Sound is recognized as a vehicle
2. Sound pitch is proportional to vehicle speed
3. Similar sound level as ICE (Internal Combustion Engine) vehicle
4. Sound has a futuristic image
5. Easily audible for pedestrians (young and elderly) under various ambient sounds, yet maintains a quiet environment for driver and neighborhoods

2.1 Sound characteristics

2.1.1 Frequency characteristic

In order to achieve this concept, Nissan considered the following information related to sound frequency in the sound design and selection process:

A. Human-beings ear frequency sensitivity

People with normal hearing are sensitive to frequencies between 2 and 5 kHz due to the resonance of the ear canal and the transfer function of the ossicles of the middle ear.

Therefore VSP sound should include a peak between 2 and 5 kHz (see Figure 2). Additionally, the ear sensitivity difference to frequency levels increases as the sound volume level decreases. Due to this phenomenon, high frequency sound (i.e. 2.5 kHz) can be heard from much longer distances than lower frequency sound (i.e. 200 Hz).

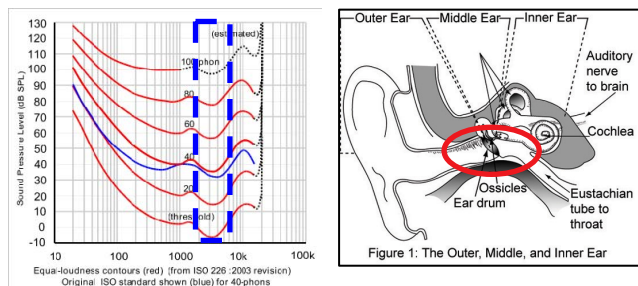


Figure 2: Human-beings ear structure and frequency sensitivity [3]

B. Hearing loss due to aging

People who are older than 60 years have difficulty detecting sound higher than 1 kHz due to age related hearing loss. More than 70% of visually impaired people are over 60 years old [4]. As a result VSP sound should include another peak lower than 1 kHz (see Figure 3).

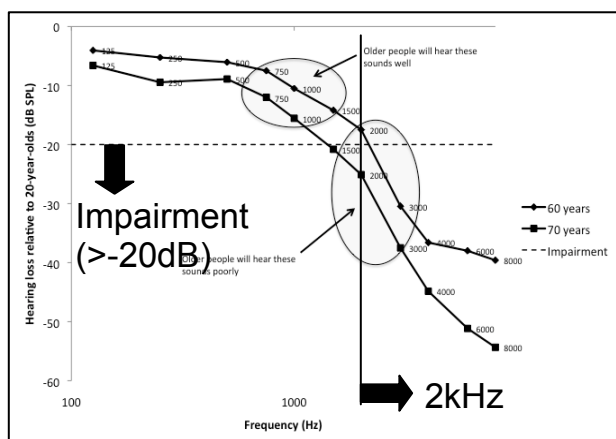


Figure 3: Hearing loss due to aging (comparison between 20 and 60,70 year olds) [5]

C. Ambient noise frequency characteristic

Ambient noise measured at busy intersection, neighborhoods near busy intersection, etc. consistently peaks at around 1 kHz. Therefore VSP sound should peak at the shoulders of 1 kHz (see Figure 4).

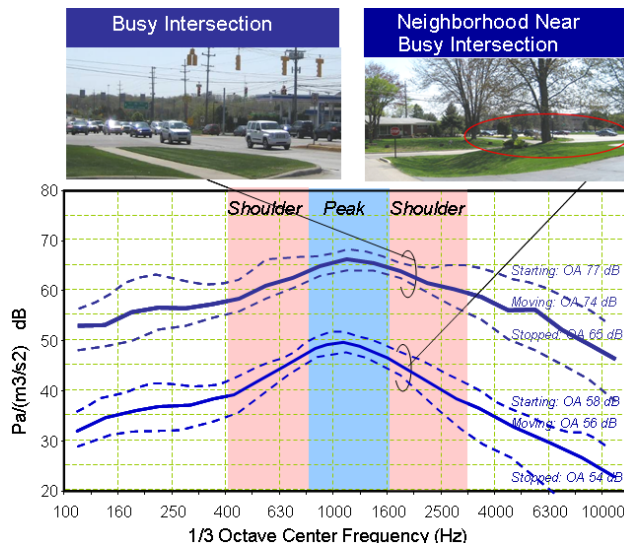


Figure 4: Ambient noise measured at busy intersection and neighborhood near busy intersection in Detroit USA

In summary, Nissan VSP sound has a “twin peaks and one dip” frequency profile (see Figure 5), including peaks at 0.6kHz and 2.5kHz, and a dip at 1kHz. The 2.5 kHz peak is intended to accommodate normal hearing. The 0.6 kHz peak is intended for elderly with high frequency hearing loss. Lastly the 1 kHz dip is for maintaining a low sound pressure level that is acceptable for neighborhoods.

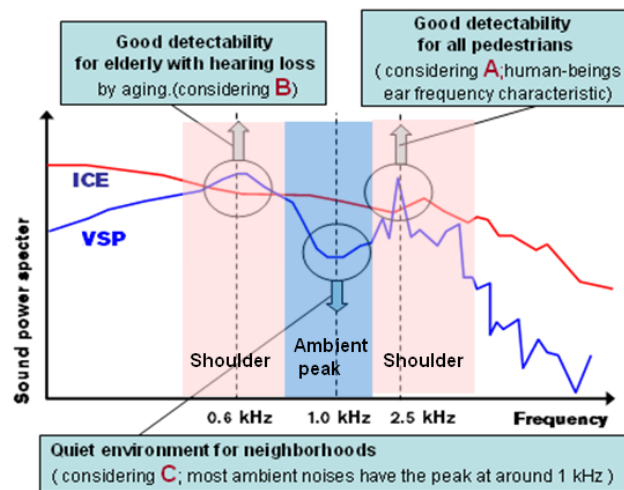


Figure 5: “Twin peaks and one dip” frequency sound characteristic explanation of Nissan VSP

2.1.2 Time domain characteristic

It is well known that sound with modulation (or rhythmic structure) stands out in ambient noise more than sound without modulation. To support the detectability of the VSP sound, subtle modulation of 0.6k Hz peak is included in the design. The time domain sound characteristic of Nissan VSP is shown in Figure 6. Another important time domain sound characteristic is “sound pitch proportional to vehicle speed”. This is an important factor that helps make it possible for pedestrians (especially the visually

impaired) to detect the approaching vehicle's behavior (accelerating or decelerating) and to recognize the sound as a vehicle .

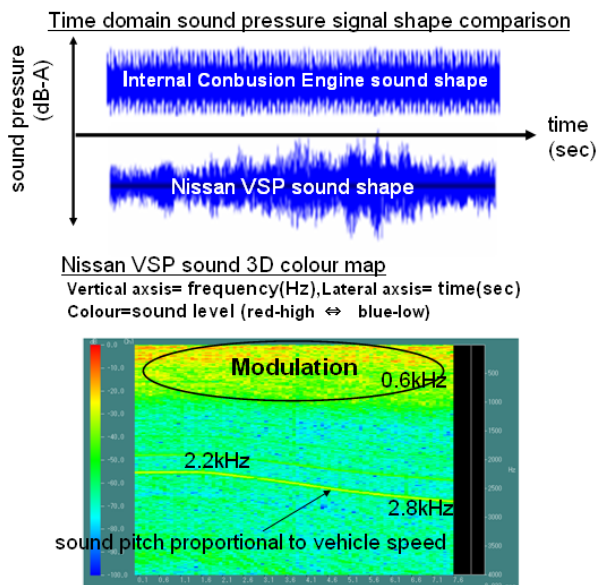


Figure 6: Time domain characteristic of Nissan VSP

2.1.3 Evaluation of sound

9 sample sounds and 1 ICE vehicle sound were evaluated for detectability (through subjective testing) and driver ear position quietness (by dB-A measurement). The sound candidates with high frequency white noise character (#3,#4,#5) were quiet inside the vehicle but the detectability was poor. The low frequency sounds with strong modulation (A,B,D) resulted in good detectability but were considerably louder inside the vehicle. The sound with 1kHz peak and medium level modulation (C,E), and the sound with twin peaks and a 1kHz dip (#1) resulted in good balance of quietness and detectability as compared to ICE sound. Taking real world ambient noise conditions (peak at 1 kHz) and other design guidelines into consideration, it was concluded that the twin peaks sound with 1 kHz dip (#1) would be most appropriate for the VSP system (see Figure 7).

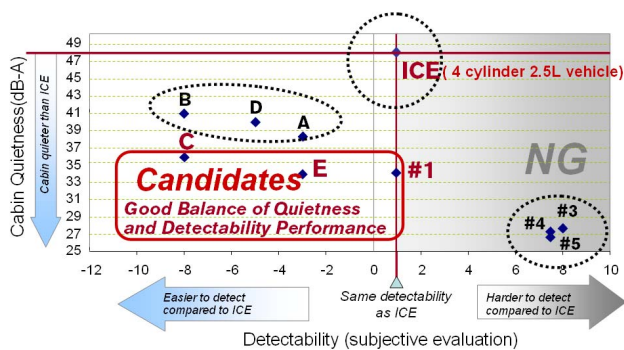


Figure 7: Detectability vs. Cabin Quietness evaluation result for 9 sample sounds

2.2 Sound volume level

The SAE J2889-1 pass-by measurement procedure was used to set the VSP forward signal sound pressure level (SPL) as measured in dB-A. First, 7 different Nissan US market vehicles were measured including 5 ICE, one Nissan HEV and one Nissan full electric vehicle when travelling at 10 kph. The results were consistent with what is shown in Figure 1 - there is a clear difference in SPL between ICE and EV vehicles.(see Figure 8) Even smaller segment vehicles such as the Nissan 1.8 L ICE vehicle2 have considerably higher SPL for pedestrian detectability as compared with vehicles in electric mode. Therefore, Nissan VSP has been set to achieve equivalent SPL as Nissan 1.8 L ICE vehicle2 at 10 kph. The actual SPL is 55 dB-A.

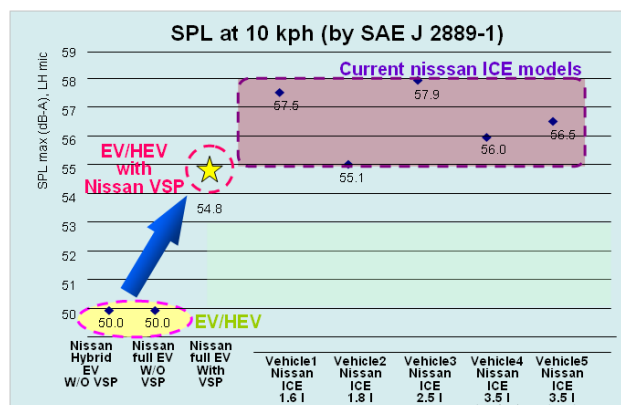


Figure 8: Comparison of SPL at 10kph (by SAE J2889-1)

Testing in a hearing research laboratory and real world testing with the visually impaired has confirmed that Nissan full EV with VSP setting 55dB-A achieves the same or better performance than Nissan vehicle2 (high sales volume ICE model in the US) in all Approach Detection and Turning Perception listening tasks. Therefore Nissan VSP will achieve equal or better performance than ICE at equivalent SPL in the two key pedestrian listening tasks. (Figure 9)

■ Testing by West Michigan University and Vanderbilt University Medical Center confirms that for Approach Detection and Turning Perception tasks, Nissan VSP is always equal or better than ICE at equivalent SPL

Pedestrian Task	Metrics	Related Common Scenarios
Approach Detection	Real world testing w/ visually impaired Vehicle Detection Distance (m)	Crossing street with no stop sign, traffic light Crossing isle in parking lot Crossing driveway while walking on sidewalk
Turning Perception	Surge Detection Lag (sec)	Crossing street at intersection, detecting traffic starting to move Walking in parking lot, listening for cars starting to move
	Path Detection Lag (sec)	Crossing street at intersection, tracking traffic movement (straight or turning)
	Lab testing w/ children, adults, elderly Min SPL (dB)	Crossing street at intersection in loud ambient conditions

Figure 9: Real world testing of Approaching detection and Turning perception of Nissan VSP

There currently is no study indicating that low speed pedestrian crash risk is higher for vehicles with SPL similar as Nissan vehicle2, as compared to noisier ICEs (i.e. vehicles with SPL at 60 dB-A and higher). Therefore the

direction to set the Nissan VSP sound at the same level as Nissan vehicle2 is reasonable. To verify that Nissan vehicle2 SPL does not pose additional pedestrian crash risk over noisier vehicles, a statistical analysis is being performed of actual pedestrian crash data.

One other consideration is the difference in difficulty between pedestrian listening tasks in terms of how loud the sound needs to be for good performance. Testing with Vanderbilt University Medical Center revealed that the Turning Perception task (perceiving if a vehicle is moving straight through an intersection or turning right into the pedestrian’s walking path) is significantly more difficult than Approach Detection. The test results show that turning perception requires approximately 11 dB-A more SPL than detection in a typical 60 db-A ambient noise condition. Therefore design elements such as time domain and activation features are very important for addressing the usefulness of VSP in motion perception tasks.(Figure 10)

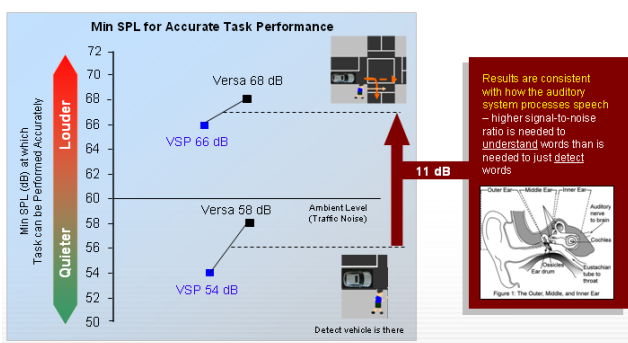


Figure 10: Minimum SPLs at which approaching detection task and turning perception task can be performed accurately

2.3 Sound activation procedure

The VSP system emits sound during low speed forward movement and reverse (see Figure 11). The reverse sound, or “cadenced backing up sound” and the “emphasized taking-off sound” were included in the final design based on feedback gathered in real world survey with visually impaired in Japan and USA.

- Sound activation procedure for “Twin Peaks” VSP based on real world study and feedback from demos with visually impaired

- No sound while stopped
- D-position & brake release -> forward sound starts
- Emphasized “take-off” sound to provide cue that vehicle is starting to move
- Over 30 kph fades out, below 25 kph fades in
- R-position & brake release -> cadenced backing-up sound starts

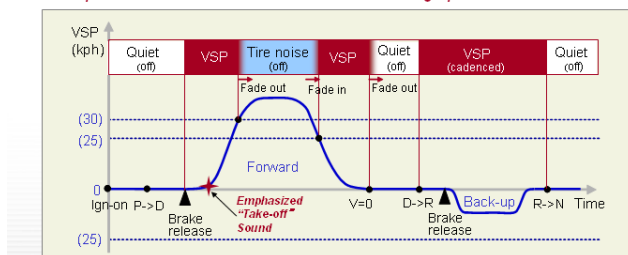


Figure 11: the Sound activation procedure of Nissan VSP

2.3.1 Sound during idle and take-off

Nissan VSP does not have idle sound, instead it has an emphasized take-off sound (starting forward motion) to clearly notify pedestrians that the vehicle is about to move. This decision is based on testing in real world pedestrian scenarios with visually impaired participants in collaboration with Western Michigan University. We tested surge detection lag (time it takes to recognize that a vehicle has started to move from a stopped position) of EV mode with VSP compared to ICE. The result show that the VSP emphasized take-off sound helps to shorten the time lag as compared to ICE. (Figure 12)

Moreover we found that no idle sound condition of VSP contributed to the shortened lag because of the noticeable gap in sound level from stopped condition to take-off condition. This is critical because a pedestrian failing to detect a vehicle surge at an intersection may increase the risk of an accidental collision in situations where the vehicle is making a right turn into the pedestrian’s crossing path. Although implementing an idle sound may prevent startling a pedestrian at an intersection, it was decided to not include sound at idle to address the risk of collision.(Figure 13)

- VSP performed statistically better than ICE at equivalent SPL
- Participants missed 0% VSP surge trials, but missed 2.5% of ICE surge trials (likely due to VSP emphasized “take-off” sound and no idle sound)

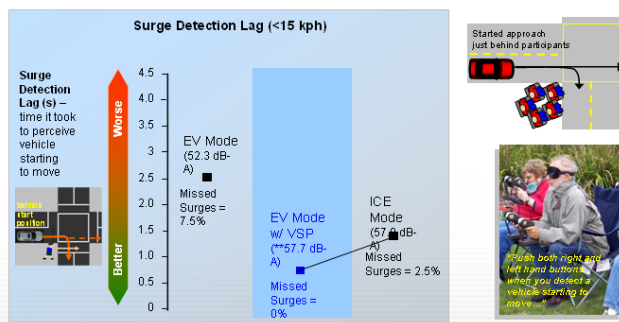


Figure 12: Surge detection lag comparison test result

- Nissan VSP has no sound at idle to enhance surge detection performance
- Idle sound may prevent “startling” a pedestrian (path perpendicular to vehicle), but it may in effect increase risk of collision with a pedestrian (path parallel to vehicle)

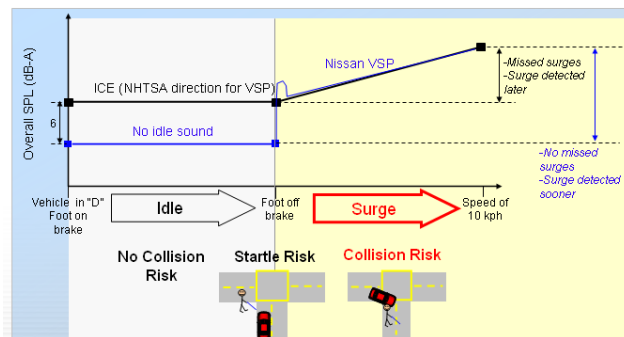


Figure 13: Explanation why no sound at idle VSP can reduce the collision risk at intersection

2.3.2 Back-up sound

The sound level is set by same SPL as ICEs at the pedestrian position in the rear. This is about 15dB smaller

than SAE J994 back-up alarm standard type E (according to SAE J994 definition, loudest type A ; 112dB-A at 1.2m distance point, type B; 107dB, type C; 97dB, type D; 87dB, and the smallest SPL type E; 77dB-A). And continuous cadenced with reverberation characteristics is added to enhance the motion perception(different sound from forward motion) and less annoyance(different sound from typical annoying backing alarms), in response to real world feedback gathered in surveys with visually impaired in Japan and USA. And nissan VSP back-up sound characteristic is supported very strongly by the visually impaired in France and USA to compare with continuous ICE like back-up sound characteristic. (Figure 14) There is an opinion that the enhanced reverse sound might cause drivers less attention to pedestrians. But VSP is a kind of ADAS(Advanced Driver Assist System) like the back view monitor system or the pedestrian detection auto brake system. Although someone might concern that such reverse sound increase the noise intrusion to neighbourhood, but nissan back-up sound is within ICE vehicles sound pressure levels and much smaller than the typical aftermarket alarm systems.

VSP reverse sound evaluation test by the visually impaired French and American

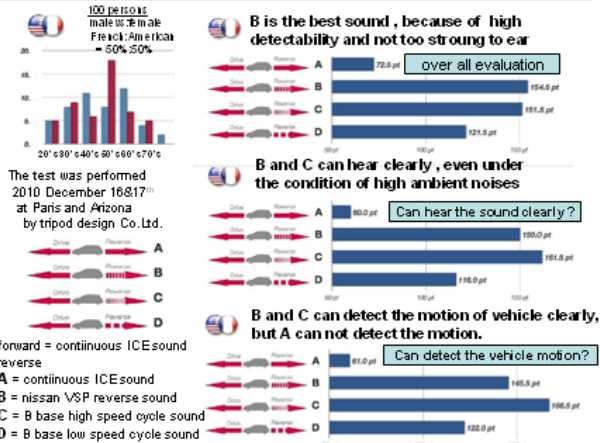


Figure 14: Nissan VSP reverse sound evaluation test by French and American visually impaired

2.4 System Configuration and diagram

The actual system applied to the Nissan new mass production electric vehicles is shown in Figure 15 and Figure 16.

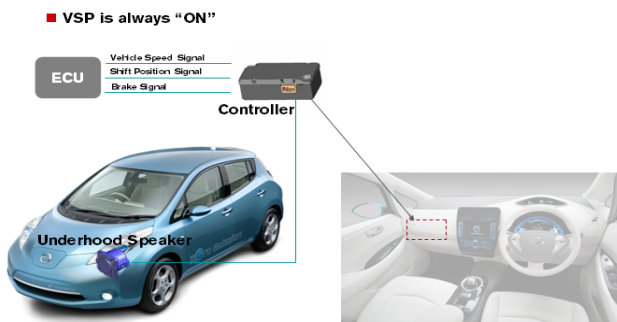


Figure 15: the System Configuration of Nissan VSP

- Software program inside Sound controller cannot be accessed from outside.
- The sound file is merged into the whole system program, and cannot be modified independently

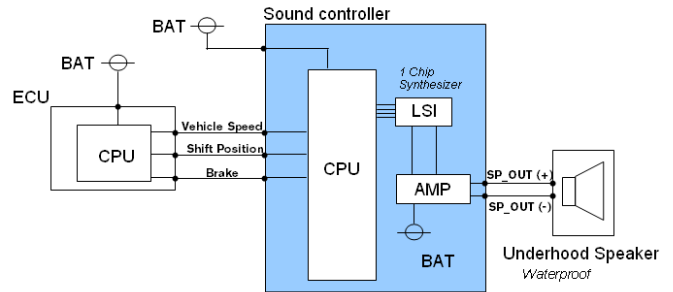


Figure 16: the System Diagram of Nissan VSP

3. Real world survey with visually impaired

Key feedback points from real world survey with the visually impaired includes: "sound should have a low pitch in order to intuitively recognize an approaching vehicle" and "distinctive sound when a vehicle is backing up and taking off (starting forward motion) helps raise awareness for motion perception and surge detection (recognizing that the vehicle has started to move from the stopped position)" (Figure 17).

- The real world survey conducted with visually impaired in US and Japan to identify the system really works in the actual traffic environment.

"Sound should have a 'low pitch' in order to intuitively recognize an approaching vehicle..."

"Distinctive sound when a vehicle is backing up helps raise awareness..."



Interview with Visually Impaired, at several traffic condition in Tokyo Metropolitan area



Interview with Visually Impaired, demo of EV sounds (prototype) at Detroit Institute of Ophthalmology (DIO)



Figure 17: The result from real world survey with visually impaired in Japan and USA

4. Smart sound as a future solution

In the future this quiet electric vehicle issue should be solved by using “Pedestrian detection technology”. There is discussion that the VSP sound volume should be higher up to the old fashion noisier vehicles’ level like 60-65dB-A to be able to detect in the very noisy ambient conditions. But this is impossible, because 60-65dB-A level sound brings unpleasant noise intrusion into car cabin and neighborhoods. Future Pedestrian detection by radar/camera on vehicles, by ITS (for example, pedestrians keep signal transmitter) will make future smarter sound system possible. Only when the system detects pedestrians and dangerous conditions should emit louder sounds, otherwise emits smaller sounds. This is the Smart sound concept. In the future, not only pedestrian detection technology but also conditions detection technology, like detection of high ambient noise, blind corner, dangerous turning at intersection, may be installed on vehicles. (Figure 18)

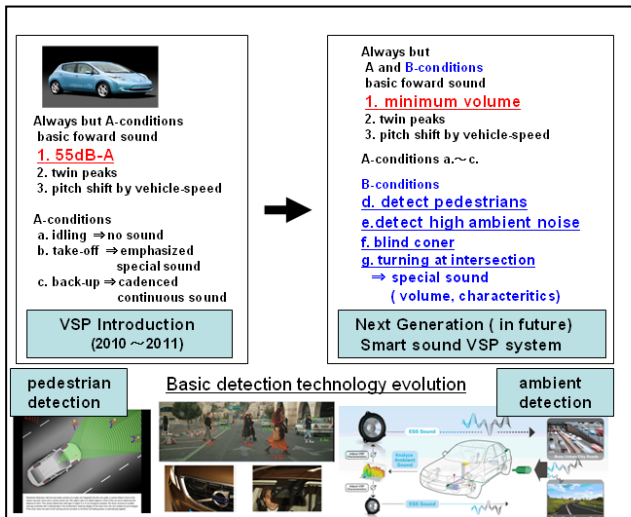


Figure 18 : Smart sound as a future solution

5. Conclusion

As research to support VSP development progressed, it became clear that the solution was much more complicated than just adding a sound effect or artificial engine noise to electric vehicles. The challenge was to provide detectability and recognition for all pedestrians, including the visually impaired, older hearing impaired adults and young children. The signals needed to be acceptable for neighborhood communities, so as not add to noise pollution, while at the same time offering a pleasant, non-intrusive sound for drivers and passengers. The final Nissan VSP system includes a unique forward driving sound with “twin peaks and one dip” frequency

signature (see Figure 19). The system also includes a distinctive cadenced sound for reverse backing. With quiet cabin performance, the system is pleasing drivers and passengers, yet it also offers good detectability for all pedestrians, along with low noise intrusion for neighboring communities.

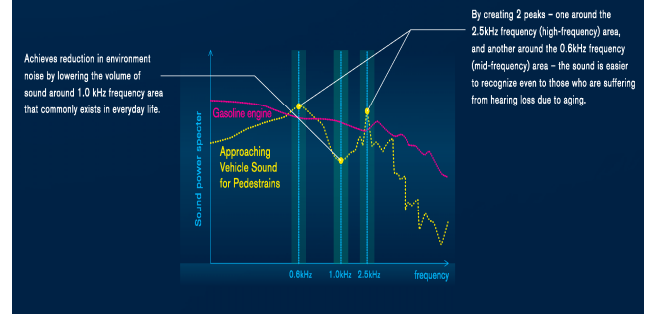


Figure 19: The final Nissan VSP system frequency signature

6. References

- [1] Japanese Automobile Standards International Centre, *A study on approaching warning systems for hybrid vehicle in motor mode*, Informal document No GRB-49-10, February 2009
- [2] National Highway Traffic Safety Administration, *Quieter cars and safety of Blind pedestrian: Phase I*, DOTHS811304, April 2010
- [3] ISO Equal Loudness Curves (ISO 226), 2003
- [4] “Visually Impaired” includes people with “Legal Blindness” and “Low Vision”
Japan Data: Brant, M. Yamada, *Ophthalmic Epidemiology*, 17(1), 50-57, 2010
US Data : National Eye Institute (NEI) - 3 million people over 60 years have blindness or low vision, Lighthouse International - 4.3 million people of all ages in US with blindness or low vision
- [5] Brant, L.J. & Fozard, J.L.. *Journal of the Acoustical Society of America*, 1990
- [6] Nissan Leaf Owners Groupe site (<http://leafownersgroup.com/leaf-media-documents/90-nissan-leaf-vsp-vehicles-sound-pedestrians.html>), then ‘ Forum’>>Media and Documents’>>Nissan Leaf VSP Vehicle Sound for Pedestrian (Video)’

THE CORRELATION BETWEEN PEDESTRIAN INJURY SEVERITY IN REAL-LIFE CRASHES AND EURO NCAP PEDESTRIAN TEST RESULTS

Johan Strandroth (1, 2)

Matteo Rizzi (3, 5)

Simon Sternlund (1)

Anders Lie (1, 4)

Claes Tingvall (1, 2)

1) Swedish Transport Administration

2) Chalmers University of Technology

3) Vectura Consulting

4) Karolinska Institutet, Department for Public Health Science
Sweden

5) Monash University Accident Research Centre
Australia

Paper Number 11-0188

ABSTRACT

The protection of pedestrians in crashes has been addressed by friendlier car fronts. This is a process driven by both regulation and consumer test programs. Since 1997, Euro NCAP has been testing and assessing the level of protection for most car models available in Europe.

In the current study, the Euro NCAP pedestrian scoring was compared with the real-life outcome in pedestrian crashes that occurred in Sweden 2003-2010. The real-life crash data was obtained from the data acquisition system STRADA, which combines police records and hospital admission data. The medical data consisted of ICD diagnoses and AIS scoring. In all approximately 500 pedestrians were included in the study. Each car model was coded according to Euro NCAP pedestrian scores. In addition, the presence or absence of Brake Assist (BA) was coded for each car involved. The injury scores for each individual were translated to Risk of Serious Consequences (RSC) at 1, 5 and 10% risk of disability level. This will indicate the total risk of a medical disability given the severity and location of injury.

The results showed a significant reduction of injury severity for cars with better pedestrian scoring, although cars with a high score could not be studied, due to lack of cases. The reduction of RSC for medium performing cars in comparison with low performing cars was 17, 26 and 38% for 1, 5 and 10% of medical impairment, respectively.

These results applied to urban areas with speed limits up to 50 km/h, although no significant reduction was found in higher speed zones.

While Brake Assist (BA) was found to contribute to a small injury reduction of about 5%, the results were non-significant. It was also found that the combined effect of BA and higher pedestrian scoring was greater than the two effects separately.

INTRODUCTION

Every year 400 000 pedestrians are killed worldwide according to Naci et al (2009). In the European Union only, more than 5 000 pedestrians are killed (CARE database, 2009). In Sweden approximately 40 pedestrians are killed each year, which is 12% of all road fatalities, and 250-300 are severely injured according to police records. Out of the injured pedestrians 260 were calculated to have got injuries with long term disability in 2009 (Swedish Transport Administration, 2010). The number of killed pedestrians per 100 000 population is 0.4, compared to approximately 6.4 globally (Swedish Transport Administration, 2010; Statistics Sweden, 2011; Naci et al., 2009).

Several studies have reported that lower extremities are the most commonly injured body region among pedestrian to car crashes (Roudsari et al., 2005, EEVC WG 17, 1998). With regard to more severe injuries (AIS 3+), head injuries are more frequent in US data (Longhitano et al., 2005), followed by leg and thorax injuries. However, Fredriksson et al (2007) reported in a study with German GIDAS data that, even among AIS 3+ injuries, leg is still the most commonly injured body part, followed by head and thorax. Fredriksson et al (2007) also concluded that 30% of all surviving pedestrians suffer from permanent medical impairment and that the head is the dominating body region regarding more severe impairment.

As recognized by the working group of Pedestrian Safety in European Enhanced Vehicle safety Committee (EEVC WG 17), many studies have shown that a large proportion of pedestrians are hit by the front of the car (EEVC WG 17, 1998).

In a typical car to pedestrian crash, the bumper first strikes the leg. The thigh, pelvis or chest then most likely is hit by the bonnet leading edge. Next, the upper body moves to the bonnet area with the shoulder or thorax hitting the bonnet. Finally, the head hits the bonnet or windshield area or/and sometimes even the roof, depending on the impact speed. Based on this impact scenario, various recommendations for the crash testing of front design have been developed (EEVC WG 17, 1998; Fredriksson et al., 2007). EEVC WG 17 recommends that main concern should be given to the leg-to-front end impacts, chest impacts to the bonnet and windscreen areas and head-to-windscreen area impacts.

The process of making the car front more pedestrian friendly has been encouraged by both regulation and consumer test programs. In 1987, EEVC Working Group 10 Pedestrian Protection was set-up in order to determine test methods for assessing pedestrian protection by the front of cars. In 1998 EEVC Working Group 17 Pedestrian Safety was formed and asked to review the test method suggested by WG 10 in 1994 which resulted in the report “EEVC Working Group 17 Report – Improved test methods to evaluate pedestrian protection afforded by passenger cars”, which was also updated in 2002 (EEVC WG 17, 1998). The assessment was based on dummy response data recorded in three test configurations; head to bonnet, upper leg to bonnet leading edge and leg to bumper impact. In the report WG 17 specifically pointed out the importance of not considering only life threatening injuries (high AIS levels) but also the risk for long term disability (EEVC WG 17, 1998).

In 2005 the test methods as proposed by EEVC were adopted by the European directive in the legal requirements on pedestrian protection (EC, 2003). Also in 2005 the Japan Ministry of Land, Infrastructure and Transport (MLIT) introduced a “Technical Standard for Protection of Heads of Pedestrians” (McLean, 2005). But already in 1997 the consumer organization European New Car Assessment Program (Euro NCAP) had started to assess pedestrian protection based on methods presented in the EEVC WG 17 report. Until 2008 the pedestrian rating was not included in the overall rating and a separate Euro NCAP star rating was given for pedestrian protection (1-9 points = one star, 10-18 points = two stars, 19-27 points = three stars and 28-36 points = four stars). In 2009 the pedestrian rating was included in the overall rating even though the test and the scoring system were still the same (Euro NCAP, 2009). During the first couple of years, the typical Euro NCAP pedestrian rating was one or two stars; in 1997 30% of the tested cars were given one star and 70% two stars.

This suggested that the score was more a result of coincidence than focused engineering. However, in 2007 the distribution of stars was 13% one star, 65% two stars and 19% three stars (Euro NCAP, 2008). In 2009 the new overall rating system was introduced and the average score was 16.8 points and in 2010 19.1 points (Euro NCAP, 2011), suggesting that the recent improvements were an effect of more engineering efforts being put on pedestrian friendly car design. Looking into the future, 21 points in the pedestrian test will in 2012 be a minimum to qualify for five stars in the overall rating.

Now, consumer testing and regulation have encouraged the manufacturers to meet the requirements of the assessment protocols. However, it is still needed to understand whether the scoring in these assessments correlate with the injury outcome for pedestrians in real-life car to pedestrian crashes. In the SARAC2-project an analysis of police reported pedestrian crash data from Great Britain, France and Germany, Delaney and Cameron (2006) used logistic regression analysis to compare injury severity from pedestrians hit by one and two stars vehicles. No evidence of a relationship between Euro NCAP pedestrian star rating and pedestrian injury severity from police recorded data was found using that method. Another study published in 2009 used case-by-case analysis on 667 real-world crashes from the GIDAS in-depth database to estimate the benefit of Euro NCAP pedestrian rating (Liers and Hannawald, 2009). The Euro NCAP test results were used to estimate the benefit of vehicles already introduced into the market. Liers and Hannawald (2009) concluded that the number of severely injured pedestrians (MAIS2+) would be reduced by 6.5-9.7%, if the vehicle fleet would consist only of currently established models. Consequently, earlier studies give no clear picture about the real-world benefits of a high pedestrian ranking and, more importantly, no study has yet evaluated the effects on long term disability, or risk for permanent medical impairment (RPMI), which is in focus for the pedestrian assessment. RPMI is an estimation of the risk for a patient to suffer from a certain level of impairment based on the diagnosed injuries. The risk is derived from risk matrices for 1, 5 and 10% medical impairment (see Appendix II) developed by Malm et al (2008). As reference amputation of foot, knee or tibia is set to an impairment of 9, 12 or 19%, respectively. The risk matrices were developed for car passengers but are considered to be suitable even for pedestrians (Fredriksson et al., 2007).

The rating system for serious consequence (RSC) is a scale from 0 to 1 and is defined as the risk of being either killed or to suffer from a permanent medical impairment according to the criteria of the Swedish Insurance Companies (Försäkringsförbundet, 2004). The fatality risk is linked to ISS calculated from the maximum AIS (Gustafsson et al., 1985; Håland et al., 1993). RSC can be calculated if all injuries of a person are coded.

In a pedestrian to car impact the injury outcome is not only affected by on the front design but also on the impact speed and the contact with the ground. The ground is considered to have a limited influence on the injury severity, as Zhang et al (2008) estimated the ground to contribute to approximately 20% of injuries. However, impact speed is crucial and highly correlated with injury severity for head, chest and leg injuries (Fredriksson et al., 2007).

Since it has been shown that more than 90% of all drivers fail to apply the brakes enough in a panic situation, Brake Assist has been introduced in order to optimize braking. Brake Assist measures the speed with which the brake pedal is pressed down, and in some models how fast the accelerator pedal is released. If a panic situation is then detected, maximum brake pressure is applied (Wikipedia, 2011). Since this system enhance braking performance and thereby potentially decreases the impact speed, it could be argued to have a positive effect on pedestrian injury severity. Hannawald and Kauer (2004) estimated that braking occurred and would activate a Brake Assist system in 50% of the crashes and Lawrence et al (2006) estimated Brake Assist to have an effect to reduce fatal and serious injuries among pedestrians by 10%.

Autonomous braking, independent of the driver, would increase the potential of injury reduction. Rosén et al (2010) estimated autonomous braking to have positive effects of 40% for fatalities and 27% for severely injured. Bearing two injury mechanisms in mind (front design and impact speed), it would also be of interest to investigate whether they could be combined to find integrated safety solutions. While few studies have been made in this area, Fredriksson and Rosén (2010) concluded that a combined system would protect 64% of the pedestrian by analyzing pedestrian to car crashes with a severe head injury (AIS3+). The potential system would consist of an active autonomous braking system and a passive system with a deployable hood and a lower windshield/A-pillar airbag, which would separately give a reduction of 34 and 44% reduction, respectively.

AIM

The aim of the present study was to:

- estimate the correlation between Euro NCAP pedestrian rating scores and injury outcome in real-life car to pedestrian crashes, with special focus on long-term disability and permanent medical impairment;
- determine whether Brake Assist systems affect the injury outcome in real-life car to pedestrian crashes;
- estimate the combined effects in injury reduction of a medium Euro NCAP ranking score and Brake Assist, compared to a low Euro NCAP ranking score without Brake Assist.

MATERIAL

Swedish real-life crash data was obtained from the data acquisition system STRADA, which combines police records and hospital admission data. Police data contained information from the national vehicle register and it was thereby possible to identify every specific car model involved in a car to pedestrian crash. The hospital data consisted of ICD diagnoses and AIS coded injuries. AIS values from the three most severely injured body regions on a pedestrian were applied on the risk matrices for RPMI calculations. All pedestrian crashes from STRADA during the period 2003-2010 were selected. The material contained 1644 pedestrians with 4105 injuries. Only pedestrians hit by the front of cars tested by Euro NCAP were then selected which limited the numbers of pedestrians to 709 and the number of injuries to 1741. In the analysis, only crashes on roads with speed limit up to 50 km/h were included (except for the analysis in figure 3). In the end, 488 patients with 1156 injuries were included in the study.

Age distribution is shown in Table 1 and confirms that the ages of the pedestrians included in the study are comparable to the national crash statistics.

Table 1.
Age distribution of pedestrians in the study compared to national crash statistics on roads with speed limit 50 km/h

Age	Study material	National crash statistics
0-9	5%	6%
10-17	18%	18%
18-24	13%	15%
25-64	36%	39%
65+	27%	22%

Table 2 shows the number of tested cars in the material and their Euro NCAP rating. As it may be seen, the number of cars with high scores is limited.

Table 2.
Number of cars with different pedestrian rating and score groups, n = 488

Stars	Score	No. of cars
1	1-3	15
1	4-6	58
1	7-9	76
2	10-12	99
2	13-15	147
2	16-18	80
3	19-21	11
3	22-24	1
3	25-27	1

Injury distribution

The injury distribution in the material can be seen in Figure 1. In both AIS1+ (n = 1156), AIS2+ (n = 464) and AIS3+ (n = 130) lower extremities are the most frequent injured body region. However, as injury severity increases the proportion of head and thorax injuries increases too, while injuries on upper extremities decrease. This is well in line with the observations made by Fredriksson et al (2007).

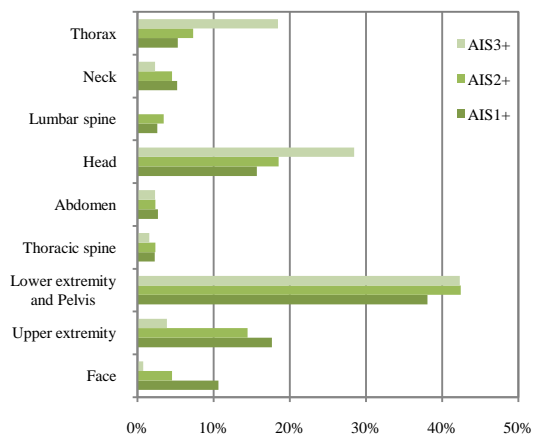


Figure 1. Injury distribution on body regions of pedestrians per AIS level, n = 1156.

Information about Brake Assist fitment was difficult to find. Hence, the assumption was made that a car fitted with Electronic Stability Control (ESC) would be also equipped with Brake Assist. In all, 129 pedestrians were hit by cars with Brake Assist and 357 pedestrians were hit by cars without. Two pedestrians were impacted by cars with unknown Brake Assist fitment. The share of one star cars in the material with Brake Assist was 23% whereas the share in two star cars was 25% (see Appendix I).

METHOD

Each car model in the crash data was linked to the corresponding Euro NCAP pedestrian scores found via the Euro NCAP web site. In addition, the presence or absence of Brake Assist was coded for each car involved, given the assumption that an ESC-equipped car would also be fitted with Brake Assist. Pedestrian injuries were then linked to each individual car model. The cars were divided into groups depending on their rating score and Brake Assist fitment. Since the pedestrian scoring is likely to have less effect in higher speed zones, pedestrians hit on roads with speed limit above 50 km/h were excluded in the analysis, except for results shown in Figure 3.

Cars with Brake Assist were compared to cars without Brake Assist regarding injury severity measured by AIS level and Rating system for Serious Consequences (RSC), which is explained in the next section. A p value < 0.05 was used as indicative of statistical significance.

The correlation between pedestrian score and real-life injuries was mainly estimated as the difference in injury severity (AIS level and RSC) between one and two star vehicles. Again, a p value < 0.05 was used as indicative of statistical significance. Linear regression was used to calculate the effect of injury reduction with increasing Euro NCAP pedestrian score.

Rating system for serious consequence

AIS values from the three most injured body regions on a pedestrian were applied on the risk matrices. RPMI was calculated according to Equation 1.

$$RPMI = 1 - (1 - risk_1) \times (1 - risk_2) \times (1 - risk_3) \quad (1)$$

RSC was calculated according to Equation 2.

$$RSC = 1 - ([1 - r_{fatality}] \times [1 - RPMI]) \quad (2)$$

To compare different groups, the mean RSC (mrsc) was calculated for each group.

RESULTS

Pedestrian score

In Table 3 injury severity for one and two stars cars are shown. For two stars cars the injury severity was significantly lower on all levels except for AIS3+ injuries. Also, the injury reduction between one and two stars cars increased with the level of mrsc from 17% in mrsc 1%+ to 38% in mrsc 10%+.

The average score in the one star and two stars groups were closer than the median value in the interval, indicating that the true difference between one and two star cars is probably larger. Further analysis of which body regions contributed to medical impairment showed no major difference between one and two stars cars.

Table 3.
Number of injuries and injured pedestrians as well as injury severity to one and two stars cars

	1 star	2 star	Rel. diff.
No. injuries	376	745	
No. pedestrian	149	326	
Average NCAP pedestrian score	6.24	13.84	
AIS2+	45.7% (172)	37.9% (282)	-17%
AIS3+	13.8% (52)	9.9% (74)	-28%
mrsc 1%+	48.6%	40.5%	-17%
mrsc 5%+	27.1%	20.0%	-26%
mrsc 10%+	14.8%	9.2%	-38%

Specific stars to illustrate the result of the pedestrian rating are not used after 2009. Consequently it is of special interest to investigate the correlation between mrsc on different levels and Euro NCAP pedestrian score. This is shown in Figure 2. Three groups of cars with similar point intervals and their corresponding mrsc values are plotted in the figure.

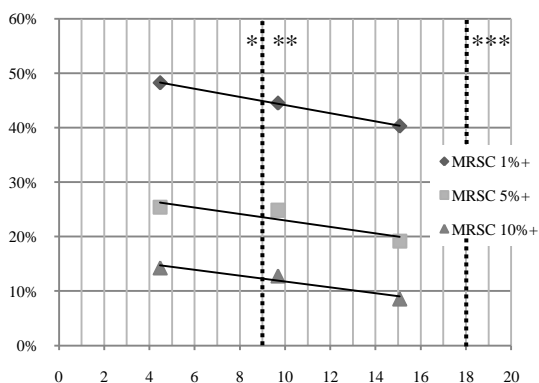


Figure 2. Correlation between Euro NCAP pedestrian score and mrsc.

The same figure is shown in Table 4. The reduction in the range 1-18 of mrsc 1, 5 and 10%+ is 1.6, 2.3 and 3.5% per points, respectively.

Table 4.
Pedestrian score divided in three groups compared to mrsc.

	Gr. I	Gr. II	Gr. III
NCAP ped. score	1-6	7-12	13-18
Average score	4.47	9.61	15.08
No. pedestrian	73	175	227
mrsc 1%+	48.2%	44.5%	40.3%
mrsc 5%+	25.4%	24.8%	19.2%
mrsc 10%+	14.3%	12.8%	8.6%

In Figure 3 pedestrian crashes on roads with speed limit 70 or 90 km/h (n = 73) are included in the analysis. A level of 5%+ medical impairment was chosen to illustrate the effect of pedestrian score on different speed limits. It was clear that the injury reduction due to a high pedestrian score was isolated only to speed limits up to 50 km/h.

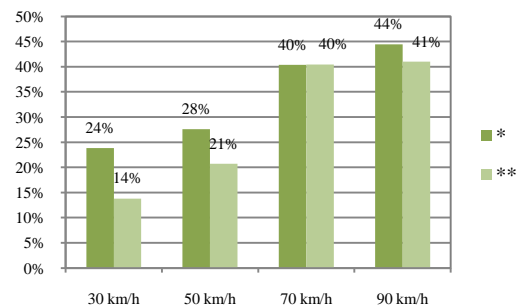


Figure 3. Comparison of mrsc in one and two star cars in different speed limits.

The effect of the Euro NCAP pedestrian score in different age groups was examined and is displayed in Figure 4. The findings showed that a two stars car gave a lower mrsc in all age groups except for small children (0-9). However, the number of pedestrians in this group is small and the estimation was considered uncertain.

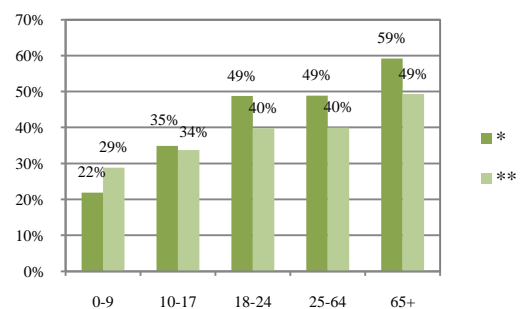


Figure 4. Comparison of mrsc 1%+ between one and two stars vehicle in different age groups.

Other factors that could affect injury severity for pedestrians and possibly confound the results (e.g. car year of manufacture, age and gender of pedestrians and car drivers, road type and road conditions as well as light conditions) were checked and no significant discrepancies were found. In all cases cars with a higher score in the pedestrian rating had a lower injury severity than poor performers.

Brake Assist

Comparisons between cars with and without Brake Assist (BA) are shown in Table 5. Pedestrians hit by BA-equipped cars had a lower proportion of AIS2+ and AIS3+ injuries, 4% and 16% respectively. However, the differences were not significant. Also, mrcs on all levels of medical impairment were lower with BA-cars. For mrcs 1, 5 and 10%+ the reduction with BA were 2, 5 and 4%, although non-significant.

Table 5.
Number of injuries and injured pedestrians as well as injury severity to cars with and without Brake Assist (BA)

	Without BA	With BA	Rel. diff.
No. injuries	839	313	
No. pedestrian	357	129	
AIS2+	40.6% (341)	39.0% (122)	-4%
AIS3+	11.8% (99)	9.9% (31)	-16%
mrcs 1%+	43.5%	42.5%	-2%
mrcs 5%+	22.6%	21.5%	-5%
mrcs 10%+	11.2%	10.8%	-4%

The combined effect of pedestrian score and Brake Assist

Finally, the combined effect of a high pedestrian scoring and Brake Assist (BA) was estimated. Two stars cars with Brake Assist were compared to one star cars without BA and a 20% significant reduction of mrcs 1%+ was found (see Figure 5). Consequently the combined effect of a higher pedestrian score and a lower impact speed (20%) is larger than the separate effects (17 and 2% respectively).

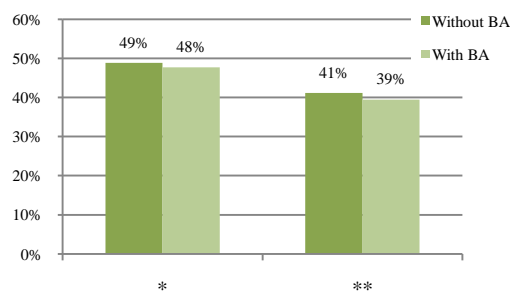


Figure 5. The combined effect of pedestrian score and Brake Assist.

DISCUSSION

This study showed a statistically significant correlation between Euro NCAP pedestrian results and real-life injury outcome for pedestrians. No correlations for specific car models are shown since the material is limited and models are grouped according to their test results. Instead this study showed that an average performing car in the pedestrian rating is in general better performing in real-life conditions too, compared to a poor performing car in the test.

In the groups of one and two stars cars the average Euro NCAP pedestrian score is 6.24 and 14.84, respectively. The reduction of fatal risk combined with risk for permanent medical impairment (mrcs) and also AIS2+ was significant, but not AIS3+ due to the limited material. Since the average score in the groups is closer than the median score, this indicates conservative results. A better correlation to the score is found with three intervals, estimating the injury reduction to between 1.5 and 3.5% per Euro NCAP point depending on injury severity. This way of evaluating the pedestrian rating will be more suitable in the future, with further good performers in the crash data and as the pedestrian stars disappear. The effect of injury reduction increases with increasing severity which is logical since the pedestrian test is design to simulate more severe crashes with focus on long term injuries.

As the number of real-life crashes was limited it was not possible to evaluate the separate tests for head, upper leg and lower leg. However, there was no difference between one and two stars cars regarding which body regions contributed to medical impairment. This can be interpreted as no specific test is more relevant than others and that the effect in real-life injuries is correlating to the total score. Further research with a larger dataset is needed to investigate this aspect.

However, it is clear that injury data with AIS coding for every injury (i.e. not only MAIS codes), is needed to find the actual correlations.

Also, the largest injury reductions are observed on mrcs. This is well in line with the ambitions of the regulation and test procedures to also focus on these impairing injuries. This could also explain why previous studies have not found any correlations. Another factor is that the front design seems to give large benefit only at lower speeds. If evaluations were to be based only on injuries with a high mortality risk one would need to include crashes in speed zones which are probably too high for the front design to be of any real significance. This study only showed an effect in crashes on roads with speed limit up to 50 km/h (and in crashes most likely with impact speeds much lower than 50 km/h). This could be a logical consequence of the fact that Euro NCAP pedestrian test is designed to simulate a crash at 40 km/h. Since about 80 % of all police reported fatal and severe crashes with pedestrians in Sweden are in speed zones up to 50 km/h (Kullgren et al., 2011) the limitation of the effect on front design to lower speeds should not be an issue.

If a high pedestrian score had been found to have benefits also in higher speed zones, there could have been reasons to suspect confounding factors in the results. Now, a number of factors such as vehicle year of manufacture, vehicle weight, road type, speed limit, light and weather conditions as well as driver and pedestrian characteristics were checked. A possible confounder could still be the absence or presence of Brake Assist, if it had been associated to large injury reductions. In this study the difference between one and two stars cars with regard to Brake Assist fitment is only 2%. Giving that the effect is approximately 10%, as shown in this and previous studies, it is highly unlikely that Brake Assist could affect the results to such degree. The assumption that Brake Assist fitment corresponds to ESC fitment is a source of uncertainty. However, it is more likely that Brake Assist exist without ESC than the other way around. This scenario would make a slight underestimation of the injury reduction due to Brake Assist, suggesting that the results are conservative.

The combined effects of two stars cars with Brake Assist compared to one star cars without Brake Assist are larger than the separate effects. Even though it is hard to draw any real conclusion out of this, it can be used to illustrate the large potential in combining friendly car fronts and impact speed reduction with e.g. autonomous braking (the reduction of impact speed due to Brake Assist could in this study be estimated to be 2-3 km/h using the relationship in the power model).

In a combined system the autonomous braking would expose the pedestrian to crashes with impact speeds were a friendlier front design would be beneficial, creating additional effects.

It is fundamental for the development of safer vehicles that test procedures as basis for safety rating are evaluated in a real-life environment too. Previous studies have shown positive correlation between the Euro NCAP occupant protection score and better real-life crashworthiness (Lie et al., 2001; Kullgren et al., 2010). This has encouraged a broader implementation of cars with a high Euro NCAP occupant rating including it as a performance indicator in traffic safety management.

The inclusion of pedestrian scores in the overall NCAP star rating seems to be relevant. Pedestrian protection might also be relevant as well as occupant protection to include as a performance indicator in traffic safety management.

CONCLUSIONS

- A significant correlation between Euro NCAP pedestrian score and injury outcome in real-life car to pedestrian crashes was found.
- Injury reduction was found to be larger with increasing severity and level of permanent medical impairment.
- The difference between one and two star cars is 17% in AIS2+, 17% in mean risk of permanent medical impairment (mrcs) 1%+, 26% in mrcs 5%+ and 38% in mrcs 10%+, for crashes in speed zones up to 50 km/h.
- Brake Assist was found to give a small injury reduction. The effects of Brake Assist were non- significant.

REFERENCES

- CARE database. 2009. "CARE - Road fatalities by Country."
http://ec.europa.eu/transport/road_safety/specialist/statistics/care_reports_graphics/index_en.htm.
(Accessed 2011-03-10).
- Delaney, A. and Cameron M. 2006. "Analysis of Pedestrian Crash Data from Great Britain, France and Germany". Report of sub-task 3.4.
- EC. 2003. "Directive 2003/102/EC of the European Parliament and of the Council of 17 November 2003 Relating to the Protection of Pedestrians and Other Vulnerable Road Users Before and in the Event of a Collision With a Motor Vehicle and Amending Council Directive 70/156/EEC." In: UNION, T.E.P.A.T.C.O.T.E. (ed.) 2003/102/EC. Brussels: Official Journal of the European Union.
- EEVC, Working Group 17. 1998. "Improved Test Methods to Evaluate Pedestrian Protection Afforded by Passenger Cars".
- European New Car Assessment Programme (Euro NCAP). 2009. Assessment Protocol Version 5.0
- Fredriksson, R. and Rosén E. 2010. "Integrated Pedestrian Countermeasures - Potential of Head Injury Reduction Combining Passive and Active Countermeasures." IRCOBI Conference, Hannover, Germany.
- Fredriksson, R., Zhang, L., Boström, O., Yang, K. 2007. "Influence of Impact Speed on Head and Brain Injury Outcome in Vulnerable Road User Impacts to the Car Hood". Stapp Car Crash Journal, 51, 155-67.
- Försäkringsförbundet. 2004. "Medicinsk invaliditet – Gradering av medinsk invaliditet" (Swedish Insurance Federation: Medical impairment – Grading of medical impairment, in Swedish). Stockholm, Sweden, Sveriges Försäkringsförbund.
- Hannawald, L. and Kauer, F. 2004. "Equal Effectiveness Study on Pedestrian Protection". Technische Universität, Dresden, Germany.
- Kullgren, A., Lie, A., Tingvall, C. 2010. "Comparison between Euro NCAP Test Results and Real-World Crash Data". 2010 Traffic Injury Prevention, 11: 6, 587-593.
- Lawrance, G. J. L., Hardy, B. J., Carroll, J. A., Donaldson, W. M. S., Visvikis, C. and Peel, D. A. 2006. "A Study on the Feasibility of Measures Relating to the Protection of Pedestrians and Other Vulnerable Road Users". EC report UPR/VE/045/06, contract ENTR/05/17.01. TRL Limited, UK.
- Lie, A., Kullgren, A., Tingvall, C. 2001. "Comparison of Euro NCAP Test Results with Folksam Car Model Safety Rating". In ESV proceedings 2001, paper number 277.
- Liers, L. and Hannawald, L. 2009. "Benefit Estimation of the Euro NCAP Pedestrian Rating Concerning Real-World Pedestrian Safety". In ESV proceedings 2009, paper number 387.
- Malm, S., Krafft, M., Kullgren, A., Ydenius, A., Tingvall, C., 2008. "Risk of Permanent Medical Impairment (RPMI) in Road Traffic Accidents." Annu. Proc. Assoc. Adv. Automot. Med. 52, 93–100.
- McLean, AJ. 2005. "Vehicle Design for Pedestrian Protection." CASR report series report no. CASR037. ISBN 1 920947 39 6.
- Naci, H., Chisholm, D. and Baker, T. D. 2009. "Distribution of Road Traffic Deaths by Road User Group: a Global Comparison." Traffic Injury Prevention, 15, 55-9.
- Rosén, E., Källhammer, J.-E., Eriksson, D., Nentwich, M., Fredriksson, R. and Smith, K. 2010. "Pedestrian Injury Mitigation by Autonomous Braking". Accident Analysis and Prevention, 42, 1949-1957.
- Roudsari, B. S., Mock, C. N. and Kaufman, R. 2005. "An Evaluation of the Association Between Vehicle Type and the Source and Severity of Pedestrian Injuries." Traffic Injury Prevention, 6, 185 - 192.
- Kullgren, A., Lie, A., Strandroth, J., Rizzi, M., Tingvall, C. 2011. "The importance of age for injury severity among car drivers and pedestrians". In ESV proceedings 2011.
- Wikipedia. (2010). Brake Assist, http://en.wikipedia.org/wiki/Brake_Assist. (Accessed 2011-03-09.)
- Zhang, G., Cao, L., Hu, J. and Yang, K. H. 2008. "A Field Data Analysis of Risk Factors Affecting the Injury Risks in Vehicle-to-Pedestrian Crashes." Annu Proc Assoc Adv Automot Med, 52, 199-214.

APPENDIX I – CAR MODELS

1 star-cars, with BA	n
AUDI A2	2
AUDI A4 01-	4
AUDI A6 04-	1
BMW 1 SERIES 04-	1
BMW 3 SERIES 98-05	1
BMW 5 SERIES 03-	4
BMW 5 SERIES 96-02	3
BMW X3	1
MAZDA 6	1
MERCEDES-BENZ A CLASS W169	1
MERCEDES-BENZ E CLASS 02-09	4
OPEL ASTRA 04-	2
OPEL VECTRA 02-	5
SAAB 9-3 04-	4
VOLVO C30	1
SUM	35

1 star-cars, without BA	n
BMW 3 SERIES 98-05	1
BMW 5 SERIES 96-02	8
CHRYSLER PT CRUISER	1
CHRYSLER VOYAGER 2	4
CITROEN XANTIA	3
FIAT PUNTO 94-98	1
FORD FIESTA 96-02	3
FORD KA	1
MERCEDES-BENZ VITO 03-	1
MINI COOPER	2
MITSUBISHI COLT 04-	3
NISSAN ALMERA 98-00	1
OPEL ASTRA 04-	4
OPEL ASTRA 99-03	8
OPEL CORSA 00-	1
OPEL MERIVA	1
PEUGEOT 306	3
RENAULT CLIO 06-	1
RENAULT CLIO 91-98	3
RENAULT MEGANE 97-03	14
RENAULT MODUS	1
SAAB 9-3 04-	2
SAAB 9-3 98-03	7
TOYOTA AVENSIS 03-	3
VOLVO S40 96-04	26
VW POLO 02-05	4
VW POLO 95-00	7
SUM	114

2 stars-cars, with BA	n
AUDI A3 97-03	1
AUDI A4 94-00	1
AUDI A6 97-04	1
CITROEN C5	1
FORD FOCUS 05-	2
FORD MONDEO 01-06	1
FORD MONDEO 07-	1
HYUNDAI I30	1
LEXUS GS 450	1
MERCEDES-BENZ B CLASS	1
MERCEDES-BENZ C CLASS 01-07	1
MERCEDES-BENZ E CLASS 96-01	7
NISSAN QASHQAI	1
OPEL ZAFIRA 05-	1
PEUGEOT 206	6
PEUGEOT 307	5
PEUGEOT 406	1
PEUGEOT 407	2
SAAB 9-5 99-10	3
TOYOTA COROLLA 02-	2
TOYOTA YARIS 05-	1
VOLVO S40/V50 04-	6
VOLVO S60	2
VOLVO V70 N 00-06	17
VOLVO V70 N2 07-	3
VOLVO XC90	2
VW PASSAT 4 97-04	5
VW PASSAT 5 05-	5
VW SHARAN 95-10	1
SUM	82

2 stars-cars, without BA	n
AUDI A3 97-03	2
AUDI A4 94-00	7
AUDI A6 97-04	1
BMW 3 SERIES 91-97	9
CITROEN BERLINGO	1
CITROEN C3	2
CITROEN C5	1
CITROEN XSARA	1
FIAT PUNTO 99-	1
FORD ESCORT 91-	5
FORD FIESTA 03-	7
FORD FOCUS 05-	2
FORD FOCUS 98-04	6
FORD MONDEO 93-00	7
FORD MONDEO 01-06	2
HYUNDAI ACCENT	3
HYUNDAI ATOS	1

2 stars-cars, without BA, cont.	n
MERCEDES-BENZ C CLASS 93-00	1
MERCEDES-BENZ E CLASS 96-01	2
MITSUBISHI SPACESTAR/WAGON 99-	4
MITSUBISHI CARISMA	2
MITSUBISHI COLT 96-04	2
MITSUBISHI WAGON/GEAR 96-	1
NISSAN ALMERA 00-06	1
NISSAN MICRA 92-03	1
NISSAN PRIMERA 98-	4
OPEL CORSA 92-00	2
OPEL OMEGA 94-99	1
OPEL VECTRA 97-02	2
OPEL ZAFIRA 05-	2
OPEL ZAFIRA 99-05	2
PEUGEOT 206	9
PEUGEOT 406	8
RENAULT CLIO 99-06	2
RENAULT LAGUNA	3
RENAULT LAGUNA 2	3
RENAULT MEGANE SCENIC 04-	1
ROVER 75	1
SAAB 900	3
SAAB 9-5 99-10	15
SEAT IBIZA/CORDOBA 93-98	1
SEAT IBIZA/CORDOBA 99-	3
SKODA FABIA	3
SKODA OCTAVIA	4
SUZUKI BALENO	2
TOYOTA AVENSIS 98-02	2
TOYOTA COROLLA 02-	1
TOYOTA COROLLA 98-	9
TOYOTA COROLLA VERSO 04-	1
TOYOTA PICNIC	1
TOYOTA PRIUS 04-	5
TOYOTA YARIS 99-05	2
VOLVO 800/S70	21
VOLVO C70	2
VOLVO S60	9
VOLVO S80	2
VOLVO V70 N 00-06	18
VW GOLF 4 98-03	9
VW LUPO	1
VW NEW BEETLE	1
VW PASSAT 4 97-04	11
VW POLO 00-02	4
SUM	163

2 stars-cars, BA fitment unknown	n
SAAB 9-5 99-10	2

3 stars-cars with BA	n
CITROEN C4	1
TOYOTA AURIS	2
VW GOLF 5 04-	7
VW TOURAN	2
SUM	12

3 stars-cars without BA	n
HONDA CIVIC 02-	1

TOT 1 star	149
TOT 2 stars	326
TOT 3 stars	13
SUM	488
TOT with BA (including 3 stars)	129
TOT without BA (including 3 stars)	357
TOT BA unknown	2
SUM	488

APPENDIX II – RISC MATRICES FOR PERMANENT MEDICAL IMPAIRMENT

Risk for 1% or more permanent medical impairment

(%)	AIS 1	AIS 2	AIS 3	AIS 4	AIS 5
Face	5.8	28	80	80	n/a
Upper extremity	17.4	35	85	100	n/a
Lower extremity	17.6	50	60	60	100
Thoracic spine	4.9	45	90	100	100
Abdomen	0.0	2.4	10	20	20
Head	8.0	15	50	80	100
Lumbar spine	5.7	55	70	100	100
Neck	16.7	61	80	100	100
Thorax	2.6	4.0	4	30	30

Risk for 5% or more permanent medical impairment

(%)	AIS 1	AIS 2	AIS 3	AIS 4	AIS 5
Face	2.4	10	60	60	n/a
Upper extremity	4.2	10	65	100	n/a
Lower extremity	1.6	20	35	60	100
Thoracic spine	0.9	20	55	100	100
Abdomen	0.0	0.0	4.5	10	10
Head	5.0	12	45	80	100
Lumbar spine	1.6	25	45	100	100
Neck	9.7	40	55	100	100
Thorax	0.0	0.5	0.7	15	15

Risk for 10% or more permanent medical impairment

(%)	AIS 1	AIS 2	AIS 3	AIS 4	AIS 5
Face	0.4	6	60	60	n/a
Upper extremity	0.3	3	15	100	n/a
Lower extremity	0.0	3	10	40	100
Thoracic spine	0.0	7	20	100	100
Abdomen	0.0	0.0	5	5	5
Head	2.5	8	35	75	100
Lumbar spine	0.1	6	6	100	100
Neck	2.5	10	30	100	100
Thorax	0.0	0	0	15	15

BENEFIT ESTIMATION OF SECONDARY SAFETY MEASURES IN REAL-WORLD PEDESTRIAN ACCIDENTS

Henrik Liers

Lars Hannawald

Verkehrsunfallforschung an der TU Dresden GmbH (VUFO)

Germany

Paper Number 11-0300

ABSTRACT

Pedestrian accidents play an important role in the area of traffic accident research. Especially in Asia, pedestrians account for large numbers of accident involvements. However, even in the US 12% of the traffic accident fatalities are pedestrians (FARS, 2008) and in Europe, every fifth person, which died in a traffic accident, is a pedestrian (EU-27, 2008).

For that reason, a study was carried out, dealing with the potential benefit of secondary safety measures for pedestrians. Thus, 669 real-world pedestrian accidents out of GIDAS (German In-Depth Accident Study) have been analyzed. The study considered the exact vehicle impact zones, the affected body regions and the injury causing parts of about 850 AIS2+ injuries. Furthermore, the relevance of the ground impact is estimated, which provides an indication about the possible benefit of primary and secondary safety systems.

On the basis of the detailed impact distribution and by using the developed injury shift method, several secondary safety measures can be estimated concerning their effectiveness. In this paper, the results for measures related to the Euro NCAP pedestrian rating tests are presented. It is calculated how well current vehicles perform in pedestrian protection. The benefit of different Euro NCAP point levels is estimated, including the limit value of 36 Euro NCAP. Furthermore, a correlation between the achieved number of Euro NCAP points and the expected real-world benefit is calculated. By using this correlation, the effect of improved secondary safety measures (e.g. due to increased requirements) can be projected to the future pedestrian accident scenario.

The analysis of injury causation in Euro NCAP test zones bases on a high number of real-world pedestrian accidents. The analysis focused on secondary safety measures which are necessary to meet the requirements of the Euro NCAP rating tests. The developed methodology further allows the evaluation of secondary safety systems like the pop-up bonnet or a pedestrian airbag. Furthermore, the results can be later compared to the benefit of primary safety systems like a brake assistant or sensor-based forward-looking systems.

INTRODUCTION

The study generally deals with the analyses of real-world pedestrian accidents involving M1 vehicles. The aim of the study was the benefit calculation of secondary safety measures for the protection of pedestrians with a focus on the Euro NCAP tests concerning pedestrian safety. The study is a part of a larger research project dealing with the benefit estimation of primary safety systems and secondary safety measures. This paper describes the methods and some results of the analysis of secondary safety measures. Most of the results are currently used in the “vFSS” project (“vorausschauende Frontschuttsysteme”) dealing with the development of test procedures for and the benefit estimation of advanced forward looking safety measures.

DATASET

The following chapter deals with the data source that was used for the analysis. The sample criteria as well as the creation of the master-dataset are described. To get an overview of the pedestrian accident scenarios some statistical information is provided.

Data source

For the study accident data from GIDAS (German In-Depth Accident Study) is used. GIDAS is the largest in-depth accident study in Germany and the data collected in the project is very extensive.

Due to a well defined sampling plan, representativeness with respect to the federal statistics is also guaranteed. Since mid 1999, the GIDAS project has collected more than 20.000 on-scene accident cases in the areas of Hanover and Dresden. GIDAS collects data from accidents of all kinds. Due to the on-scene investigation and the full reconstruction of each accident, it gives a comprehensive view on the individual accident sequences and the accident causation.

The project is funded by the Federal Highway Research Institute (BASt) and the German Research Association for Automotive Technology (FAT), a department of the VDA (German Association of the Automotive Industry).

Use of the data is restricted to the participants of the project. However, to allow interested parties the direct use of the GIDAS data, several models of participation exist. Further information can be found at <http://www.gidas.org>.

Sample criteria

The GIDAS database currently consists of more than 2.500 accidents involving pedestrians. These are accidents with passenger cars, trucks, trams, motorcycles and bicycles. For the present study, special filter criteria are used not least because of the intended comparison between the benefits of primary and secondary safety measures. Thus, a common dataset (usable for the simulation on the one hand and for the analysis of secondary safety measures on the other hand) has to be created.

First and foremost, only reconstructed accidents are used as only these do include information regarding the initial speed, braking deceleration, collision speed etc. Accidents with unknown parameters (where an exact reconstruction was not possible) are excluded, as well as cases where the pedestrian kinematics is unknown or where no injury information could be investigated due to missing declarations of consent of the involved persons.

The next sample criterion is the vehicle class. The study considers all accidents with passenger cars of the M1 type (according to the UN-ECE definition). Furthermore, only accidents with impacts in zones tested by Euro NCAP are taken into account. These are mostly pure frontal impacts and few lateral impacts. Furthermore, special types of accidents were excluded from the analysis. These are rare cases such as run-over accidents, where the person already laid/sat on the road or accidents where the pedestrian was crushed between two cars.

Descriptive statistics of the master-dataset

The application of all filter criteria to the GIDAS database gives a master-dataset of 669 accidents that can be analysed regarding the benefit of primary and secondary safety measures.

The large majority (97%) of these accidents occur in urban areas. Looking on the accident types, the following results can be derived from the data:

- 85% of the cases are crossing accidents
- 9% of the cases are turning accidents
- 6% of the cases are other accidents (loss of control, longitudinal traffic, resting traffic)
- in 58% of the crossing accidents the pedestrian is not obstructed
- in 60% (crossing accidents) the pedestrian crosses the road from the right to the left.

Considering the collision speeds (figure 1) it can be seen, that approximately 80% of the accidents occur at speeds up to 40kph. Half of the pedestrians are hit with speeds between 11 and 30 kph.

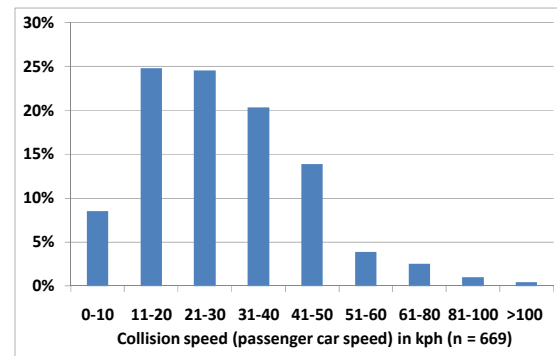


Figure 1. Distribution of collision speed (speed of the passenger car).

Another important parameter is the age of the pedestrian as it is known that the age has a large influence on the injury severity outcome, beside the collision speed and the impacted part of the vehicle. Due to the human physiological properties, elderly people often sustain worse injuries than younger people. Otherwise, children are often hit by other vehicle parts than adults, due to their smaller body height. Especially the head impact areas of children differ substantially from the impact zones of adults.

The following graph shows the distribution of the pedestrian's age in the master-dataset (figure 2).

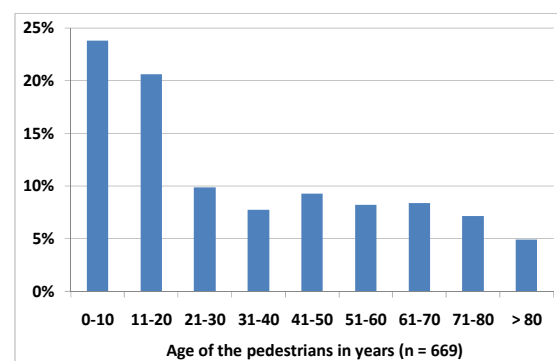


Figure 2. Distribution of pedestrian age.

Every third injured pedestrian is aged up to 14.

Finally, the injury severity is analysed. According to the official definition, the dataset contains:

- 321 slightly injured pedestrians (48,0%)
- 319 seriously injured pedestrians (47,7%)
- 29 fatally injured pedestrians (4,3%)

Furthermore, the distribution of the MAIS is shown in figure 3. The present study is consistently done on the basis of the AIS edition 2005.

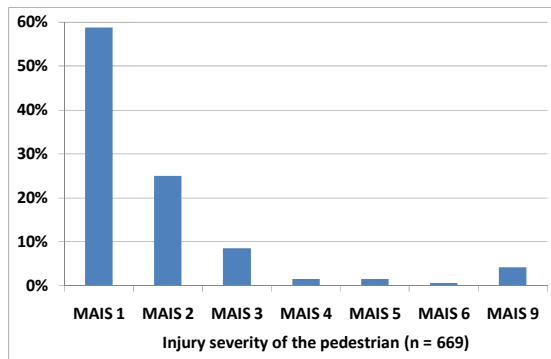


Figure 3. Injury severity distribution (MAIS).

As seen in the figure, approximately 40% of the pedestrians have been MAIS2+ injured. Following many other studies, this group of seriously and fatally injured persons is the interesting group for the development and improvement of safety systems. The analyses within the present study also focus on AIS2+ injuries respectively MAIS2+ injured pedestrians. All in all, the dataset contains 276 MAIS2+ injured pedestrians that sustained about 850 AIS2+ injuries.

METHODOLOGY

This chapter describes the used methods for the benefit estimation. It concentrates on the more sophisticated methodologies basing on the methods published in previous studies.

Summary of known methodologies

As mentioned the aim of the study is the benefit estimation of secondary safety measures on the basis of single injuries sustained in real-world pedestrian accidents. For the intended evaluation of different secondary safety measures resulting in different Euro NCAP test results, a detailed impact distribution of AIS2+ injuries is necessary. To derive this basic information, the following steps have to be done.

The estimation of the Euro NCAP test zones is done for every vehicle model that was involved in one of the 276 accidents with an MAIS2+ injured pedestrian. The determination of the 60 single test zones is done on the basis of CAD models, according to the Euro NCAP testing protocol [2]. After that, every actually sustained injury in the 669 real-world accidents can be allocated to a particular Euro NCAP test zone if it occurred in such an area.

A case-by-case analysis is necessary to link impact data (Wrap Around Distance and lateral distance from the vehicle mid of every AIS2+ injury) with injury data such as the type of injury, the injury severity value (AIS), the injury location

(exact body region) and the injury causing part. As shown in figure 4 all relevant data is combined to derive the required impact distribution.

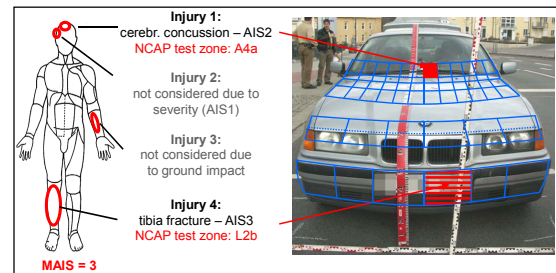


Figure 4. Combination of injury data, measured impact points and the Euro NCAP test zones.

This is done for all 276 accidents with an MAIS2+ injured pedestrian. As a result, the injury causation of pedestrian's AIS2+ injuries in Euro NCAP test zones, in other vehicle zones or due to the ground impact can be displayed.

Improved injury shift method

Previous studies dealing with secondary safety measures for pedestrians vary in relation to the question as to whether all injuries (in all body regions) benefit from improvements that were made to pass a special (body region related) test or if only the injuries in addressed body regions may be affected from secondary safety measures.

For the study, all injuries in all body regions are taken into account. Child head injuries for instance are also considered if they are caused by the bonnet leading edge, although this part is essentially addressed by a test covering upper leg and pelvis injuries. By using this approach it is assumed that all injuries in all body regions will benefit from secondary safety measures. Although this assumption is an optimistic one and may lead to an overestimation of the benefit it can be expected that an optimised impact zone will even have a positive effect on injuries of other body regions. An optimised head test zone on the bonnet will surely mitigate injuries to the thorax or abdomen, too.

Contrary to that, the next step of the benefit estimation, the injury shift method, is intentionally done with a pessimistic approach. The aim is the performance estimation of particular Euro NCAP test zones. Due to the fact, that real-world accident databases do not contain any information about the Euro NCAP testing parameters like HIC, bending moment, knee bending angle, leg impact force or lower leg acceleration, the evaluation cannot directly be done on the basis of these parameters. Thus, the Euro NCAP test zones are estimated on the basis of their colour [1].

The performance of all 60 Euro NCAP test zones is judged on the basis of physical parameters. Depending on the results in the test, a characteristic colour is assigned to every zone, namely green for a good pedestrian protection, yellow for an adequate pedestrian protection and red for a marginal one. This colour code was here used for the estimation of effectiveness of single test zones. It is assumed that the original injury severity could be reduced by a green or yellow test zone. That means the AIS value is shifted downwards if the injury was sustained in a green or yellow Euro NCAP zone. Figure 5 shows the extent of the injury severity reduction depending on the colour of the particular test zone.

One of the most important assumptions within the entire study is that the injury shift method is only applied to AIS2+ injuries if they were sustained in accidents with collision speeds up to 40kph. It is assumed that there is hardly any potential of secondary safety measures for the reduction or mitigation of injuries. That means that about 500 AIS2+ injuries are not considered by the injury shift.

Injury shift method	
→ is applied to all AIS2+ injuries in all body regions but only in accidents with collision speeds up to 40kph	
green Euro NCAP test zone (good protection potential)	original injury severity is shifted by two AIS levels
yellow Euro NCAP test zone (adequate protection potential)	original injury severity is shifted by one AIS level
red Euro NCAP test zone (marginal protection potential)	original injury severity is not shifted

Figure 5. Injury shift method (assumptions).

It is assumed that the injury severity in a green Euro NCAP test zone decreases stronger than in a yellow one. Injuries in red Euro NCAP test zones are never shifted. Generally, the injury severity can be shifted towards AIS1 at the maximum. It is assumed that no injury is entirely avoided (AIS0).

Benefit estimation

Out of the case-by-case analysis it is known which injuries have been sustained by the pedestrian and which impact zones were responsible for them. Along with the measured Euro NCAP test zones for every vehicle model it is possible to evaluate any Euro NCAP colour distribution regarding its expected real-world benefit; theoretical distributions as well as real test results.

The colour distribution that has to be evaluated is assumed to all vehicles in the dataset. Using the injury shift method, it is calculated how the injury

severity outcome will be if all vehicles in the dataset would have this Euro NCAP distribution.

One important thing that has to be assumed is that the vehicles in the original GIDAS dataset have zero Euro NCAP points. Due to the fact that most of the vehicles in the GIDAS dataset are rather old, this assumption seems to be suitable. However, the actual pedestrian protection performance is unknown for the majority of the vehicles, due to missing Euro NCAP test results for older vehicles.

Keeping this in mind, the benefit can be calculated. The injury severity (represented by the MAIS) is re-calculated for every pedestrian, using the maximum AIS value of all single injuries. Depending on the number, the severity and the causation of the injuries, the MAIS of a pedestrian is reduced or remains constant.

Analysis of real Euro NCAP test results

The central aim of the study is the evaluation of measures related to the Euro NCAP pedestrian tests. It is intended to evaluate all currently tested vehicles concerning their real-world effectiveness in pedestrian accidents. Furthermore the state of the art as well as the minimum expectable safety level of recently introduced vehicles is considered.

For that reason, the real test results of all vehicles tested by Euro NCAP according to the 2010 rating method are derived from the official homepage [3]. Finally, 66 different vehicle models (tested between January 2010 and February 2011) are used for the analysis. The performances of these vehicles range between 9 and 28 Euro NCAP points with an average of 17,9 points and a median of 18 points.

The colour distributions of these vehicles are then used for the characterisation of the state of the art, representing the pedestrian protection potential of currently tested vehicles. Therefore, the proportion of green, yellow and red test zones within the 66 vehicle models is calculated. Figure 6, for instance, shows the proportions of green test results for every zone each. Zones where the proportion is clearly above the half ($\geq 55\%$) are coloured green.

AH	0%	6%	33%	36%	41%	39%	41%	39%	39%	36%	8%	0%
	3%	8%	32%	41%	42%	42%	41%	42%	41%	29%	6%	3%
CH	9%	23%	48%	64%	73%	74%	79%	77%	65%	53%	20%	5%
	11%	15%	42%	48%	65%	64%	64%	64%	50%	39%	15%	8%
UL	14%	12%	12%	14%	12%	14%						
LL	79%	88%	95%	94%	88%	77%						

Figure 6. Proportion of green tested Euro NCAP zones (66 currently tested vehicles).

It can clearly be seen that the vast majority of currently tested vehicles achieve good test results in the lower leg test areas. Furthermore, the child head impactor test zones in the vehicle mid perform relatively well. Contrary to that, the tested vehicles show worse results in nearly all other head impactor test zones, especially in the outermost test zones. Looking on the upper leg test zones it can be derived from the figures that only every sixth vehicle achieves a “green” result on average.

Figure 7 shows the proportion of red tested zones. Again, zones with a proportion above 55% are coloured. As expected, the distribution is inverted compared to the green one; leading to the same conclusions as mentioned in the paragraph above.

AH	100%	88%	56%	47%	44%	47%	48%	48%	50%	52%	86%	100%
	94%	82%	56%	42%	39%	39%	38%	36%	42%	56%	83%	94%
CH	77%	58%	18%	9%	11%	9%	2%	3%	11%	20%	61%	80%
	77%	59%	26%	24%	17%	20%	18%	15%	26%	32%	58%	80%
UL	62%	70%	62%				65%	73%	64%			
LL	9%	0%	0%				0%	0%				9%

Figure 7. Proportion of red tested Euro NCAP zones (66 currently tested vehicles).

Finally, the proportions of yellow tested Euro NCAP zones are shown, including the remaining percentages per test zone (figure 8).

AH	0%	6%	13%	21%	15%	13%	11%	13%	13%	15%	6%	0%
	2%	9%	15%	21%	17%	17%	21%	21%	17%	15%	11%	2%
CH	6%	17%	42%	32%	21%	21%	25%	25%	25%	30%	17%	8%
	6%	21%	36%	32%	23%	19%	23%	26%	25%	28%	25%	6%
UL	25%	19%	23%				21%	15%	23%			
LL	9%	13%	6%				8%	13%	11%			

Figure 8. Proportion of yellow tested Euro NCAP zones (66 currently tested vehicles).

In the upper leg test zones, about every fifth tested vehicle achieves “yellow” test results on average. The lower leg test areas of few vehicles also show yellow zones and some head impactor test areas are covered with yellow test fields, too.

These three distributions represent the state of the art of current vehicles (model years 2009 and 2010). In the next step, a “minimum expectable safety level” is derived from this information. Therefore, all zones with frequencies of at least 55% of one colour automatically get this colour in the “basic shape”. Furthermore, the colour distribution has to be symmetrical. That means, for

instance, if the test zone on the left vehicle side is already red, the related test zone on the right vehicle side is also defined as red. Zones with high frequencies of yellow test zones and/or similar proportions of red and green zones are defined as yellow. In doing so, the following Euro NCAP colour distribution was created (figure 9).

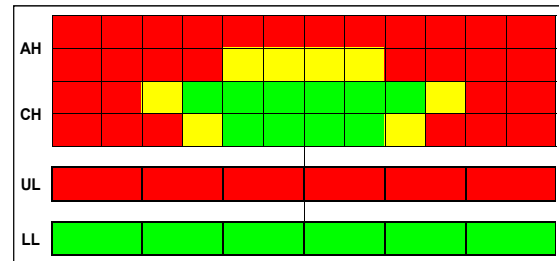


Figure 9. “Basic Euro NCAP shape” (Current minimum expectable safety level).

The following points are assumed per zone:

- lower/upper leg: green = 1.0 point
- head test zones: green = 0.5 points
yellow = 0.25 points
red = 0 points

Applying these scores to the above shown distribution leads to an overall rating result of 13 Euro NCAP points. This can be assumed to be the minimum expectable safety level of recently introduced vehicle models. Compared to the single test results, 86% of the tested vehicles achieve this result. Furthermore, it has to be mentioned that the test results now (June 2011) are on average already one year old and it can be expected that the “basic pedestrian protection level” increases steadily.

ANALYSES AND RESULTS

This chapter gives a summary about some results of the study. At first, the impact distribution is shown. Afterwards, the results of the benefit estimation for different Euro NCAP rating results are described. In addition, the performance of the above shown “basic Euro NCAP distribution” and some theoretical shapes is compared to real vehicles.

Impact distribution

At first, the results of the case-by-case analysis are presented. All AIS2+ injuries have been either allocated to a Euro NCAP test zone, to another (not tested) vehicle zone or to the ground impact. Figure 10 shows the general areas of injury causation for all AIS2+ injuries. In addition, the numbers for accidents up to 40kph are given in brackets.

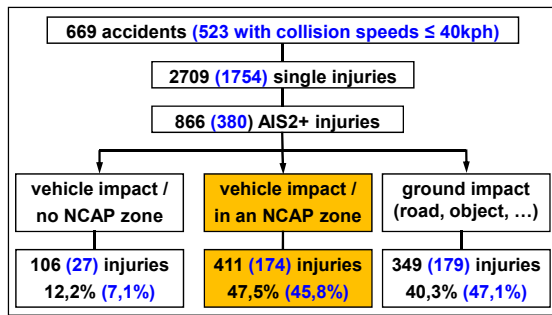


Figure 10. Injury causation of AIS2+ injuries.

The first conclusion that can be drawn from the figures is that about every second AIS2+ injury occurs in a Euro NCAP test zone. The ground (= secondary) impact plays a very important role, especially in low speed accidents. The relevance of other vehicle parts (not tested) obviously increases with the collision speed. This is caused by more impacts in areas with a WAD above 2100mm.

It can be further seen from the figure that the majority (56,1%) of all severe injuries in the dataset occurred in accidents with collision speeds above 40kph although they make up only 22% of all accidents. Another important fact is that pedestrians in accidents with high collision speeds often suffer more than one severe injury. Especially fatally injured pedestrians can have up to 70 single injuries (given that the information from the autopsy is very detailed). As a consequence, one pedestrian can be responsible for more than one AIS2+ injury in one Euro NCAP zone.

This is confirmed by figure 11 that shows the distribution of all AIS2+ injuries in Euro NCAP zones. The majority of the pedestrians account for one or two AIS2+ injuries per test zone, but there are two (fatally injured) pedestrians who suffered about 10 thorax injuries in one Euro NCAP zone, leading to a small bias in the shown distribution. However, the impact distribution leads to clear conclusions concerning the occurrence of AIS2+ injuries. The majority of these injuries are sustained in the lower leg test zones, followed by the rearmost und outermost head impact test zones.

	right vehicle side				left vehicle side			
AH	4%	7%	1%	0%	1%	-	-	4%
	2%	2%	1%	2%	1%	1%	0%	1%
CH	1%	-	2%	1%	0%	0%	-	1%
	1%	1%	2%	-	-	-	0%	2%
UL	2%	2%	2%	2%	1%	-	-	3%
LL	6%	8%	6%	7%	9%	7%	-	-

Figure 11. Distribution of AIS2+ injuries in Euro NCAP zones (all collision speeds / n=411).

Figure 12 shows the same distribution for accidents with collision speeds up to 40kph. As described above, the injury shift method is only applied to these 174 AIS2+ injuries.

	right vehicle side				left vehicle side			
AH	6%	4%	-	1%	-	-	-	1%
	3%	3%	-	-	-	1%	-	2%
CH	-	-	5%	1%	1%	-	-	1%
	-	-	1%	-	-	-	-	1%
UL	3%	5%	3%	1%	1%	-	-	3%
LL	6%	11%	8%	10%	10%	3%	-	-

Figure 12. Distribution of AIS2+ injuries in Euro NCAP zones (coll. speed ≤40kph / n=174).

As expected, the proportions in accidents with smaller collision speeds are slightly shifted towards the lower leg test zones. This is especially a result of fewer thoracic and abdominal injuries.

Evaluation of real Euro NCAP test results

On the basis of the case-by-case analysis and the detailed impact distribution, various analyses can be done with the available data. On the one hand it is possible to directly estimate the benefit of existing secondary safety measures (like an active bonnet or an external pedestrian airbag). On the other hand, the safety performance of single vehicles models can be estimated if their Euro NCAP test results are available. It can be analysed how the pedestrian accident scenario would be if all vehicles would feature the given Euro NCAP colour distribution.

Furthermore, the impact distribution can be inverted to conclude which zones/parts of the vehicle should be better addressed or improved by secondary safety measures. In doing so, all pedestrian impact points should be considered, not only the ones tested by Euro NCAP.

For the present paper, all 66 real test results are estimated regarding their benefit in the real pedestrian accident scenario. In addition, three theoretical shapes are evaluated. The first one only has optimised lower leg test zones; the second one represents the best possible Euro NCAP test result (upper limit of 36 points) and the last one is the created “basic shape” out of the 66 recently tested vehicle models ((figure 13).

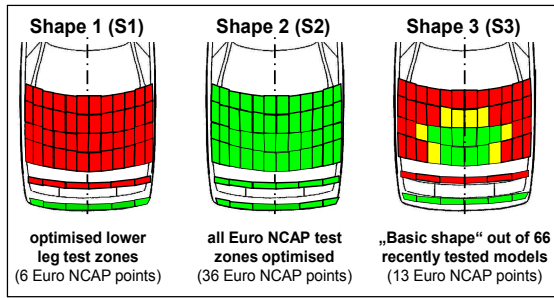


Figure 13. Evaluated theoretical shapes.

All in all, the 69 colour distributions each are assumed to all vehicles in the dataset and the new number of MAIS2+ injured pedestrians is calculated following the above mentioned method. Assuming that the vehicles in the original GIDAS dataset have zero Euro NCAP points and that the 669 accidents were responsible for 276 MAIS2+ injured pedestrians, every model or colour distribution will lead to a decreasing number of seriously injured pedestrians.

The following graph shows the calculated reduction of MAIS2+ injured pedestrians for all 69 colour distributions (figure 14).

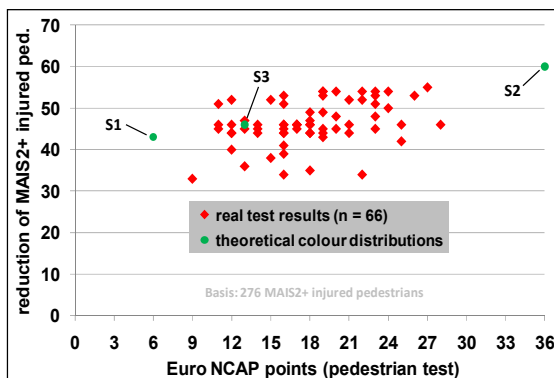


Figure 14. Reduction of the number of MAIS2+ injured pedestrians for 69 colour distributions.

Various conclusions can be derived from the figure.

- I) In general, the reduction of MAIS2+ injured pedestrians will increase with an increasing number Euro NCAP points.
- II) The maximum possible reduction amounts to 60 MAIS2+ injured pedestrians, assuming that all vehicles achieve 36 Euro NCAP points (shape S2). That means the other way round that 216 (of the original 276) pedestrians remain MAIS2+ injured due to other severe injuries sustained during the ground impact or on other vehicle parts.
- III) If all vehicles would feature completely optimized lower leg zones (point S1 in the figure),

the number of MAIS2+ injured pedestrians would already decrease by 43 persons.

IV) Although some vehicle models achieve good test results (represented by many Euro NCAP), their benefit in the real-world pedestrian accident scenario is smaller than the benefit of the 6-point-distribution (S1). One vehicle model, for instance, performs worse than the S1 shape.

V) There are partially considerable variations within one point level. In the most frequent group of (16 Euro NCAP points), the reduction varies between 34 and 53 MAIS2+ injured pedestrians.

VI) The result of the “basic shape” S3 (achieving “only” 13 Euro NCAP points) shows a notable reduction of 46 seriously injured pedestrians. That means that the large majority of current vehicle models (which built the colour distribution of the shape) already have acceptable pedestrian safety performances.

SUMMARY AND CONCLUSIONS

In the study 669 real-world pedestrian accidents involving M1 vehicles have been analysed concerning the pedestrian’s impact points on the vehicle and the injury causation. More than 850 AIS2+ injuries are analysed with regard to their severity, body region and causation. A detailed impact distribution for injuries in Euro NCAP test zones is generated both for all accidents and only for accidents with collisions speeds up to 40kph.

Various analyses can be done on the basis of this information. It is possible to evaluate secondary safety measures like pop-up bonnets or external pedestrian airbags. Furthermore, the benefit of system ideas or future secondary safety measures can be estimated prospectively. In this study the data is used for the evaluation of different Euro NCAP pedestrian rating results. Therefore, the benefit is defined as the reduction of MAIS2+ injured pedestrians, resulting from single injury severity reductions in yellow and green Euro NCAP test zones.

At first, 66 vehicle models recently tested by Euro NCAP have been used to describe the state of the art and to create a “basic shape”. This shape represents the current expectable pedestrian protection performance. Afterwards, these 66 vehicle models and three theoretical shapes have been evaluated concerning their effectiveness in the real-world pedestrian accident scenario. Taking the actual real-world impact points as a basis, different Euro NCAP colour distributions achieve different real-world benefits, depending on the individual position of their red, yellow and green fields.

Vehicles with equal Euro NCAP pedestrian ratings (point scores) may have great as well as small real-world benefits.

The results of the study show that there is a correlation between the number of Euro NCAP points and the reduction of MAIS2+ injured pedestrians. However, the expected real world benefit may vary considerably within one Euro NCAP point level. Another important fact is that even a vehicle achieving 36 Euro NCAP points is incapable to reduce the number of seriously injured pedestrians to an acceptable extent. Therefore, combinations of primary and secondary safety measures will be the number one way to make great progresses in reducing the number of seriously and fatally injured pedestrians.

REFERENCES

- [1] Liers, H., Hannawald, L. 2009. "Benefit estimation of the Euro NCAP pedestrian rating concerning real-world pedestrian safety". Final report, available on www.vufo.de
- [2] Euro NCAP. 2008. Pedestrian testing protocol, Version 4.2, derived from www.euroncap.com
- [3] Euro NCAP. 2011. Results of the pedestrian rating tests, derived from www.euroncap.com

BIO-INSPIRED NEUROMORPHIC IDENTIFICATION OF PEDESTRIAN AND OBJECT FOR THE ROAD USER SAFETY

Woo Joon, Han
Il Song, Han
KAIST, Korea, i.s.han@kaist.ac.kr
Paper Number 11-0217

ABSTRACT

There has been much research and development in pedestrian detection to minimize accidents. The fast changing environment presents a challenge for reliable detection. In this paper, an algorithm inspired from human eye was implemented. The detection of pedestrian from an image taken from a moving car and a second deck of a moving bus proved to be successful with same algorithm even the condition of the image taken was quite different. The feasibility of applying this idea is further extended when it can be implemented electronically using 0.18 μ m CMOS technology.

INTRODUCTION

The pedestrian detection techniques in real-world images have emerged as a solution to protect pedestrians against fatal accident. The vision-based pedestrian detection is very challenging due to the wide range of outdoor lighting condition and pedestrians' appearance. In this paper, we propose a pedestrian detector based on bio-inspired neuromorphic system of mimicking human or animal, for the robust and reliable operation on the road. The video image or still image of pedestrians on the road is analyzed by a neuromorphic system, which is based on the Hubel and Wiesel's experimentation of cat's visual cortex and the spiking neuron of Hodgkin-Huxley formalism. The research of visual signal processing aims to identify pedestrians or other vulnerable non-occupant road users of bicyclist or motorcyclist. The current development stage is the recognition of pedestrians crossing the road or bicyclist/motorcyclist on the road. The detection of pedestrian and other vulnerable road users is monitored using the CCTV video image taken from the urban road intersection.

The analysis methodology is developed by mimicking the principle of visual cortex with similar robust characteristics, while there is practical feasibility of VLSI implementation for low cost device. The directional elements in images are utilized as in Hubel and Wiesel's experimentation, and the neural networks with template as well as the histogram analysis are used to recognize the pedestrian or vulnerable objects.

The successful detection of a pedestrian or bicyclist demonstrates the feasibility of adopting the

video-based road user detection, with video taken from commercial IP CCTV camera as database in the experiment. The challenge of abrupt illumination change is managed by mixed processing of neuromorphic and frame difference.

The video sequence, with resolution of 720x480 and 30 frames per second, is successfully evaluated for detecting the pedestrian, the bicyclist, and the motorcyclist on the road. During the sequence, the video sample is taken at different time of the day with different illumination conditions. The human head is also identified regardless of the facial direction, while the wheel of bicycle or other objects is successfully recognized. The robust and flexible detection of objects is enabled by the particular directional image processing together with neural weight template. The neuromorphic vision system is applied to the video image of pedestrians taken by the commercial car black box, while the vehicle is in motion at various locations of Korea and UK.

The neuromorphic vision based pedestrian detection system targets to develop the pedestrian protection system, which warns the driver from the road infrastructure or the on-vehicle system. The neuromorphic system improves the robustness and reliability of the vision-based pedestrian detection for the wide range of application environment.

Bio-inspired detection

The environment of the pedestrian may differ greatly between each person since the vehicle is in motion. So a robust detection algorithm is needed to perform accurately under this fast changing environment. Much of computer vision algorithms are effective in their specific usage, however they lack the robustness of human vision and for most times will underperform in varied conditions. [1]

Although there is not a definite model of visual cortex, Hubel and Wiesel's research on cat's striate cortex confirmed the idea on the functioning of simple cell [2]. It is from this discovery which motivated various theories of object recognition from characters to complex natural images [3]. These researches on neurophysiology introduced the principles of biologically plausible electronic implementation. One of the electronic implementation is the Hodgkin and Huxley's model of neuron which is utilized in this paper to show

feasibility of implementation of proposed bio-inspired visual processing electronically. The motivation for it was found from the result of the well-known experimentation of simple cell by Hubel and Wiesel as shown in figure 1. By mimicking the simple cell, similar robustness of visual cortex can be achieved.

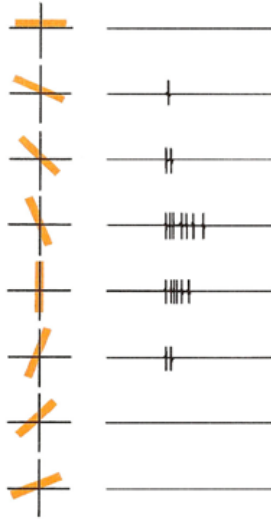


Figure 1. Response of the cat's cortex when a rectangular slit of light of different orientations is shown [1]

Neuromorphic neuron based on voltage-controlled CMOS conductance The Hodgkin-Huxley (H-H) is a widely adopted idea of neuron's biophysical characterization as shown in figure 2. H-H formalism is not used as much in neural networks as it does not give any major advantages however the asynchronous spikes are considered as principle element of high level or large scale neural computing system.

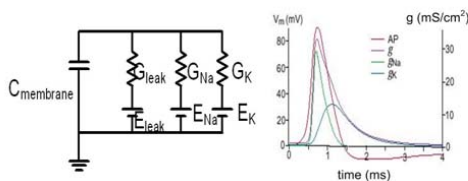


Figure 2. An electrical equivalent circuit of neuron, H-H formalism where the asynchronous spike of a neuron as shown on the right can be reproduced. [4]

A circuit of Fig. 3a was proposed as a voltage-controlled linear conductance circuit by a PMOS transistor and a pair of identical NMOS transistors M1 and M2, while the conductance of MOS transistors is one of essential components in the analogue circuit design. The circuit of Fig. 3 has

been investigated for various neural networks applications, from implementing synapses to neurons [5, 6].

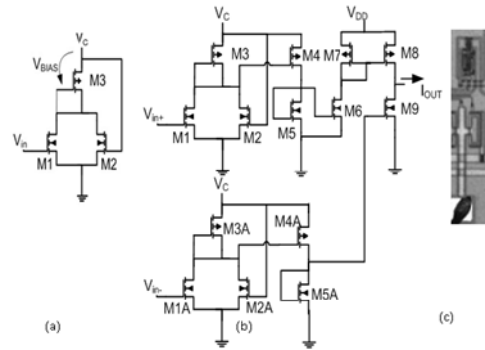


Figure 3a. Voltage-controlled linear conductance by a pair of MOSFETs in the triode region, b. the tunable linear transconductance circuit, c. the chip photograph of CMOS transconductor.

The empirical mathematical formulae of conductance element in the formalism is expressed as (1) where b is the sigmoid function of membrane potential. And V_m is a membrane potential and the overall dynamic modeled by an Action potential and related ionic conduction.

$$G_{ion} = G_{ionmax} \cdot x$$

$$dx/dt = \alpha(b - x)$$

$$i_{ion} = G_{ion}(V_m - E_{ion}) \quad (1)$$

Functional components of eq 1 are controlled conductance, multiplication, addition (or subtraction), and differential equation. The differential equation in eq 1 can be implemented by the low pass filter, which induces a delayed response. From these relationships dynamic behavior of biological neuron can be implemented electronically by the ion-based conductance controlled by membrane potential as shown in figure 3.

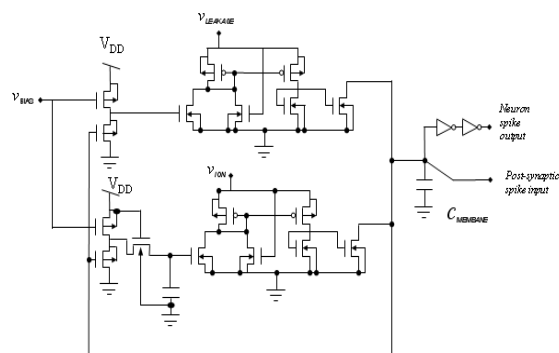


Figure 4. Neuromorphic implementation of a neuron.

The implemented system was simulated with different orientation inputs as it is believed that the tuning properties of orientation selectivity plays key role for perception in visual cortex as it was shown in figure 1. For the simulation, a tuned feature map of 5 x 5 synaptic weights, shown in figure 5, is based on the reference stimulus to match, with the minor adjustment depending on the output was prepared to mimick the orientation selectivity property of the simple cell. The synaptic weights are in the ratio of 1:-0.6:0.1 for black: grey: white respectively. The stimulus were six 50 x 50 pixel sized rectangles at different angles as to give same effect as the inputs give to the cat in Hubel and Wiesel's experiment. The result of stimulation shown in figure 6 showed consistent outcome as the outcome of Hubel and Wiesel's experiment shown in figure 1 where the tuned feature orientations (-45° , 25°) are evaluated.

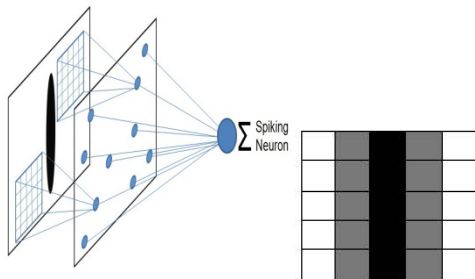


Figure 5. The artificial primary visual cortex model with orientation selective synaptic weights to mimick the simple cell.

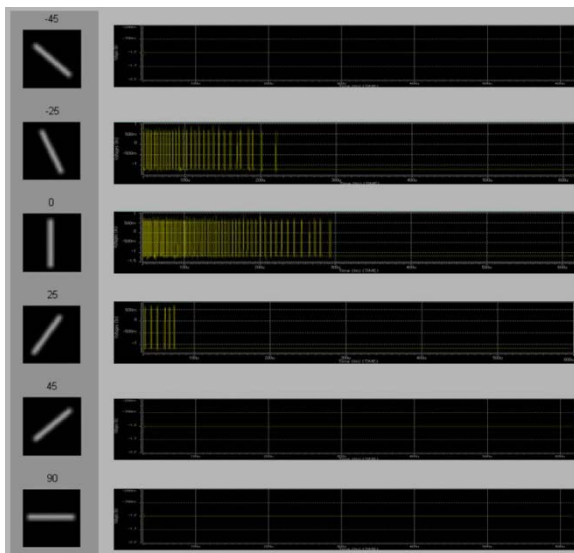


Figure 6. The simulated spike burst of VLSI visual cortex to stimulus in various orientations.

DETECTION OF PEDESTRIANS

Pedestrians are detected in two different environments; moving car and second floor of moving double decker bus.

For detection of pedestrians using bio-inspired approach, orientation features from the input image is extracted first. The number of different orientation angles to be extracted will be different depending on the type of the target to be extracted. For example, a vehicle or man-made objects tend to have lot of straight edges whereas a biological object such as pedestrian do not have much of pre-defined features so much more orientation feature extractors are used.

Figure 7 shows the result of detection of the cyclist from a video stream captured from inside the car using commercially available car black box. The orientation feature map shows much of background are extracted as well however after carrying out an neural network function the cyclist is detected at the end.

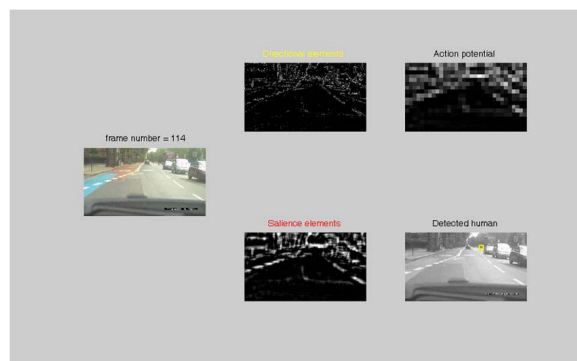


Figure 7. The detection of cyclist from input image from a car. (from right in clockwise direction) Input image, orientation feature image, action potential of neuron, detected image and salience image.

Detection of pedestrian from an image captured from the second deck of a typical bus in city of London is shown in figure 8. The video stream from the bus is quite different to the one captured from the car as shown in figure 7. Firstly, the angle at which the image is captured is different thus the effect of luminance level however the results show that the proposed idea is robust.



Figure 8. The input image captured from second deck of a bus in London.

The figure 9 shows the orientation features extracted from figure 8. From the initial orientation feature extracted, it is not easy to easily identify the pedestrian. But since video stream is being used, the difference of orientation feature reduces noise and outline of pedestrian can be more clearly seen.



Figure 9. Orientation features extracted from figure 8.

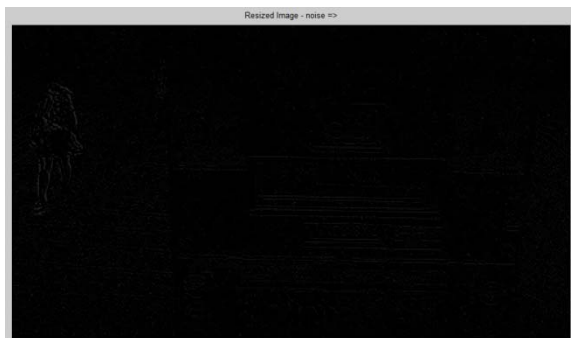


Figure 10. Difference of orientation feature map extracted from figure 8 and previous frame. Note that pedestrian is more clearly visible.

The difference image is then passed through a neural network which uses template of upper torso of human. The action potential of the resulting neural network shows strong signal from the pedestrian and figure 12 shows the successful detection of the pedestrian in the image.

Cyclist on the road can be just as dangerous as the pedestrian so the proposed idea is tested with a motorcyclist as shown in figure 13. The orientation features extracted, shown in figure 14, from this figure shows much of the image is extracted so that the motorcyclist is not so clearly seen. The orientation features of previous frame is used to difference the image as seen in figure 15, the motorcyclist is still not clearly seen as it did in figure 10. However when the neural network shown in figure 16 is applied most of the noise is diminished since the most of the background noise detected are from man-made objects such as vehicles or road signs and the template of the neural network is such that only the human-like objects are left. Then the resulting action potential shows clearly the motorcyclist and as expected the detection was successful as shown in figure 17.

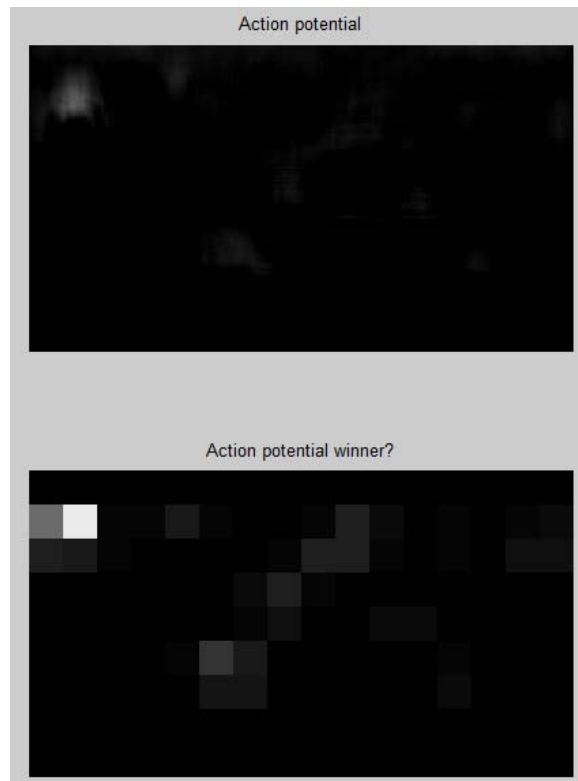


Figure 11. The top image shows the result after neural network is applied to figure 10. Then (bottom image) shows the action potential of the neural network.



Figure 12. Successful detection of the pedestrian.



Figure 13. Captured image of motorcyclist from the second deck of a bus in London.



Figure 14. Orientation features extracted from figure 13. There is much noise extracted as well.

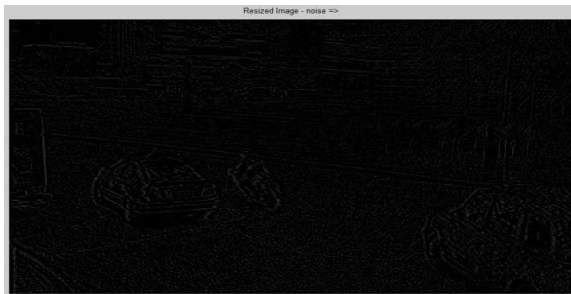


Figure 15. Orientation feature difference of orientation extracted from figure 13 and previous frame. Note that the outline of the vehicle is still quite strong.

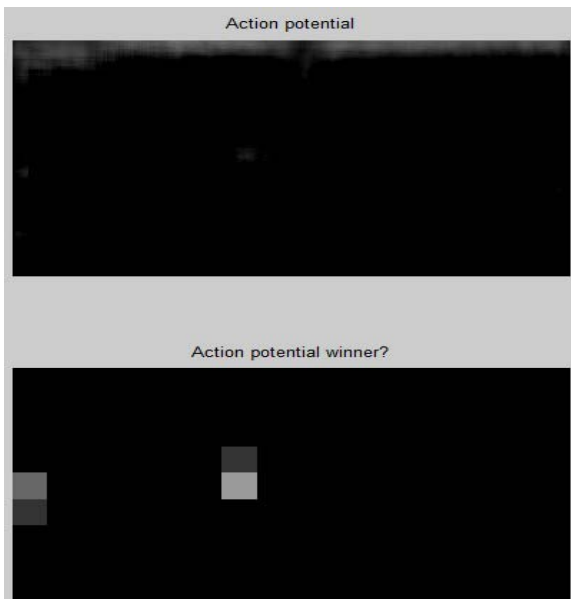


Figure 16. The result after neural network is applied. Note that after the neural network is applied much of noise is diminished and motorcyclist is detected clearly.



Figure 17. Successful detection of motorcyclist.

CONCLUSION

The bio-inspired approach to pedestrian detection was explored. The challenges of pedestrian detection are the quick changing of the environment and the condition so a robust algorithm is a must especially if such system were to be applied to actual vehicle as pedestrian detection system.

The detection of pedestrian and a cyclist taken from images captured from a car and a bus proved to be successful even if the conditions were different. Also the application of the proposed idea into a CMOS technology was explored as well with SPICE simulation of the idea.

ACKNOWLEDGEMENT

This research was funded by NRF, Korea. Grant No. 2010-0022245.

REFERENCES

- [1] Yilmaz, A, Javed, O and Shah, M, "Object Tracking: A Survey", ACM Computing Surveys, vol. 38, Article 13, 2006, pp.1-45.
- [2] Hubel, D. H and Wiesel, T, "Receptive fields of single neurones in the cat's striate cortex", J. Physiol., 148, 1959, pp 574-591.
- [3] Risenhuber, M and Poggio T, "Hierarchical models of object recognition in cortex", Nature Neuroscience, 1999, pp 1019-1025.
- [4] Hausser, M, "The Hodgkin-Huxley theory of action potential", Nature neuroscience supplement, vol. 3, 2000, pp. 1165.
- [5] Han, I. S, "Mixed-signal neuron-synapse implementation for large scale neural networks", *Journal of Neurocomputing*, pp. 1860-1867, 2006.
- [6] Han, W. J and Han, I. S, Bio-Inspired Visual Signal Processing based on Neuromorphic Circuit, in *Proc. WSEAS(IMCAS'10)*, (Hangzhou, 2010), pp. 131-136.

TYPICAL PEDESTRIAN ACCIDENT SCENARIOS FOR THE TESTING OF AUTONOMOUS EMERGENCY BRAKING SYSTEMS

James Lenard

Russell Danton

Loughborough University

UK

Matthew Avery

Alix Weekes

Thatcham

UK

David Zuby

Insurance Institute for Highway Safety

USA

Matthias Kühn

German Insurers Accident Research

Germany

Paper Number 11-0196

ABSTRACT

The research objective of this work was to describe typical accident scenarios for pedestrian accidents.

The accident analysis forms a component of work by the AEB Test Group which aims to develop test procedures for assessing Autonomous Emergency Braking (AEB) systems. This technology is penetrating the vehicle market and is designed to offer protection against the occurrence and severity of collisions; however there is a need to evaluate the systems and their effectiveness since they are not yet subject to regulation or standardised assessment.

Case files for 175 pedestrians who were struck by the front of a passenger car were extracted from an in-depth accident database and reviewed in detail to establish the position and movement of road users before impact. A dataset of key parameters was formed from the detailed case reviews and subjected to a hierarchical cluster analysis to identify groups of similar accident scenarios. A second cluster analysis was performed on a dataset derived from the British national accident database for over 10,500 accidents where a pedestrian was struck by the front of a passenger car. This led to a second set of typical accident circumstances based on a comprehensive coverage of the accident population.

The national accident database for Great Britain, STATS 19, is compiled annually from police reports and effectively defines the national road accident population. In 2008 it registered over 28,000 pedestrian casualties from a total of around 230,000 road user casualties. The UK On-the-Spot (OTS) in-depth accident database was compiled by

research teams at the scene of accidents in two regions of England from 2000 to 2010, including some non-injury accidents. Each team attended approximately 250 accidents per year, resulting in a total of over 4,700 accidents involving over 11,000 road users (including 288 pedestrians). This study was designed to collect a representative sample of accidents.

The cluster analyses show the association of accident circumstances such as speed limit, light conditions, weather, vehicle manoeuvre, pedestrian size, pedestrian movement, obstruction of line of sight, vehicle travel speed and change of speed to impact. The proportion of fatal, serious and slight casualties associated with these scenarios is quantified, showing for example that one scenario covered 12% of the population but 23% of fatal casualties.

Typical circumstances for pedestrian accidents in the dataset include (1) crossing from the kerb side without obstruction of the driver's line of sight, (2) smaller pedestrians crossing from the kerb side with at least partial obstruction of the driver's line of sight and (3) adult pedestrians crossing in inclement light and weather conditions. These scenarios were computed mathematically from large in-depth and national accident databases using cluster analysis and provide relevant information for the formulation of controlled tests of AEB systems.

INTRODUCTION

Autonomous Emergency Braking is one of a number of modern safety technologies designed to prevent or mitigate the severity of vehicle impacts. There is scope for considerable variation among

AEB systems depending on the type of sensors fitted, the decision logic programmed into the control units, how and when the driver is alerted, how and when braking is activated and other factors. For this reason there is interest in developing and conducting physical tests to assess performance, compare systems and inform consumers.

The AEB Test Group is formed from insurance-based research centres around the world with a common interest in assessing AEB systems for their effectiveness in mitigating and preventing collisions. The members include Thatcham, the Insurance Institute for Highway Safety (IIHS), the German Insurers Accident Research (UDV) and Folksam. The Group is involved with assessing the effectiveness of these systems in real accidents, but since they show potential benefit of collision mitigation the group is authoring test procedures to assess the effectiveness of the systems. It is important to assess these systems since there is not yet any regulation or other consumer assessment that might influence the development of the AEB systems. The consumer rating of the systems will help to inform consumers of the most effective systems and help to drive design and development of systems that are best suited to addressing real-world collisions.

AEB systems can already work in collisions involving pedestrians and rear impacts and in the future will be able to address frontal, head-on collisions. However since the head-on systems are not yet widely fitted, this type of collision is not currently being considered by the AEB Test Group, but will be incorporated at a later date.

The setting of test conditions involves many considerations, one of which is the desirability of subjecting the vehicles to realistic accident conditions, i.e. circumstances that are encountered in real accidents, or at least to understand clearly how proposed test conditions relate to the circumstances of real accidents. The aim of this paper is to describe typical accident scenarios for pedestrian accidents based on empirical data. Some examples are given of possible test scenarios that could be based on this factual information.

MATERIALS AND METHODS

Source databases

Two major sources of information about accidents in Britain were used in this work: the national accident database STATS 19 and the in-depth On-the-Spot study (OTS). STATS 19 is compiled annually by the Department for Transport (DfT) based primarily on police reports and it effectively

defines the road casualty population of Great Britain. OTS was a study run from 2000 to 2010 for the DfT and Highways Agency to collect in-depth information about a representative sample of road accidents based on approximately 500 at-scene investigations per year. Some key facts about these databases are presented in Table 1 and both are described more fully in the literature [1] [2] [3]. The analysis in this paper used STATS 19 for 2008 and OTS from 2000 to mid-2009, the latest versions available when work commenced.

A note on the relationship between the STATS 19 and OTS databases. While STATS 19 describes the whole reported road accident population for a year, the in-depth accident database OTS contains a sample of cases from two regions but over a greater period of time, 2000–2010. In addition, unlike STATS 19, OTS includes a proportion of non-injury accidents. There should consequently be some coverage of the same accidents, i.e. roughly one-third of the casualty accidents that occurred in the two OTS sample regions in 2008; however this overlap constitutes a distinct minority of both databases. Furthermore, as an in-depth database, OTS contains more information about accidents than STATS 19, especially quantitative information about velocity, location, injuries and causal factors based on accident investigation, reconstruction and follow-up data collection.

Table 1.
Source databases STATS 19 and OTS

STATS 19	OTS
<i>Period</i> 2008	2000–2010
<i>Sample region</i> Great Britain	South Nottinghamshire Thames Valley
<i>Purpose</i> National statistics	Detailed information to support casualty reduction programmes
<i>Source</i> Police reports	At-scene investigations by research teams at Loughborough University and TRL
<i>Inclusion criteria</i> Casualty on public road	Police attendance on rotating 8-hour shift
<i>Number of accidents</i> 170,591	4,744

The summary datasets prepared for the clusters analyses (described below) contain a selection of the most suitable fields available in each dataset. This resulted, for example, in taking vehicle speed from OTS but speed limit, the best available proxy,

from STATS 19. The datasets derived from STATS 19 and OTS therefore contain only a partial overlap in (a) the variables used to describe the accidents and (b) the accidents covered. The two sources of information can accordingly be regarded as largely independent, the main link being that OTS was designed to be representative of the accident population as far as possible within the scope of the study.

The fields selected for detailed analysis were chosen in the context of their relevance to test conditions and the design of AEB technology. So for example an AEB system will be engineered to optimise its field of view, processing (recognition) speed and decision logic against the pre-impact location, speed, trajectory and size of pedestrians encountered in real accidents. Detrimental ambient light and weather conditions could diminish the effectiveness of certain sensors. It is highly relevant whether vehicles are typically turning or proceeding straight ahead in their approach to the point of impact and whether the line of sight from the vehicle to the struck pedestrian is fully or partially obscured by other vehicles or roadside objects in the seconds before impact. Information on the frequency and extent of braking before impact is relevant to the choice and effectiveness of a system that is fully automated or that reinforces avoidance actions initiated by the driver.

Summary datasets

The fields used for the STATS 19 and OTS cluster analyses are shown in Table 2 and Table 3. The fields derived from STATS 19 are mostly simplified versions of the originals obtained by aggregating and thereby reducing the number of categories, the exceptions being ‘pedestrian injury severity’ which is unchanged and ‘pedestrian age-sex’ which combines the original age and sex fields into a quasi-size category. The fields derived from OTS were recorded by an analyst after a review of full case materials.

The categorisation of each field as nominal, ordinal or scale is relevant to the operation of the cluster analysis algorithm. The basic concept is that scale variables are continuous parameters measured in units such as seconds or metres, ordinal variables provide categories with a natural order such as injury severity or speed limit, and nominal variables provide categories without a natural order such as vehicle type or precipitation.

Table 2.
Variables in STATS 19 cluster analysis

	Field	Type
1	Pedestrian injury severity	Ordinal
2	Speed limit	Ordinal
3	Light conditions	Nominal
4	Precipitation	Nominal
5	Vehicle manoeuvre	Nominal
6	Pedestrian age-sex	Ordinal
7	Pedestrian movement	Nominal
8	Pedestrian masked by vehicle	Nominal

As mentioned above, the choice of fields in the summary datasets was guided by their relevance for physical testing. While items such as light conditions, precipitation, vehicle speed and pedestrian crossing direction were included, other items such as the age and sex of the driver or the time of day of the accident were not, even though there could well be patterns in how these factors correlate in real accidents with other characteristics, for example it could be that female drivers experience a higher exposure to pedestrian accidents involving children in the morning and afternoon ‘school runs’. The underlying reasoning was that driver characteristics and time of day would not be reflected in the setup of physical tests of AEB performance.

Table 3.
Variables in OTS cluster analysis

	Field	Type
1	Pedestrian injury severity	Ordinal
2	Light conditions	Nominal
3	Precipitation	Nominal
4	Vehicle manoeuvre	Nominal
5	Pedestrian age-sex	Ordinal
6	Pedestrian movement	Nominal
7	Pedestrian speed	Ordinal
8	Line of sight obscured (1 sec)	Nominal
9	Vehicle speed	Scale
10	Change of speed to impact	Scale

Cluster analysis

The method employed in this analysis to move the from accident data to the formulation of accident scenarios was a data mining technique known as cluster analysis, in particular the hierarchical, ascending (agglomerative) variety. This works by progressively grouping together the most similar records of a dataset, where the notion of similarity is defined mathematically. As applied here, each record describes an accident and so the cluster analysis identifies groups of similar accidents. These groups or clusters have (by definition) common characteristics and can be interpreted as constituting accident scenarios. The foremost

advantage of applying this method is that the results are objective and reproducible, with an additional benefit that the representativeness of the resultant accident scenarios is clearly defined.

The algorithm for computing the similarity or, on the analogy of points in space, ‘distance’ between clusters of accidents requires specification at three levels:

- at field level, the algorithm was set to compute a distance or (dis)similarity in the range 0–1 for any two values of a field with 0 signifying identity and 1 signifying maximum difference
- at record level, the distance between two accidents was defined as the sum of the distances between the fields—the *city block* or *Manhattan* distance
- at cluster level, the distance between two clusters was defined as the average of the distances between each pair of records in the groups—the *average linkage method*.

Table 4.
Illustration of the assignment of numeric values for quantifying similarity

Field	Type	Numeric value	Field value
Vehicle manoeuvre	Nominal	1	Ahead
		2	Turning
		3	Other
Age-sex	Ordinal	0.00	0–7 years
		0.33	8–15 years
		0.67	Adult female
		1.00	Adult male
Vehicle speed (km/h)	Scale	0.0	40 (min.)
		0.2	50
		0.8	80
		1.0	90 (max.)

For nominal fields, the distance or dissimilarity between two values is always either 0 or 1, depending whether the characteristic is the same or different for two accidents. Making reference to Table 4, if in two accidents the vehicles are both ‘Turning’, the distance is 0; if one is ‘Going ahead’ and the other ‘Other’, the distance is 1. For ordinal and scale values, the range is set to span 0–1 in equal increments for ordinal variables or continuously for scale variables. Accordingly the distance between an adult female and an adult male is 0.33 (1.00-0.67) and the distance between 50 and 80 km/h would be 0.6 (0.8-0.2) assuming minimum and maximum speeds in the dataset of 40 and 90 km/h respectively.

It remains to state briefly how the number of clusters for each analysis was determined. The hierarchical cluster analysis begins with one cluster for each record and iterates through a grouping

procedure until it ends with one cluster for the whole dataset. No particular set of clusters is right or wrong: each is a valid representation of the data. The question is rather the usefulness of a set of clusters for a particular purpose. Clearly neither extreme—one for each record or one for the whole population—adds value. For the purpose of contributing to the design of testing procedures, it was considered relevant to have a relatively small number of clusters that covers much of the population. To this end supplementary programming code was written to assist in the identification of around six clusters to contain about 75–80% of the population, including the fatal and seriously injured sub-populations. In conjunction with further code to identify ‘natural’ gaps between the clusters, the final number of clusters for each accident type and source database was chosen manually after examination of the data.

The technical specifications of the algorithm underlying the cluster analysis were selected from a range of standard methods. Further details are available in the literature [4] [5]. This style of analysis has been applied to accident data before [6] but not, to the authors’ knowledge, to STATS 19, OTS or another major British accident database. The details provided above are intended to suffice in principle for the clusters to be independently derived starting from the same datasets using any software. The order of cases in the input dataset should make no difference.

RESULTS

National accident database STATS 19

The casualty file for STATS 19 (2008) contains information on 230,905 road users, among whom were 28,482 pedestrians. There is provision to nominate a vehicle with which each pedestrian interacted. These constitute the pool of cases from which the pedestrian accidents were drawn. The primary criteria for the selection of pedestrian accidents from STATS 19 were:

- cars, including taxis and private hire cars, associated with a pedestrian casualty
- first point of impact of the front surface.

There were 13,257 vehicles that met these criteria (Table 5). A second filter was made (a) of vehicles that were parked or reversing and (b) of records with missing or unknown information in any field. This resulted in a drop in the number of cases from 13,257 to 10,574, the main contributor being unknown pedestrian movement (2,263).

Table 5.
Vehicle type and first point of contact for pedestrian accidents (STATS 19)

	First point of contact		Total
	Front	Other	
Car	13257	9857	23114
Other	2833	2535	5368
Total	16090	12392	28482

Table 6 shows the distribution of maximum pedestrian injury severity for the cases with complete and partially incomplete information, providing a check on the number of fatally or seriously injured casualties excluded at this stage. The proportions are reasonably evenly distributed among the fatal, serious and slight categories and, as a practical matter, 13,257 was slightly beyond the technical capacity of the hardware and software to process in a standard manner. The cluster analysis of STATS 19 was therefore performed on the basis of 10,574 vehicles.

Table 6.
Availability of information for pedestrian accidents of interest (STATS 19)

	Complete	Partially incomplete	Total
Fatal	240	79	319
Serious	2463	559	3022
Slight	7871	2045	9916
Total	10574	2683	13257

The outcome of the cluster analysis is shown in Table 8 at a level where the accident population was partitioned into 23 groups. The characteristics of the largest six clusters which comprise 85% of the population are shown in detail. Cells printed in bold font indicate (a) that the distribution of numbers for the given field is significantly different from the distribution in the total population (chi-squared test to 99.5% significance) and (b) that the particular numbers highlighted are over-represented. To take an example, all cases in Cluster 1 occurred in daylight compared to a distribution of 67% daylight and 33% darkness in the overall population of 10,574. The probability that this would happen by chance is less than 0.5% and the value of 100% is over-represented.

The figures on cluster representativeness in Table 7 express the numbers for pedestrian injury severity in Table 8 as row percentages. This is useful in highlighting for example that Cluster 3, which comprises 12% of the overall population, contains 23% of the pedestrian fatalities. It can therefore be construed as a particularly dangerous scenario.

Table 7.
Cluster representativeness by pedestrian injury severity (STATS 19): N=10,574 vehicles

	Cluster %							Total
	1	2	3	4	5	6	7-23	
Slight	41	15	11	8	7	3	16	100
Serious	35	14	15	13	5	4	15	100
Fatal	24	4	23	19	3	14	14	100
Total	39	14	12	9	6	3	15	100

Table 8.
Pedestrian accident clusters derived from national data (STATS 19): N=10,574 vehicles

	Cluster %							Total
	1	2	3	4	5	6	7-23	
Pedestrian injury severity								
Slight	78	77	68	63	81	60	76	74
Serious	21	22	28	32	17	30	22	23
Fatal	1	1	4	5	1	9	2	2
Speed limit (mph)								
10-30	92	97	90	90	97	71	92	92
40-50	5	3	8	7	2	8	4	5
60-70	3	0	2	3	1	21	4	3
Light conditions								
Light	100	100	0	0	98	0	46	67
Dark	0	0	100	100	2	100	54	33
Precipitation								
No	96	100	71	73	100	79	42	83
Yes	4	0	29	27	0	21	58	17
Vehicle manoeuvre								
Ahead	100	100	100	100	0	98	62	88
Turning	0	0	0	0	100	2	38	12
Pedestrian age-sex								
0-7 yrs	11	23	2	3	5	1	7	10
8-15 yrs	34	42	18	16	11	9	26	28
Female	26	16	26	27	46	20	33	27
Male	28	18	53	55	38	71	34	35
Pedestrian crossing from...								
Left	59	57	100	0	63	0	59	57
Right	33	40	0	100	31	0	37	36
Other	7	2	0	0	6	100	4	7
Masked by vehicle								
No	100	0	100	100	100	100	54	79
Yes	0	100	0	0	0	0	46	21
Total	100	100	100	100	100	100	100	100

The highlighting of cells in bold font assists in four ways to interpret the clusters. Firstly, where all of the cases fall into a single category, the cluster can be thought of as "purely" something. For example in Cluster 1 all of the accidents occurred in daylight, all vehicles were going ahead and no pedestrians were masked by a vehicle. As a starting point in building up the concept of a scenario based on this cluster, these characteristics are unambiguous. Secondly, where a category or associated group of categories is over-represented

and constitutes a majority of the cases, it also lends its character to the cluster. In Cluster 2 the vast majority of accidents occurred in a 10–30 mph speed zone where the pedestrian was either crossing from the left or from the right. Thirdly, where a category or associated group of categories is over-represented but constitutes a minority of the cases, this can be thought of as a tendency. In Cluster 6, serious and fatal casualties are significantly over-represented along with the higher speed limits 40–50 and 60–70 mph. Finally, where no cell is marked in bold, the column of numbers for a given characteristic is not significantly different from the overall population. This can be seen in the speed limit zones of Cluster 4.

Table 8 defines the accident scenarios precisely and succinctly and it would not necessarily be informative to re-express them in words. A few ‘higher level’ observations may however be of interest. The two largest clusters, 1 and 2, mostly amplify the dominant characteristics of the overall population (slight injury, 10–30 mph, daylight, fine, going ahead and pedestrian crossing) with two exceptions, (a) an over-representation of children and (b) in cluster 2, the pedestrian being masked (obscured) by a vehicle. Clusters 3 and 4, on the other hand, are weighted towards serious and fatal injury, occur in darkness with a tendency towards wet weather and adult males who are not masked, the really substantial difference between these two clusters being that the pedestrian was crossing from the left in one case and from the right in the other. Cluster 5 introduces a turning scenario at low speeds and low injury outcomes, mostly matching the dominant features of the overall population except for an over-representation of adults. Apart from the higher severity levels and speed zones in Cluster 6 already mentioned, it is worth noting that this group of accidents occurred in darkness with mostly men who were stationary in or moving along the carriageway, this being the meaning of the “Other” category. This is the only major cluster not dominated by pedestrian movement across the carriageway.

In-depth accident database OTS

The On-the-Spot study had compiled records on 7,665 vehicles at the commencement of work for this analysis, among which were 216 passenger cars that struck (219) pedestrians. After filtering out non-frontal impacts and cases where inadequate information from the scene of the accident was available to support a quantitative assessment of the movement of the pedestrian and striking vehicle before impact, 175 were subjected to a detailed case-by-case review.

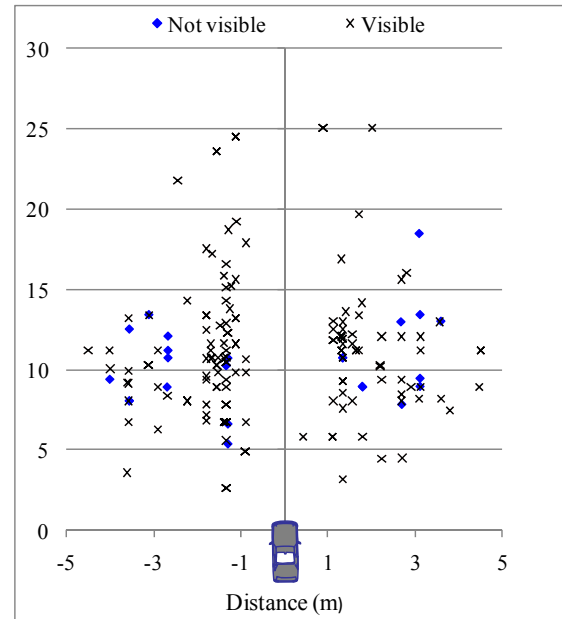


Figure 1. Vehicle travel speed for clusters 1–6 (OTS): N=175 vehicles

A focus of these reviews and reconstructions was the speed, direction of movement and distance apart of the road users and the presence or absence of a clear line of sight between the driver and pedestrian for up to five seconds before impact using established protocols where possible [7]. This is illustrated in Figure 1 which shows the location of the pedestrian relative to the striking vehicle one second before impact and whether there was a clear line of sight between the driver and pedestrian at this time. This parameter was not explicitly included in the cluster analysis because it is highly correlated with two items that were included: vehicle travel speed and change of speed to impact (braking). Including it would have provided double weight to essentially the same information.

The results of the cluster analysis of the OTS dataset are detailed at the level of 14 clusters. The largest six of these contain 79% of the population of the dataset (Table 9). The cells printed in bold font in Table 10 indicate (a) that the distribution of numbers for the given field is significantly different from the distribution in the whole population (chi-squared test to 95% significance) and (b) that the particular value highlighted is over-represented. This is similar to the treatment of STATS 19 above except that the statistical test is evaluated at 95% confidence instead of 99.5%. This level is better suited to the lower number of cases in OTS for providing an objective guide to differences between the clusters and the overall population.

Table 9.
Cluster representativeness by pedestrian injury severity (OTS): N=175 vehicles

	Cluster %							Total
	1	2	3	4	5	6	7-14	
Slight	29	20	12	9	8	0	23	100
Serious	30	9	15	24	4	0	19	100
Fatal	20	0	40	10	0	20	10	100
Total	29	15	14	14	6	1	21	100

Table 10.
Pedestrian accident clusters derived from in-depth data (OTS): N=175 vehicles

	Cluster %							Total
	1	2	3	4	5	6	7-14	
Pedestrian injury severity								
Slight/nil	64	81	52	42	82	0	69	63
Serious	32	19	32	54	18	0	28	31
Fatal	4	0	16	4	0	100	3	6
Light conditions								
Light	100	100	0	0	100	100	56	63
Dark	0	0	100	100	0	0	44	37
Precipitation								
No	90	85	100	38	82	100	61	77
Yes	10	15	0	63	18	0	39	23
Vehicle manoeuvre								
Ahead	100	100	72	100	55	100	69	87
Turning	0	0	28	0	45	0	31	13
Pedestrian (age-sex)								
0-7 years	8	22	4	0	55	50	14	13
8-15 years	24	44	8	4	45	0	42	27
Female	36	11	24	38	0	0	14	23
Male	32	22	64	58	0	50	31	37
Pedestrian movement from...								
Left	58	100	100	29	0	50	39	59
Right	34	0	0	58	100	50	58	37
Other	8	0	0	13	0	0	3	5
Pedestrian speed								
Walking	100	0	96	100	0	0	42	65
Running	0	100	4	0	100	100	58	35
Line of sight obstructed (1 sec)								
No	90	74	100	100	100	100	69	87
Yes	10	26	0	0	0	0	31	13
Vehicle travel speed (km/h)								
Mean	43	35	48	51	37	87	-	44
Change of speed to impact (km/h)								
Mean	-7	-6	-6	-7	-11	-7	-	-7
Total	100	100	100	100	100	100	100	100

Cluster 1, the largest in the set comprising 29% of the population, has accidents in daylight involving vehicles going ahead and pedestrians walking (Table 10). Other majority characteristics are fine weather and an unobstructed line of sight one second before impact. The mean travel speed was 43 km/h with a reduction of 7 km/h before impact. The range of these last two parameters are shown

in Figure 2 and Figure 3. Cluster 2, the second largest, has an over-representation of children running from the left with a tendency to be obscured. This compares interestingly with the corresponding STATS 19 cluster. There are also parallels with the STATS 19 results in clusters 3 and 4, with the tendencies towards serious injury outcomes, darkness, wet weather and adults. Cluster 5 is the closest that a major cluster approaches to a turning scenario, involving children running across from the right side; the mean travel speed is 37 km/h with 11 km/h reduction in speed before impact. This is consistent with the STATS 19 turning scenario which has speed limits and injury outcomes at the lower end of the range. Two of the ten fatalities are in cluster 6 which is too small to support any generalisations, but noteworthy for very high vehicle speeds.

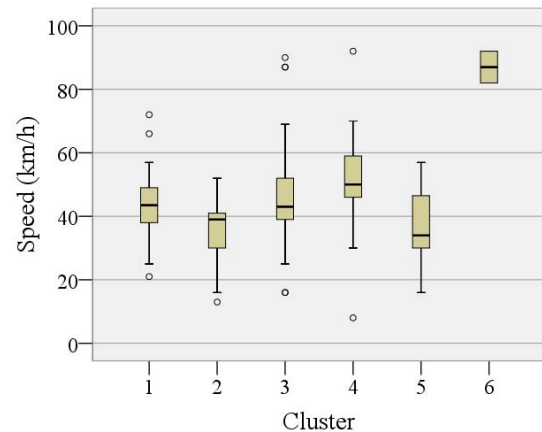


Figure 2. Vehicle travel speed for clusters 1-6 (OTS): N=175 vehicles

Figure 2 and Figure 3 show the median values, interquartile ranges (IQR) and outliers for vehicle travel speed and change of speed to impact using Tukey's hinges and outliers denoted as 'o' for 1.5-3 IQR and '*' for 3+ IQR [8].

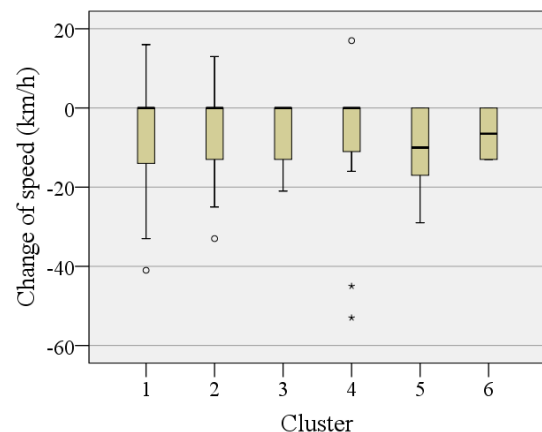


Figure 3. Change of speed to impact for clusters 1-6 (OTS): N=175 vehicles

DISCUSSION

The decisive reason for using cluster analysis to identify groups and associated characteristics in the accident data is that the procedure is objective, reproducible and multivariate. It would not make sense to provide a subjective interpretation of the data to over-ride the key findings presented in Table 8 and Table 10. With this caveat, it is possible to discern some striking parallels between the two sets of clusters.

Firstly the set of characteristics of the largest clusters derived from STATS 19 and OTS mirror the most common features of the accident population, establishing a type of baseline scenario (Table 11).

Table 11.
Baseline scenario

STATS 19 Cluster 1	OTS Cluster 1
<ul style="list-style-type: none"> ● 39% of population ● Daylight ● Fine ● Vehicle going ahead ● 10–30 mph limit ● Pedestrian crossing, especially from left ● Not masked ● Children over-represented minority 	<ul style="list-style-type: none"> ● 29% of population ● Daylight ● Fine ● Vehicle going ahead ● Speed 43 km/h ● Pedestrian crossing, especially from left ● Walking ● Not obstructed

The set of characteristics from the second largest clusters of each dataset differs from the first in having a smaller pedestrian who may be partially or fully obstructed from the line of sight of the driver and (in OTS) is moving faster than walking pace (Table 12).

Table 12.
Smaller pedestrian with obstructed line of sight

STATS 19 Cluster 2	OTS Cluster 2
<ul style="list-style-type: none"> ● 14% of population ● Daylight ● Fine ● Vehicle going ahead ● 10–30 mph limit ● Children over-represented majority ● Pedestrians crossing, especially from left ● Masked by vehicle 	<ul style="list-style-type: none"> ● 15% of population ● Daylight ● Fine ● Vehicle going ahead ● Speed 35 km/h ● Children over-represented majority ● Pedestrian crossing, especially from left ● Running ● Obstructed for over-represented minority

The set of characteristics from the third and fourth largest clusters of each dataset involves darkness and potentially wet conditions, with a large

pedestrian crossing at walking pace from either side of the carriageway without sight obstruction (Table 13).

Table 13.
Larger pedestrian in darkness and some precipitation

STATS 19 Clusters 3–4	OTS Cluster 3–4
<ul style="list-style-type: none"> ● 21% of population (combined) ● Darkness ● Not fine over-represented minority ● Vehicle going ahead ● 10–30 mph limit ● Adult male over-represented majority ● Pedestrian crossing from both directions ● Not masked 	<ul style="list-style-type: none"> ● 28% of population (combined) ● Darkness ● Fine (cluster 3) and not fine (cluster 4) ● Vehicle going ahead ● Speed 48–51 km/h ● Adults ● Pedestrian crossing from both directions ● Walking ● Not obstructed

Having used cluster analysis on the accident data to define a set of pedestrian collision types that have similar features and represent over 75% of the selected cases, it is considered reasonable to use these as relevant scenarios for generation of an AEB testing protocol. In further on-going work, the UK data is being compared to other data sources from different countries to ensure that a global set of pedestrian collisions is represented and initial indications are of a high level of commonality. It is also necessary to ensure that testing procedures are feasible, repeatable and reproducible. The AEB Group is currently considering a number of provisional test conditions which are not, it must be stressed, a final precise list, but are subject to further discussion, definition and finalisation. These are:

- Pedestrian walks from near-side pavement into path of car
- Pedestrian walks from near-side pavement from behind an obstruction into path of car
- Pedestrian runs from far-side pavement into path of car
- Pedestrian walks along near side of carriageway ahead of car
- Pedestrian walks across junction from near-side pavement into path of car turning towards far side into junction.

This data analysis method has also been applied to car-to-car rear and head-on collision types [9]. For each of these collision types, including pedestrian collisions, the AEB Test Group is developing a test scenario along with procedures and targets that will evaluate the effectiveness of the AEB systems for preventing or mitigating these collisions [10].

A restriction on the scope of the results presented in this paper is that they are based on data from a single country. The frequency with which a certain event or combination of factors occurs is naturally dependent on the local road environment, vehicle fleet, driver characteristics and various social and legal factors. At a different level, the formation of clusters is determined in a substantial part by the fields on which accidents are compared. As mentioned above, fields relevant to physical testing were used in this work. If other factors were added or substituted for these, it would not be surprising to see this reflected in the constitution of the clusters. A further consideration relating to the effect of fields is that the number of fields that can be used meaningfully in a cluster analysis is limited by the number of cases. The risk of using too many fields is overfitting of the data with the consequential danger that at least some of the patterns observed would not be maintained with the addition of extra cases. With 175 cases for the OTS analysis and thousands of cases for the STATS 19 analysis, this is a relatively minor concern for the current work. Experience also indicates that the results obtained above are relatively insensitive to fine-tuning of the computational algorithm.

CONCLUSION

The most common scenarios for pedestrian accidents identified in the STATS 19 and OTS databases are described in Table 8 and Table 10. These include a baseline scenario where a pedestrian steps out from the kerb without obstruction of the driver's line of sight; a similar second scenario where the pedestrian is smaller and at least partially obscured; and a third scenario in adverse meteorological conditions with adult pedestrians. The derivation of these situations from the accident data using cluster analysis is objective and mathematically reproducible, also providing a clear definition of the proportion of the accident population represented by the scenarios.

REFERENCES

- [1] Department for Transport. 2009. Reported road casualties Great Britain, Transport Statistics DfT, London.
<http://www.dft.gov.uk/pgr/statistics/datatablespublications/accidents/casualtiesgbar/rrcgb2008>
- [2] Department for Transport. 2004. Instructions for the completion of road accident reports.
<http://www.dft.gov.uk/collisionreporting/Stats/stats20.pdf>
- [3] Cuerden R., M. Pittman, E. Dodson and J. Hill. 2008. The UK On-the-Spot accident data collection study—Phase II report, Road Safety Research Report No. 73, Department for Transport, London.
<http://www.dft.gov.uk/pgr/roadsafety/research/rsrr/theme5/onthespotaccident.pdf>
- [4] Romesburg, H.C. 2004 Cluster analysis for researchers, Lulu Press, North Carolina.
- [5] Martinez, W.L. and A.R. Martinez. 2005. Exploratory data analysis with MATLAB®, Chapman & Hall, London.
- [6] For example: Skyving, M., H-Y. Berg and L. Laflamme. 2009. A pattern analysis of traffic crashes to older drivers, Accident Analysis and Prevention 41, pp. 253–8.
- [7] Erbsmehl, C. 2009. Simulation of real crashes as a method for estimating the potential benefits of advanced safety technologies, ESV, 09-0162.
- [8] SPSS Inc. 2009. PASW® statistics 18 command syntax reference, release 18.0.0, p. 683.
- [9] Lenard, J. and R. Danton. 2010. Accident data study in support of development of autonomous emergency braking test procedures, project reference LUEL 5989/6175, Thatcham Research Centre, England.
- [10] Further details at www.thatcham.org/AEB.

ACKNOWLEDGEMENTS

The funding for this analysis of UK accident data was provided by Thatcham (Motor Insurance Repair Research Centre) and the Insurance Institute for Highway Safety.

The OTS project was funded by the Department for Transport (DfT) and the Highways Agency. This project was not possible without help and support from many individuals, especially the Chief Constables of Nottinghamshire and Thames Valley Police Forces and their officers. Permission from the DfT to use STATS 19 (2008) for the analysis of pedestrian, rear-end and head-on accidents is also gratefully acknowledged.

The views expressed in this work are those of the authors and do not necessarily reflect the views of the DfT, Highways Agency or any other body. The Department for Transport does not guarantee the accuracy or completeness of information inferred from its data. It cannot accept liability for any loss or damages of any kind resulting from reliance on the information or guidance this document contains.

ASSESSMENT OF ACTIVE AND PASSIVE TECHNICAL MEASURES FOR PEDESTRIAN PROTECTION AT THE VEHICLE FRONT

Michael Hamacher

fka - Forschungsgesellschaft Kraftfahrwesen mbH Aachen
Germany

Lutz Eckstein

ika - Institut für Kraftfahrzeuge RWTH Aachen University
Germany

Matthias Kühn

Thomas Hummel

German Insurers Accident Research

Germany

Paper Number 11-0057

ABSTRACT

Structural improvements at the vehicle front are state of the art in the field of pedestrian safety today. But due to raising requirements further measures will be needed. The active bonnet for example is the first deployable system that has entered the market. Other passive safety systems, like the windscreen airbag, are part of current research. This applies also to systems of active safety such as autonomous braking. Hereby the collision speed can be reduced or an accident can be even avoided. To assess and compare the safety potential of active and passive pedestrian safety measures on one scale, an assessment procedure has been developed and applied to various measures and vehicle fronts.

An important characteristic of the assessment procedure is its modular design, combining structural characteristics of a vehicle front with accident kinematics and accident research data. Each module can be enhanced or substituted independently. The assessment procedure uses the vehicle model specific Euro NCAP results and adapts the HIC values to the real accident kinematics derived from numerical simulations. Since the kinematics strongly depend on the front design of a car, a categorization has been developed. For each vehicle class respective simulation data is available. Kinematics parameters are the head impact velocity, impact angle and impact probability determined for the particular wrap-around-distance zones of the vehicle front.

The assessment procedure primarily provides an index value which indicates the risk for an AIS3+ head injury due to the primary impact at a collision speed of 40 km/h. It is calculated for children and adults by an injury risk curve. In addition the dependency of this index value from the collision speed is determined based on corresponding simulation data. Beside the head loading also the

leg loading is assessed. This is carried out by a simplified index calculation. The secondary impact is evaluated qualitatively.

The assessment procedure brings the evaluation of active and passive safety together. Index values have been calculated for good as well as poor rated vehicles within Euro NCAP and under consideration of varying additional safety systems. It could be shown that the benefit of today's measures applied to the vehicle front is limited. Legal test requirements and consumer ratings insufficiently reflect the vehicle-class-specific relevance of particular front areas. Simulation data points out the A-pillars and the lower windscreen area, which need to be addressed by technical measures. Furthermore there is no "one fits all" measure which performs on the same positive level at all vehicle fronts and for all pedestrian sizes. Therefore measures have to be selected and adjusted for each car front. A windscreen airbag is able to improve adult pedestrian safety significantly. Children however profit more by emergency brake systems with pedestrian detection due to the limited safety potential of an active bonnet. Consequently, future cars should offer both adequate passive pedestrian protection and additional active safety systems. The benefit of relevant passive safety systems as well as reductions in collision speed has been demonstrated by Polar-II dummy tests with an experimental vehicle.

INTRODUCTION

Due to increasing requirements on the part of European legislation as well as consumer ratings pedestrian protection measures have become more important over the past years. Structural improvements at the vehicle front are state of the art in the field of pedestrian safety today. But further measures will be needed. The active bonnet for example is the first deployable system that has entered the market. Other passive safety systems, like the windscreen airbag, are part of current

research. This applies also to systems of active safety such as autonomous braking. Hereby the collision speed can be reduced or an accident can be even avoided. To assess and compare the safety potential of active and passive pedestrian safety measures on one scale, an assessment procedure has been developed within a joint research project of fka and the German Insurers Accident Research.

ASSESSMENT PROCEDURE

An important characteristic of the assessment procedure is its modular design. The particular modules will be presented by means of the experimental vehicle used for the final Polar-II dummy tests.

Modules

The assessment procedure is divided into six modules. Within the first three modules all vehicle characteristics required for the assessment are determined (Table 1).

Table 1.
Modules of the assessment procedure

1	Measurement and classification into vehicle class	Vehicle characteristics
2	Simulation and accident kinematics	
3	Structural properties and safety systems	
4	Weighting and adaptation of structural properties	Assessment
5	Index calculation	
6	Qualitative assessment of secondary impact	

The first module is based upon a categorization, which has been developed to consider the different front designs of modern cars and their impact on pedestrian accident kinematics.

Measurement and classification into vehicle class The categorisation comprises six vehicle classes. For each class a representative front has been defined. Figure 1 shows the front contours of those class representatives. Three geometrical parameters are used for the classification of a new car model. The first one is the height of the bonnet leading edge, which has significant influence on the accident kinematics of a pedestrian. The wrap around distance (WAD) up to the bonnet rear edge is relevant for the location of the head impact relative to the vehicle front. The lower the values for this parameter, the higher is the probability for a head impact in the windscreen area. The third characteristic parameter is the bonnet angle, which has an effect on the throw-up distances.

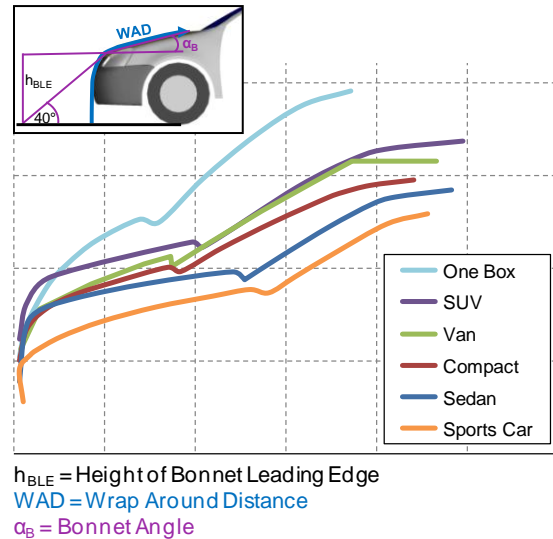


Figure 1. Classification into vehicle class.

Since the utilisation of Euro NCAP results is an essential part of the assessment procedure, the vehicle zoning is orientated towards the Euro NCAP grid. For the representation of the relevant impact areas an expansion as well as a finer raster of the grid in longitudinal direction is necessary. Hence, the four Euro NCAP test zones are subdivided and expanded by two more zones. Each zone offers twelve fields. Figure 2 illustrates the defined segmentation using the example of the experimental vehicle, which belongs to the class Sedan.

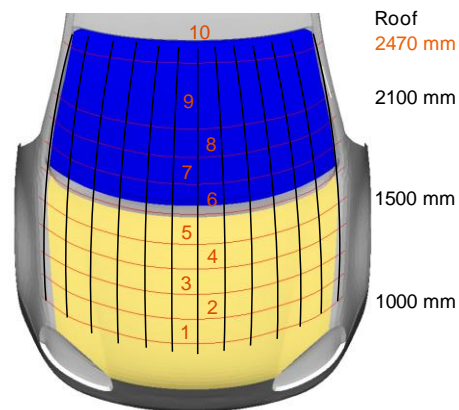


Figure 2. Vehicle segmentation.

The following module assigns values for different kinematics parameters to each of the ten WAD-zones.

Simulation and accident kinematics The kinematics parameters used within the assessment procedure are the head impact velocity, impact angle and impact probability. The kinematics is determined by simulations with the MADYMO multi-body solver. The simulated scenario is based

on accident research data and describes a pedestrian crossing in front of a vehicle. The collision speed for the assessment of passive safety measures is 40 km/h. For the assessment of active safety systems additional simulations with reduced collision speeds (20, 30, 35 km/h) are necessary. The consideration of four pedestrian models, three impact positions and two walking postures leads to the simulation matrix described by Table 2.

Table 2.
Simulation matrix

4 collision speeds	40, 35, 30 and 20 km/h
4 pedestrian models	6 year old child, 5 %-female, 50 % & 95 %-male
3 impact positions	Centred, staggered, edge
2 walking postures	Leg facing the vehicle is backwards and forwards respectively
4 x 4 x 3 x 2	96 simulations per vehicle

For the assessment of additional passive safety systems (module 3), like a pop-up bonnet, additional simulations with a collision speed of 40 km/h have to be performed ($1 \times 4 \times 3 \times 2 = 24$). Figure 3 visualises the head impact for the 50 %-male in central position and at a collision speed of 40 km/h.

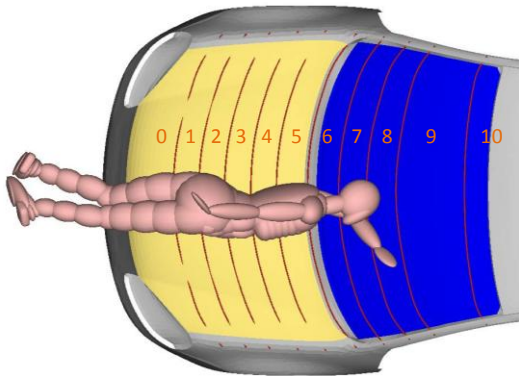


Figure 3. Multi-body simulation.

The interpretation of the simulation data is carried out separately for every velocity and related to the pedestrian models. For each model the area of head impact as well as the highest head impact velocity and angle occurred in the simulations are determined. The head impact area of a model is described by its minimal and maximal WAD for the head impact locations. This interval is used to calculate the throw-up factor f_a , which is a measurement for the throw-up distances achieved by the particular pedestrian height. The values identified for each pedestrian model are used as supporting points for the description of the vehicle-specific accident kinematics.

With the help of a best-fit curve a functional correlation between throw-up factor and body height can be derived, which allows a complete description of the throw-up behaviour. This is the first step towards WAD-zone-related impact probabilities. A second step combines the throw-up behaviour with a pedestrian size distribution. Since the assessment is carried out for children and adults, two separate size distributions have been defined. The outcome of this procedure is shown in Figure 4. Here the WAD-distribution regarding the head impact is given for adults. It is apparent that the WAD-zones 7 and 8, i.e. the lower windscreen area, possess the highest relevance in this regard. The impact locations of the children are more evenly distributed. Relevant are the WAD-zones 2 to 5, all lying on the bonnet.

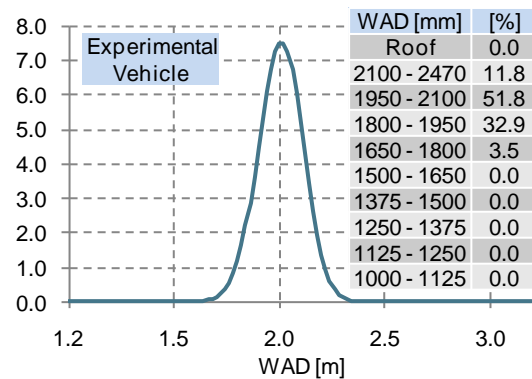


Figure 4. Relevance of the WAD-zones (adults).

After assigning impact probabilities to each WAD-zone, the throw-up behaviour is used for the specification of impact velocities and angles. Therefore the discrete heights of the pedestrian models are transferred into WAD-values. Through linear interpolation between the corresponding velocities and angles respectively, both kinematics parameters can be determined for every WAD. Figure 5 illustrates the correlation between head impact velocity and throw-up distance for a collision speed of 40 km/h.

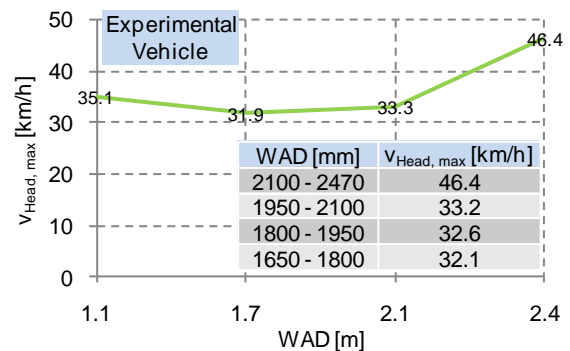


Figure 5. Correlation between maximal head impact velocity and throw-up distance.

In the upper windscreen area the values lie above the collision speed. Therefore the head impact velocities in the relevant WAD-zones of the adults range from 32 to 46 km/h (see table in Figure 5) while the children achieve values from 32 to 35 km/h. To obtain the maximal head impact angels for the particular WAD-zones the procedure has to be carried out analogue.

For every vehicle class representative (Figure 1) generic 3D simulation models have been generated. Those models provide vehicle-class-specific kinematics data. Since this data is available for all of the six class representatives, it is not mandatory to perform and analyse additional simulations. The class-specific kinematics parameters are implemented into the index calculation. They are assigned through the classification of a new car model into the corresponding vehicle class. Alternatively, vehicle-model-specific kinematics data can be used for the application of the assessment procedure, as it has been done in case of the experimental vehicle.

After transferring the accident kinematics parameters to every WAD-zone, the structural properties of the vehicle front have to be devolved.

Structural properties and safety systems The structural properties are described by the Head Injury Criterion (HIC). These data is taken from the respective Euro NCAP spreadsheet of the car to be assessed. Rules have been defined for a reasonable assignment of the HIC-values to the particular fields of the vehicle segmentation. Since the Euro NCAP test zones have been subdivided the respective WAD-zones receive the same HIC-values, however possess different impact probabilities (Figure 6). When an additional passive safety system like a windscreen airbag is implemented, the structural properties have to be adapted within the protected area. In case of the windscreen airbag, the HIC-values of all fields fully covered by the airbag are reduced to a general value of 500, an advanced airbag design assumed. The performed Polar-II dummy test with a prototype airbag confirms the specified HIC-value.

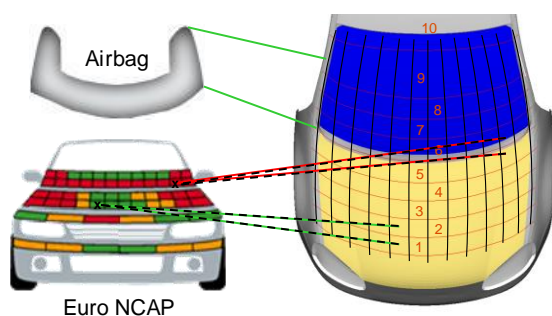


Figure 6. Assignment of structural properties.

In addition to the HIC-values, the results of the legform impactor tests are considered as well for the assessment of a car. Those results can be directly used for the calculation of the leg index (module 5).

Additional passive safety systems usually not only influence the structural properties but also the accident kinematics. This also applies to the adaptive bumper and the active bonnet (pop-up bonnet), which are regarded beside the windscreen airbag. Those systems have been assessed individually and in combination. The consideration of the kinematics influence requires additional simulations with revised models. Figure 7 shows the modified simulation model of the experimental vehicle for a combination of adaptive bumper and active bonnet.

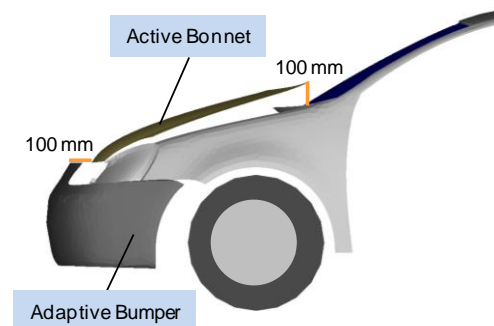


Figure 7. Simulation of adaptive bumper and active bonnet.

The retraction of the bumper happens inertia controlled with an artificially increased bumper weight. The deployment of the bonnet is rigid (locking system). With the help of coupled simulations (multi-body pedestrian models and FE vehicle models) the modelling of additional safety systems could be enhanced. The assessment of the windscreen airbag resorts to the kinematics of the active bonnet.

In contrast to the adaptive bumper, which only affects the values for the leg loading, the active bonnet leads to reduced HIC-values in the corresponding WAD-zones. If the active bonnet is part of the standard equipment of a car (e.g. current BMW 5 series and Mercedes E-class) those values can be taken from the Euro NCAP spreadsheet. Otherwise generic HIC-values have to be used for a simplified assessment. In this case a general value of 700 is defined for the fields lying on the bonnet. Only the lateral and rear boundary areas keep their values. The risk coming from the gap at the bonnet rear edge is addressed by a minimum value of 1500. The implementation of a windscreen airbag minimises the risk due to the rear bonnet gap, so that most of the front is rated “green”.

Weighting and adaptation of structural properties Within the fourth module of the assessment procedure the structural properties are combined with the accident kinematics. For the weighting and adaption of the HIC-values several factors are defined. Those factors are integrated into the calculation formula of the head index (module 5). Each factor represents one of the kinematics parameters evaluated in module 2.

The weighting of the particular vehicle fields with regard to the impact probabilities is carried out by relevance factors. Two relevance factors are defined, one for the lateral and one for the longitudinal direction. Data of the German Insurers Accident Research reveals an approximately equal distribution of the impact locations in lateral direction, so that the associated relevance factor ($R_{j,lateral}$) gets a constant value. The relevance factor in longitudinal direction ($R_{i,WAD}$) represents the impact probabilities of the particular WAD-zones at a specific collision speed.

The Euro NCAP tests are performed with definite boundary conditions, i.e. constant values for impactor velocity and angle [1]. The velocity factor ($V_{i,j}$) adapts the standardised Euro NCAP head impactor results to the maximal head impact velocities coming from the kinematics analysis. The definition of the velocity factor is based on analytical approaches and simulation results. Figure 8 illustrates the relationship between HIC-value and impact velocity. On the basis of the Euro NCAP result at the regarded test location it enables the determination of correspondent HIC-values for both reduced and increased impact velocities without conducting further tests.

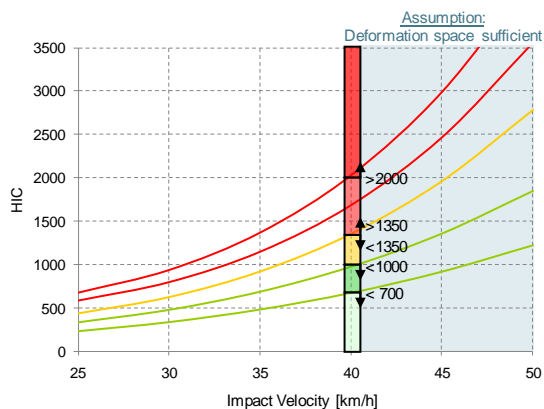


Figure 8. HIC-velocity diagram.

The correlation between head impact velocity and HIC-value is related to the stiffness at the test location. The behaviour for a stiff area with high HIC-values is more dependent on impact velocity than for a flexible area. Although the presented velocity factor definition is primarily validated for

the bonnet, the stiffness based approach behind it in principle allows an application to the windscreen area. Hence, and due to the complex and unpredictable behaviour of the windscreen, no separate definition of the velocity factor is used here.

Finally, the velocity related HIC-values are adapted to the maximal head impact angles of the particular WAD-zones. This is done qualitatively by the angle factor ($W_{i,WAD}$). Criterion is the deviation from the particular Euro NCAP impactor angle. A deviation of more than 10° results in a reduction and increase respectively of the HIC-value by 10 % (Table 3).

Table 3. Definition of angle factor

$W_{i,WAD}$	Maximal head impact angle (α_{max})	
	Child zone (50°)	Adult zone (65°)
0,9	$\alpha_{max} < 40^\circ$	$\alpha_{max} < 55^\circ$
1,0	$40^\circ \leq \alpha_{max} \leq 60^\circ$	$55^\circ \leq \alpha_{max} \leq 75^\circ$
1,1	$\alpha_{max} > 60^\circ$	$\alpha_{max} > 90^\circ$

Simulations with varied impactor angles demonstrate, that the defined adaptation is a conservative estimate. With regard to real accident events this is reasonable, since the free-flying impactors do not represent the biomechanics of the neck and upper body area.

Index calculation The assessment of the primary impact is divided into a head as well as a leg index, with the head index representing the fundamental part of the procedure. While the head index resorts to all of the previously presented modules, the assessment of the leg loading is based on a simplified index calculation that only requires the results of the legform impactor.

The assessment of the head loading is geared to the VERPS-index [2]. In contrast to the VERPS-index the simulation results are not used to define boundary conditions for separate impactor tests but for the described adaptation of existing Euro NCAP results towards the accident kinematics. Furthermore, the vehicle categorisation and segmentation as well as the simulation set-up are different. Commonalities can be found regarding the definition of the relevance factors and the underlying injury risk curve for the head loading.

The injury risk curve shown in Figure 9 assigns a probability for an AIS 3+ (Abbreviated Injury Scale) head injury to each HIC-value, i.e. a severe to fatal injury (AIS 0 = uninjured, AIS 6 = fatally injured). For an exemplary HIC-value of 1000 the risk of a AIS 3+ head injury is stated with 24 %. The appropriate function forms the basis of the

index calculation and enables the assignment of an injury risk to every vehicle field.

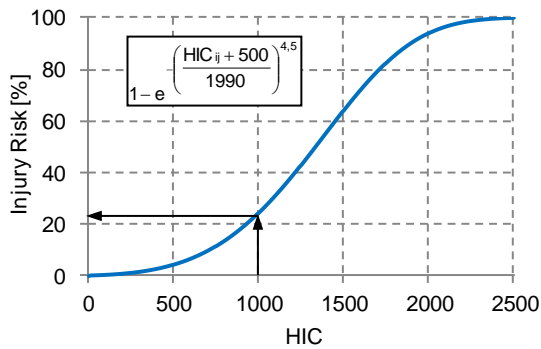


Figure 9. Injury risk curve for a AIS 3+ head injury [3].

The index calculation is based on a totals formula, which sums up the HIC-dependent injury risk of the individual vehicle fields in consideration of their relevance (Equation 1).

$$\sum_{i=1}^{10} R_{i,WAD} \cdot \left(\sum_{j=1}^{12} 1 - e^{-\left(\frac{HIC_{ij} \cdot V_{ij} \cdot W_{i,WAD} + 500}{1990}\right)^{4.5}} \cdot R_{j,lateral} \right) \quad (1).$$

i	Number of WAD-zones in longitudinal direction
R _{i,WAD}	Relevance factor in longitudinal direction, dependent on WAD-zone
j	Number of fields in lateral direction
HIC _{ij}	Euro NCAP HIC-value in particular field of vehicle front
V _{ij}	Velocity factor in particular field of vehicle front
W _{i,WAD}	Angle factor in particular WAD-zone
R _{j,lateral}	Relevance factor in lateral direction, constant = 1/12

The head index reaches values between 0 and 1. It becomes apparent how the data out of the particular modules goes into the index calculation. The definition of the vehicle segmentation is represented by the indices i and j. By means of the relevance factor in longitudinal direction the impact probabilities due to the throw-up behaviour and the pedestrian size distribution are assigned to each of the ten WAD-zones. The velocity and the angle factor are directly integrated into the injury risk function, where they adapt the HIC-value of the individual vehicle fields to the simulated accident kinematics.

The leg index is also based upon an injury risk curve. The leg test zone within Euro NCAP comprises six fields arranged at the bumper in lateral direction [1]. The measured results require no further adaptation due to the initial contact characteristic of the leg impact. For the leg loading three injury parameters are defined by Euro NCAP, tibia acceleration, knee bending angle and knee

shear displacement. For each of these parameters corresponding injury risk curves for the EEVC lower legform impactor are applied on the basis of [4] and [5]. The crucial injury criterion regarding the tibia acceleration is the tibia fracture, while for the knee bending angle and the shear displacement the risk of a collateral ligament damage and cruciate ligament damage respectively is relevant. For the index calculation the injury risk of each parameter is added up over the six leg impact areas, which are weighted equally. For the assessment only the injury parameter with the highest injury risk is considered. In case of the experimental vehicle the tibia acceleration causes the highest value. Here the injury risk for a tibia fracture is 13 % and thus results in a leg index of 0.13 for the experimental vehicle.

Since the legform impactor represents the leg of a 50 %-male the leg index can only be specified for adults. Furthermore, vehicles possessing very high bumpers are not tested with the legform impactor, so that for those vehicles no leg index values can be calculated. In general the approach is also transferable to the Flex-PLI legform, corresponding injury risk curves presupposed.

The whole assessment procedure is processed automatically with the help of a MS Excel-tool. When using vehicle-class-specific kinematics data the only input needed for the calculation of head and leg index are the impactor results stated in the Euro NCAP spreadsheet.

Assessment of active safety systems Within the index calculation module the assessment of active safety systems is regarded separately. Assessment criterion is the reduction in collision speed achieved by the particular system. The approach is based on the conducted simulations with reduced collision speed. For those reduced velocities the corresponding head index values are calculated and act as supporting points for the velocity related index calculation. By interpolation between the respective supporting points an index value can be determined for every speed reduction (Figure 10).

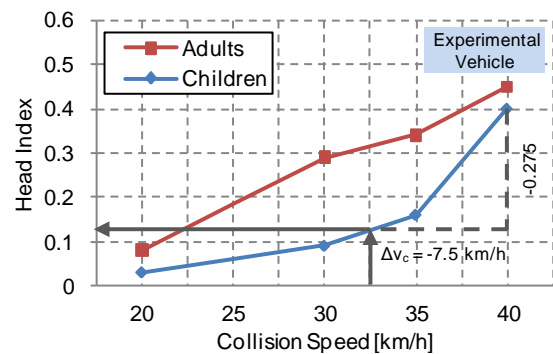


Figure 10. Velocity related index calculation.

The index values given in Figure 10 are calculated for the basic version of the experimental vehicle, i.e. no additional safety systems are implemented. Starting point for the assessment of active safety systems marks the passive safety index at a collision speed of 40 km/h, which amounts to 0.45 for adults and 0.4 for children. The additional supporting points describe the influence of a reduced collision speed on the index value. For children an assumed decrease in velocity of 7.5 km/h leads to an index reduction from 0.4 to 0.125. The children benefit from the homogeneous structural properties of the bonnet area. Here the forward displacement of the head impact locations due to the reduced collision speeds implicates no negative consequences, since the children still impact in the bonnet area. This does not apply to adults. At the initial collision speed of 40 km/h the area of the central windscreen, including the accordant A-pillar sections, is most relevant for the head impact of this pedestrian group (>60 %). Since the central windscreen is rated “green” by Euro NCAP, the resulting passive safety index is moderate. For reduced collision speeds the relevance of the critical cowl area rises due to the forward displacement of the head impact locations coming along. At a collision speed of 30 km/h more than 75 % of the adults impact in the cowl und lower windscreen area. The poor Euro NCAP results within the corresponding WAD-zones counteract the positive effect due to the reduced head impact velocity, so that adults do not benefit in the same manner as children.

The illustrated correlation between collision speed and head index value forms the interface between active and passive safety. For the application of the presented approach to a real system, the average deceleration in relevant accident scenarios has to be known. Such system-specific data can only be determined on the basis of an external test protocol. The underlying boundary conditions should correspond to the general assessment scenario, which describes a pedestrian crossing in front of a vehicle driving with a velocity of 40 km/h. Thereby, the comparability to the assessment of passive safety measures is guaranteed.

However, the general capability of different generic systems can be estimated with the help of an accident analysis and transferred into according head index values. Based on given system specifications speed reductions can be derived for all accident cases conforming to the defined scenario. To demonstrate the potential of autonomous braking, three generic systems are specified. For those systems the percentage of avoidable and unavoidable cases referred to the relevant accident events within the database of the German Insurers Accident Research is identified.

All accidents not avoided by the particular system are classified with respect to the achieved speed reduction. Furthermore, a failure rate is defined by means of the number of cases where the active safety system did not come into action.

For all three generic systems equal braking performances on dry and wet road ($a_{\max, \text{dry}} = 9.5 \text{ m/s}^2$, $a_{\max, \text{wet}} = 7 \text{ m/s}^2$) as well as an autonomous braking are assumed. Differences arise regarding the time of braking prior to the collision (TTC) and the capability of the sensor technology. A driver model is not considered since here only the general methodology for the assessment of active safety systems is to be demonstrated.

The first system defined does not work in rain and snow and brakes 500 ms prior to the collision with the pedestrian. The index calculation for this system is illustrated in Figure 11 using the example of the experimental vehicle. The assessment is exemplary conducted for adults, starting with the index value at 40 km/h (0.45). Each branch of the scheme possesses a probability based on the performed accident analysis. For the accidents mitigated by the system the analysis groups the achieved speed reductions in 5 km/h intervals and assigns corresponding percentages. For the index calculation (see Figure 10) the average speed reduction of each interval is used, which is a simplification. It would also be possible to calculate a separate index value for each individual accident case instead of grouping them. When an accident is avoided by the active safety system, the resulting injury risk of the pedestrian is zero, which leads to an analogous index value. The opposite case occurs when the system fails in a particular accident case. Here the index value is not reduced.

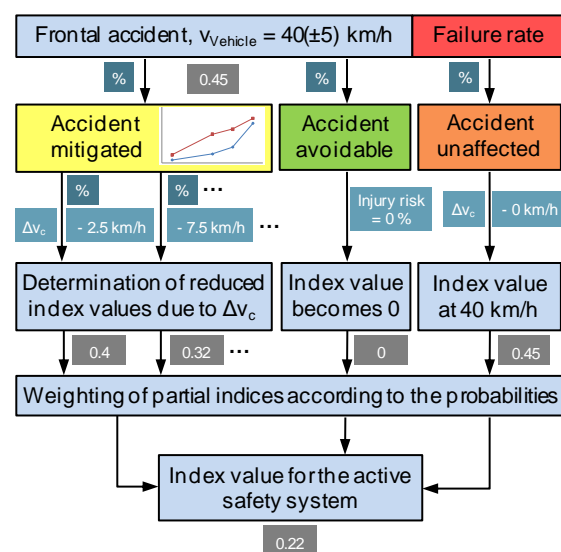


Figure 11. Assessment of an autonomous brake system (system 1, adults, experimental vehicle).

The partial indices are weighted by the assigned probabilities and add up to the total index value for system 1, which is 0.22. Compared to the passive safety index the value is halved.

The second generic system detects pedestrians in rain and snow but does not operate in darkness. The time of braking is equal to system 1. Finally an optimal braking system is defined with no restrictions on sensing and an increased braking initiation time (TTC = 700 ms). The corresponding index results for children and adults will be discussed together with the passive safety values after the presentation of the last assessment module.

Qualitative assessment of secondary impact

For the assessment of the secondary impact additional multi-body simulations have been conducted with each of the generic vehicle class representatives. A validation of the simulation models on the basis of real accident cases has shown, that characteristic parameters like the vehicle-sided contact points as well as the longitudinal and the lateral throwing range of the pedestrian can be reproduced realistically. The throwing range describes the distance between the place of collision and the final position of the pedestrian on the road in longitudinal and lateral direction.

The assessment of the secondary impact is based on three pillars, the general kinematics, the probability of an initial head contact and the contact forces during head impact. Those criteria are transferred into qualitative statements on secondary impact (moderate, critical, very critical).

The assessment of kinematics is conducted with the help of four general scenarios (Table 4), conditional on the different vehicle geometries.

Table 4.
General scenarios

Scenario	Description
1	Pedestrian is thrown forwards after the impact (distinct flight phase)
2	Pedestrian is thrown backwards over the vehicle (high velocities), dropping to the side or backwards
3	Pedestrian is thrown up on the vehicle and slips off the bonnet. (dependent on vehicle deceleration)
4	Pedestrian is immediately thrown on the ground and possibly overrun by the vehicle

Decisive for the kinematics is the ratio of the vehicle sided initial impact point to the centre of gravity height of the pedestrian as well as the

overlap of pedestrian and vehicle due to the height of the bonnet leading edge. The kinematics parameters regarded for assessment of the secondary impact are the vertical and rotatory velocity components as well as the dropping angle of the pedestrian while disengaging from the vehicle. The dropping angle enables a general estimation with respect to the danger of overrun.

For the determination of the head impact probability the simulation results are analysed at the time of the initial contact of the pedestrian with the road. The corresponding snap-shot reveals the position of the pedestrian. Does the head contact the road first, i.e. in advance of the other body parts, the head loading is particularly high. Those cases are referenced to the total number of simulations with the particular vehicle class representative. Thus, the head impact probability can be specified qualitatively with the help of an assessment schema for every generic model.

The head loading due to the impact on the road is considered by the last part of the approach. For this purpose the head contact force recorded by MADYMO is analysed. Criterion forms the maximum value in z-direction, which is averaged over the respective vehicle class.

Table 5 summarises the outcome of the assessment and shows a qualitative comparison of the particular vehicle classes.

Table 5.
Qualitative comparison of the vehicle classes regarding secondary impact

Vehicle Class	Children	Adults
Compact		
Sedan		
Van		
SUV		
One Box		
Sports Car		
 moderate	 critical	 very critical

The vehicle classes SUV and One Box turn out to be particularly critical due to disadvantageous kinematics combined with a high head loading. The classes Compact, Sedan and Sports Car show more favourable kinematics, coming from the distinct throw-up behaviour, which trends to cause a less critical secondary impact. This does not apply in an analogous manner to the class Van. Here the steeper bonnet angle affects the results adversely.

A reduction in collision speed benefits the kinematics within the simulations and leads to a

decrease in altitude and throwing range. At an appropriate speed reduction the pedestrian does not disengage from the vehicle but slips off the bonnet. Overall, the probability of an initial head contact as well as the contact forces during head impact are reduced. Hence, an autonomous brake system also addresses the secondary impact, which increases its safety potential and forms an advantage compared to measures of passive safety.

INDEX RESULTS

The head index values calculated for the experimental vehicle are illustrated in Figure 12. For the sake of clarity, the results of the second generic brake system are omitted. The given correlation between head index and collision speed enables a conversion of the safety potential of passive measures into an equivalent reduction in collision speed.

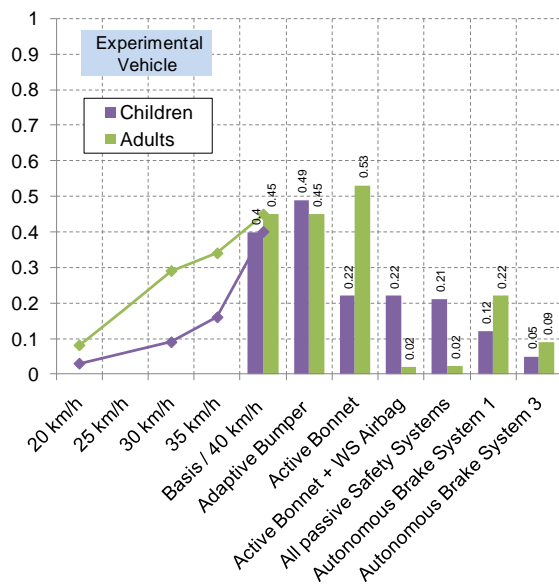


Figure 12. Head index results.

For children the sole implementation of an adaptive bumper has negative consequences for the head loading since it causes increased head impact velocities. This also applies to the active bonnet but due to the reduced HIC-values within the relevant impact area, the index can be almost halved compared to the basic value. As expected, a windscreen airbag offers no additional protection for children. The covered area is not relevant with respect to small pedestrian heights. The index value for the combination of all regarded passive safety systems lies only slightly below, coming from lower head impact angles caused by the adaptive bumper. The highest safety potential for children offer autonomous brake systems. The velocity dependent index progression illustrates, that small velocity reductions already lead to a significant

decrease of injury risk. For the optimal generic braking system the index is eight times lower than the basic value. System 2 adds up to 0.24 and lies slightly above the passive safety level.

For adults the index results show a different behaviour. Due to the good Euro NCAP results of the windscreen area, the resulting safety index of the basic vehicle is comparable to the value of the children. However, the corresponding Polar-II dummy test (see next chapter) reveals, that the HIC-values for the windscreen can be considerably higher in a real-life accident. Against this background, the determined safety potential of a windscreen airbag has to be rated even higher. A windscreen airbag forms the most effective safety measure for adults, while the adaptive bumper as well as the active bonnet offer no benefit for the head loading as long as they are applied separately. The active bonnet even has a negative effect in case that no windscreen airbag is implemented, coming from the forward displacement of the head impact locations. Thereby the relevance of the critical cowl area as well as the gap at the bonnet rear edge increases significantly. At the same time, this behaviour is the reason for the high protective function of the windscreen airbag, which forms an enhancement of the active bonnet. Due to the forward displacement caused by the deployed bonnet the inflated airbag is able to cover most of the relevant impact area. Hence, the adult risk of a severe head injury amounts only to 2 %, which is confirmed by the low HIC-value measured in the corresponding Polar-II dummy test. Autonomous brake systems offer a high safety potential for adults as well. But even the value for the optimal generic braking system does not reach the level of a combination of active bonnet and windscreen airbag. As for the children the index values of the particular braking systems are strongly dependent on the sensor technology. System 2 for example reaches only a value of 0.32.

As already mentioned above, the leg index value for the experimental vehicle adds up to 0.13, representing the injury risk for a tibia fracture. To calculate a leg index value for the adaptive bumper, additional legform impactor tests have to be conducted. Since such tests have not been part of the research project, only an estimated value based on the available Polar-II dummy test results can be given. Here, the measured reduction in tibia acceleration between the basic and adaptive bumper design is 23 %. Applying this percentage decrease to the Euro NCAP legform results of the basic vehicle leads to a leg index of 0.09 for the adaptive bumper. The achieved injury risk mitigation is quite small, since the results of the basis vehicle are already on a low level due to its pedestrian friendly bumper design.

Besides the experimental vehicle further cars out of all classes have been assessed. Index values have been calculated for good as well as poor rated vehicles within Euro NCAP and under consideration of the presented additional safety systems. The assessment is carried out based on the kinematics data of the particular vehicle class representatives. The corresponding index values reflect the differences in passive safety and amplify poor test results in cases where they occur in relevant WAD-zones.

Additionally, the calculated index results enable a direct comparison of the regarded passive and active safety measures. While autonomous braking systems are beneficial for all vehicle classes, passive safety systems have to be selected and adjusted for each individual car front. The application of an active bonnet for example reduces the injury risk for children but can be disadvantageous for adults. With regard to sedan shaped vehicles adults benefit strongly from the additional implementation of a windscreen airbag, whereas it offers only little protection for SUVs. Here the impact locations of both pedestrian groups lie on the bonnet, so that the cowl area is not relevant.

In general the basic index values for children are below those for adults, since children profit from the good passive safety level in the bonnet area nowadays. For adults however the simulation data points out the A-pillars and the lower windscreen area, which need to be addressed by technical measures. Currently legal test requirements and consumer ratings insufficiently reflect the high relevance of those areas.

Autonomous braking systems offer the advantage, that they address both pedestrian groups in a similar manner. For children they show the highest safety potential of all assessed measures due to the limited impact of an active bonnet on the structural properties. This does not apply to a windscreen airbag, which is able to reduce the critical HIC-values in the cowl and lower windscreen area significantly. Apart from the class SUV an autonomous brake system has to possess a high performance as well as reliability to protect adults in the same way than a windscreen airbag does. Active systems generally require an adequate passive safety to be most effective. The more capable an active system is, the less relevant the differences in passive safety of a good and a poor rated car become.

POLAR-II DUMMY TESTS

With the help of the experimental vehicle the effectiveness of the assessed safety systems is

demonstrated in tests with the Polar-II pedestrian dummy from Honda. The selected vehicle represents an average front design with a high relevance in road traffic and it is designed to current pedestrian safety standards.

Experimental Vehicle

The experimental vehicle is equipped with an adaptive bumper, an active bonnet and a windscreen airbag. These systems are implemented in a way, that the basic as well as the modified version of the vehicle can be tested. Figure 13 illustrates the modifications made to the vehicle.

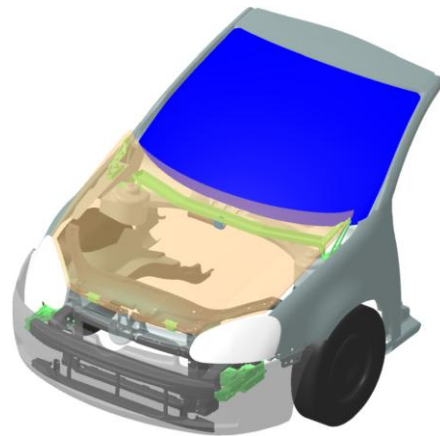


Figure 13. Implementation of safety systems.

The adaptive bumper is realised by linear guides combined with gas springs, which damp the impact of the pedestrian legs. Since both front cross members are moved together with the foam element and the covering, the existing passive pedestrian protection of the basic vehicle is preserved. The bumper is tested in deployed position, i.e. no actuating elements as well as sensor technology are used. As in the simulations its travel distance is 100 mm. Tail hooks fix the bumper after retraction.

Due to the implementation of a windscreen airbag beneath the bonnet rear edge, additional actuating elements for the lifting of the bonnet are not required. The bonnet deployment is carried out by the inflating airbag. Therefore additional hinges are applied in the area of the bonnet leading edge while the series bonnet hinges are modified in a way, that they allow an upward movement of 120 mm.

The windscreen airbag has been designed and implemented in cooperation with Takata. For the integration of the folded airbag an appropriate receptacle is necessary. It is designed as a three-piece tray that follows the curved run of the bonnet leading edge. The airbag receptacle is mounted to the strut towers and additionally fixed in the

middle. This implicates a disassembly of the wiping system. The inflator is installed central at the underside of the airbag receptacle, where an opening is provided. An identical hole pattern of airbag and inflator allows a gastight connection. The U-shaped windscreen airbag reaches at its outer side, i.e. the area of the A-pillars, till a WAD of about 2250 mm. The covering of the middle section goes till a WAD of about 2000 mm. Hence, together with the active bonnet a major part of the Euro NCAP test range is protected.

Tests

Four tests are conducted. At first the basic vehicle is tested with a collision speed of 40 km/h (basic test), corresponding to the general accident scenario used for the assessment of passive safety. This test is repeated with the modified vehicle (system test), demonstrating an optimised passive safety equipment. Finally, the benefit of a reduction in collision speed is exemplified by two additional tests carried out with the basic vehicle at collision speeds of 30 as well as 20 km/h.

Pedestrian dummy The Honda Polar-II dummy has been specially developed for the performance of full-scale tests and is supposed to reproduce the kinematics and loadings of a 50 %-male during a vehicle-pedestrian collision. It is subdivided into eight body regions with own sensing elements. The Polar-II dummy possesses a detailed reproduction of the thorax as well as a complex knee joint. The deformable tibia is designed to have human-like force-deflection characteristics in lateromedial bending up to the point of fracture. [6]

The dummy is positioned centred in walking posture with the head orientated normal to the driving direction of the experimental vehicle. The leg facing the vehicle is backwards and the wrists are tightly bound. The adjustment of the dummy is carried out according to the posture and the joint alignments respectively given in [7]. Hence, a consistent and repeatable test setup is guaranteed. The dummy is connected via a belt with a release mechanism, which is activated by running over a trigger. This happens ca. 50 ms prior to the impact, so that the dummy is free-standing at contact with the vehicle. After the primary head impact a full braking of the vehicle is initiated, corresponding to the recommendation in [7]. Conclusions regarding secondary impact cannot be drawn since the dummy is caught by a net, which is mounted 12 m behind its initial position.

Test evaluation At first the results of the basic and the system test are compared to illustrate the improvement of passive safety. The extended bumper of the modified vehicle causes a time offset

regarding the hip impact, which is compensated in the following by the deployed bonnet and the inflated airbag. Therefore the primary head impact occurs almost isochronous in both tests. For the system test the head impact time is 118 ms while the basic test achieves a head impact time of 120 ms. Here, the head subsequently strikes through the windscreen and hits the instrument panel at $t = 130$ ms (Figure 14). The vehicle velocity reached at the basic test lies about 1 km/h above the intended collision speed.

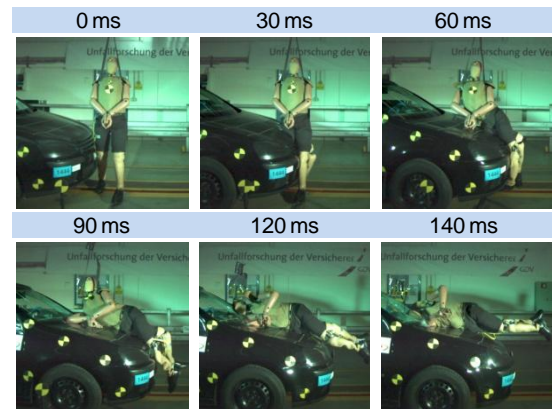


Figure 14. Basic test with a collision speed of 41 km/h.

Figure 15 illustrates the system test. The yellow black tapes sideways at the bumper visualise its retracting movement. At the same time the bonnet is lifted by 120 mm due to the inflating airbag, which subsequently absorbs the head impact.

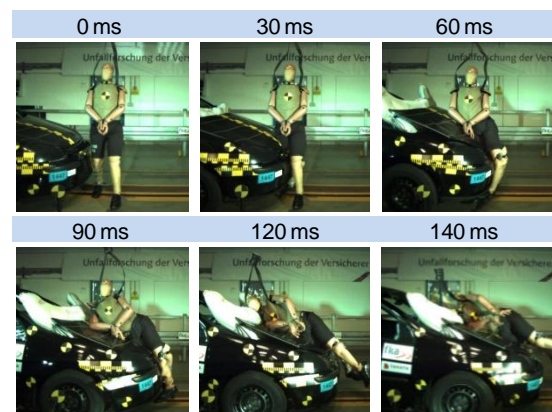


Figure 15. System test with a collision speed of 40 km/h.

The WAD for the head impact location amounts to 1940 mm in case of the basic test and 1860 mm (measured with undeployed bonnet) for the system test. The forward displacement of the head impact location is caused by the bonnet deployment. Both tests show a good conformance to the simulation results.

The measurement results confirm the high safety potential of the windscreen airbag. A comparison of basic and system test shows a reduction of the maximum head acceleration from 203 g to 72 g (Figure 16). The second peak in the acceleration curve of the basic test results from the head impact on the instrument panel. The curve occurring in the system test is smoother. Here the deceleration phase is longer and on a lower level. This is also reflected by the corresponding HIC₁₅-values. While the basic test reaches a value of 1736, the system test exhibits only a value of 566, which equals a reduction by 67 %.

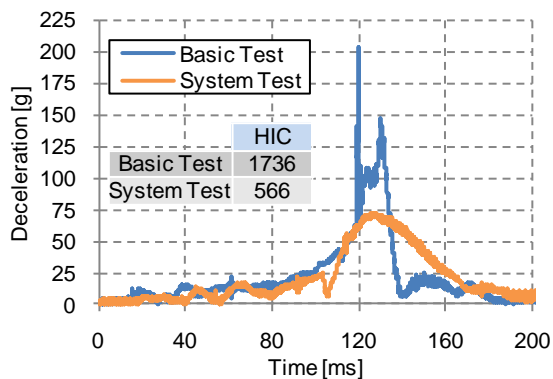


Figure 16. Head acceleration progression.

For the adaptive bumper the measurement results prove an increased safety potential as well. In Figure 17 this is exemplary demonstrated for the tibia acceleration in y-direction. The coordinate system of the dummy is oriented such that the positive x-axis is normal to the front of the dummy while the positive y-axis points laterally towards the right, i.e. towards the vehicle. Besides the tibia acceleration, also the maximum values for the resultant force as well as the bending moment in x-direction are reduced significantly. The maximum force value decreases from 4167 to 2330 N. For the bending moment a reduction from 216 to 163 N is achieved. The values for the opposite leg behave in a similar manner.

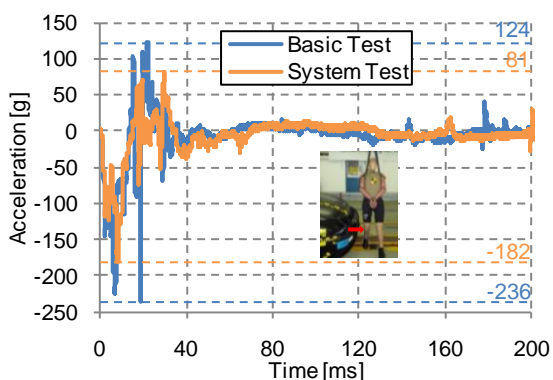


Figure 17. Tibia acceleration a_y of vehicle-oriented leg.

The benefit of a reduction in collision speed is demonstrated by two additional tests with a collision speed of 30 as well as 20 km/h. Those tests are conducted with the basic vehicle. Figure 18 shows the 30 km/h test. The reduced velocity leads to an increased head impact time of 143 ms, going along with a forward displacement of the head impact location (WAD = 1820 mm). The maximum head acceleration amounts to 162 g.



Figure 18. Test with a reduced collision speed of 30 km/h (basic vehicle).

The described effect becomes even more apparent for a collision speed of 20 km/h (Figure 19). Here the head impact time is 211 ms, which is almost 100 ms longer than for the basic test with 40 km/h. A significant difference also exists regarding the location of the head impact. Compared to the basic test the forward displacement adds up to 240 mm, resulting in a WAD of 1700 mm. This leads to a primary head impact on the bonnet rear edge, followed by an impact on the lower windscreen frame. The maximum head acceleration of 116 g lies above the value achieved by the airbag.

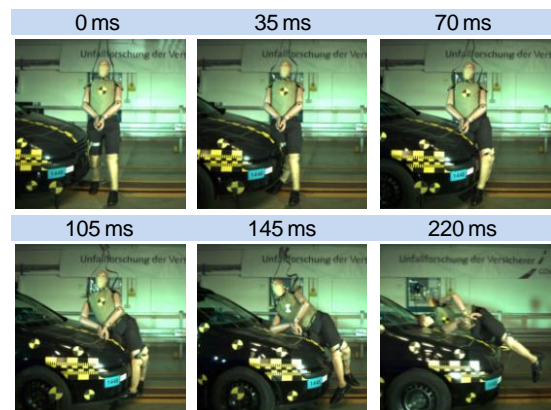


Figure 19. Test with a reduced collision speed of 20 km/h (basic vehicle).

Figure 20 illustrates the rise in head impact time as well as the reduced head loading due to a lower

collision speed. For all three tests conducted with the basic vehicle the corresponding head acceleration curves are given together with the HIC₁₅-values. In case of the basic vehicle a speed reduction about 10 km/h brings the HIC-value measured by the polar dummy below the common threshold of 1000. A collision with 20 km/h results in a further significant reduction of the HIC-value, which also becomes apparent within the assessment procedure. Here, the velocity related HIC-value calculated for the corresponding field of the vehicle segmentation amounts to 396, which is close to the test result of 340 and corroborates the presented approach (Figure 8).

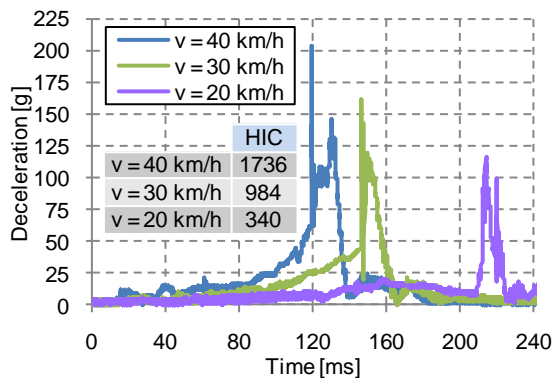


Figure 20. Velocity-dependent head acceleration progression (basic vehicle).

The low HIC-value reached in the 20 km/h test does not imply, that the safety potential regarding the primary head impact is generally higher compared to a windscreen airbag. The head impact occurred in that part of the cowl area, which achieved the best Euro NCAP test result (HIC = 1444). Therefore higher values have to be expected for other impact locations within the cowl area. Furthermore, a head impact on the rear bonnet edge, as it happens in the 20 km/h test, is always critical. For such a contact both the area of force application and the force magnitude are decisive for the arising injuries. The measurement of the acceleration at the centre of gravity of the head allows no direct conclusions regarding the area of force application. [8] Therefore the HIC does not reflect this critical loading case. The problem becomes apparent by an exemplary comparison of the resulting upper neck force measured by the dummy. For the 20 km/h test the maximum magnitude amounts to 6.5 kN while the airbag achieves a value of 2.9 kN at a collision speed of 40 km/h.

The windscreen airbag forms a very effective measure for the protection of adult pedestrians since it is able to reduce the head injury risk significantly in the most relevant impact area of sedan shaped vehicles. On the other hand, a speed

reduction due to an active brake system is beneficial for both pedestrian groups as well as all affected body regions. Additionally there is a positive influence on secondary impact. Nevertheless, a hundred percent reliability cannot be guaranteed for an active system and a speed reduction by 20 km/h is a challenge which demands high system requirements. Hence, the best pedestrian protection is provided by an integrated approach, combining measures of active and passive safety in a reasonable way.

CONCLUSIONS

The presented assessment procedure brings the evaluation of active and passive safety together and allows a general estimation of the risk for a severe head injury due to the primary impact. To validate the assessment procedure index values have been calculated for good as well as poor rated vehicles within Euro NCAP and under consideration of varying additional safety systems. It could be shown that the benefit of today's measures applied to the vehicle front is limited. Legal test requirements and consumer ratings insufficiently reflect the vehicle-class-specific relevance of particular front areas. For adults the simulation data points out the cowl, the A-pillars and the lower windscreen area, which need to be addressed by technical measures. Furthermore there is no "one fits all" passive measure which performs on the same positive level at all vehicle fronts and for all pedestrian sizes. Therefore measures have to be selected and adjusted for each car front. A windscreen airbag is able to improve adult pedestrian safety significantly. Children however profit more by emergency brake systems with pedestrian detection due to the limited safety potential of a pop-up bonnet.

The effective use of active safety systems generally demands an adequate passive pedestrian safety, as shown by the velocity related index calculation within the assessment procedure. Consequently, future cars should follow an integrated safety approach. Besides the head loading, this is moreover beneficial with respect to the leg loading as well as the secondary impact, which are also considered by the assessment procedure. The performed Polar-II dummy tests demonstrate the benefit of both the regarded passive safety systems and the reductions in collision speed.

REFERENCES

- [1] N.N.
European New Car Assessment Programme (Euro NCAP)
Pedestrian Testing Protocol, Version 5.1
January 2010

[2] KÜHN, M.; FRÖMING, R.; SCHINDLER, V.
Fußgängerschutz - Unfallgeschehen, Fahrzeuggestaltung, Testverfahren
Springer-Verlag, Berlin, 2007

[3] INTERNATIONAL STANDARD
Motorcycles - Test and analysis procedures for research evaluation of rider crash protective devices fitted to motorcycles
Part 5: Injury indices and risk/benefit analysis
Reference number: ISO 13232-5:2005(E)
Geneva, 2005

[4] MATSUI, Y.
New injury reference values determined for TRL legform impactor from accident reconstruction test
International Journal of Crashworthiness.
Vol. 8 No. 2 pp. 89-98, 2003

[5] MATSUI, Y.
Biofidelity of TRL Legform Impactor and Injury Tolerance of Human Leg in Lateral Impact
STAPP Car Crash Journal Vol45, 2001

[6] N.N.
POLAR II User's Manual, Version 2.2
HONDA R&D CO., LTD. TOCHIGI R&D CENTER
Japan, 2008

[7] N.N.
Surface Vehicle Recommended Practice
SAE International Document j2782
Dummy Task Group, Draft Recommended Practice for Pedestrian Dummy
Performance Specifications for a 50th Percentile Male Pedestrian Dummy
SAE International, 2007

[8] BOVENKERK, J.
Fußgängerschutz Testverfahren für den Frontscheibenbereich am Kraftfahrzeug
Schriftreihe Automobiltechnik
Institut für Kraftfahrzeuge, RWTH Aachen University, 2009